

Springer Theses

Recognizing Outstanding Ph.D. Research

Estefanía Cuenca

On Shear Behavior of Structural Elements Made of Steel Fiber Reinforced Concrete



Springer

Springer Theses

Recognizing Outstanding Ph.D. Research

Aims and Scope

The series “Springer Theses” brings together a selection of the very best Ph.D. theses from around the world and across the physical sciences. Nominated and endorsed by two recognized specialists, each published volume has been selected for its scientific excellence and the high impact of its contents for the pertinent field of research. For greater accessibility to non-specialists, the published versions include an extended introduction, as well as a foreword by the student’s supervisor explaining the special relevance of the work for the field. As a whole, the series will provide a valuable resource both for newcomers to the research fields described, and for other scientists seeking detailed background information on special questions. Finally, it provides an accredited documentation of the valuable contributions made by today’s younger generation of scientists.

Theses are accepted into the series by invited nomination only and must fulfill all of the following criteria

- They must be written in good English.
- The topic should fall within the confines of Chemistry, Physics, Earth Sciences, Engineering and related interdisciplinary fields such as Materials, Nanoscience, Chemical Engineering, Complex Systems and Biophysics.
- The work reported in the thesis must represent a significant scientific advance.
- If the thesis includes previously published material, permission to reproduce this must be gained from the respective copyright holder.
- They must have been examined and passed during the 12 months prior to nomination.
- Each thesis should include a foreword by the supervisor outlining the significance of its content.
- The theses should have a clearly defined structure including an introduction accessible to scientists not expert in that particular field.

More information about this series at <http://www.springer.com/series/8790>

Estefanía Cuenca

On Shear Behavior of Structural Elements Made of Steel Fiber Reinforced Concrete

Doctoral Thesis accepted by
Universitat Politècnica de València, Spain

Author

Dr. Ing. Estefanía Cuenca
Department of Construction Engineering
and Civil Engineering Projects, Concrete
Science and Technology Institute
(ICITECH)
Universitat Politècnica de València (UPV)
Valencia
Spain

Supervisors

Prof. Dr. Ing. Pedro Serna
Department of Construction Engineering
and Civil Engineering Projects, Concrete
Science and Technology Institute
(ICITECH)
Universitat Politècnica de València (UPV)
Valencia
Spain

Prof. Dr. Ing. Giovanni A. Plizzari
Department of Civil Engineering,
Architecture, Environment, Land
Planning and Mathematics
University of Brescia
Brescia
Italy

ISSN 2190-5053

Springer Theses

ISBN 978-3-319-13685-1

DOI 10.1007/978-3-319-13686-8

ISSN 2190-5061 (electronic)

ISBN 978-3-319-13686-8 (eBook)

Library of Congress Control Number: 2014956871

Springer Cham Heidelberg New York Dordrecht London

© Springer International Publishing Switzerland 2015

This work is subject to copyright. All rights are reserved by the Publisher, whether the whole or part of the material is concerned, specifically the rights of translation, reprinting, reuse of illustrations, recitation, broadcasting, reproduction on microfilms or in any other physical way, and transmission or information storage and retrieval, electronic adaptation, computer software, or by similar or dissimilar methodology now known or hereafter developed.

The use of general descriptive names, registered names, trademarks, service marks, etc. in this publication does not imply, even in the absence of a specific statement, that such names are exempt from the relevant protective laws and regulations and therefore free for general use.

The publisher, the authors and the editors are safe to assume that the advice and information in this book are believed to be true and accurate at the date of publication. Neither the publisher nor the authors or the editors give a warranty, express or implied, with respect to the material contained herein or for any errors or omissions that may have been made.

Printed on acid-free paper

Springer International Publishing AG Switzerland is part of Springer Science+Business Media
(www.springer.com)

Parts of this thesis have been published in the following documents:

Referred Journal Papers

- J1** Estefanía Cuenca; Pedro Serna. FAILURE MODES AND SHEAR DESIGN OF PRESTRESSED HOLLOW CORE SLABS MADE OF FIBER-REINFORCED CONCRETE. *Composites Part B: Engineering*, 45(1), pp. 952–964. Elsevier, 2013. DOI: <http://dx.doi.org/10.1016/j.compositesb.2012.06.005> ISSN: 1359-8368
- J2** Estefanía Cuenca; Pedro Serna. SHEAR BEHAVIOR OF PRESTRESSED PRECAST BEAMS MADE OF SELF-COMPACTING FIBER REINFORCED CONCRETE. *Construction and Building Materials*, 45, pp. 145–156. Elsevier, 2013. DOI: <http://dx.doi.org/10.1016/j.conbuildmat.2013.03.096>
- J3** Fausto Minelli; Antonio Conforti; Estefanía Cuenca; Giovanni Plizzari. ARE STEEL FIBRES ABLE TO MITIGATE OR ELIMINATE SIZE EFFECT IN SHEAR? *Materials and Structures*. March 2014, Volume 47, Issue 3, pp 459–473. Springer. DOI: [10.1617/s11527-013-0072-y](http://dx.doi.org/10.1617/s11527-013-0072-y)

Book Chapters

- B1** Estefanía Cuenca; Pedro Serna. SHEAR BEHAVIOR OF SELF-COMPACTING CONCRETE AND FIBER-REINFORCED CONCRETE PUSH-OFF SPECIMENS. *Design, Production and Placement of Self-Consolidating Concrete*. 36, pp. 429–438. RILEM Bookseries, Springer, 2010. DOI: [10.1007/978-90-481-9664-7_36](http://dx.doi.org/10.1007/978-90-481-9664-7_36); Print ISBN: 978-90-481-9663-0; Online ISBN: 978-90-481-9664-7.
- B2** Pedro Serna; Estefanía Cuenca; Mariela Alves De Oliveira. SELF-COMPACTING FIBER REINFORCED IN PRECAST ELEMENTS PRODUCTION FOR SHEAR RESISTANCE. *Dedicated to Innovation: 50 Years MC-Bauchemie*. MC-Bauchemie Müller GmbH Co. KG., 2011. ISBN-13:978-3-89355-989-3.

International Conferences

- C1** Estefanía Cuenca; Pedro Serna; María José Pelufo. STRUCTURAL BEHAVIOR OF SELF-COMPACTING AND FIBER REINFORCED CONCRETE UNDER SHEAR LOADING. *Book of Abstracts. Evolution and Trends in Design, Analysis and Construction of Shell and Spatial Structures IASS 2009*. ISBN: 978-84-8363-459-2. Valencia (Spain), 2009.
- C2** Estefanía Cuenca; Pedro Serna. SHEAR BEHAVIOR AND MODE OF FAILURES ANALYSIS OF DIFFERENT STRUCTURAL ELEMENTS MADE WITH FIBER REINFORCED CONCRETE. *Proceedings of the 8th fib Ph.D. Symposium*. ISBN: 9788778773012. Technical University of Denmark (DTU). Kgs. Lyngby (Denmark), 2010.

- C3** Estefanía Cuenca; Pedro Serna. RESPUESTA FRENTE A CIZALLAMIENTO EN PROBETAS TIPO Z FABRICADAS CON HACS DE DIFERENTE ESTRUCTURA GRANULAR. Actas del 2° Congreso Ibérico sobre Hormigón Autocompactante/Congresso Iberico sobre betao auto-compactavel. ISBN: 978-972-8692-46-9. Universidad do Minho. Guimaraes (Portugal), 2010.
- C4** Estefanía Cuenca; Pedro Serna. COMPORTAMIENTO A CORTANTE DE VIGAS PREFABRICADAS CON HORMIGÓN TRADICIONAL Y HORMIGÓN AUTOCOMPACTANTE. Actas del 2° Congreso Ibérico sobre Hormigón Autocompactante/Congresso Iberico sobre betao auto-compactavel. ISBN: 978-972-8692-46-9. Universidad do Minho. Guimaraes (Portugal), 2010.
- C5** Estefanía Cuenca; Pedro Serna. SHEAR BEHAVIOR OF SELF-COMPACTING CONCRETE AND FIBER REINFORCED CONCRETE BEAMS. Design, Production and Placement of Self-Consolidating Concrete. Proceedings of the 6th International RILEM Symposium on Self-Compacting Concrete, SCC2010. Montreal (Canada), 2010.
- C6** Antonio Conforti; Fausto Minelli; Estefanía Cuenca; Giovanni Plizzari. COMPORTAMENTO A TAGLIO DI TRAVI ALTE IN CALCESTRUZZO ARMATO FIBRORINFORZATO. Atti del 26° Convegno Nazionale Giornate AICAP 2011. Padova (Italy), 2011.
- C7** Antonio Conforti; Estefanía Cuenca; Fausto Minelli; Giovanni Plizzari. CAN WE MITIGATE OR ELIMINATE SIZE EFFECT IN SHEAR BY UTILIZING STEEL FIBERS? Proceedings of the fib Symposium in Concrete Engineering for Excellence and Efficiency. ISBN: 978-80-87158-29-6. Prague (Czech Republic), 2011.
- C8** Estefanía Cuenca; Pedro Serna. HORMIGÓN REFORZADO CON FIBRAS DE ACERO PARA PREFABRICADOS ESTRUCTURALES. CONTRIBUCIÓN AL ESFUERZO CORTANTE. V Congreso de ACHE. ISBN: 978-84-89670-73-0. Barcelona, (España), 2011.
- C9** Estefanía Cuenca; Javier Echegaray; Pedro Serna; Andrea Pasetto. DUCTILITY ANALYSIS ON THE POST-PEAK BEHAVIOR OF SELF-COMPACTING FIBER REINFORCED CONCRETE (SCFRC) BEAMS SUBJECTED TO SHEAR. 8th RILEM International Symposium on Fibre Reinforced Concrete: Challenges and Opportunities (BEFIB 2012). ISBN: 978-2-35158-132-2. E-ISBN: 978-2-35158-133-9. Guimaraes, (Portugal), 2012.
- C10** Javier Echegaray; Juan Navarro; Estefanía Cuenca; Pedro Serna. UPGRADING THE PUSH-OFF TEST TO STUDY THE MECHANISM OF SHEAR TRANSFER IN FRC ELEMENTS. VIII International Conference on Fracture Mechanics of Concrete and Concrete Structures (FraMCoS-8). ISBN: 978-84-941004-1-3. Toledo (Spain), 2013.
- C11** Estefanía Cuenca; Pedro Serna; Giovanni Plizzari. SHEAR DATABASE FOR REINFORCED AND PRESTRESSED BEAMS MADE WITH FIBER REINFORCED CONCRETE. VIII International Conference on Fracture Mechanics of Concrete and Concrete Structures (FraMCoS-8). ISBN: 978-84-941004-1-3. Toledo (Spain), 2013.

Supervisors' Foreword

Estefanía worked in the hostile habitat of a laboratory or a precast concrete industry and in a foreigner laboratory imposing her personality and working with the technicians and other colleagues. She got used to the new environment and assumed the coordination of work of other students from different universities or Erasmus.

When difficulties seemed overcome, she sought others to be solved. With the aim of achieving the International Mention in the title of doctor, she wrote the thesis in English (rare in Spain) and did not hesitate to make a very productive stay in Brescia with the group led by Giovanni A. Plizzari. Her stay allowed to increase collaborative relations between the two research groups. An important part of Estefanía's work was done at the University of Brescia and her attitude, also there, was highly evaluated.

The work of the thesis provides significant data on shear behavior of fiber reinforced concrete. These data have been manufactured, tested, and analyzed. She tested shear beams of significant size, with a very wide range of characterization tests, manufacturing several cubic meters of concrete. The structure of this document allows the reader to analyze each chapter independently. Each one deals with issues relating to effect of the concrete properties as material or related to the concrete structural system. The incorporation of an additional database with results from other researchers allows the reader an easy access to information not always available.

We are sure that everywhere that Estefanía is involved in teaching, research, or other activities, she will be able to overcome the obstacles that will come in her way.

The reader will find in this thesis many unclear points but they are not mistakes since they are points that allow us to further investigate the problem and we hope that this will encourage more people to be involved in the research work.

Estefanía, we wish you every success possible. It was a pleasure working with you and we hope that we continue taking advantage of your last job and we raise more for the future.

Valencia, July 2014
Brescia

Prof. Dr. Ing. Pedro Serna
Prof. Dr. Ing. Giovanni A. Plizzari

Acknowledgments

Maybe this is the most difficult part of the entire thesis. Difficult because in only one page, I am supposed to write my acknowledgments to all those people who have supported, listened, and understood me during this path called “Ph.D. thesis.” This thesis is dedicated to a small but selected group of people who told me those words that I needed to listen in determined moments, those people who always have believed in me, and have been with me not only in the nice moments (that is easy) but also in the difficult ones. Thanks to all people who have made me happy, offering me smiles and affection.

First of all, I want to thank Prof. Dr. Pedro Serna; my mentor and main supervisor of this Ph.D. thesis. Thank you Pedro for all. Thank you for the numerous knowledge and principles that you transmitted to me and for encouraging me to love what I did in the laboratory. I will always remember your attitude, friendliness, kindness, human touch, affection, humility, and your smiles. Since the first day you always treated me as an equal, thank you for being with me since the first moment I arrived at your office and for the funding. Thank you also for listening to me, for understanding me, and for the flexibility, liberty, and confidence that you gave me during all this time.

I would like to express my special appreciation also to Prof. Dr. Giovanni A. Plizzari for receiving me into their research group in Brescia (Italy) and for his important advices. Since the first day in Brescia, he always was very kind with me. Thank you to my colleagues, technicians, and faculty members of Brescia as well.

A special recognition has to be given to the big family of the ICITECH, professors and researchers, especially to Paco Martorell, who worked hard with me in the lab along these years with a fantastic sense of humor. Thank you to all my friends from the department, especially to Javier Echegaray (my officemate during the last years) and Karen Caballero. Two big friendships that were born in the department and continue in the present.

To my friends, thank you for the good moments.

To my parents, thank you for all, for your kindness, for your unconditional support, love, comprehension, wise advices, and for being the best example of life. I am very, very proud of you. Thank you mum for being always so comprehensive with me

and for your enormous patience. Thank you dad for being an example for overcoming difficulties and for demonstrating to me that if you want something, you can achieve it. Thank you for believing in me. Thank you also to my sister, Natalia, for being always there, for your sincerity and clear advices when I asked you.

Thank you to my grandparent Honorio. I know you always take care of me from the top.

The Ph.D. period has been also significant, because it has permitted me to meet Antonio, the biggest surprise of all this period. Thank you for all, from the first day.

Madrid, July 2014

Dr. Ing. Estefanía Cuenca

Contents

Part I Introduction and Objectives

1	Introduction	3
1.1	Outline	3
1.2	Foreword	4
1.3	Contents	6
	References.	7
2	Objectives and Research Significance.	9
2.1	Objectives	9
2.2	Specific Objectives	9
2.3	Final Considerations	10
	References.	10

Part II State of the Art

3	Literature Survey on Shear in FRC Beams	13
3.1	Introduction	13
3.2	On Steel Fiber Reinforced Concrete (SFRC).	13
3.2.1	Introduction About FRC.	13
3.2.2	Classification	15
3.2.3	Constitutive Laws	16
3.2.4	Partial Safety Factors	17
3.3	Fibers Effects on Shear Behavior	18
3.3.1	Fibers Concept	18
3.3.2	Effect of Fibers on Shear Strength and Stiffness	18
3.3.3	Effect of Fibers on Ductility (Postcracking Response).	19
3.3.4	Effect of Fibers on Shear Cracking	20
3.3.5	Effect of Fibers on Yielding of Longitudinal Bars	20

- 3.3.6 Effect of Fibers on Cracking Distribution 20
- 3.3.7 Effect of Fibers on Rotation Capacity 21
- 3.3.8 Effect of Fibers on Tensile Properties 21
- 3.3.9 Effect of Fibers on Crack Spacing 21
- 3.3.10 Effect of Fibers on Tension Stiffening 21
- 3.3.11 Effect of Fibers on Characteristic Length (L_r) 22
- 3.4 Steel Fibers as Shear Reinforcement 23
 - 3.4.1 Fibers as Minimum Shear Reinforcement 23
 - 3.4.2 Fibers Totally Replacing Stirrups 23
 - 3.4.3 Fibers Partially Replacing Stirrups 24
 - 3.4.4 Shear Crack Pattern in FRC Elements 24
- 3.5 Failures Modes 24
 - 3.5.1 Can Fibers Alter the Collapse from Shear to Flexure? 24
 - 3.5.2 Ductile Failure Mode Due to Fibers 25
 - 3.5.3 Influence of Fibers in Compression Zone 25
- 3.6 Fibers Influence on Size Effect 25
 - 3.6.1 Influence of Depth in Shear Strength 25
 - 3.6.2 Influence of Depth on the Shear Crack Width 26
- 3.7 Fibers Influence on Serviceability Limit State (SLS) and Durability 27
- 3.8 Reduction of Production Cost 27
- 3.9 Combination of Steel Fibers and Stirrups 28
- 3.10 Shear Models and Design Codes 28
 - 3.10.1 Design Codes 28
- 3.11 Parameters Influencing in Shear Behavior of FRC Beams 36
 - 3.11.1 Amount of Fibers 37
 - 3.11.2 Relation Between Casting Procedure and Fiber Length 37
 - 3.11.3 Fiber Type 37
 - 3.11.4 Relation Between Fiber Type and Beam Size 38
 - 3.11.5 Depth of the Beam 38
 - 3.11.6 Flange Width 39
 - 3.11.7 Flange Depth 39
 - 3.11.8 Effect of Longitudinal Ratio 40
 - 3.11.9 Influence of Prestressing 40
 - 3.11.10 Influence of Concrete Strength 40
- 3.12 Fibers Influence on Deflections 40
- 3.13 Fibers Influence on Dowel Action 41
- 3.14 Hollow Core Slabs (HCS) Made with FRC 41
 - 3.14.1 Introduction 41
 - 3.14.2 Manufacturing of HCS Made with FRC 42
 - 3.14.3 Advantages of Adding Fibers into Concrete Mix for HCS Production 42
 - 3.14.4 Shear Behavior of HCS 42

3.14.5	Failure Modes	44
3.14.6	Design of HCS	44
	References.	45

Part III Experimental Tests

4	Experimental Tests on Parameters Influencing on Shear.	59
4.1	Introduction	59
4.2	Concrete Mix Designs	59
4.3	Concrete Properties and Production Control	61
4.4	Experimental Program and Results Analysis	63
4.4.1	Main Variables and Beams Production	63
4.4.2	Testing Procedure	65
4.4.3	Results.	65
4.4.4	Shear Values Calculated with the Current Design Codes	70
4.5	Conclusions	76
4.6	Publication of These Results.	77
	References.	77
5	Experimental Tests on Fibers Influence on the Size Effect on Shear.	79
5.1	Introduction	79
5.2	Materials	79
5.3	Concrete Properties and Production Control	81
5.4	Experimental Program	84
5.4.1	Main Variables and Beam Production	84
5.4.2	Testing Procedure	85
5.4.3	Results.	89
5.4.4	Study of the Size Effect	95
5.4.5	Shear Values Calculated with the Current Design Codes	103
5.5	Conclusions	104
5.6	Publication of These Results.	105
	References.	105
6	Experimental Tests to Study the Influence on the Shear Behavior of Fibers of Different Characteristics.	107
6.1	Introduction	107
6.2	Experimental Program	108
6.3	Result of the Concretes Characterization	109
6.4	Results of the Shear Tests on Beams	114
6.5	Conclusions	122
	References.	123

7	Experimental Tests on Hollow Core Slabs Made with FRC	125
7.1	Introduction	125
7.2	Experimental Investigation	125
7.2.1	Hollow Core Slabs' Geometry	125
7.2.2	Concrete Mix Design	127
7.2.3	HCS Production	128
7.2.4	Test Set-Up	129
7.3	Tests Results and Analysis	133
7.3.1	Failure Modes	133
7.3.2	Load-Deflection Response	135
7.3.3	Shear Values According to Current Design Codes and Failure Modes Discussion	138
7.4	Conclusions	145
7.5	Publication of These Results	146
	References	146

Part IV Shear Database

8	Shear Database and Study of the Parameters Influencing Shear Behavior	149
8.1	Introduction	149
8.2	Data Selection	150
8.3	Case 1: Beams Made Without Shear Reinforcement (Concrete Neither Fibers Nor Stirrups)	151
8.3.1	Influence of the a/d Ratio	151
8.3.2	Influence of the Effective Depth, d . Size Effect	154
8.3.3	Influence of the Concrete Compressive Strength, f_c	154
8.3.4	Influence of the Amount of Longitudinal Reinforcement, ρ_l	155
8.3.5	Influence of the Prestressing Stress, σ_c	155
8.3.6	General Behavior of Codes for Beams Without Shear Reinforcement	157
8.4	Case 2: Beams with Stirrups (No Fibers)	158
8.4.1	Parameters Influence on Shear for Beams with Only Stirrups	158
8.4.2	General Behavior of Codes for Beams with Only Stirrups	158
8.5	Case 3: Beams with Fibers (No Stirrups)	159
8.5.1	Influence of the a/d Ratio and the Effective Depth, d	159
8.5.2	Influence of the Concrete Compressive Strength, f_c	159
8.5.3	Influence of the Residual Tensile Strength (CMOD = 2.5 mm), f_{R3}	160

8.5.4	Influence of the Amount of Longitudinal Reinforcement, ρ_l	160
8.5.5	Influence of the Stress Due to Prestressing Actions, σ_c	161
8.5.6	Influence of the Amount of Fibers, Kg/m^3	164
8.5.7	General Behavior of Codes for Beams with Only Fibers	164
8.6	Case 4: Beams with Fibers and Stirrups	165
8.6.1	Influence of the Residual Tensile Strength, f_{R3}	166
8.6.2	Influence of the Longitudinal Reinforcement Percentage, ρ_l	166
8.6.3	Influence of the Stress Due to Prestressing Actions, σ_c	167
8.6.4	General Behavior of Codes for Beams with Stirrups and Fibers	167
8.7	Particular Cases	169
8.7.1	Introduction	169
8.7.2	Brite Series 1	170
8.7.3	Brite Series 2	174
8.7.4	Brite Series 3	175
8.7.5	Study of Size Effect on Shear	181
8.7.6	Beams with Different Types of Fibers	185
8.8	Conclusions According to the Analyzed Shear Database	192
8.8.1	Influence of Effective Depth, d	192
8.8.2	Influence of the a/d Ratio	193
8.8.3	Influence of the Concrete Compressive Strength, f_c	193
8.8.4	Influence of the Residual Tensile Strength, f_{R3}	194
8.8.5	Influence of the Amount of Longitudinal Reinforcement, ρ_l	195
8.8.6	Influence of the Stress Due to the Prestressing Actions, σ_c	196
8.9	Suggestions for Design Codes According to Shear	197
	References	203

Part V Conclusions and Future Research

9	Conclusions	207
10	Recommendations for Future Research	209

Symbols and Abbreviations

a	Shear span
A_p	Cross-sectional area of prestressed reinforcement
A_s	Cross-sectional area of longitudinal tension reinforcement
A_α	Traditional shear reinforcement area
b_f	Flange width
b_o	Web width
d	Effective depth
f_{bpt}	Constant bond stress at which the prestress is transferred to the concrete at release of tendons
$f_{ctd(t)}$	Design tensile value of strength at time of release
f_{ctk}	Characteristic tensile strength value for the concrete matrix
f_{Ftu_k}	Characteristic ultimate residual tensile strength value for fiber-reinforced concrete
f_{p0}	Stress in strands when the strain in the surrounding concrete is zero
f_{R3k}	Residual flexural tensile strength corresponding to $CMOD = 2.5$ mm (according to EN 14651)
f_{R4k}	Residual flexural tensile strength corresponding to $CMOD = 3.5$ mm (according to EN 14651)
$f_{y\alpha,k}$	Yielding strength of shear reinforcement steel
I	Second moment of area
k_f	Factor to take into account the flanges contribution in the T-sections (EHE08 and RILEM)
l_{crit}	Critical length
l_{pt}	Transfer length
l_{pt2}	Upper bound value of the transmission length of the prestressing element: $l_{pt2} = 1.2 \cdot l_{pt}$
l_x	Distance of section considered from starting point of the transmission length
S	First moment of area above and about the centroidal axis
V_{cu}	Design shear resistance attributed to concrete
V_{fu}	Design shear resistance attributed to fibers

V_{su}	Design shear resistance provided by shear reinforcement
V_{u2}	Design shear resistance
z	Internal lever arm corresponding to the maximum bending moment In the shear analysis, an approximate value $z = 0.9 \cdot d$ can be normally used
α	Inclination of stirrups in relation to the beam axis
α_l	$= l_x/l_{pt2} \leq 1$ for pretensioned tendons
β	Reduction factor referred to the transmission length ($\beta = 0.9$)
γ_c	Partial safety factor for concrete material properties
γ_s	Partial safety factor for the material properties of reinforcement and prestressing steel
ϵ_x	Longitudinal strain at the mid-depth of the member
η_{p1}	Coefficient that takes into account the type of tendon and the bond situation at release
θ	Inclination of the compression stresses
θ_e	Reference angle of cracks inclination
ξ	Factor that takes into account the size effect
ρ_l	Reinforcement ratio for longitudinal reinforcement
ρ_w	Percentage of shear reinforcement
σ_{ck}	Average stress acting on the concrete cross-section for an axial force due to prestressing actions
σ_{pm0}	Tendon stress just after release
φ	Reduction factor ($\varphi = 0.8$)
ϕ	Nominal diameter of the tendon

About the Author



(Photo by Zaida del Río Martín)

Dr. Ing. Estefanía Cuenca achieved her B.S. and M.S. degrees in Civil Engineering from Universitat Politècnica de València (València, Spain) in 2008, and obtained her Ph.D. degree with International Mention and honors from the same University in 2012. Estefanía’s primary research interests include the concrete technology and mechanical behavior of self-compacting concrete and fiber reinforced concrete, specifically shear behavior of both reinforced and prestressed concrete structural elements reinforced by steel fibers, as well as structural applications of fiber reinforced concrete.

From September 2008 to May 2013, she worked as a researcher in the Science and Concrete Technology Institute (ICITECH) of the Universitat Politècnica de València (Spain) in the research team headed by Prof. Dr. Pedro Serna. During this period she designed new mix designs of self-compacting concretes and steel fiber reinforced concretes, analyzing their mechanical behavior. After that, she performed several shear tests on beams, hollow core slabs, and push-off specimens made with those concretes. Moreover, most of these works were done with a close collaboration with a precast industry, in order to achieve structural applicability of the research results.

After her Ph.D. defense, she was faculty member of the Universitat Politècnica de València, teaching courses on design of: reinforced and prestressed concrete structural elements and foundations.

During her Ph.D. research period, from April 2010 to October 2010, she joined the research team headed by Prof. Dr. Giovanni A. Plizzari in the University of Brescia (Italy). During this time she performed shear tests on reinforced concrete beams made with fiber reinforced concrete to study the influence of steel fibers on the size effect. In October 2010, she had the opportunity to participate as organizing staff of the International Workshop on “Recent developments on shear and punching shear in RC and FRC elements” in Salò, Italy.

Since June 2013, Estefanía is a faculty member at the Nebrija University (Madrid, Spain) where she teaches courses on structural design.

Estefanía is author of 16 scientific papers, including journal and conference papers.

She is official reviewer of the following international scientific journals: Construction and Building Materials (Elsevier), Materials and Structures (Springer) and Scientific Research and Essays.

Part I
Introduction and Objectives

Chapter 1

Introduction

1.1 Outline

Research on shear in reinforced concrete has been carried out for about a century, so there are many published papers in existence related to this subject.

With the arrival on the market of new materials, such as Fiber Reinforced Concrete (FRC), studies began to focus on the shear behavior of elements made of this material.

The present thesis tries to shed some new light on the shear behavior of FRC elements by means of a thorough analysis of the most important studies in order to detect any deficiencies or issues that have not yet been examined.

Many researchers have presented new formulas for evaluating shear resistance and have compared them with others already in existence.

This thesis does not propose a new formula to add to the already long list, but the objective is to verify the reliability of the current codes by means of comparing experimental tests.

One of the issues dealt with was to verify the influence of flange size on shear and whether to include the flange factor in the design formulas (it appears in one shear formulation for FRC elements, but not in those for non-fiber elements).

Tests were also performed on beams made of concrete of different compressive strengths and fiber reinforcements (quantity and quality) to study their influence on shear, including the size effect.

Finally, FRC hollow core slabs were produced to achieve the benefits of fibers under shear forces, due to the impossibility of including transverse reinforcement in this type of slab.

1.2 Foreword

In 1955, the partial collapse of the Wilkins Air Force Depot warehouse in Shelby, Ohio, called into question the shear provisions of the ACI Building Code. This Code for many years had permitted, under service conditions, shear stresses in beams without stirrups equal to $0.03:f'_c$, which meant an allowable working shear stress of 0.62 MPa for the 20 MPa Wilkins concrete. As a matter of fact, the beams in the Air Force warehouse failed due to a shear stress of about 0.5 MPa (see Fig. 1.1), pointing to serious deficiencies in the design practice of the time. Further analyses demonstrated that tensile stresses due to the restraint of shrinkage and thermal movements explained why the low shear stresses applied caused the failure [1]. This accident led to a revision of the shear provisions in the 1956 ACI Building Code and triggered a considerable number of studies on shear strength.

Even after many years of intensive research, the shear behavior of concrete structures is still not complete and is a topic of continuous debate between researchers and practitioners looking for models and methods to describe and determine the shear capacity of structural concrete members (Fig. 1.2).

Some of the parameters usually considered in shear behavior are: element dimensions (for the size effect), presence of axial forces, amount of longitudinal reinforcement, concrete compressive strength, load conditions, cross-section shape and the shear span/depth ratio (a/d).

General shear models are now being extended to cover newer materials such as fiber reinforced concrete (FRC).

The following are some of the main concepts included in papers related to FRC elements subjected to shear forces:

- fibers are used to enhance the shear capacity of concrete, or to partially or totally replace stirrups in RC structural members [4, 5]
- FRC is characterized by enhanced toughness due to the bridging effects provided by fibers [5, 6]
- fibers provide substantial post-peak resistance and ductility [5, 7–9]



Fig. 1.1 Shear failure of air force warehouse beams ([2, 3] respectively)

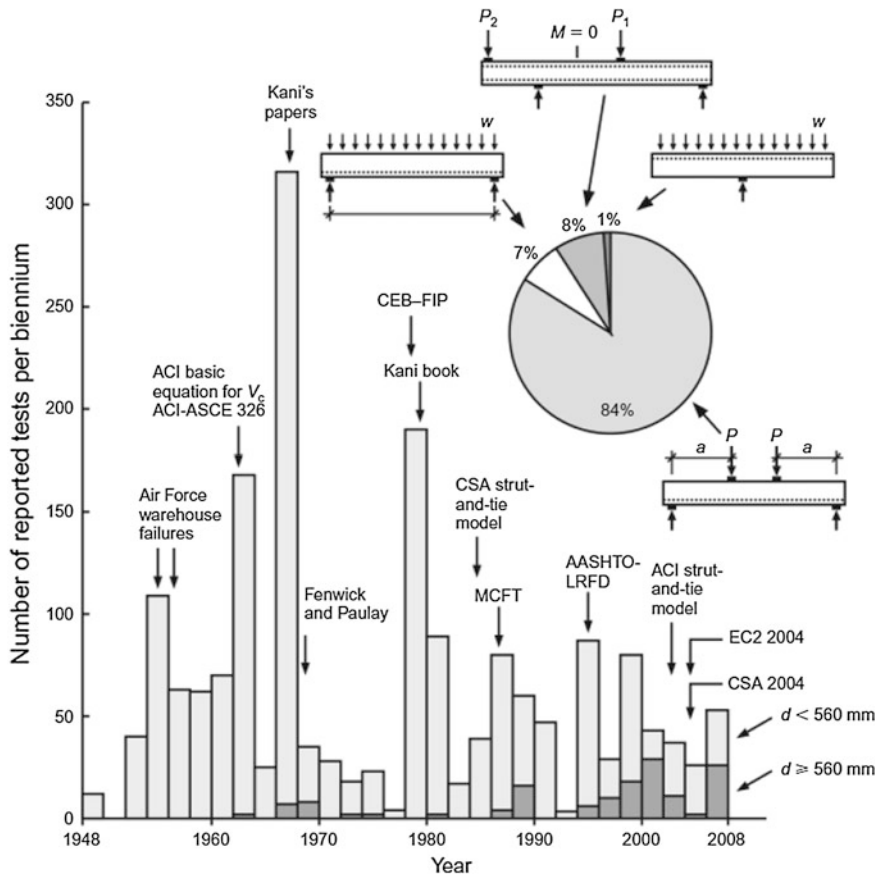


Fig. 1.2 Shear research on members without shear reinforcement [2]

- adding fibers means fewer brittle shear failures take place e.g., [10,11]
- test results indicate that adding fibers reduces maximum crack width, average crack width and average crack spacing [7, 12–14]
- FRC is suitable for structures where diffused stresses are present, and improves reinforcement in structures with both localized and diffused stresses in combination with rebars [5].

RILEM TC162-TDF [15] produced pioneer design guidelines in which the fibers' contribution to shear resistance is added to that of the concrete as a separate term, based on the fiber's toughness properties.

The approach presented in the Final Draft of the Model Code 2010 [16] for shear resistance of FRC members is based on the Eurocode 2 [17], used to determine shear contribution in concrete members without shear reinforcement, by adding a factor based on Minelli's proposal, which includes the FRC mechanical properties by modifying the effect of the longitudinal reinforcement ratio. Thus, by

considering FRC as a composite with enhanced toughness, the fiber effects are included as a concrete contribution. This was done to obtain a more representative modeling of the actual effect of fibers, which basically make the concrete matrix tougher after cracking by improving both the transfer of residual tensile stresses and the aggregate interlock (the latter, by keeping cracks smaller). However, it should be noted that the two formulations require toughness properties. When combining fibers with stirrups, both Codes include an additional term to consider the effect of stirrups. The proposed model and the RILEM formulation were compared with of a wide experimental database. Although the fit is less promising when dealing with high strength concrete specimens or prestressed members, the RILEM results are slightly more refined for small-sized elements than for deep beams.

The ACI 318-11 Code [18] does not include a formula to calculate the shear strength of SFRC beams and only assumes a minimum shear strength which fibers can withstand. In 2006, Parra-Montesinos [19] ensured that hooked steel fibers in an FRC with a 0.75 % by volume fraction of steel fibers can be used in lieu of minimum stirrup reinforcement in beams. A limit based on FRC toughness properties (that does not only depend on the amount of fibers) would be a better criterion to justify substitution of transverse reinforcement.

Other countries have produced design guidelines, including: France (AFGC-SETRA, 2002), Sweden (Stålfiberbeton, 1995), Germany (DAfStb, 2007), Austria (Richtlinie Faserbeton, 2002), Italy (CNR, 2006) and Spain (EHE: Appendix 14 [20]) (the latter based on RILEM guidelines [15]).

The FRC shear design workshop held in Salò (Italy) proved to be an interesting advance in the development of the Model Code provisions [16] and in inspiring future research into these topics. Lectures were included in a *fib* Bulletin [21].

1.3 Contents

This Ph.D. thesis is divided into five parts:

The **Part I: Introduction and Objectives** consists of Chaps. 1 and 2

- Chapter 1 is an introduction to the shear behavior of concrete structural elements, with and without fibers, with a brief historical review on the research to date on this topic. Also included are the main topics in papers related to FRC elements subjected to shear and the benefits on shear behavior of the addition of steel fibers. Current Codes are cited that include fibers' contribution to shear. Finally, there is a brief summary of the contents of this Ph.D. thesis.
- Chapter 2 describes the objectives pursued in this thesis and its contribution to the research in its field.

Part II: State of the Art describes the state-of-the-art of the shear behavior of structural concrete elements made with fiber reinforced concrete (Chap. 3).

Chapter 3 describes the state-of-the-art of the shear behavior of concrete structural elements made with steel fibers. This chapter starts with a general introduction on steel fiber reinforced concrete, followed by the use of steel fibers as shear reinforcement.

Part III: Experimental Tests deals with the experimental tests (Chaps. 4–7).

- Chapter 4 presents the results of studies with large beams to assess the influence of the size effect.
- Chapter 5 examines the shear behavior of concrete containing fibers of different characteristics and different concrete compressive strengths.
- In Chap. 6 shear tests on prestressed beams are analyzed, with special attention to the possible influence of parameters such as flange size on shear strength.
- Chapter 7 describes a complete experimental program consisting of the shear behavior of hollow core slabs (HCS) made of fiber reinforced concrete.

Part IV: Shear Database Chapter 8 focuses on the analysis of an extensive shear database of concrete elements with and without steel fibers, and studies the effect of each parameter on shear behavior and discusses the reliability of the Design Codes.

Part V: Conclusions and Future Research Chapter 9 contains the final conclusions and possible future lines of research.

References

1. Bhide and Collins. 1989. Influence of axial tension on the shear capacity of reinforced concrete members. *ACI Structural Journal* 86(5): 570–581.
2. Collins, Bentz, Sherwood and Xie. 2008. An adequate theory for the shear strength of reinforced concrete structures. *Magazine of Concrete Research* 60(9): 635–650.
3. MacGregor and Wight. 2005. *Reinforced Concrete, Mechanics and Design*. Upper Saddle River: Pearson Prentice Hall.
4. Imam, Vandewalle, Mortelmans and V. Gemert. 1997. Shear domain of Fibre-Reinforced High-Strength Concrete Beams. *Engineering Structures* 19(9): 738–747.
5. Di-Prisco, Plizzari and Vandewalle. 2010. MC2010: Overview on the shear provisions for FRC. In *Shear and punching shear in RC and FRC elements*, vol. 57, ed. F. Minelli and G. Plizzari, 61–76. Italy: University of Brescia.
6. Kim, Lee, Hwang and Kuchma. 2012. Shear behavior model for steel fiber-reinforced concrete members without transverse reinforcements. *Composites: Part B* 43: 2324–2334.
7. Balázs. 2010. A historical review of shear. In *Shear and punching shear in RC and FRC elements*, vol. 57, ed. F. Minelli and G. Plizzari, fib-Bulletin 1–13. Italy: University of Brescia.
8. Bencardino, Rizzuti, Spadea and Swamy. 2010. Experimental evaluation of fiber reinforced concrete fracture properties. *Composites: Part B* 41: 17–24.
9. Minelli and Plizzari. 2013. On the Effectiveness of Steel Fibers as Shear Reinforcement. *ACI Structural Journal* 110(3): 379–390.
10. Minelli and Plizzari. 2010. Shear strength of FRC members with little or no shear reinforcement: a new analytical model. In *Shear and punching shear in RC and FRC elements*, vol. 57, ed. F. Minelli and G. Plizzari, 211–225. Italy: University of Brescia.
11. Cucchiara, La-Mendola and Papia. 2004. Effectiveness of stirrups and steel fibers as shear reinforcement. *Cement and Concrete Composites* 26(7): 777–786.

12. Susetyo and Vecchio. 2010. Effectiveness of steel fiber as minimum shear reinforcement: panel tests. In *Shear and punching shear in RC and FRC elements*, vol. 57, ed. F. Minelli and G. Plizzari, 227–241. Italy: University of Brescia.
13. Kovács and Balázs. 2003. Structural behavior of steel fiber reinforced concrete. *Journal of Structural Concrete*, pp 57–63.
14. Parra-Montesinos, Wight, Dinh and Cheng. 2010. Use of steel fiber reinforcement for shear resistance in beams and slab-column connections. In *Shear and punching shear in RC and FRC elements*, vol. 57, ed. F. Minelli and G. Plizzari, 243–262. Italy: University of Brescia.
15. RILEM-TC-162-TDF. 2003. Test and design methods for steel fibre reinforced concrete, Stress-strain design method. Final Recommendation 36: 560–567.
16. MC2010. 2012. Fib Bulletin 65–66. Model Code—final draft.
17. EC2. 2005. Eurocode 2: Design of concrete structures—EN 1992-1-1.
18. ACI.Committee.318. 2011. Building Code requirements for structural concrete (ACI 318-11), American Concrete Institute.
19. Parra-Montesinos. 2006. Shear strength of beams with deformed steel fibers. *Concrete International* 28(11): 57–66.
20. EHE-08. 2008. Instruccion de hormigon estructural EHE-08 (in Spanish), Madrid, Spain: Ministerio de Fomento.
21. Fib-Bulletin57, Shear and punching shear in RC and FRC elements, Salò, Italy, 2010.

Chapter 2

Objectives and Research Significance

2.1 Objectives

The main objective of this Ph.D. thesis is to study the different parameters affecting the shear behavior of concrete reinforced with steel fibers. It also aims to determine the influence of the different parameters involved and examine certain design Codes, with particular reference to the role of fiber reinforcement.

2.2 Specific Objectives

After a thorough study of the literature dealing with shear forces, the behavior of fiber reinforced concrete (FRC) beams was analyzed. Particular attention was devoted to the behavior of both precast elements and those made in situ in a number of experimental tests.

This Ph.D. thesis tries to provide answers to some issues that are still the subject of enquiry in the research community.

The specific objectives are the following:

- To conduct a review of the literature with particular attention to how the phenomenon has been analyzed in both traditional reinforced concrete and prestressed elements. An additional aim is to compile an extensive bibliographical database to facilitate consistent parametric analysis.
- To analyze the influence of fibers in the context of size in the form of the shear behavior of large concrete beams.
- To study the influence of flange size in prestressed double-T beams.
- To analyze the different shear responses obtained from concretes of different toughness by the use of different fiber content and geometry. For this, the shear behavior, failure modes and the validity of design formulas recommended by a number of building codes were analyzed.

- To analyze the shear behavior of Hollow Core Slabs made of fiber reinforced concrete, which is of great interest due to the difficulties involved in fitting transverse reinforcement in these elements.
- Analysis of an extensive database to verify the standards in Current Codes.

2.3 Final Considerations

Possible improvements of the current building codes was considered to be more important than proposing a new shear formula as Regan has pointed out [1]: “The most imposing analyses have often given excellent correlation with known results but failed miserably to predict behavior in untried circumstances. For simpler models the problem is mostly that of the need to neglect secondary factors, while what is secondary in one case may be primary in another. This is not to question the desirability of models, or of refined analysis at least as a research tool, but to point to the need for very careful verifications. It also points to the fact that significant improvements for design are very likely to be initiated by experimental observation”.

This thesis will therefore focus on a deeper understanding of the parameters that influence shear strength and try to identify any possible defects in existing design formulas.

On the other hand, “the use of steel fibers in concrete mixtures has not yet been fully utilized by the concrete industry for several reasons: steel fibers are often considered expensive and [2] the shear behavior of concrete containing steel fibers is still not fully understood. It is important to better understand and predict the shear behavior of SFRC for its wider applications in the concrete industry” [3].

Without any doubt Regan’s claim [1] invites us to reflect and leaves no-one indifferent: “Research on shear: a benefit to humanity or a waste of time?”

References

1. Regan, P.E. 1993. Research on shear: a benefit to humanity or a waste of time? *The Structural Engineer* 71(19): 337–347.
2. Chanh, N. 2004. Steel fiber reinforced concrete, 108–116. Vietnam: Faculty of Civil Engineering, Ho Chi Min City University of Technology.
3. Slater, E., Moni, M., and Alam, M.S. 2012. Predicting the shear strength of steel fiber reinforced concrete beams. *Construction and Building Materials* 26: 423–436.

Part II
State of the Art

Chapter 3

Literature Survey on Shear in FRC Beams

3.1 Introduction

This chapter appears as inspiration for the affirmation of Fenwick and Paulay in 1968: “An inquiring designer will not only want to know how to apply a safe design procedure, but also wish to see the reason why a particular structural member is likely to fail in a particular mode” [1].

Therefore, this chapter seeks to know in depth the shear behavior of structural concrete elements made of fiber reinforced concrete in order to understand the failure modes and to understand existing formulations of the Design Codes thus may be suggestions, suggest any amendments or even propose new methods of calculation that more faithfully reproduce the behavior of these elements. So, this chapter presents the state-of-the-art on the shear behavior of fiber reinforced concrete elements, complete and fully updated. Initially, the basic theory of shear will be explained; then, the shear behavior of concrete with and without transverse reinforcement, parameters influencing the shear behavior; Codes (formulas, comments and criticisms) and finally, the shear behavior of hollow core slabs.

3.2 On Steel Fiber Reinforced Concrete (SFRC)

3.2.1 Introduction About FRC

What is fiber-reinforced concrete (FRC)?

The Model Code 2010 [2] defines FRC as a “composite material characterized by a cement matrix and discrete fibers (discontinuous)”.

The matrix is made of either concrete or mortar. Fibers can be made of steel, polymers, carbon, glass or natural materials, although this PhD will be entirely focused in steel fibers.

Different FRC properties for structural applications can be obtained using different fibers materials. From the post-cracking residual strength of the composite, design constitutive laws are obtained [2].

For structural applications with normal and high-strength concrete the material classification is based on the post-cracking residual strength.

A minimum mechanical performance of FRC is needed for structural use. Fibers improve durability and the behavior at SLS because they reduce crack width and crack spacing. Fibers also improve ULS because they substitute partially or totally conventional reinforcement. Unless a high percentage of fibers is used, fibers do not change elastic properties nor compressive strength (Fig. 3.1), but they can modify mechanical properties [2].

In uniaxial tension, Fiber Reinforced Concretes (FRC) can show hardening or softening behavior depending of their composition (Fig. 3.2). Deformations are localized in one crack when FRC has a softening behavior (Fig. 3.2a). On the other hand, multiple cracking occurs before reaching the peak load in the case of hardening behavior (Fig. 3.2b).

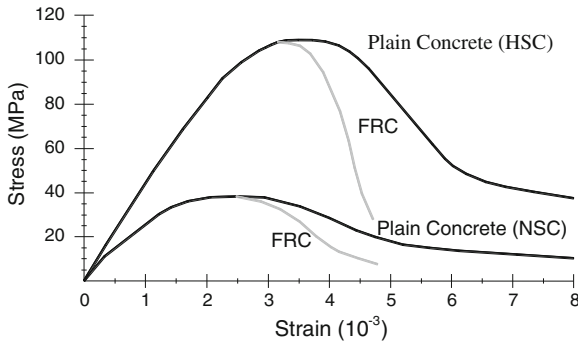


Fig. 3.1 Main differences between plain and fiber reinforced concrete having both normal and high strength under uniaxial compression [2]

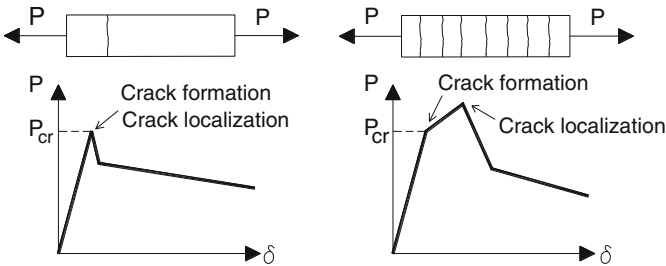


Fig. 3.2 Softening (a) and hardening (b) behavior in axial tension [2]

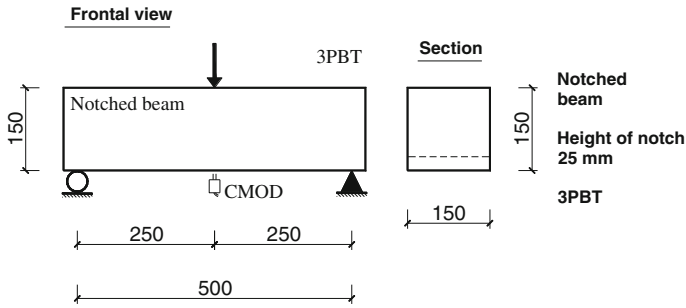
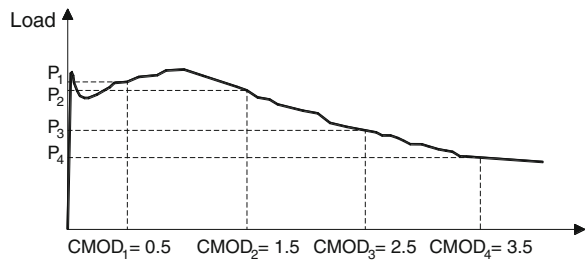


Fig. 3.3 Test set-up required by EN 14651 (dimensions in mm) [2]

Fig. 3.4 Typical load F-CMOD curve for FRC [2]



The test EN 14651 gives the guidelines to obtain the nominal values of the material properties by means of a 3 point bending test (Fig. 3.3). This test permits to obtain a curve Load-Crack Mouth Opening Displacement (CMOD), Fig. 3.4. The residual flexural tensile strength (f_{Rj}) for different values of $CMOD_j$, are evaluated as follows:

$$f_{R,j} = \frac{3F_j l}{2b h_{sp}^2} \tag{3.1}$$

where: f_{Rj} (MPa): residual flexural tensile strength corresponding to $CMOD = CMOD_j$; F_j (N): load corresponding to $CMOD = CMOD_j$; l (mm): is the span length; b (mm): specimen width; h_{sp} (mm): distance between the notch tip and the top of the specimen (125 mm).

3.2.2 Classification

In order to classify the post-cracking strength of FRC, a linear elastic behavior can be assumed by considering the characteristic residual strength significant for serviceability (f_{R1k}), and for ultimate conditions (f_{R3k}).

For structural use, the designer has to specify the residual strength class (f_{R1k}) and the ratio (f_{R3k}/f_{R1k}). Fiber reinforcement can substitute (also partially) conventional reinforcement (rebars) at ULS, if the following relationships are fulfilled:

$$f_{R1k}/f_{Lk} > 0.4 \quad (3.2)$$

$$f_{R3k}/f_{R1k} > 0.5. \quad (3.3)$$

3.2.3 Constitutive Laws

For the post-cracking behavior of FRC, a stress-crack opening law in uniaxial tension is defined. The rigid-plastic model takes the static equivalence into account (Fig. 3.5), where f_{Ftu} results from the assumption that the whole compressive force is concentrated in the top fiber of the section:

Two simplified stress-crack opening constitutive laws may be deduced from the bending test results: a plastic rigid behavior, or a linear post-cracking behavior (hardening or softening), Fig. 3.6, where f_{Fts} represents the residual strength

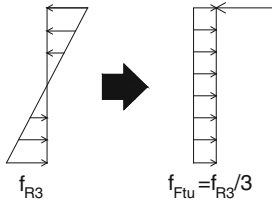
$$M_u = \frac{f_{R3} b h_{sp}^2}{6} = \frac{f_{Ftu} b h_{sp}^2}{2}$$


Fig. 3.5 Simplified model adopted to compute the ultimate tensile strength in uniaxial tension f_{Ftu} by means of the residual nominal bending strength f_{R3} [2]

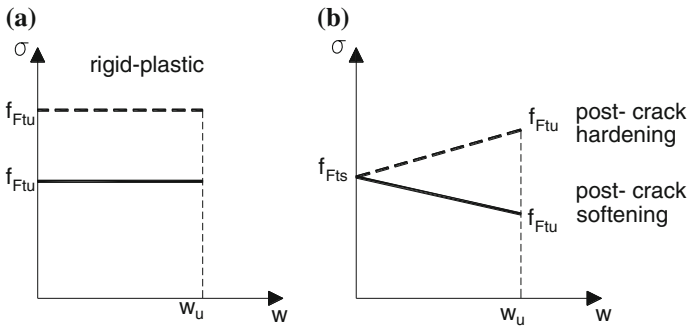
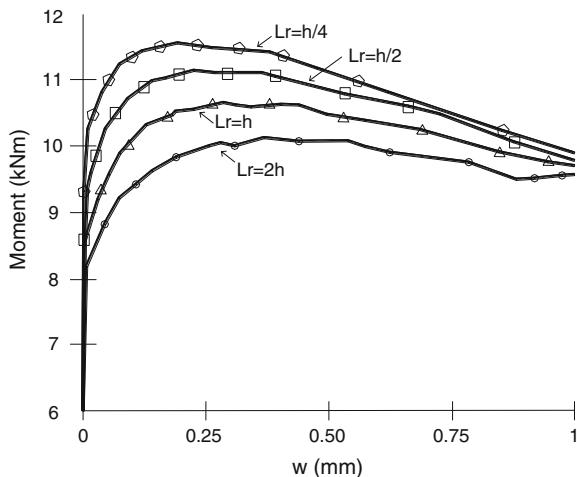


Fig. 3.6 Simplified post-cracking constitutive laws: stress-crack opening (*continuous and dashed lines* refer to softening and hardening post-cracking behavior respectively) [2]

Fig. 3.7 Influence of L_r on the flexural behavior of SFRC beam [49]



significant for serviceability crack openings and f_{Fu} represents the residual strength significant for ULS when assuming the rigid-plastic behavior (Fig. 3.7a), f_{Fu} equal to $f_{R3}/3$.

The stress-strain law is based on the identification of the crack width and on the corresponding structural *characteristic length*, l_{cs} , of the structural element for softening materials. The strain can be assumed as:

$$\varepsilon = w/l_{cs} \quad (3.4)$$

And, in elements with conventional reinforcement (rebars), l_{cs} , as:

$$l_{cs} = \min\{s_{rm}, y\} \quad (3.5)$$

where:

s_{rm} : mean distance value between cracks; y : distance between the neutral axis and the tensile side of the cross section, evaluated in the elastic cracked phase by neglecting the residual tensile strength of FRC, and for a load configuration corresponding to the serviceability state of crack opening and crack spacing.

3.2.4 Partial Safety Factors

Design values for the post-cracking strength parameter at ULS, according to the MC2010 [2], can be determined as:

Table 3.1 Partial safety factor [2]

Material	Partial safety factors
FRC in compression	As plain concrete
FRC in tension (limit of linearity)	As plain concrete
FRC in tension (residual strength)	$\gamma_F = 1.5$

$$f_{Ftsd} = f_{Ftsk} / \gamma_F \quad (3.6)$$

$$f_{Ftud} = f_{Ftuk} / \gamma_F \quad (3.7)$$

The recommended values for the partial safety factors are given in Table 3.1. For serviceability limit states (SLS), the partial factors should be taken as 1.0.

3.3 Fibers Effects on Shear Behavior

3.3.1 Fibers Concept

Fibers can be considered as reinforcement spread out all over the depth of a structural element [3].

3.3.2 Effect of Fibers on Shear Strength and Stiffness

Steel fibers increase the shear strength [4, 5] and the load corresponding to the first crack [4].

The effectiveness of fibers to increase shear strength is dependent on several factors related to: matrix properties, fiber properties (materials properties, aspect ratio, and shape), fiber content, and bond stress versus slip response of fibers [6].

In 1987, Narayanan and Darwish [7] claimed that ultimate shear strength increased in higher rates when higher values of fiber aspect ratio were used but, using higher fiber content resulted in little improvement in shear strengths. On the other hand, other authors claimed the opposite. In fact, other authors like di-Prisco et al. [8], Lim et al. [9], Oh et al. [10] and Conforti [11] found that the shear strength of concrete beams could be increased significantly even incorporating low amounts of steel fibers. Conforti [11] also ensured that fibers can alter the mode of failure of the structural elements from shear to flexure enhancing ductility and bearing capacity.

Other authors link the increase of shear strength to the volume of fibers. Greenough and Nehdi [12] ensured that a volume of steel fibers equal to 1 % can increase shear capacity up to 128 % with respect of reference beams, on the other hand, Dinh et al. [6] ensured that beyond volumes of 1 % the increase in shear

strength is relatively small. Majdzadeh et al. [13] affirmed that a volume of 1 % is optimal and no benefits are detected with volumes beyond 1 % [13]. By contrast, Oh et al. [10] ensured that the increase was approximately 100 % from volumes between 0 and 2 %.

Furthermore, fiber reinforcement enhanced the shear capacity of RC beams, but a fiber volume fraction of 1 % is seen as optimal; in fact, no benefits were noted when the fiber volume fraction was increase beyond 1 % [13]. The increase of the shear strength was about 100 % when the fiber content was increased from 0 to 2 % [10]; the use of hooked steel fibers in a volume fraction greater than 0.75 % led to an enhanced inclined cracking pattern (multiple cracks) and improved shear strength in beams (without stirrup reinforcement), of $0.33 \cdot \sqrt{f_c}$ (MPa). The increase in shear strength was associated with an increase in fiber content beyond 1 % by volume, however, it was relatively small [6]; the maximum increase of shear strength at first crack in fully prestressed beams due to the addition of fibers was 5, 10 and 20 % for the volume fraction of fiber of 0.5, 1.0, and 1.5 %, respectively. In the case of partially prestressed beam specimens, the increase of peak load due to addition of fibers was found to be 12 and 17.5 % for partially prestressed beams with fiber content of 1.0 and 1.5 %, respectively [14]. The addition of fiber reinforcement in full depth for partially prestressed concrete beams improved the shear-resisting capacity by approximately 11–20 % when compared with the corresponding control beams not containing fibers. The maximum benefit due to the addition of fibers was observed for high-strength prestressed concrete beams. The increase in the shear capacity due to the presence of fiber reinforcement only in the web portion, when compared with the control beams, was found to be 6, 9, and 14 % for normal, moderately high strength, and high strength concrete beams, respectively. Hence, the addition of fibers only in the web portion of the T-beam is recommended for enhancing the shear capacity of the prestressed concrete beam [15].

As far as the beam stiffness is concerned, the presence of fiber reinforcement delays and controls dowel cracking and, thereby, improves the stiffness and deformation characteristics of the dowel crack zone. The first shear-crack load forms and ultimate dowel strength are both found to increase almost linearly with the flexural strength of the composite. The inclusion of steel fibers in concrete deep beams resulted in enhanced stiffness and increased spall resistance at all stages of loading up to failure; fibers also reduced crack width [16].

3.3.3 Effect of Fibers on Ductility (Postcracking Response)

Fibers increase ductility in FRC beams versus beams without fibers [4, 7, 14, 17–23]; also, the increase in ductility of concrete in compression is due to fiber addition depends, among other factors: amount, geometry, orientation, strength of the steel fibers, bond between fibers and concrete [24] and post-cracking strength because of fibers addition [8, 18, 19, 25, 26]. In order to get a ductile post-peak behavior, fibers having a higher aspect ratio are required [20].

Experimental tests showed that beams made with FRC with a volume of fibers equal to 0.64 % had similar or even better postcracking behavior than beams with minimum amount of transverse reinforcement [27].

3.3.4 Effect of Fibers on Shear Cracking

Fibers are very effecting containing the dowel crack growth by means of the crack arrester controlling the propagation and widening of the dowel crack [6, 7, 16, 19, 21, 22, 28–32]. The aggregate interlock increases due to the reduction of crack spacing and widths providing a better durability of the structure [6, 19].

Structural elements made with high concrete compressive strength had smaller crack widths due to denser concrete matrix, better bond to the fibers and also due to the load transfer across the cracks [4]. The stabilization of the action of the fibers takes place at ULS with values close to a crack width of 1.2–1.4 mm [33].

3.3.5 Effect of Fibers on Yielding of Longitudinal Bars

Fibers increase the load level at which the longitudinal reinforcement yields [4]; therefore, the load bearing capacity of tensile members and bending beams increase with the presence of fibers [24].

3.3.6 Effect of Fibers on Cracking Distribution

Increased fiber volumes allow the development of multiple cracking, distributed and complex in the shear span [4, 5, 11, 32, 34–40] avoiding or delaying the localization of a major shear-critical crack responsible of a brittle collapse [3, 9, 11, 17]. The multiple cracking produces a redistribution of stresses [31, 41] giving visible warning prior the collapse of the structure [11, 32].

Steel fibers became effective after formation of shear crack and resist the principal tensile stressed until the complete pullout or yielding of fibers occurs at one critical crack [41]. After the occurrence of the first crack, fibers start working, carry the entire applied load and tend to avoid the localization of microcracks in macrocracks. Consequently, the post-cracking strength increases and a considerable ductility can be achieved due to the ability of the fibers to bridge and carry the stresses crossing the crack faces [18, 20].

3.3.7 Effect of Fibers on Rotation Capacity

The specimens without fibers had a larger rotation capacity than those with fibers. This decrease in deformation capacity is explained by localization of the deformations in one large crack in case of the FRC specimens due to the higher bond between rebars and concrete [24].

3.3.8 Effect of Fibers on Tensile Properties

Steel fibers enhance: the tensile properties of concrete, the resistance to cracking, the pull-out resistance of tension reinforcement [9, 21]. And the ultimate tensile strength [42].

Fiber reinforcement enhances shear resistance by transferring tensile stresses across diagonal cracks [6]. Fibers improve the resistance of tensile cracks both in the web and in the tension zone [31].

3.3.9 Effect of Fibers on Crack Spacing

Fibers reduce crack spacing and widths giving place to a redistribution of stresses, consequently, aggregate interlock is increased giving to FRC beams more stiffness and a high load carrying capacity [6–8, 16–29, 41].

3.3.10 Effect of Fibers on Tension Stiffening

While plain concrete is assumed to carry tension between the cracks only, FRC is able to carry significant tensile forces at a crack. Tension stiffening reflects the ability of concrete to carry tension between cracks, which increase member stiffness before the reinforcement yields [43]. Tension stiffening in FRC depends on the behavior between cracks and, at the cracks [44, 45]. Tension stiffening improves crack control and permits the use of higher-strength reinforcing steels while still maintaining control of crack widths [46] provides an additional strength after yielding of the reinforcement [47], depending on the type and amount of fibers used.

Results from tension-stiffening tests can be used to determine the average tensile strength carried by the cracked FRC, representing behavior between the cracks of a reinforced concrete member [48].

3.3.11 Effect of Fibers on Characteristic Length (L_r)

The characteristic length (L_r) is the key parameter linking strains (ϵ) and crack opening (w), [49]. In an analytical model, L_r is an indication of the crack spacing considered in calculations. L_r is influenced by several parameters: type and volume of fibers, matrix strength, cross-section geometry, presence of conventional reinforcement (longitudinal or transverse), load level (service, ultimate), etc., therefore no consensus has yet been achieved to determine it.

Figure 3.7 shows the influence of L_r on a member response, where L_r varies from $h/4$ to $2h$ for a 150 mm deep and 400 mm wide SFRC beam. The parametric analysis done by De-Montaignac et al. [49] showed that increasing L_r reduces the bending strength and thus estimates wider cracks for a given bending moment. De-Montaignac et al. [49] ensured that it is more conservative to adopt a larger L_r for predicting crack width in service conditions or for predicting ultimate strength [49].

For FRC members, some researchers have proposed the utilization of a constant value for L_r (Table 3.2) while other researchers suggest that this value should vary depending on load.

De-Montaignac et al. [49] concluded that:

Fibers in a high amount (0.75–1.25 %) confers to concrete a better structural behavior, proving a hardening behavior in bending, limiting crack opening in SLS and giving a ductile behavior in ULS [49].

If the structural behavior is governed by the maximum crack width the use of a single value of L_r in a section analysis gives good correlation with experimental values [49].

De-Montaignac et al. [49] recommends the use of $L_r = 2h$ for FRC members without conventional reinforcement and $L_r = \min(h, s_m)$ for members with conventional reinforcement [49].

Table 3.2 Proposed values for L_r [49]

Reinforcement	Past studies for deflection, average curvature and crack width		This study for maximum crack width
	Rule	References	
SFRC	$h/2$	RILEM [77], Massicotte [117], Uitkjaer et al. [118], Kooiman [119], Iyengar et al. [120], Pedersen [121]	$2h$
	$2h/3$	AFGC [122]	
	h	<i>fib</i> [2], CNR [123]	
	$2h$	Strack [124]	
SFRC and reinforcing bars	$\text{Min } [s_m; h/2]^a$	Massicotte [117]	$\text{Min } [s_m; h]^d$
	$\text{Min } [s_m; y]^a$	<i>fib</i> [2], CNR [123]	

^a s_m is estimated with the Eurocode 2 [125]

3.4 Steel Fibers as Shear Reinforcement

In the literature, it is shown that FRC can substitute, at least partially, transverse reinforcement. For this reason, some authors emphasize the usefulness of fibers for industrial applications.

3.4.1 Fibers as Minimum Shear Reinforcement

The minimum transverse reinforcement requirement can be met by using fibers in sufficient amount and with minimum performance in terms of toughness [3, 32, 50].

Fibers can replace the minimum amount of transverse reinforcement satisfying the minimum shear reinforcement criteria in ACI 318-11 [32, 51, 52] and other Codes for precast high performance concrete structures [53].

According to ACI 318-11 [52], a minimum V_f of 0.75 % is recommended [6, 54]. On the other hand, the beams reinforced only with steel fibers ($V_f = 0.64$ %) show a similar, or even better, post-cracking behavior than the beams with the minimum amount of transverse reinforcement [27].

According to the *fib* Model Code 2010 [2], it is possible to prevent the use of the minimum amount of conventional shear reinforcement (stirrups) if the following condition is fulfilled:

$$f_{Fruk} \geq \frac{\sqrt{f_{ck}}}{20} \quad (3.8)$$

where f_{Fruk} (MPa) is the characteristic value of the ultimate residual tensile strength for FRC, by considering $w_u = 1.5$ mm. This allows limiting the development and the diffusion of the inclined cracking and, as a consequence, can ensure sufficient member ductility.

3.4.2 Fibers Totally Replacing Stirrups

Fibers clearly acted as shear reinforcement [19, 28, 55, 56] and they can be used to replace stirrups in beams without reduction of the moment capacity [57]; in precast pretensioned beams [58], the use of FRC can significantly reduce production costs [27] since handling and placing of reinforcement [53] are no longer required.

From a practical point of view, steel fibers can successfully replace the shear reinforcement, but it is senseless to use steel fibers as a complementary reinforcement of longitudinal bars [55].

3.4.3 Fibers Partially Replacing Stirrups

Shear reinforcement can be substituted partially or totally with steel fibers [15, 53]. Anyway, the use of fiber reinforcement can reduce the amount of shear stirrups required [9, 10], even though this substitution may not be attractive from a practical point of view.

3.4.4 Shear Crack Pattern in FRC Elements

The pattern of cracks developed in FRC beams subjected to shear was similar to those observed in reinforced concrete beams with minimum amount of stirrups [7], when FRC satisfies the minimum performance requirements [57], reaching the maximum flexure capacity [59]; therefore, fibers represent an effective shear reinforcement [28].

3.5 Failures Modes

3.5.1 Can Fibers Alter the Collapse from Shear to Flexure?

The inclusion of fibers can modify the brittle shear mechanism into a ductile flexural mechanism, thus allowing a larger dissipation of energy [39] and a significant increase of ductility and load-bearing capacity [11, 53]. Therefore catastrophic failures are avoided when using FRC.

This change of shear failure due to fibers was analyzed by different authors [7, 11, 25, 28, 39, 53, 57, 60, 61].

Some authors assert this change in failure mode type, depending on the fiber content:

Normal-strength concrete beams changed the failure mode from shear to flexure with a volume fraction of 2 % of fibers, while high-strength concrete beams were subjected to a bending failure (no shear failure) with a volume fraction of about 1.5 % of fibers. Furthermore, normal-strength concrete involved a large increase of shear resistance up to 1 % of fibers, whereas most increase occurred at 0.5 % of fibers in high-strength concrete [62]. However, as mentioned above, the key-parameter is FRC performance expressed in terms of post-cracking residual strength.

Narayanan and Darwish [7] and, Lim and Oh [9, 10] ensured that beyond an amount of 1 % the mode of failure change from shear to flexure, but Narayanan highlighted that beyond a volume fraction of 1 % the improvement on shear strength is very little. By contrast, according to some authors, due to the high

flexural capacity of the beams, steel fibers alone could not change the modes of failure to the flexural type; while the use of steel fibers in combination with stirrups can change the mode of failure to shear-flexure type [63, 64].

3.5.2 Ductile Failure Mode Due to Fibers

Steel fibers can make the failure mode more ductile especially in high-strength concrete beams due to the material brittleness [14, 18, 41].

In shear critical beams having stirrups, with or without fibers, or in beams having fibers only in the shear span but without stirrups, the mode of failure was altered from one of brittle shear to one of ductile flexure in both fully and partially pre-stressed beams [14].

Especially for larger values of a/d , steel fibers can transform the mode of failure into a ductile one [65].

3.5.3 Influence of Fibers in Compression Zone

While the primary flexure-shear crack in FRC beam has an angle close to that of PC beams, it deviated from the original path much earlier than the one in PC beams. This is due to the fact that higher stresses were required for the crack propagation in FRC beam. This premature deviation of primary flexure-shear crack led to a much larger compression zone in FRC beam, moving the arch action as the primary shear transfer mechanism. The larger compression zone, together with the higher compressive strains at failure of FRC materials [66, 67], led to a concrete arch with greater strength and ductility under compression. In some cases, it can be clearly seen that shear failure was not caused by the primary flexure-shear crack. Contrary to PC beam, it was found that FRC beam exhibited much ductile behavior at the crushed compression zone [68].

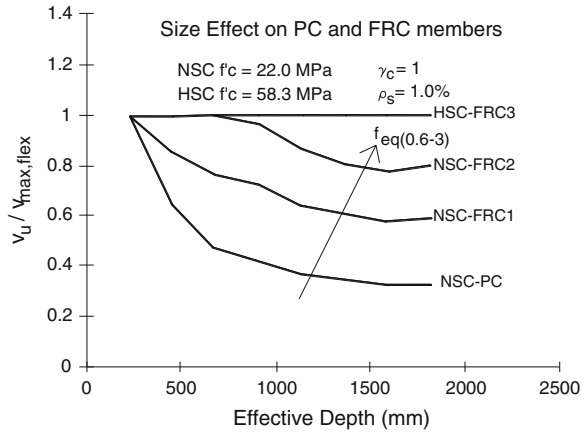
The addition of steel fibers did not prevent longitudinal crack formation in the compressive zone in case of compressive failure, but it prevented concrete spalling [24].

3.6 Fibers Influence on Size Effect

3.6.1 Influence of Depth in Shear Strength

Size effect is a key factor to take into account on shear capacity. The larger the structure, the greater is the energy release and more fracture energy is needed to avoid a sudden failure [20].

Fig. 3.8 Size effect in FRC beams without stirrups. *Lines* mean numerical analysis results and *single points* are experimental results [32]



Fibers could reduce or even eliminate the shear size effect in beams without transverse reinforcement due to the reduction in crack spacing producing the decrease of shear strength as the beam depth increases [6].

The minimum quantity of fibers to be used as minimum reinforcement increases when the size of the structural member also increases [69]. A numerical study with the software VecTor2 evidence that the decreasing of the ultimate shear stress is lower with the increase in toughness provided by fibers (see Fig. 3.8). Size effect can be mitigated or even eliminated providing sufficient amount of steel fibers [32].

When beam size increases is preferred the use of longer fibers due to their better anchorage to the concrete. This fact allows carrying the residual strength for longer crack openings.

Gustafsson and Noghabai [20] found from their tests that the failures of small beams were considerably more ductile than large beams.

The larger the structure, the greater is the energy release and the more fracture energy is needed to avoid a sudden failure. Earlier studies [70, 71] have shown that the brittleness of a beam loaded in shear is proportional to the effective depth, d . The larger the beam the greater amounts of strain energy is stored in the structure. When the tensile strength is exceeded and a critical diagonal crack is created (Fig. 3.9), the residual tensile stresses acting across the crack have to resist the impulse load that is connected to the energy release. The requirements on the tensile properties of the fibers concrete will increase as the beam size increases [20].

3.6.2 Influence of Depth on the Shear Crack Width

Steel fibers in concrete deep beams enhance stiffness, increase spall resistance at all stages of loading up to failure, and reduce crack widths [16].

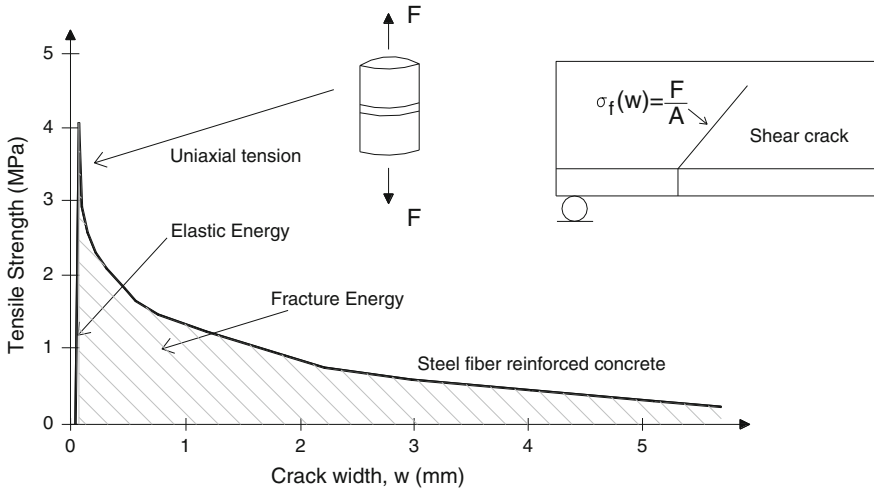


Fig. 3.9 Comparison of stress-strain relationship for plain and fiber reinforced concrete in tension. Also, some fracture mechanical properties are shown. G_E equals the stored energy per unit area and G_f is the fracture energy per unit area [20]

For large beams better tensile properties are needed than for small beams. Also, larger fibers with high strength are required for large beams than for small ones to have a proper anchorage into the concrete [20].

3.7 Fibers Influence on Serviceability Limit State (SLS) and Durability

Tension stiffening effects are useful for assessing postcracking behavior at service loads [44].

Steel fibers improve the SLS and the structural durability, because post-crack stiffness increases with the formation of closer cracks with smaller crack width [17, 19, 24, 27].

3.8 Reduction of Production Cost

Fibers give very interesting solutions. They facilitate the industrialization of the production and improve the durability of the products. Fibers give the possibility of substitute stirrups and, this fact can reduce production costs due to the fact that it is not needed to place stirrups [27, 53, 59].

3.9 Combination of Steel Fibers and Stirrups

The addition of fibers to conventional stirrups leads to the following effects:

Crack spacing: Cracks are less separated due to the presence of fibers. As a consequence, a smaller characteristic length (L_r) should be used [49].

Shear strength: Steel fibers improve the shear resisting mechanism of the concrete represented by the aggregate interlocking and dowel action so, the shear strength significantly increases [27, 29, 63]. Fibers can also be combined with stirrups, in this situation, the stresses in the stirrups are reduced [29].

Crack control: Fibers control the cracking process alone or in combination with stirrups [62, 72].

Stresses in stirrups and fibers: Fibers retarded the appearance of inclined cracks and, consequently, the stirrups are tensioned later [34]. At the same time, when stirrups and fibers work together, a further reduction in the working stress of fibers can be observed [34, 39, 61, 73, 74]. Other benefit of the combinations of fibers and stirrups is that fiber can reduce the amount of stirrups required satisfying strength and ductility requirements [9].

3.10 Shear Models and Design Codes

3.10.1 Design Codes

The current Design Codes to determine shear strength of structural elements made with FRC are basically, the RILEM approach [75] and the MC2010 [2]. RILEM has evolved, having presented different versions up to the current formulation. Firstly, RILEM approaches used equivalent flexural tensile strengths up to the current version which uses residual flexural tensile strengths according to the Standard EN 14651.

3.10.1.1 Previous Versions of RILEM Approach

Original RILEM Design Method

The original RILEM design method [74, 76] calculated the shear capacity (V) as consisting of 3 separate contributions:

$$V = V_c + V_s + V_f \quad (3.9)$$

where:

- V_c shear resistance of the member without shear reinforcement
- V_s contribution of the shear reinforcement (stirrups and/or inclined bars)
- V_f contribution of steel fiber shear reinforcement.

The first term, V_c , is calculated in the same way as in EC2 defined as:

$$V_c = 0.12 \cdot \xi \cdot (100 \cdot \rho_l \cdot f_{ck})^{1/3} \cdot b \cdot d \quad (3.10)$$

with: f_{ck} = characteristic cylinder compressive strength; b = width of the beam; d = effective depth of the beam; A_{sl} = tensile reinforcement in the critical section; ξ = size factor = $200d \leq 2$; ρ_l = tensile reinforcement ratio = $\frac{A_s}{b \cdot d} \leq 0.02$.

The second term, V_s , was also identical as in EC2 (assuming $\theta = 45^\circ$):

$$V_s = \frac{A_{sw}}{s} \cdot 0.9 \cdot d \cdot f_{ywd} \quad (3.11)$$

where:

f_{ywd} design value of the yield strength of the stirrups

$$\frac{A_{sw}}{s} = \frac{\text{Area of stirrups}}{\text{spacing between stirrups}} \quad (3.12)$$

The third term takes into account the contribution of the steel fibers (V_f) and it is determined as:

$$V_f = k_f \cdot k_l \cdot \tau_{fd} \cdot b \cdot d \quad (3.13)$$

with:

k_f factor to take into account the contribution of the flanges in a T-section. For rectangular sections: $k_f = 1$

k_l factor to take into account the size effect of the element = $\frac{(1600-d)}{1000} \geq 1$

$$\tau_{fd} = 0.12 \cdot f_{eq,3} \quad (3.14)$$

RILEM2 Design Method

In the next RILEM version (*RILEM2 design method* [74, 75]), Eqs. 3.9 and 3.13 remained unchanged compared with the previous version (showed in Sect. [Original RILEM Design Method](#)), in Eq. 3.10 the factor 0.12 took into account the influence of the shear span to depth ratio. By taking this factor constant, it is possible to make the shear as a problem for section design rather than for structural design. The factor is replaced by its original formula:

$$0.15 \sqrt[3]{3 \cdot d/a} \quad (3.15)$$

Also, the average value of the cylinder compressive strength is used instead of the characteristic one. As results Eq. 3.10 becomes:

$$V_c = 0.15 \sqrt[3]{3 \cdot \frac{d}{a} \cdot \xi \cdot (100 \cdot \rho_i \cdot f_{cm})^{1/3}} b \cdot d \quad (3.16)$$

where: a = shear span; f_{cm} = average cylinder compressive strength.

In Eq. 3.11; only the design value of the yield strength of the stirrups (f_{ywd}) is changed into the average yield strength (f_{ywm}), giving:

$$V_s = \frac{A_{sw}}{s} \cdot 0.9 \cdot d \cdot f_{ywm} \quad (3.17)$$

In Eq. 3.14, the parameter 0.12 was originally derived from the following formula:

$$\tau_{fd} = \frac{d/a \cdot 0.5 \cdot \frac{f_{eqk,3}}{0.7}}{\gamma_c} \quad (3.18)$$

where:

- $f_{eqk,3}$ characteristic equivalent flexural tensile strength;
- 0.5 factor to convert the flexural tensile strength into the axial tensile strength;
- 0.7 factor to convert the characteristic equivalent flexural tensile strength into the average equivalent flexural tensile strength;
- γ_c partial safety factor equal to 1.5 to obtain the design value of the shear resistance τ_{fd} .

Since the average flexural tensile strength is used, the factor 0.7 may be omitted. Also the partial safety coefficient (γ_c) will be left out in order to get a “real ultimate steel fiber contribution”. The Eq. 3.13 results:

$$V_f = k_f \cdot k_1 \cdot 0.5 \cdot \frac{d}{a} \cdot f_{eqm,3} \cdot b \cdot d \quad (3.19)$$

Material Parameter: Equivalent or Residual Flexural Tensile Strength

The main material parameters for the design of FRC elements in RILEM guidelines [76] were the equivalent flexural tensile strength $f_{eq,2}$ and $f_{eq,3}$. The related strain to the value $f_{eq,3}$ was 10 ‰. These parameters are replaced in the Final Draft [77] by the residual flexural tensile strength $f_{R,i}$. The equivalent flexural tensile strength is derived from the contribution of the steel fibers to the energy absorption capacity (area under the load-deflection curve) while the residual flexural tensile strength is derived from the load at a specified Crack Mouth Opening Displacement (CMOD) or midspan deflection (Fig. 3.10). The value which is used for the ULS is $f_{Rk,4}$ (CMOD = 3.5 mm) which is related to the strain of 25 ‰ [51].

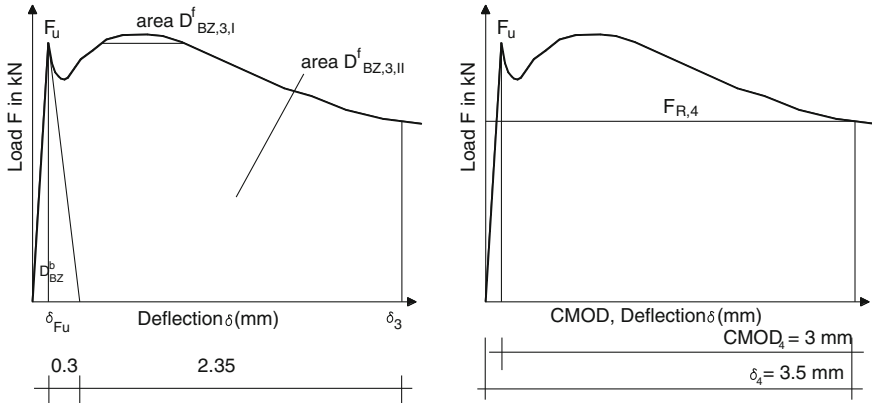


Fig. 3.10 Equivalent flexural tensile strength (*left*) and residual flexural tensile strength (*right*), [75]

where:

$$f_{eq,3} = \frac{3}{2} \left(\frac{D_{BZ,3,I}^f}{2.65} + \frac{D_{BZ,3,II}^f}{2.5} \right) \frac{L}{bh_{sp}^2}$$

$$f_{R,4} = \frac{(3F_{R,4}L)}{(2bh_{sp}^2)}$$

Due to the change from the equivalent to the residual flexural tensile strength, it might be necessary to tune the design formulas. The relation between $f_{eq,I}$ and $f_{R,I}$ for the fibers used within the Brite/Euram project is shown in Fig. 3.11. For shear design $f_{eq,3}$ replaced by $f_{R,4}$, by considering a factor $1/0.87$. The relation shown in Fig. 3.11 depends on the post-cracking behavior of the FRC.

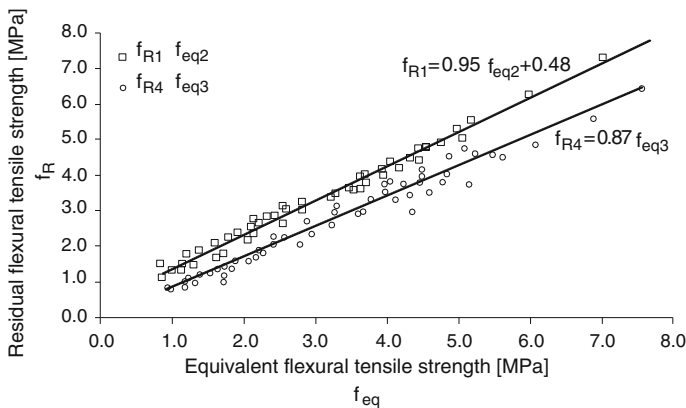


Fig. 3.11 Relation between equivalent flexural tensile strength and residual flexural tensile strength for the fibers used within the Brite/Euram project [75, 94]

3.10.1.2 RILEM Current Version 2003

The formulation to calculate shear strength in beams made with FRC according to the current version of RILEM (2003) [77] is:

$$V = V_c + V_s + V_f \quad (3.20)$$

$$V_c = \left[0.12 \cdot \xi \cdot (100 \cdot \rho_l \cdot f_{ck})^{1/3} + 0.15 \cdot \sigma_c \right] b \cdot d \quad (3.21)$$

In the case of prestressing “ h ” should be used instead of “ d ” in formula (Eq. 3.21) with:

$$\begin{aligned} \xi &= \sqrt{\frac{200}{d}} \leq 2 \\ \rho_l &= \frac{A_s}{bd} \leq 0.02 \\ \sigma_c &= \frac{N_{sd}}{A_c} \leq 0.02 \end{aligned}$$

The second term, V_s , is also identical as in Eurocode 2 (assuming $\theta = 45^\circ$)

$$V_s = \frac{A_{sw}}{s} \cdot 0.9 \cdot d \cdot f_{ywd} (1 + \cot \alpha) \cdot \sin \alpha \quad (3.22)$$

$$V_f = 0.7 \cdot k_f \cdot \xi \cdot \tau_{fd} \cdot b \cdot d \quad (3.23)$$

with:

$$\tau_{fd} = 0.12 \cdot f_{R,4} \quad (3.24)$$

τ_{fd} design value of the increase in shear strength due to steel fibers;
 k_f factor for taking into account the contribution of the flanges in a T-section:

$$\begin{aligned} k_f &= 1 + n \left(\frac{h_f}{b_w} \right) \left(\frac{h_f}{d} \right); \quad k_f \leq 1.5 \\ n &= \frac{b_f - b_w}{h_f} \leq 3; \quad n \leq \frac{3b_w}{h_f} \end{aligned}$$

with:

h_f height of the flanges;
 b_f width of the flanges;

- b_w width of the web;
 α angle of the shear reinforcement in relation to the longitudinal axis ($45^\circ \leq \alpha \leq 90^\circ$);
 θ angle of the concrete struts in relation to the longitudinal axis.

3.10.1.3 EHE-08, 14th Appendix

The 14th Appendix: “*Recommendations for the use of FRC*” of the EHE-08 [78] includes all matters concerning the FRC. This Appendix is comprised of the following parts: bases of the project, structural analysis, technological materials properties, durability, calculation, execution and control of the FRC. The design shear resistance (V_{u2}) has the following structure:

$$V_{u2} = V_{cu} + V_{fu} + V_{su} \quad (3.25)$$

The design shear resistance attributed to concrete (V_{cu}) and the design shear resistance provided by shear reinforcement (V_{su}) are both calculated in the same manner as concrete without fibers.

The design shear resistance attributed to fibers (V_{fu}) is calculated with a formulation based on RILEM approach. The only difference is the way to calculate the calculating value of the increased shear strength due to the fibers (τ_{fd}), taking the value in the EHE-08:

$$\tau_{fd} = 0.5 \cdot f_{ctR,d} \quad (3.26)$$

with: $f_{ctR,d} = 0.33 \cdot f_{R3,d}$ if a rectangular calculation diagram is assumed.

So, finally, the design shear resistance attributed to fibers (V_{fu}) is calculated with the following expression:

$$V_{fu} = 0.7 \cdot \xi \cdot \tau_{fd} \cdot b_0 \cdot d \quad (3.27)$$

where: ξ factor that takes into account the size effect: $\xi = 1 + \sqrt{(200/d)} \leq 2.0$; b_0 web width and d effective depth.

3.10.1.4 MC2010 Formulation for FRC According to the Final Draft [2]

Since FRC is a concrete having an enhanced toughness, the fiber contribution should be included within the concrete contribution (and not as a separate fiber shear contribution). That conclusion is based on the experiments and on the numerical evidence, which demonstrates the ability of simulating FRC structures by just adopting a proper tension softening model [53]. So, an equation for shear strength of FRC without transverse reinforcement [79] was proposed and then, it

was incorporated in the *Final Draft of the Model Code 2010* [2]. It includes the shear contribution of fibers as an enhancement of the concrete contribution by modifying the longitudinal reinforcement ratio considered by EC2. As it increases, the longitudinal reinforcement limits the growth of shear-critical crack, allowing a greater transfer of stresses (whether tensile or shear). The proposed equation is based on FRC performance (residual post-cracking strength), which is the more significant index for FRC structural design. It can be easily applied and transferred into practice [50].

The formula of MC2010 for FRC is based on the results obtained in the Ph.D. thesis of Minelli [79]:

$$V_c = \left[\frac{0.18}{\gamma_c} \xi \cdot \left(100\rho_l \cdot \left(1 + 7.5 \cdot \frac{f_{Fruk}}{f_{ctk}} \right) \cdot f_{ck} \right)^{1/3} + 0.15\sigma_{cp} \right] b_w d \quad (3.28)$$

where:

γ_c	is the partial safety factor for the concrete without fibers;
ξ	is a factor that takes into account the size effect and it is equal to: $\xi = \sqrt{\frac{200}{d}} \leq 2$
d (mm)	is the effective depth of the cross-section;
ρ_l	is the reinforcement ratio for longitudinal reinforcement equal to: $\rho_l = \frac{A_s}{b d} \leq 0.02$;
A_{sl} (mm ²)	is the cross-sectional area of the reinforcement which extends $\geq l_{bd} + d$ beyond the considered section;
f_{Fruk} (MPa)	is the characteristic value of the ultimate residual tensile strength for FRC, by considering $w_u = 1.5$ mm;
f_{ctk} (MPa)	is the characteristic value of the tensile strength for the concrete matrix;
f_{ck} (MPa)	is the characteristic value of cylindrical compressive strength;
$\sigma_{cp} = N_{Ed}/A_c < 0.2 \cdot f_{cd}$ (MPa)	is the average stress acting on the concrete cross-section, A_c (mm ²), for an axial force N_{Ed} (N), due to loading or prestressing actions ($N_{Ed} > 0$ for compression);
b_w (mm)	is the smallest width of the cross-section in the tensile area.

The shear resistance, $V_{Rd,F}$, is assumed to be not smaller than the minimum value, $V_{Rd,Fmin}$, defined as:

$$V_{Rd,Fmin} = (v_{min} + 0.15 \cdot \sigma_{cp}) \cdot b_w \cdot d \quad (3.29)$$

where: $v_{min} = 0.035 \cdot k^{3/2} \cdot f_{ck}^{1/2}$

On the other hand, in the recent Final Draft [2] a recent model computes the term V_{RdF} as follows:

$$V_{Rd,F} = \frac{1}{\gamma_F} \left(k_v \sqrt{f_{ck}} + k_f f_{Ftuk} \cot \theta \right) z b_w \quad (3.30)$$

where f_{Ftuk} is the characteristic value of the ultimate tensile strength for FRC, as determined by direct tensile tests, taken at the crack width at ultimate, w_u ; $k_f = 0.8$:

$$k_v = \frac{0.4}{1 + 1500\varepsilon_x} \cdot \frac{1300}{1000 + k_{dg}z} \quad \text{for } \rho_w < 0.08 \sqrt{f_{ck}/f_{yk}} \quad (3.31)$$

$$k_v = \frac{0.4}{1 + 1500\varepsilon_x} \quad \text{for } \rho_w \geq 0.08 \sqrt{f_{ck}/f_{yk}} \rho_w$$

In Eq. 3.31, ε_x is the longitudinal strain at the mid-depth of the effective shear depth, as determined by the same expressions for concrete without fibers; z is the internal lever arm (in mm) between the flexural tensile and compressive forces and k_{dg} is an aggregate size influence parameter.

The aggregate size influence parameter in Eq. 3.31, k_{dg} , is given by:

$$k_{dg} = \frac{32}{16 + d_g} \geq 0.75 \quad (3.32)$$

where d_g is the maximum aggregate size in mm. If the size of the maximum aggregate particles is not less than 16 mm, this parameter may be taken as $k_{dg} = 1.0$.

The limits of the angle of the compressive stress field, θ , relative to the longitudinal axis of the member are:

$$\theta_{min} \leq \theta \leq 45^\circ \quad (3.33)$$

where the minimum inclination angle is:

$$\theta_{min} = 29^\circ + 7000\varepsilon_x \quad (3.34)$$

For the determination of where f_{Ftuk} , the crack width at ultimate (w_u) is taken as:

$$w_u = 0.2 + 1000 \cdot \varepsilon_x \geq 0.125 \text{ mm.} \quad (3.35)$$

3.10.1.5 ACI-318 (2011): Recommendations for FRC

The ACI Code 2011 [52] does not include a formula to calculate the shear strength of SFRC beams.

The provision in the ACI Code assumes a minimum shear strength for SFRC beams of $2\sqrt{f_c}$. From test results reported in the literature, Dinh et al. [6] found that $3.6\sqrt{f_c}$ was a lower bound for the shear strength of SFRC beams with a minimum fiber volume fraction of 0.75 %. Dinh et al. [6] then established a minimum performance criterion for the SFRC such that the material used would not have a lower performance compared to those used in previous beam tests. The ACI Code Committee 318 thought that the difference between, in $3.6\sqrt{f_c}$ and $2\sqrt{f_c}$, in combination with the strength reduction factor and factored loads, provides sufficient safety margin.

3.11 Parameters Influencing in Shear Behavior of FRC Beams

The parameters which have a clear influence on the shear behavior of structural concrete elements without transversal reinforcement are: shear slenderness, element dimensions (size effect), presence or not of axial forces (tensile or compressive), amount of longitudinal reinforcement, compressive concrete strength, load conditions, cross-section shape and longitudinal reinforcement distribution inside the transversal section [59].

On the other hand, the parameters relevant to the structural part of FRC have the same effects as in reinforced concrete; those parameters can be taken into account globally through the post-cracking tensile behavior of the FRC used [19] and, therefore, the contribution of the fibers and their efficiency are the result of the global behavior of the fiber-reinforced concert [33].

In the experimental study of Li et al. [80], it was found that the material strength of steel FRC is significantly affected by the volume ratio, aspect ratio, and shape of the steel fiber. Also, the main variables studied for Imam's model and Slater et al. [81] were: shear span/depth ratio (a/d), the steel fiber content (V_f), and the percentage of the longitudinal flexural reinforcement (ρ) [41].

Swamy and Bahia [28] concluded that steel fibers clearly enhance the ultimate shear strength of reinforced concrete beams, the extent of such increase depending on the shape of the cross section, the amount of tension steel, and the fiber volume.

Of all these influencing parameters, below will go into depth on some of them:

3.11.1 Amount of Fibers

It is well known that crack widths clearly decreased with increasing fiber content [82]. Also, the volume of fibers has a strong influence on the ultimate shear load due to the improvement of toughness and ductility [83].

Susetyo et al. [26] found that a fiber content of 1 % is required to improve shear strength, deformation ductility, crack width, and crack spacing. Dinh et al. [6] added that with a 0.75 % volume fraction the increase in shear strength is significant. With minor contents (0.5 %) no improvements can be guaranteed [26] and, with contents greater than 1 % no more improvements are observed respected with 1 %, probably due to the saturation [6, 26].

The beams with fibers exhibited less deflection and larger ultimate load carrying capacity than those without fibers [41].

After analyzing the results of an extended campaign of bending tests, Altun et al. [84] concluded that the addition of a 30 kg/m^3 of fibers produced a clear improvement compared to concretes without fibers. However, when the amount of fibers was 60 kg/m^3 the benefits observed were small compared with an amount of 30 kg/m^3 .

Recently, Kim et al. [85] proposed a volume fraction of steel fibers of 1.5 % as the optimal value.

Regarding to self-compacting concretes (SCC), Khayat et al. [86] found that a volume of fibers of 0.5 % could be an upper limit for the production of SCC. A greater amount of fibers could hinder the SCC characteristics.

3.11.2 Relation Between Casting Procedure and Fiber Length

The mechanical behavior of the composite improves when decreases the fiber length in extruded composites and when increase the fiber length in cast composites. This contradictory trend is due to the difference in fiber failure mechanism, fiber distribution and fiber orientation in these two systems. In extruded composites the critical fiber length is shorter than in the cast composites due to the strong fiber-matrix bond in the extruded composites [87].

3.11.3 Fiber Type

Strength and geometry of fiber have a direct influence on the load bearing capacity of High Strength Fiber Reinforced Concrete beams without bar reinforcement. The ductile behavior was better in the postcracking range due to the use of high strength

fibers, compared to normal strength ones but the load bearing capacity reached the same level as concrete with normal strength fibers [88].

Fiber aspect ratio has a greater effect on the effectiveness of fiber reinforcement than fiber length, in fact, fibers with a high aspect ratio resulted in much improved post-cracking deformation capacities and crack control characteristics compared to fibers with a low aspect ratio [26, 89, 90].

Gustafsson and Noghabai [20] ensured that the best fracture toughness was provided by the mixed fibers. Short fibers have a good behavior in the pre-peak range because they improve the elastic modulus and tensile strength preventing microcracks. On the other hand, long fibers improve the post-peak behavior giving place to a ductile behavior.

Dinh et al. [6] recommended that the horizontal space between reinforcement bars should be less than the fibers length because long fibers allowed a greater inclined crack opening before failure compared to short fibers.

Regarding to the fiber shape, Banthia et al. [91] recently has ensured that, in mixes reinforced with a single fiber, the hooked-end fiber was significantly better in shear than the double deformed fiber.

Regarding to the material of the fiber, Kovler and Roussel [92] affirmed that the addition of steel fibers generally contributed towards the energy absorbing mechanism (bridging action), whereas the nonmetallic fibers delayed microcracking. Increased fiber availability in the hybrid fiber systems (due to the lower densities of non-metallic fibers), in addition to the ability of non-metallic fibers to bridge smaller microcracks, are suggested as a tool for the enhancement of mechanical properties.

3.11.4 Relation Between Fiber Type and Beam Size

The requirements on the fibers become greater as the beam dimensions increase. For small beams a shorter type of fibers may be sufficient, whereas for larger beams, fibers that are better anchored and have a higher strength are required [20].

3.11.5 Depth of the Beam

Barragán [93] ensured that, in rectangular beams made with FRC, the ultimate shear, the first crack load and the first crack deflections increase with the increase of the height; however the ultimate-load deflections are relatively unaffected to this variation.

On the other hand, Ding et al. [6] observed that, for a range of $d = 381\text{--}610$ mm, deeper beams exhibited wider crack spacings.

3.11.6 Flange Width

The presence of a flange increases the ultimate shear load-carrying capacity significantly in comparison with a rectangular beam, however, the increase of the flange width does not seem to affect the ultimate shear load (Fig. 3.12) compared with other flange widths [51, 93, 94].

3.11.7 Flange Depth

Tests on T-beams without stirrups suggested that, over a limit value of flange depth, resulted increased shear ultimate loads and better ductility but, for flange depths lower than the limit value and rectangular beams no influence was detected on the shear ultimate load [51, 93, 94], see Fig. 3.13.

Fig. 3.12 Influence of the flange width on the load-deflection response [94]

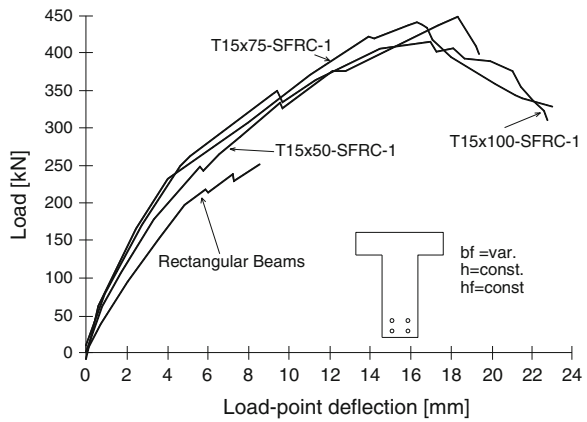
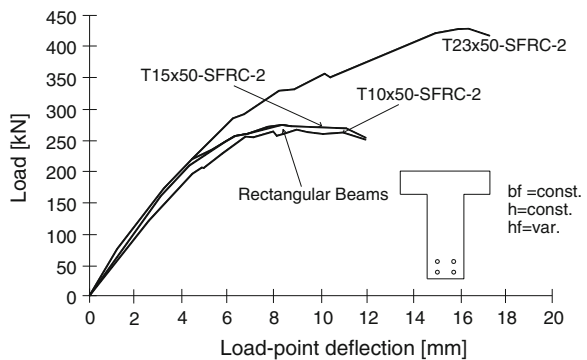


Fig. 3.13 Influence of the flange height on the load-deflection response [94]



3.11.8 Effect of Longitudinal Ratio

The main effect of longitudinal reinforcement ratio (ρ) is on beam ductility [6]. Flexural yielding was observed in several beams tested by Dinh et al. [6] with a longitudinal reinforcement ratio of approximately 2 %, whereas no yielding occurred in any of the beams with a reinforcement ratio greater than 2 %. For beams with a 2 % longitudinal reinforcement ratio, the shear strength of beams with a 0.75 % fiber volume fraction (prior to flexural yielding) was believed to be close to the shear demand associated with flexural yielding [6].

Imam et al. [41] ensured that the increase of ρ , increases the shear and the flexural strength, but the increase of the latest one is higher.

Longitudinal reinforcement affects beam shear strength by influencing the size of the compression zone and by providing shear resistance through dowel action by enhancing the tensile strength of the concrete in the splitting plane along the bars [6, 7]. Depending on the amount of steel reinforcement used, flexural yielding might develop first, followed by shear failure of the beam [6].

3.11.9 Influence of Prestressing

Furlan and Bento-de-Hanai [34] ensured that shear strength is increased more due to the prestressing than due to the fibers. Other effect of prestressing is that it decreases the slope of the compression struts and increases the extent of the non-cracked area [34].

3.11.10 Influence of Concrete Strength

Narayanan ensured that, for the same fiber factor, the shear strength increases with cube strength [7].

Tiberti et al. [95] affirmed that the use of High Strength Concrete reduces the crack spacing with respect to the Normal Strength Concrete.

3.12 Fibers Influence on Deflections

Fibers make possible smaller deflections [22, 28, 34], in fact, deflections can be visible before collapse [5, 11, 17, 32]; these deflections are reduced because of increased stiffness [41, 65] so deformation characteristics are improved [21, 72]. On the other hand, if fibers acted compositely with stirrups, larger deflections are observed [21, 28].

3.13 Fibers Influence on Dowel Action

The interaction between fiber contribution and the various resistant mechanisms is always favorable for strut-bending and dowel action and unfavorable for aggregate interlock. It involves a significant reduction in the role of aggregate interlock, and an increase in dowel action, especially in reinforced concrete beams when the stirrup spacing is not altered even if fibers are added [96].

On the other hand, the dowel resistance of reinforced concrete beams depends on the tensile strength of the concrete and the bending resistance of tension steel [21]. The presence of fibers improved the tensile strength of the concrete in the splitting plane along the reinforcement [7].

The stiffness of the dowel zone increases if the fiber content, amount of tension steel, or amount of tension steel, or amount of web reinforcement also increases. The fiber reinforcement is very effective in containing the dowel crack growth due to the crack arrester, and make failures very ductile. Beams with web reinforcement showed similar load capacity and ductility but suffered spalling and disintegration of the concrete cover. The first crack and ultimate dowel strength increase almost linearly with the flexural strength of the composite and also they are very sensitive to the distribution of fiber in the dowel zone being affected by the spacing and concrete cover of the main reinforcement and the presence of stirrups which could lead to non-uniform fiber distribution [21].

In conclusion, fibers clearly control the cracking and displacement in the dowel zone, and enable the beams to fully use the contribution to shear due to dowel action [28].

3.14 Hollow Core Slabs (HCS) Made with FRC

3.14.1 Introduction

The Hollow Core Slabs (HCS) are manufactured by a long-line extrusion system which imposes restrictions on the placing of transverse reinforcement. HCS are therefore exempt from the minimum shear reinforcement requirements found in Design Codes [97, 98]. This lack of transverse reinforcement leads to a number of potential problems in the use of HCS [99]. In 1994, a study [100] suggested that the inclusion of steel fibers in HCS would be an economic solution to some of these problems [101].

3.14.2 Manufacturing of HCS Made with FRC

Adding fibers in a concrete mix with zero slump concrete is possible if fibers are added before any free water. However, to use this type of concrete to produce Hollow Core Slabs (HCS) by extrusion it would be necessary to make the concrete mix slightly wetter [101].

ACI Committee 544 [102] and JCI [103] recommended that fibers should be added to the concrete mix as the final component after all other ingredients have been introduced. However, with this mixing procedure fibers remained together. Therefore, Paine [101] proposed to add finally the water. With this method no balling of fibers occurred due to the scouring action of aggregates on the fibers.

Initially, in 1996, Peaston and Paine FRC was performed with the extrusion machine with no apparent difficulties but, it was detected a lack of compaction on the top surface of the HCS [101, 104]. Some years ago, in 1999, Peaston et al. [104] ensured that extruded HCS with FRC could be practicable but it was detected that the fiber orientation was not random and was strongly influenced by the extrusion process.

Recently, Cuenca and Serna [105, 106] has ensured that it is possible to produce fiber-reinforced concrete Hollow Core Slabs (HCS) without encountering technical problems.

3.14.3 Advantages of Adding Fibers into Concrete Mix for HCS Production

Fibers considerably improve the shear strength of HCS and also help to maintain strength after shear cracking giving more ductile shear failures. Fibers may also improve the bond between strand and concrete resulting in greater dowel resistance to shear. This is a key advantage given the impossibility of placing transverse reinforcements on HCSs [101, 105, 106]. Fibers improve mechanical behavior of the concrete giving a solution to overcome shear failure since fibers are capable of increasing element strength to its full flexural capacity, thus attenuating Kani's valley [105, 106].

3.14.4 Shear Behavior of HCS

The shear failures were abrupt, brittle and occurred with little or no warning. As a/d increased the explosiveness of the failure increased. Figure 3.14 compares the failure mechanisms of the slabs, showing how a tendency for flexural-type failures increased with a/d and fiber volume [101].

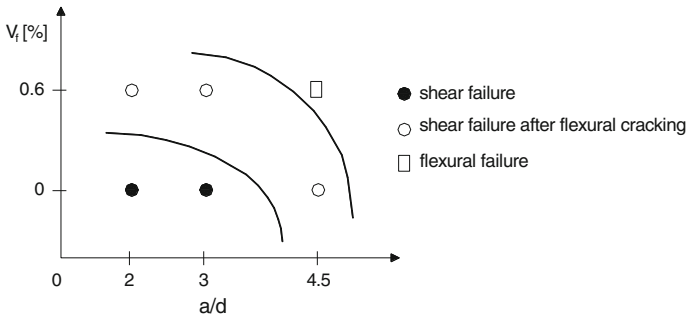


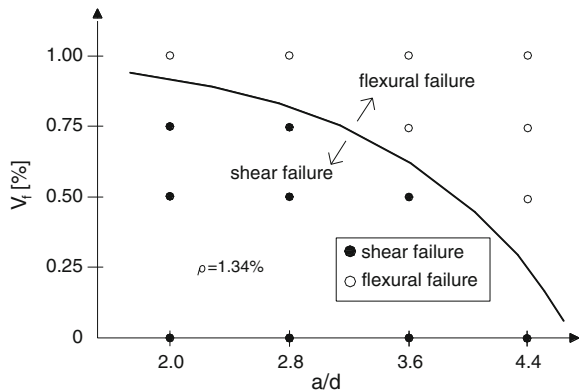
Fig. 3.14 Observed failure modes for HCS [101]

Figure 3.15 shows the failure modes for reinforced concrete and reinforced FRC beams [101].

Due to the presence of fibers in the mix for producing HCS, many advantages take place: FRC slabs had a much greater post-peak strength, with a reduced spalling giving place to safer and controlled failures. The increase in strength could therefore be due to the fibers in the compression zone and the enhanced post-cracking performance is associated with the energy that is required to pull the fibers out of the cracked matrix. At large deflections fibers have pulled-out and are not bridging the majority of the crack [101, 104, 107–109]. The shear capacity increases with increased fiber content, fiber aspect ratio and with improved fiber-matrix interfacial bond.

In conclusion, if steel fibers are dispersed correctly is known that they increase the post-cracking tensile performance and, if they are introduced into the hollow core extrusion and they are properly distributed, fibers improve both, the shear strength of the structural element and also its ductility behavior [110].

Fig. 3.15 Observed failure modes for FRC beams [60]



3.14.5 Failure Modes

The main modes of failure in HCS are: flexural shear and web shear tension. Flexural shear occurs when a flexural crack develops into a shear crack and leads to a relatively ductile failure. Web shear tension is brittle failure and may not be preceded by any warning of impending failure [104, 111].

Precast HCSs do not have web widths exactly equal, therefore, once a shear failure occurs in the critical web, it propagates rapidly throughout the unit of HCS [110].

3.14.6 Design of HCS

3.14.6.1 BS 8110 Modified Method

To determine the fiber contribution to shear, Paine [101] used the Narayanan and Darwish's equation [112].

To account for FRC beams failing in web shear tension, Narayanan and Darwish altered the equation of BS 8110 [98] to:

$$V_{Rd} = 0.67bh\sqrt{f_{fct,sp}^2 + 0.8\sigma_{cp}f_{fct,sp}} \quad (3.36)$$

where the tensile split cylinder strength, $f_{fct,sp}$, is found empirically from cube compression tests:

$$f_{fct,sp} = \frac{f_{fc,cub}}{20 - \sqrt{F}} + 0.7 + \sqrt{F} \quad (3.37)$$

and:

$$F = \eta_b \cdot V_f \cdot \lambda_f \quad (3.38)$$

where V_f is the fiber volume fraction, λ_f is the fiber aspect ratio and η_b is a bond efficiency factor to account for different fiber types.

The use of the split cylinder strength in plain HCS design has been shown to produce exaggeteratingly high results [109]. Equations for shear strength of prestressed FRC, with the tensile strength derived indirectly from flexural strength or toughness may be more acceptable.

3.14.6.2 Fiber Supplement Additive Method

$$V_u = V_c + V_b \quad (3.39)$$

where V_c is the concrete contribution to shear capacity, a combination of concrete compressive resistance V_{cc} , prestressing V_p , and dowel resistance V_d . The term V_b is usually the sole measure of the improved shear resistance due to fibers [113].

$$V_u = V_{cc} + V_p = \left[0.4\sqrt{f_{cu}} + 0.45\sigma_{cpk} \right] b_w d \quad (3.40)$$

V_b According to Lim

$$V_b = f_{tu} b_w d \quad (3.41)$$

where f_{tu} can be calculated theoretically as $\eta_\theta \cdot V_f \cdot \tau_f \cdot \lambda_f$ according to Lim et al. [114], where V_f is the fiber volume fraction, τ_f is the fiber matrix interfacial bond, λ_f is the fiber aspect ratio, and η_θ is fiber orientation factor.

V_b According to Dramix Guidelines

Dramix guidelines [115] defined V_b as:

$$V_b = 0.54f_{ct,ax}R_t b d \quad (3.42)$$

where R_t is the ratio of the tensile strength before and after cracking and is given by Nemegeer and Tatnall [116] as:

$$R_t = \frac{1.1W_f\lambda_f}{(180C + W_f\lambda_f)} \quad (3.43)$$

where W_f is the fiber content (in kg/m^3) and C is a function of the anchorage effect of the fibers.

References

1. Fenwick, R.C., and T. Paulay. 1968. Mechanisms of shear resistance of concrete beams. *Proceedings of the ASCE* 94(10): 2325–2350.
2. MC2010. 2012. Fib Bulletin 65–66. Model Code—final draft.
3. Minelli, F., and G. Plizzari. 2006. Steel fibers as shear reinforcement for beams. In *Proceedings of the second fib congress*, Naples, Italy.
4. Juárez, C., P. Valdez, A. Durán, A., and K. Sobolev. 2007. The diagonal tension behavior of fiber reinforced concrete beams. *Cement and Concrete Composites* 29: 402–408.

5. Conforti, A., F. Minelli, and G.A. Plizzari. 2013. Wide-shallow beams with and without steel fibers: A peculiar behaviour in shear and flexure. *Composites Part B: Engineering* 51: 282–290.
6. Dinh, H.H., G.J. Parra-Montesinos, and J.K. Wight. 2010. Shear behavior of steel fiber-reinforced concrete beams without stirrup reinforcement. *ACI Structural Journal* 107(5): 597–606.
7. Narayanan, R., and I.Y.S. Darwish. 1987. Use of steel fibers as shear reinforcement. *ACI Structural Journal* 84: 216–227.
8. di-Prisco, M., M. Colombo, and D. Dozio. 2013. Fibre-reinforced concrete in fib Model Code 2010: Principles, models and test validation. *Structural Concrete* 14(4): 342–361.
9. Lim, D.H., and B.H. Oh. 1999. Experimental and theoretical investigation on the shear of steel fibre reinforced concrete beams. *Engineering Structures* 21: 937–944.
10. Oh, B., D. Lim, K. Hong, S. Yoo, and S. Chae. 1999. Structural behavior of steel fiber reinforced concrete beams in shear. *ACI Special Publication* 182: 9–27.
11. Conforti, A. 2014. Shear behavior of deep and wide-shallow beams in fiber reinforced concrete. Ph.D. thesis, Department of civil, architectural, environmental, land planning engineering and of mathematics, University of Brescia, May 2014, Aracne Editrice, Roma, p. 232, ISBN 978-88-548-7009-3.
12. Greenough, T., and M. Nehdi. 2008. Shear behavior of fiber reinforced self-consolidating concrete slender beams. *ACI Materials Journal* 105(5): 468–477.
13. Majdzadeh, F., S.M. Soleimani, and N. Banthia. 2006. Shear strength of reinforced concrete beams with a fiber concrete matrix. *Canadian Journal of Civil Engineering* 33: 726–734.
14. Padmarajaiah, S.K., and A. Ramaswamy. 2001. Behavior of fiber-reinforced prestressed and reinforced high-strength concrete beams subjected to shear. *ACI Structural Journal* 98(5): 752–761.
15. Thomas, J., and A. Ramaswamy. 2006. Shear strength of prestressed concrete T-beams with steel fibers over partial/full depth. *ACI Structural Journal* 103(3): 427–435.
16. Narayanan, R., and I.Y.S. Darwish. 1988. Fiber concrete deep beams in shear. *ACI Structural Journal* 85(2): 141–149.
17. Minelli, F., A. Conforti, E. Cuenca, and G.A. Plizzari. 2014. Are steel fibres able to mitigate or eliminate size effect in shear? *Materials and Structures* 47(3): 459–473.
18. Imam, M., and L. Vandewalle. 2000. Role of fibers in controlling failure modes of high-strength concrete beams. *ACI Special Publication* 193: 503–515.
19. Casanova, P., P. Rossi, and I. Schaller. 1997. Can steel fibers replace transverse reinforcements in reinforced concrete beams? *ACI Materials Journal* 94(5): 341–354.
20. Gustafsson, J., and K. Noghabai. 1999. Steel fibers as shear reinforcement in high strength concrete beams. *International Journal of Nordic Concrete Research* 22: 1–18.
21. Swamy, R.N., and H.M. Bahia. 1979. Influence of fiber reinforcement on the dowel resistance to shear. *ACI Journal* 76(2): 327–356.
22. Balaguru, P.N., and A.S. Ezeldin. 1987. Behavior of partially prestressed beams made with high strength fiber reinforced concrete. *ACI Special Publication* 105: 419–436.
23. Minelli, F., and G. Plizzari. 2013. On the effectiveness of steel fibers as shear reinforcement. *ACI Structural Journal* 110(3): 379–390.
24. Schumacher, P., J.C. Walraven, J.A. Den-Uijl, and A. Bigaj. 2009. Rotation capacity of self-compacting steel fiber reinforced concrete beams. *HERON* 54(2/3): 127–161.
25. Khuntia, M., B. Stojadinovic, and S.C. Goel. 1999. Shear strength of normal and high-strength fiber reinforced concrete beams without stirrups. *ACI Structural Journal* 96(2): 282–290.
26. Susetyo, J., P. Gauvreau, and F.J. Vecchio. 2011. Effectiveness of steel fiber as minimum shear reinforcement. *ACI Structural Journal* 108(4): 488–496.
27. Meda, A., F. Minelli, G. Plizzari, and P. Riva. 2005. Shear behaviour of steel fibre reinforced concrete beams. *Materials and Structures* 38: 343–351.
28. Swamy, R.N., and H.M. Bahia. 1985. The effectiveness of steel fibers as shear reinforcement. *Concrete International* 7: 35–40.

29. Calixto, J.M., L.V. Filho, and F. Gonçalves. 2002. Shear behavior of reinforced concrete beams with the addition of short steel fibers. *ACI Special Publication* 207: 449–466.
30. Vandewalle, L. 2000. Cracking behaviour of concrete beams reinforced with a combination of ordinary reinforcement and steel fibers. *Materials and Structures* 33: 164–170.
31. Noghabai, K. 2000. Beams of fibrous concrete in shear and bending: Experiment and model. *Journal of Structural Engineering, ASCE* 126(2): 243–251.
32. Minelli, F., G. Plizzari, and F. Vecchio. 2007. Influence of steel fibers on full-scale RC beams under shear loading. In *Proceedings of the international conference framcos—high performance concrete, brick-masonry and environmental aspects*, Catania, Italy.
33. Pujadas, P., A. Blanco, A. De-La-Fuente, and A. Aguado. 2012. Cracking behavior of FRC slabs with traditional reinforcement. *Materials and Structures* 45: 707–725.
34. Furlan, S., and J.B. Bento-de-Hanai. 1999. Prestressed fiber reinforced concrete beams with reduced ratios of shear reinforcement. *Cement and Concrete Composites* 21: 213–221.
35. Cuenca, E., and P. Serna. 2010. Shear behavior of self-compacting concrete and fiber reinforced concrete beams. In *Proceedings of 6th RILEM symposium on self-compacting concrete SCC*, Montreal, Canada.
36. Minelli, F. and G. Plizzari. 2006. Progetto a taglio di travi in calcestruzzo fibrorinforzato prive di armatura trasversale (in Italian). In *Atti del 16° Congresso C.T.E.*, Parma, Italy.
37. Cuenca, E., and P. Serna. 2013. Shear behavior of prestressed precast beams made of self-compacting fiber reinforced concrete. *Construction and Building Materials* 45: 145–156.
38. Cuenca, E., P. Serna, and M.J. Pelufo. 2009. Structural behavior of self-compacting and fiber reinforced concrete under shear loading. In *Proceedings of international symposium of shell and spatial structures IASS*, Valencia, Spain.
39. Cuchiara, C., L. La-Mendola, and M. Papia. 2004. Effectiveness of stirrups and steel fibers as shear reinforcement. *Cement and Concrete Composites* 26: 777–786.
40. Sharma. A.K. 1986. Shear strength of steel fiber reinforced concrete beams. *ACI Journal* 83 (4): 624–628.
41. Imam, M., L. Vandewalle, and F. Mortelmans. 1994. Shear capacity of steel fiber high-strength concrete beams. *ACI Special Publication* 149: 227–241.
42. Batson, G., E. Jenkins, and R. Spatney. 1972. Steel fibers as shear reinforcement in beams. *ACI Journal* 69(10): 640–644.
43. Collins, M.P., and D. Mitchell. 1991. *Prestressed Concrete Structures*. Englewood Cliffs: Prentice-Hall.
44. Bischoff, P.H. 2003. Tension stiffening and cracking of steel fiber-reinforced concrete. *Journal of Materials in Civil Engineering* 15(2): 174–182.
45. Abrishami, H.H., and D. Mitchell. 1997. Influence of steel fibers on tension stiffening. *ACI Structural Journal* 94(6): 769–776.
46. Samarrai, M.A., and R.H. Elvery. 1974. The influence of fibers upon crack development in reinforced concrete subject to uniaxial tension. *Magazine of Concrete Research* 26(89): 203–211.
47. Massicotte, B., A. Belanger, and K. Moffatt. 2000. Analysis and design of SFRC bridge decks. In *5th RILEM symposium on fiber reinforced concrete*, RILEM Publications, Cachan Cedex, France.
48. Bischoff, P.H., and B. Massicotte. 1999. Structural design with fiber reinforced concrete: A North American perspective. In *Proceedings of 2nd Asia-pacific specialty conference on fiber reinforced concrete*, Singapore.
49. De-Montaignac, R., B. Massicotte, and J.P. Charron. 2012. Design of SFRC structural elements: Flexural behaviour prediction. *Materials and Structures* 45(4): 623–636.
50. Minelli, F., and G. Plizzari. 2008. Shear design of FRC members with little or no conventional shear reinforcement. In *Proceedings of the fib symposium “tailor made concrete structures-new solutions for our society”*, Amsterdam, The Netherlands.
51. Rosenbusch, J., and M. Teutsch. 2003. Shear Design with sigma-epsilon method. In *Proceedings of the RILEM TC 162-TDF workshop test and design methods for steel fibre*

- reinforced concrete—background and experiences*, ed. by Schnütgen and Vandewalle. RILEM Publications, 2003.
52. ACI Committee. 318. 2011. Building Code requirements for structural concrete (ACI 318-11), American Concrete Institute.
 53. Minelli, F., and F. Vecchio. 2006. Compression field modeling of fiber-reinforced concrete members under shear loading. *ACI Structural Journal* 103(2): 244–252.
 54. Parra-Montesinos, G.J. 2006. Shear strength of beams with deformed steel fibers. Evaluating an alternative to minimum transverse reinforcement. *Concrete International* 28: 57–66.
 55. Imam, M., L. Vandewalle, F. Mortelmans, and D.V. Gemert. 1997. Shear domain of fibre-reinforced high-strength concrete beams. *Engineering Structures* 19(9): 738–747.
 56. Imam, M., L. Vandewalle, and F. Mortelmans. 1995. Shear-moment analysis of reinforced high-strength concrete beams containing steel fibers. *Canadian Journal of Civil Engineering* 22: 462–470.
 57. Williamson, G.R. 1978. Steel fibers as web reinforcement in reinforced concrete. de Proceedings, U.S. Army Service Conference, West Point, N.Y.
 58. De-Pauw, P., L. Taerwe, N. Van-den-Buverie, and W. Moerman. 2008. Replacement of shear reinforcement by steel fibers in pretensioned concrete beams. Taylor Made Concrete Structures, 391–397. London: Taylor & Francis Group. ISBN: 978-0-415-47535-8.
 59. Minelli, F., and G. Plizzari. 2007. Un nuovo modello analitico per il progetto a taglio di elementi in calcestruzzo fibrorinforzato privi di armatura trasversale (in italian). In *Atti del 24° Convegno Nazionale Giornate AICAP*, Salerno, Italia.
 60. Mansur, M.A., K.C.G. Ong, and P. Paramasivam. 1986. Shear strength of fibrous concrete beams without stirrups. *Journal of Structural Engineering, ASCE* 112(9): 2066–2079.
 61. Campione, G. 2008. Simplified flexural response of steel fiber-reinforced concrete beams. *Journal of Materials in Civil Engineering, ASCE* 20(4): 283–293.
 62. Cho, S.H., and Y.I.L. Kim. 2003. Effects of steel fibers on short beams loaded in shear. *ACI Structural Journal* 100(6): 765–774.
 63. Sarhat, S.R., and R.B. Abdul-Ahad. 2006. The combined use of steel fibers and stirrups as shear reinforcement in reinforced concrete beams. *ACI Special Publication* 235: 269–282.
 64. Furlan, S., and J.B. Bento-de-Hanai. 1997. Shear behavior of fiber reinforced concrete beams. *Cement and Concrete Composites* 19: 359–366.
 65. Ashour, S.A., G.I.S. Hasanain, and F.F. Wafa. 1992. Shear behavior of high-strength fiber reinforced concrete beams. *ACI Structural Journal* 89(2): 176–184.
 66. ACI-Committee-544. 2002. State of the Art Report on Fiber Reinforced Concrete. Report 544-1R-96 (Reapproved 2002).
 67. Bencardino, F., L. Rizzuti, G. Spadea, and R.N. Swamy. 2008. Stress-Strain behavior of steel fiber-reinforced concrete in compression. *Journal of Materials in Civil Engineering, ASCE* 20(3): 255–263.
 68. Cho, J.S, J. Lundy, and S.H. Chao. 2009. Shear strength of steel fiber reinforced prestressed concrete beams. In *ASCE structures congress '09*, Austin, Texas.
 69. Kuchma, D.A., P. Véghe, K. Simionopoulos, B. Stanik, and M.P. Collins. 1997. The influence of concrete strength, distribution of longitudinal reinforcement, and member size, on the shear strength of reinforced concrete beams. In *Concrete tension and size effect*, CEB Bulletin 237, Lausanne, 1997, 258 pp.
 70. Bazant, Z.P. and H.H. Sun. 1987. Size effect in diagonal shear failure: Influence of aggregate size and stirrups. *ACI Materials Journal* 84(4): 259–272.
 71. Bazant, Z.P., and S.S. Kim. 1984. Size effect in shear failure of longitudinally reinforced beams. *ACI Journal* 81(5): 456–468.
 72. Mansur, M.A., and K.C.G. Ong. 1991. Behavior of reinforced fiber concrete deep beams in shear. *ACI Structural Journal* 88(1): 98–105.
 73. Campione, G., C. Cucchiara, and L. La-Mendola. 2003. Role of fibers and stirrups on the experimental behavior of reinforced concrete beams and flexure and shear. In *Proceedings of international conference on composites in construction*, Rende, Italy.

74. Dupont, D., and L. Vandewalle. 2003. Shear capacity of concrete beams containing longitudinal reinforcement and steel fibers. *ACI Special Publication* 216: 79–94.
75. RILEM-TC-162-TDF. 2003. Test and design methods for steel fibre reinforced concrete—background and experiences. Bagnoux: RILEM Publications s.a.r.l.
76. RILEM. 2003. Recommendations of RILEM TC 162-TDF: Sigma-epsilon design method. *Materials and Structures* 33: 75–81.
77. RILEM. 2003. RILEM TC 162-TDF: Test and design methods for steel fibre reinforced concrete. Sigma-epsilon design method. Final Recommendation. *Materials and Structures* 36: 560–567.
78. EHE-08. 2008. Instrucción de Hormigón Estructural EHE-08 (in Spanish), Ministerio de Fomento.
79. Minelli, F. 2005. Plain and fiber reinforced concrete beams under shear loading: Structural behavior and design aspects. PhD thesis, Starrylink Editrice, Brescia, Italy.
80. Li, V.C., R. Ward, and A.M. Hamza. 1992. Steel and synthetic fibers as shear reinforcement. *ACI Materials Journal* 89(5): 499–508.
81. Slater, E., M. Moni, and M.S. Alam. 2012. Predicting the shear strength of steel fiber reinforced concrete beams. *Construction and Building Materials* 26: 423–436.
82. Jansson, A., M. Flansbjer, I. Löfgren, K. Lundgren, and K. Gylltoft. 2012. Experimental investigation of surface crack initiation, propagation and tension stiffening in self-compacting steel-fiber-reinforced concrete. *Materials and Structures* 45: 1127–1143.
83. El-Niema, E.I. 1991. Reinforced concrete beams with steel fibers under shear. *ACI Structural Journal* 88(2): 178–183.
84. Altun, F., T. Haktanir, and K. Ari. 2007. Effects of steel fiber addition on mechanical properties of concrete and RC beams. *Construction and Building Materials* 21: 654–661.
85. Kim, K.S., D.H. Lee, J.H. Hwang, and D.A. Kuchma. 2012. Shear behavior model for steel fiber-reinforced concrete members without transverse reinforcements. *Composites: Part B* 43: 2324–2334.
86. Khayat, K.H., F. Kassimi, and P. Ghoddousi. 2014. Mixture design and testing of fiber-reinforced self-consolidating concrete. *ACI Materials Journal* 111(2): 143–152.
87. Akkaya, Y., A. Peled, and S.P. Shah. 2000. Parameters related to fiber length and processing in cementitious composites. *Materials and Structures* 33: 515–524.
88. Holschemacher, K., T. Mueller, and Y. Ribakov. 2010. Effect of steel fibers on mechanical properties of high-strength concrete. *Materials and Design* 31: 2604–2615.
89. Johnston, C.D., and A. Skarendahl. 1992. Comparative flexural performance evaluation of steel fiber-reinforced concretes according to ASTM C1018 shows importance of fiber parameters. *Materials and Structures* 25(4): 191–200.
90. Bencardino, F., L. Rizzuti, G. Spadea, and R.N. Swamy. 2013. Implications of test methodology on post-cracking and fracture behavior of steel fiber reinforced concrete. *Composites: Part B* 46: 31–38.
91. Banthia, N., F. Majdzadeh, J. Wu, and V. Bindiganavile. 2014. Fiber synergy in hybrid fiber reinforced concrete (HyFRC) in flexure and direct shear. *Cement and Concrete Composites* 48: 91–97.
92. Kovler, K., and N. Roussel. 2011. Properties of fresh and hardened concrete. *Cement and Concrete Research* 41: 775–792.
93. Barragán, B.E. 2002. Failure and toughness of steel fiber reinforced concrete under tension and shear. PhD thesis, Universitat Politècnica de Catalunya (UPC).
94. Rosenbusch, J., and M. Teutsch et al. 2002. Trial beams in shear, Final Report Sub Task 4.2, Brite Euram project 97-4163: Test and design methods for steel fibre reinforced concrete.
95. Tiberti, G., F. Minelli, G. Plizzari, and F. Vecchio. 2014. Influence of concrete strength on crack development in SFRC members. *Cement and Concrete Composites* 45: 176–185.
96. Di-Prisco, M. and J.A. Romero. 1996. Diagonal shear in thin-webbed reinforced concrete beams: Fibre and stirrup roles at shear collapse. *Magazine of Concrete Research* 48(174): 59–76.
97. FIP-Recommendations. 1988. Precast Prestressed Hollow Core Floors.

98. BS-8110, BS 8110. 1985. Part 1: structural use of concrete, code of practice for design and construction. Part 2: code of practice for special circumstances, British Standards Institution.
99. Angelakos, D., E.C. Bentz, and M.P. Collins. 2001. Effect of concrete strength and minimum stirrups on shear strength of large members. *Journal of Structural Engineering* 98(3): 290–300.
100. Glavind, M., C. Munch-Petersen, and E.J. Pedersen. 1994. Framework programme 1989–92 fibre reinforced concrete. Publication No. 14 1/94. Nordic Concrete Research.
101. Paine, K. 1996. Trial production of fibre reinforced hollow core slab. Research Report SR 96 007. Department of Civil Engineering, University of Nottingham.
102. ACI-544. 1993. Guide for specifying, proportioning, mixing, placing and finishing steel fiber reinforced concrete. ACI 544.3R-93. *ACI Materials Journal* 90(1): 94–101.
103. JCI. 1983. Method of making fiber reinforced concrete in the laboratory. JCI Standard SF1. JCI Standards for Test Methods of Fiber Reinforced Concrete, 35–36.
104. Peaston, C.H., K.S. Elliott, and K.A. Paine. 1999. Steel Fiber Reinforcement for extruded prestressed hollow core slabs. *ACI Special Publication* 182: 87–107.
105. Cuenca, E., and Serna, P. 2013. Failure modes and shear design of prestressed hollow core slabs made of fiber-reinforced concrete. *Composites Part B: Engineering* 45(1): 952–964.
106. Cuenca, E., and P. Serna. 2010. Shear behavior of self-compacting concrete and fiber-reinforced concrete push-off specimens. In *Design, production and placement of self-consolidating concrete*, vol. 1, ed. K.H. Khayat, and D. Feys, 429–438., RILEM Bookseries Netherlands: Springer.
107. Swamy, R.N., and S. Al-Ta'an. 1981. Deformation and ultimate strength in flexure of reinforced concrete beams made with steel fiber concrete. *ACI Journal* 78(5): 395–405.
108. Bentur, A., and S. Mindess. 1990. *Fibre reinforced cementitious composites*. England: Elsevier Applied Science, 449 pp.
109. Pisanty, A. 1992. The shear strength of extruded hollow-core slabs. *Materials and Structures* 25: 224–230.
110. Elliott, K.S., C.H. Peaston, and K.A. Paine. 2002. Experimental and theoretical investigation of the shear resistance of steel fiber reinforced prestressed concrete X-beams-part 1: Experimental work. *Materials and Structures* 35: 519–527.
111. Girhammar, U.A. 1992. Design principles for simply supported hollow core slabs. *Structural Engineering Review* 4(4): 301–316.
112. Narayanan, R., and I.Y.S. Darwish. 1987. Shear in prestressed concrete beams containing steel fibers. *International Journal of Cement Composites and Lightweight Concrete* 9(2): 81–87.
113. Elliott, K.S., C.H. Peaston, and K.A. Paine. 2002. Experimental and theoretical investigation of the shear resistance of steel fiber reinforced prestressed concrete X-beams-part 2: Theoretical analysis and comparison with experiments. *Materials and Structures* 35: 528–535.
114. Lim, T.Y., P. Paramasivam, and S.L. Lee. 1987. Analytical model for tensile behavior of steel-fiber concrete. *ACI Materials Journal* 84(4): 286–298.
115. Dramix-Guidelines. 1995. Design of concrete structures. Steel wire fiber reinforced concrete structures with or without ordinary reinforcement.
116. Nemegeer, D., and R. Tatnall. 1995. Measuring toughness characteristics of SFRC—a critical view of ASTM C1018. Testing of fiber reinforced concrete. *ACI Special Publication* 155: 77–92.
117. Massicotte, B. 2004. Implementing SFRC design into North American Codes: Application to a building floor. In *International workshop on the advanced in fibre reinforced concrete*, Bergamo, Italia.
118. Ultkjaer, J.P., S. Krenk, and E. Brincker. 1995. Analytical model for fictitious crack propagation in concrete beams. *ASCE Journal of Engineering Mechanics* 121(1): 7–15.
119. Kooiman, A.G. 2000. Modelling SFRC for structural design. PhD thesis, University of Delft, Delft, The Netherlands.

120. Iyengar, K., S. Raviraj, and P.N. Ravikumar. 1998. Analysis study of fictitious crack propagation in concrete beams using a bilinear stress-crack width relation. In *3th International conference on fracture mechanics of concrete and structure (FRAMCOS III)*, Japan.
121. Pedersen, C. 1996. New production processes, materials and calculation techniques for fiber reinforced concrete pipes. Ph.D. thesis, University of Denmark, Denmark.
122. AFGC-SETRA. 2002. *Ultra high performance fibre-reinforced concretes, interim recommendations*. France: AFGC Publication.
123. CNR-DT-204. 2006. *Guidelines for design, construction and production control of fiber reinforced concrete structures*. Rome: National Research Council of Italy.
124. Strack, M. 2008. Modelling of crack opening of SFRC under tension and bending. In 7th international RILEM symposium on fr: design and application.
125. EC2, Eurocode 2. 1992. *Design of concrete structures. Part 1: General rules and rules for buildings*. Brussels: European Committee for Standardization (CEN).

Part III

Experimental Tests

Contents of Part III

After making a thorough study of the literature on the shear behavior of structural elements made of fiber-reinforced concrete—FRC—(Chap. 3) and concrete without fibers, it is possible to detect some possible aspects to take a step that allows to better understand the shear behavior of structural elements made with FRC.

In the literature it is not entirely clear the contribution of the flange size of double-T beams to shear strength. In the current Codes, this effect does not appear for the determination of shear strength in concrete without fibers but it appears in the RILEM guidelines for FRC. It seems of practical interest to better understand whether or not the flange helps to resist shear. To this aim, an experimental campaign was carried out consisting of eight FRC prestressed beams and a concrete without fibers was used as reference. The beams had different top flange widths (260, 400, and 600 mm); two of the nine beams had both stirrups and fibers, one was reinforced only with stirrups and the other six beams were reinforced only with fibers for shear resistance. As additional variable, one of the beams was done with a larger flange (with an increase in height of 50 mm). Chapter 4 explains in detail the experimental program: procedure, testing, data collection, analysis of results and conclusions.

Today it is well known that the size of the beam has a clear influence on the shear strength of the element. As the depth of the element increases, the lower is the shear strength achieved. This is due to the great influence that exists between the depth and the shear crack width. In large beams such opening is larger and this is detrimental to shear capacity. Collins et al. came to the conclusion that longitudinal reinforcement distributed along the beam depth could eliminate the size effect, as the same happens if stirrups are added. The question raised was if fibers could mitigate somewhat the size effect or even eliminate it as the stirrups can do. In order to give an answer to this question, an experimental program was carried out for shear tests on nine large beams, where three beams had a depth of 500 mm, the next three a depth of 1000 mm, and the last three had a depth of 1500 mm. In turn, each

depth was made from three types of concrete with the following amount of fibers: 0, 50, and 75 kg/m³. This research is explained in detail in Chap. 5.

Another aspect that has attracted interest is to know the influence of fibers on shear behavior of beams. It is well known that fibers give rise to more ductile behavior with more dynamic failure modes in which, *a priori*, it cannot be made sure which of the shear cracks that were generated will provoke the beam failure. Furthermore, it is known that the presence of fibers results in a more distributed cracking pattern; in fact, in FRC beams, shear cracks appear more but thinner and closer. Another aspect to note is that Codes currently use f_{R3} to take into account the mechanical properties concerning FRC. This has been widely studied and justified, but it is not evident that the value of f_{R3} is the one that better represents the mechanical behavior of FRC for all combinations of compressive strength and fiber type. To this aim, in Chap. 6, a comprehensive experimental program consisting of 22 FRC beams has been carried out. In this program, three different compressive strength levels (low, medium, and high; 30, 50, and 80 MPa, respectively) have been used. Also, five different types of fibers have been used, where three types of steel fibers had normal strength (45/50BN, 65/40BN, 80/50BN) and two types of fibers were made of high-strength steel (80/30BP, 80/30BP).

After studying the literature, it was found that the addition of fibers can be very positive in structural elements where it is difficult to incorporate transverse reinforcement such as Hollow Core Slabs (HCS), manufactured by extrusion. The literature on HCS made with FRC is very scarce; also in addition, during manufacturing some problems raised up due to the addition of fibers. Therefore, an experimental program was carried out on HCS made with FRC, in which no manufacturing problems were detected, since the most interesting issue would be to take advantage of the fiber for industrial use. The experiments also seek to study different failure modes to analyze the contribution of the fibers, using different amounts of fibers and different a/d ratio. This experimental program is presented in Chap. 7.

Design Codes Used in Part III

For determining the shear strength, the most widely used international Design Codes have been used, such as the Eurocode 2 (EC2) and the Final Draft of the Model Code 2010 (MC2010). In this Ph.D. thesis, when MC2010 is used, it is going to be used as its Final Draft. The Final Draft of the MC2010 proposes formulations to determine the shear value of elements with and without fibers. On the contrary, the EC2 does not have a formulation to determine the fiber contribution to shear; therefore RILEM formulation is added to determine such contribution. Furthermore, as this thesis is mainly done in a Spanish university, shear values have also been calculated according to the Spanish Code “EHE08.” The latter is based on EC2 for the part of concrete without fibers and on RILEM to determine fiber contribution to shear.

Table III.1 Current codes shear formulas

Code	Theoretical shear (V)		Parameters	
	Concrete contribution V_{cu}	Fibers contribution V_{fu}	Without stirrups	With stirrups
EHE-08	$V_{cu} = [(C_1/\gamma_c) \cdot \xi \cdot (100 \cdot \rho_1 \cdot C_2)^{1/3} + 0.15 \cdot \sigma_{ck}] \cdot \beta \cdot b_o \cdot d$	$V_{fu} = k_f \cdot 0.7 \cdot \xi \cdot 0.5 \cdot 0.33 \cdot (f_{R3k}/\gamma_c) \cdot b_o \cdot d$	$C_2 = f_{cv}$ $C_1 = 0.18$ $\beta = 1$	$C_1 = 0.15$ $\beta = (*)$
EC-2 + RILEM	$V_{cu} = [(C_1/\gamma_c) \cdot \xi \cdot (100 \cdot \rho_1 \cdot C_2)^{1/3} + 0.15 \cdot \sigma_{ck}] \cdot \beta \cdot b_o \cdot d$	$V_{fu} = k_f \cdot 0.7 \cdot \xi \cdot 0.18 \cdot (f_{R4k}/\gamma_c) \cdot b_o \cdot d$	$C_2 = f_{ck}$ $C_1 = 0.18$ $\beta = 1$	$\beta = 0$ $V_{cu} = 0$
MC2010 (*) Without fibers	$V_{cu} = k_v \cdot (\sqrt{f_{ck}}/\gamma_c) \cdot z \cdot b_o$ (level III approximation)			
MC2010 (*) With fibers	$V_{cu} + V_{fu} = [(C_1/\gamma_c) \cdot \xi \cdot (100 \cdot \rho_1 \cdot C_2)^{1/3} + 0.15 \cdot \sigma_{ck}] \cdot \beta \cdot b_o \cdot d$ $C_2 = (1 + 7.5 \cdot (f_{ftuk}/f_{ctk})) \cdot f_{ck}$		$C_1 = 0.18$ $\beta = 1$	

(*) Final Draft of the MC2010

Table III.2 Parameters for the determination of the shear strength and their limitations

Common limitations for all Codes	
$\xi = 1 + \sqrt{(200/d)} \leq 2.0$	(1)
$\rho_1 = (A_s + A_p)/(b_o \cdot d) \leq 0.02$	(2)
Particular limitations of each Code	
$\sigma_{ck} = [(N_k + P_k)/(b_o \cdot d)] < 0.30 \cdot f_{ck} \leq 12 \text{ Mpa}$ (EHE-08)	(3)
$\sigma_{ck} = [(N_k + P_k)/(b_o \cdot d)] < 0.2 \cdot f_{ck}$ (EC2 and MC2010 for FRC)	(4)
$k_f = 1 + n \cdot (h_f/b_o) \cdot (h_f/d) \leq 1.5$ (EHE08 and RILEM)	(5)
$n = [(b_f - b_o)/h_f] \leq 3$ and $n \leq (3 \cdot b_o/h_f)$ (EHE08 and RILEM)	(6)
$V_{cu,min} = [(0.075/\gamma_c) \cdot \xi^{3/2} \cdot f_{cv}^{1/2} + 0.15 \cdot \sigma_{ck}] \cdot b_o \cdot d$ (EHE-08)	(7)
$V_{cu,min} = [0.035 \cdot \xi^{3/2} \cdot f_{cv}^{1/2} + 0.15 \cdot \sigma_{ck}] \cdot b_o \cdot d$ (EC2 and MC2010 for FRC)	(8)
$0.5 \leq \cotg \theta \leq 2.0 \rightarrow 26.57^\circ \leq \theta \leq 63.43^\circ$ (EHE-08)	(9)
$1 \leq \cotg \theta \leq 2.5 \rightarrow 22^\circ \leq \theta \leq 45^\circ$ (EC2)	(10)
β determination (EHE-08)	
$\beta = (2 \cdot \cotg \theta - 1)/(2 \cdot \cotg \theta_e - 1)$; if $0.5 \leq \cotg \theta < \cotg \theta_e$	(11)
$\beta = (\cotg \theta - 2)/(\cotg \theta_e - 2)$; if $\cotg \theta_e \leq \cotg \theta \leq 2.0$	(12)
Parameters influencing V_{cu} (MC2010)	
$\theta = 29^\circ + 7000 \cdot \varepsilon_x$	(13)
$\varepsilon_x = [M_{Ed}/z + V_{Ed} + 0.5 \cdot N_{Ed} - A_p \cdot f_{p0}]/[2 \cdot (E_s \cdot A_s + E_p \cdot A_p)]$	(14)
$k_v = 0.4 \cdot 1300/[1 + 1500 \cdot \varepsilon_x] \cdot (1000 + 0.7 \cdot k_{dg} \cdot z)$ if $\rho_w = 0$	(15)
$k_v = 0.4/(1 + 1500 \cdot \varepsilon_x)$ if $\rho_w \geq 0.08 \cdot \sqrt{f_{ck}/f_{yk}}$	(16)

Table III.3 Notations

a	Shear span
A_p	Cross-sectional area of prestressed reinforcement
A_s	Cross-sectional area of longitudinal tension reinforcement
A_α	Traditional shear reinforcement area
b_f	Flange width
b_o	Web width
d	Effective depth
f_{bpt}	Constant bond stress at which the prestress is transferred to the concrete at release of tendons
$f_{ctd}(t)$	Design tensile value of strength at time of release
f_{ctk}	Characteristic tensile strength value for the concrete matrix
f_{Fmk}	Characteristic ultimate residual tensile strength value for fiber-reinforced concrete
f_{p0}	Stress in strands when the strain in the surrounding concrete is zero
f_{R3k}	Residual flexural tensile strength corresponding to CMOD = 2.5 mm (according to EN 14651)
f_{R4k}	Residual flexural tensile strength corresponding to CMOD = 3.5 mm (according to EN 14651)
$f_{y\alpha,k}$	Yielding strength of shear reinforcement steel
I	Second moment of area
k_f	Factor to take into account the flanges contribution in the T-sections (EHE08 and RILEM)
l_{crit}	Critical length
l_{pt}	Transfer length
l_{pt2}	Upper bound value of the transmission length of the prestressing element: $l_{pt2} = 1.2 \cdot l_{pt}$
l_x	Distance of section considered from starting point of the transmission length
S	First moment of area above and about the centroidal axis
V_{cu}	Design shear resistance attributed to concrete
V_{fu}	Design shear resistance attributed to fibers
V_{su}	Design shear resistance provided by shear reinforcement
V_{u2}	Design shear resistance
z	Internal lever arm corresponding to the maximum bending moment. In the shear analysis, an approximate value $z = 0.9 d$ can be normally used
α	Inclination of stirrups in relation to the beam axis
α_l	$= l_x / l_{pt2} \leq 1$ for pretensioned tendons
β	Reduction factor referred to the transmission length ($\beta = 0.9$)
γ_c	Partial safety factor for concrete material properties
γ_s	Partial safety factor for the material properties of reinforcement and prestressing steel
ϵ_x	Longitudinal strain at the mid-depth of the member
η_{p1}	Coefficient that takes into account the type of tendon and the bond situation at release
θ	Inclination of the compression stresses
θ_e	Reference angle of cracks inclination

(continued)

Table III.3 (continued)

ξ	Factor that takes into account the size effect
ρ_l	Reinforcement ratio for longitudinal reinforcement
ρ_w	Percentage of shear reinforcement
σ_{ck}	Average stress acting on the concrete cross-section for an axial force due to prestressing actions
σ_{pm0}	Tendon stress just after release
φ	Reduction factor ($\varphi = 0.8$)
ϕ	Nominal diameter of the tendon

Table III.1 summarizes the formulations used in Part III, which includes Chaps. 4–7. The limitations of the shear design formulas are reported in Table III.2. Finally, a list with the notation of the main parameters used in Chaps. 4–7 of Part III is presented (Table III.3).

Chapter 4

Experimental Tests on Parameters Influencing on Shear

4.1 Introduction

This chapter develops and explains the criteria for obtaining self-compacting fiber reinforced concrete (SCFRC) and the analysis of its production quality continuity in a precast industry and its ulterior application to produce prestressed concrete beams to minimize traditional transverse rebars.

An experimental program consisting in nine prestressed I-beams with unequal flange dimensions was developed to analyze fiber contribution to shear behavior.

The main objective of the research described in this chapter is to analyze the shear behavior of real mass-produced prestressed beams made with high-strength self-compacting fiber-reinforced concrete (SCFRC). The main goals of the study were to:

- Propose a consistent SCFRC mix design adapted for continuous use in the precast industry.
- Evaluate the possibility of replacing all the transverse reinforcement and secondary rebars by steel fibers.
- Analyze the theoretical shear strength values according to the safety margins of current international Codes, which are obtained as the experimental-to-theoretical shear strength ratio.
- Check the possible influence of flange size on shear behavior.

4.2 Concrete Mix Designs

Reference SCC and a SCFRC with 60 kg/m^3 ($V_f = 0.75 \%$) of steel fibers, a nominal slump flow of 600 mm and an average compressive strength of about 60 MPa at 28 days were used in the study. This performance was chosen to obtain

self-compacting concretes with good compressive strength at an early age which could be poured without vibration, in line with precast prestressed beam production demands.

The materials used were: cement CEM I 52.5R and calcareous crushed aggregates based on filler, sand and 7/12 mm size coarse aggregates. The steel fibers (RC65/40BN) were low carbon with hooked-ends (40 mm long, 0.62 mm diameter and a nominal aspect ratio (length/diameter) equal to 65) and a tensile strength of 1,225 MPa.

The water/cement ratio and superplasticizer dosage were determined to reach the required strength and slump flow, respectively.

SCC mix design criteria [1], most of which are based on laboratory tests, suggest an increase in fines content. The final application needs experimental verification under working conditions, as when SCC contains fibers the fines content must be higher.

Based on the authors' previous research work [2], the concrete mix design was determined by adapting solid grading (including cement) to the theoretical Bolomey particle size distribution curve [3], defined as:

$$p = a + (100 - a)(d / D)^{1/2} \quad (4.1)$$

where “p” is the percentage passed through a “d” sieve, “D” is the concrete's maximum aggregate size and “a” is the Bolomey parameter [3], which depends on the desired workability of the concrete and aggregates properties.

For the concretes in this study, the “a” values used were: a = 16 for SCC and a = 20 for SCFRC. The relatively low “a” parameter was due to the inclusion of well graded sand.

Table 4.1 shows the mix design for both concretes. The theoretical and actual particle size distribution curves are plotted in Fig. 4.1.

Table 4.1 Mix design adaptation (kg/m³)

(kg/m ³)	SCC	SCFRC
7/12 aggregate	846	721
Sand	924	985
Filler	41	50
Cement	440	460
Water	198	205
Fibers (RC65/40BN)	0	60
Superplasticizer	11.1	12.8
W/C ratio	0.45	0.45

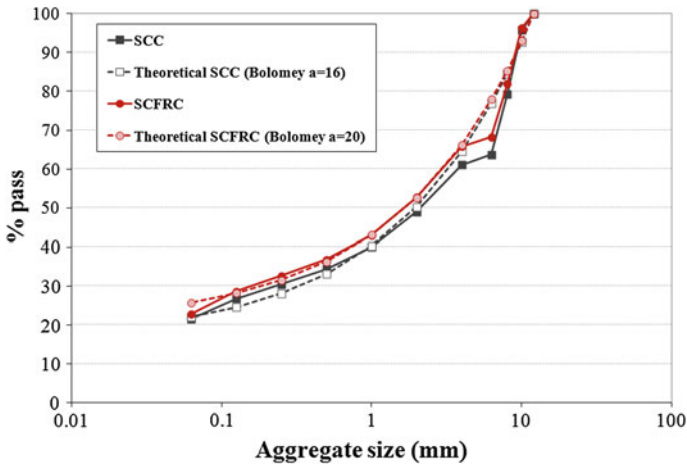


Fig. 4.1 Theoretical versus actual particle size distribution curves for selecting the mix design

4.3 Concrete Properties and Production Control

Figure 4.2 shows SCFRC concrete being poured into a beam formwork with no compacting process. A consistent mix design was used, suitable for continuous precast production processes.

In order to analyze the mix robustness, an exhaustive production quality control took place in the experimental program and a 2 m³ mix was used to cast all nine beams. The following tests were done on samples from each mix: slump-flow test (EN 12350-8), compressive strength test on 150 × 300 mm cylinder specimens (EN 12390-3) and flexural tensile strength test (EN 14651). The flexural test gave the

Fig. 4.2 Concrete pouring into the formwork



following results: the limit of proportionality (f_{ct1}) and the residual flexural tensile strength ($f_{R,j}$) of the crack mouth opening displacements (CMOD) linked to the crack openings of 0.5, 1.5, 2.5 and 3.5 mm ($j = 1, 2, 3, 4$ respectively). All the mixes reached slump flow test values of between 550 and 710 mm, which were sufficient to be able to pour the concrete into the beam formwork.

Table 4.2 shows the mechanical properties of the different concrete mixes for each beam. Each of them had a Specimen ID for identification (Table 4.2) as follows:

{Concrete: with fibers (HF) or without fibers (H)}–{Top flange width, b_f (mm)}–{“h” if the depth of the beam is 800 mm, otherwise = 750 mm}–{“TR” with transverse reinforcement equal to $\phi 8@300$ mm-2 legs}–{number of the beam}

For example, beam HF600TR/1 was made with fiber reinforced concrete transversally reinforced with stirrups and had a top flange width equal to 600 mm.

All the mechanical values (Table 4.2) were obtained as the average of three specimens 28 days after casting. In order to analyze production continuity, the mean values, standard deviations (SD) and coefficients of variation (CoV) of the results are included.

It is noteworthy that the FRC was observed to have brittle behavior during the flexural tensile strength tests, as can be seen from the fact that $f_{R,3}$ and $f_{R,4}$ are clearly lower than $f_{R,2}$. A 2 mm crack opening was often reached with the severance of several fibers without them sliding out of the concrete, and sometimes a brittle rupture occurred before being able to determine the residual strength of $f_{R,3}$ and $f_{R,4}$. A possible reason for this could be the combination of a high-strength concrete matrix with steel fibers and low carbon (65/40BN). This should be taken into account in future work. The values in Table 4.2 are those of at least two specimens.

Table 4.2 Mechanical concrete properties (average values)

Specimen ID	f_c (MPa)	f_{ct1} (MPa)	f_{R1} (MPa)	f_{R2} (MPa)	f_{R3} (MPa)	f_{R4} (MPa)
HF600TR/1	61.1	3.36	5.26	5.13	–	–
HF600TR/2	65.7	4.39	9.36	9.56	6.89	4.96
H600TR/3	52.4	3.64	–	–	–	–
HF600/4	65.4	4.70	10.46	7.99	6.24	5.12
HF600/5	65.9	4.20	8.55	8.43	5.55	3.92
HF400h/6 ^a	59.5	4.45	8.96	7.49	5.96	4.57
HF400/7	63.5	4.08	6.64	6.70	4.77	3.41
HF400/8	70.0	4.33	8.10	7.02	4.68	3.13
HF260/9	65.0	3.11	6.45	4.38	–	–
Average	63.17	4.03	7.97	7.09	5.68	4.18
SD	4.75	0.51	1.61	1.59	0.79	0.75
CoV (%)	8	13	20	22	14	18

^a All the beams have a height of 750 mm with the exception of the HF400h/6 beam having a height equal to 800 mm (this is indicated with the letter “h” whose significance is explained in the text)

The smallest variation was obtained for compressive strength, with 8 % CoV. The residual flexural strengths values were in a wider range, with CoV between 13 and 22 %. This means that for residual flexural strength, dispersion can only be controlled at levels higher than those obtained for compression strength in traditional concrete production. In fact, it should be noted that high CoV for residual strength values is very common in flexural testing, no matter how it was cast (FRC cast in a controlled laboratory environment typically has a CoV of 20 % [4]).

di Prisco et al. [5] obtained a higher dispersion for the residual parameters from an SCFRC used as a top slab (26.8–34.6 %) when casting concrete with a small proportion of fibers and under in situ production conditions.

4.4 Experimental Program and Results Analysis

4.4.1 Main Variables and Beams Production

Nine six meter-long prestressed I-beams were cast with different flange dimensions. Figure 4.3 shows the beams’ cross-section and reinforcement.

Prestressed beams were over-reinforced longitudinally with 11 tendons (0.6" diameter with a nominal cross-section equal to 140 mm²) of 7 wires (Y 1860 S7). Their initial tension was 1,354 MPa (before pre-stress losses, which can account for approximately 26.2 %). This reinforcement guarantees the shear failure of the beam. This longitudinal reinforcement means that $p_l = 1.83\%$ for all the beams, except for specimen HF400h/6, with $p_l = 1.71\%$. All the rebars used for stirrups or additional reinforcement were made out of type B 500 S steel.

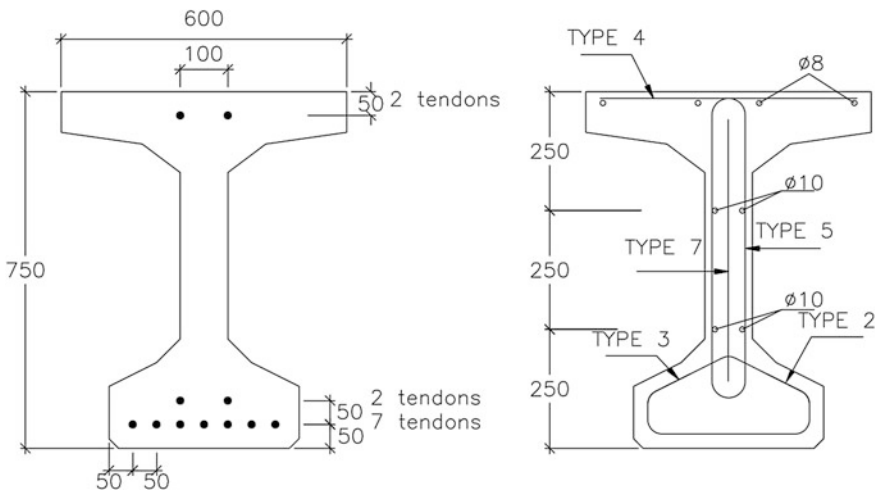


Fig. 4.3 Cross-section. Dimensions in mm

The experimental program variables were:

- Top flange width (260 mm; 400 mm; 600 mm)
- Concrete type (SCC or SCFRC)
- Presence or absence of traditional transverse reinforcement ($\phi 8$ stirrups each 300 mm, amount indicated in Table 4.3 as $\phi 8@300 \text{ mm}^{-2}$ legs)
- Use of additional reinforcement, which is normally placed in beams made with SCC to control secondary failures (Fig. 4.4)
- The effect of increasing the depth of the top flange was also analyzed, when the depth of the beam (h) was either 750 or 800 mm.

Additional reinforcement (type 7) was placed at both ends of all the beams to avoid shear failures caused by the direct application of the tensile force (Fig. 4.4).

Table 4.3 shows the combination of variables for each beam tested.

Table 4.3 Main study variables

Specimen ID	Top flange width (mm)	Transverse reinforcement	Fibers (kg/m^3)	Depth (mm)	Additional reinforcements (types)
HF600TR/1	600	$\phi 8@300 \text{ mm}^{-2}$ legs	60	750	2, 3, 4
HF600TR/2	600	$\phi 8@300 \text{ mm}^{-2}$ legs	60	750	2
H600TR/3	600	$\phi 8@300 \text{ mm}^{-2}$ legs	0	750	2, 3, 4
HF600/4	600	0	60	750	2, 3, 4
HF600/5	600	0	60	750	–
HF400h/6	400	0	60	800	–
HF400/7	400	0	60	750	–
HF400/8	400	0	60	750	2, 3, 4
HF260/9	260	0	60	750	–

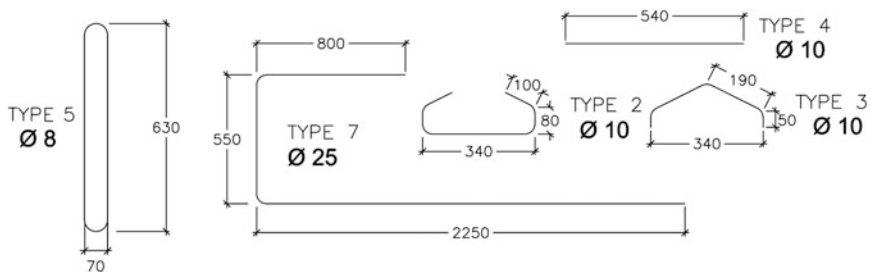


Fig. 4.4 Additional reinforcement typologies. Dimensions in mm

4.4.2 Testing Procedure

The beams were tested with simple supports and were subjected to two point loads. The distance between supports was 5.00 m and the shear span/depth ratio (a/d) was 3.0 in all cases, except for beam HF400h/6, with $a/d = 2.8$.

The two loads were applied to the beams by one 2,500 kN hydraulic jack applied at a rate of 0.5–2.0 kN/s. To monitor the behavior of the beams, the applied loads and vertical deflections were measured using a load cell and three displacement transducers placed on the middle span at the center of each shear span. All the variables were continuously registered by the data acquisition system. Photography and video cameras were also utilized in both the shear span zones on both sides of the beams. A synchronized recording system allowed us to assign each photogram to the corresponding load. The maximum shear crack opening versus load curve was obtained from a photo analysis. Figure 4.5 shows the test set-up.

4.4.3 Results

As expected, all the beams suffered shear failure and presented diagonal cracks accompanied by minor flexural cracks. Table 4.4 shows the maximum load obtained for each beam. Greater shear capacity was obtained when stirrups and fiber acted simultaneously (Beams HF600TR/1 and HF600TR/2), reaching a value of 18.5 % higher than that of the beam with traditional stirrups only (Beam H600TR/3). No significant difference was found between the two beams with both stirrups



Fig. 4.5 Beam during shear test

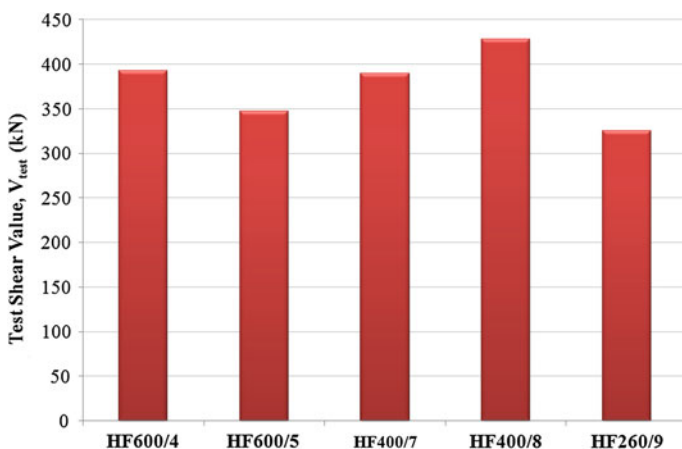
Table 4.4 Experimental shear strength (kN) for each tested beam

Specimen ID	V_{test} (All beams)	V_{test} (Beams only with fibers, not stirrups)
HF600TR/1	571.61	–
HF600TR/2	592.70	–
H600TR/3	491.34	–
HF600/4	392.44	392.44
HF600/5	347.17	347.17
HF400h/6	420.03	–
HF400/7	389.95	389.95
HF400/8	428.31	428.31
HF260/9	325.58	325.58
Average	–	376.69
SD	–	36.26
CoV (%)	–	9.62

and fibers. The additional reinforcement types 3 and 4 (Fig. 4.4) in Beam HF600TR/1 did not improve the shear capacity.

The beam with stirrups only also showed greater shear strength (an average of 30.4 %) than all the other beams with only fibers as shear reinforcement.

The differences among the fiber-only beams were clearly less significant. Although beam HF260/9 had the lowest shear strength, it is not possible to confirm any clear influence of flange width, as no clear differences in shear strength were observed for beams with flange widths between 400 and 600 mm (Fig. 4.6). Table 4.4 provides the test values of the shear strength of fiber-only reinforced beams of the same height. The low CoV value (9.62 %) was similar to the

**Fig. 4.6** V_{test} (kN) comparison of fiber-reinforced beams with a variable top flange width

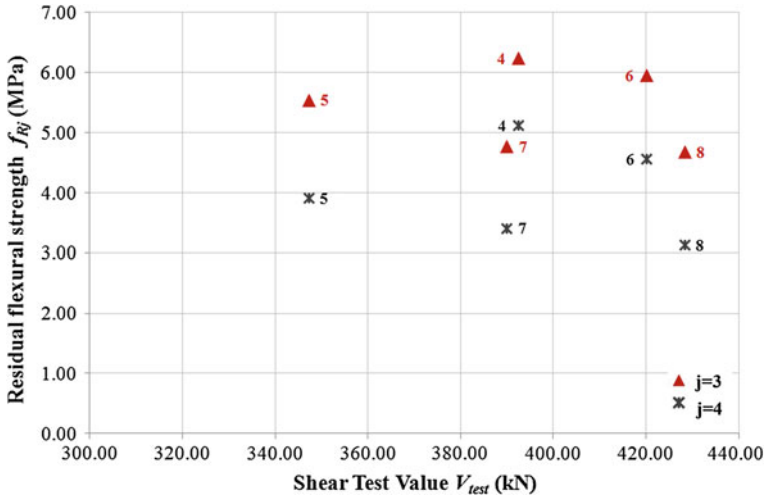


Fig. 4.7 V_{test} - f_{Rj} response for each beam (the number of the beam is next to each point)

compressive strength dispersion found in this study and indicates the absence of flange influence.

It seems that these additional reinforcements (types 2, 3, and 4) could have an influence on fiber-only beams without stirrups, although there are not enough data to confirm this.

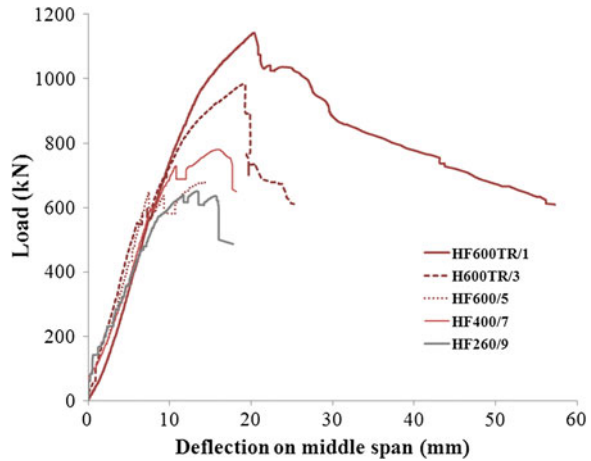
Since the fibers contribution to shear-bearing capacity depends on the efficiency of the fibers, it should be possible to find a correlation between the shear strength of the beams and their concrete flexural residual strength. However, in this experimental campaign the dispersion of the residual strength (see Table 4.2) did not show a clear trend (Fig. 4.7).

Based on these results, when analyzing the parameters influencing shear capacity, concrete residual flexural strength was considered a constant parameter and was evaluated as the average of the residual strengths obtained from the eight beams containing fibers. Identical criteria were applied for the concrete compressive strength.

4.4.3.1 Load-Deflection Response

Figure 4.8 shows the load versus mid span deflection response for one beam for each combination of top flange width and shear reinforcement conditions. The other beams were eliminated for clarity's sake. The beams with stirrups and fiber shear reinforcement showed a ductile failure with controlled post-peak behavior. All the others, including the one with stirrups-only and no fibers, revealed brittle failure with a sharp drop after the peak. No clear differences in ductility (post-peak behavior) were observed between the beams reinforced with only fibers or only stirrups.

Fig. 4.8 Load-deflection responses on middle span



4.4.3.2 Crack Patterns and Load-Crack Width Responses

The crack pattern evolution on shear span at different loads is shown in Fig. 4.9 as a selection of the main types of beams with the same geometry. The crack widths were measured by means of video recording and image analysis. Figure 4.10 gives the load-crack width response of the beams. These figures make it possible to analyze the influence of the type of reinforcement: transverse, stirrups (TR) or fibers or both. The other variables analyzed did not significantly affect this behavior. As can be seen in Fig. 4.9, HF600TR/2 achieved the highest ultimate load and its first visible crack appeared at a higher load than the other beams. Comparing H600TR/3 (stirrups only) with HF600/4 (fibers only), Fig. 4.9 clearly shows that stirrups reduce the number of cracks but they are wider than those in HF600/4. The fiber-only beams (HF600/4) showed thinner cracks that were closer together.

The average crack inclination was very close to 22° for all the beams.

BEAM			
	HF600TR/2	H600TR/3	HF600/4
	Load level for each crack line color		
	750 kN	600 kN	600 kN
	900 kN	700 kN	700 kN
	1100 kN	800 kN	750 kN
	FAILURE		

Fig. 4.9 Cracking patterns. Crack appearance and its corresponding load level

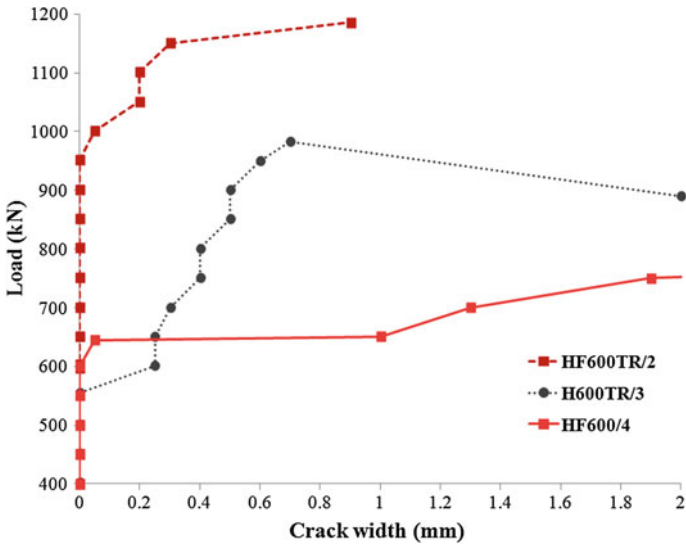


Fig. 4.10 Crack widths (mm) on beams for different shear reinforcement combinations

In the fiber-only beams (HF600/4) only a few cracks developed at low loads (≈ 600 kN), but one of them opened quickly. In H600TR/3, which had only traditional reinforcement, the cracks were more noticeable, very straight and highly parallel. At very low loads (≈ 600 kN) some crack openings of about 0.3 mm were noted and advanced rapidly. In all the SCFRC and stirrups-only beams the crack which produced the failure either coincided with a previous crack or was generated from previous cracks. HF600TR/2 (traditional reinforcement and fibers) developed a larger number of smaller cracks fairly close together. Shear cracks only appeared at high loads and reached widths of 0.2 mm only near ultimate loads. The cracks grew slowly but were easy to control. The crack that finally caused the failure appeared at a very high load from two existing parallel cracks and had a flatter final crack slope.

To sum up, clearly improved ductility was detected only in SCFRC beams with stirrups and when fibers plus traditional transverse reinforcement led to a 35 % increment in maximum load for the same crack width. In fact, the crack width of the beam with traditional transverse reinforcement only (H600TR/3) was 0.4 mm for a load of 750 kN. The same beam with fibers (HF600TR/2) reached an ultimate load (1,150 kN) 35 % higher than the fiber-only beams.

4.4.4 Shear Values Calculated with the Current Design Codes

Shear strength capacities were calculated from current Codes EHE08 [6], EC2 [7] and the final draft of MC2010 [8]. The formulations are shown in *Introduction to Part III*.

It is important to clarify that the first complete draft of the Model Code was used as it was the latest version available when the results were analyzed. On the other hand, as EC2 has no formulation which includes the fiber contribution, it was calculated by following the RILEM approach [9].

The notation (see *Introduction to Part III*) and formulas were adapted to facilitate comparisons and have the following general structure:

$$V_{u2} = (V_{cu} + V_{fu}) + V_{su} \quad (4.2)$$

All the Codes consider the contribution of the traditional transverse reinforcement (V_{su}) in the same way and are evaluated according to the following expression:

$$V_{su} = z \cdot \text{sen } \alpha \cdot (\text{cotg } \alpha + \text{cotg } \theta) \Sigma A\alpha \cdot f_{y\alpha, k} \quad (4.3)$$

No Code considers the explicit influence of crack inclination on the evaluation of the fiber contribution or proposes a fiber effect on the θ value considered in the shear reinforcement contribution (V_{su}). The fibers are therefore considered separately from stirrups.

The theoretical shear strength values were calculated by the following criteria (for each Code):

- MC2010: Beam H600TR/3 (without fibers) was calculated by applying the most accurate form (Level III of Approximation), which permits the calculation of ϵ_x and directly calculates the corresponding inclination of the compression stresses (θ). Level III of Approximation was based directly on the equations of the Modified Compression Field Theory (MCFT) [10]. Other beams (with fibers) were calculated by applying the formula proposed in MC2010, which includes the effect of fibers inside the concrete matrix contribution.
- EHE08: This reference angle of cracks inclination (θ_e) was taken to be equal to the inclination of compression stresses (θ) calculated according to the general method of the EHE (analogous to the MCFT): $\theta = \theta_e$.
- EC2: When considering shear in beams with stirrups, EC2 neglects the concrete contribution to shear (V_{cu}). Several authors, including the EC2, have doubts about the concrete contribution to shear when stirrups are needed. Cladera and Marí [11, 12] concluded that the EC2 procedure is very easy to use but its results are very scattered. On the one hand, it may be too conservative for slightly shear-reinforced beams or for prestressed beams; and on the other it may prove slightly underestimated for heavily reinforced members. For the EC2, θ value

was determined by equaling the ultimate capacity for yielding stirrups with the ultimate capacity for crushing of concrete struts (see Commentary to Eurocode [13]). For all beams, $\theta \approx 13^\circ$ was obtained, so θ values were lower than the minimum bound value 21.8° , corresponding to $\cotg \theta = 2.5$; $\theta = 21.8^\circ$ was therefore used for the calculations.

To obtain predictable concrete resistance, partial safety factors for material properties were considered in the calculation as $\gamma_c = 1$ and $\gamma_s = 1$ and average values were utilized when a characteristic value appeared in a formula.

Code formulas include limitations on several parameters such as the ρ_l reinforcement ratio for longitudinal reinforcement, the ξ factor which takes into account the size effect, the σ_{ck} average stress acting on the concrete cross-section for an axial force due to prestressing actions and minimum concrete contribution to shear V_{cu} , as presented in the *Introduction to Part III*. None of these limitations affected the values calculated in the beams tested in this study.

Table 4.5 presents the theoretical shear strength values calculated with the current Codes for each beam. Figures 4.11 and 4.12 represent contributions to shear by means of concrete, stirrups and fibers for the Spanish Code EHE08, the EC2 and the MC2010, for all of the beams tested. In Fig. 4.11, the results were evaluated by considering average values without applying safety factors. Figure 4.12 reproduces the values evaluated by considering design values (obtained by dividing the characteristic value by its corresponding material safety factor).

As all the formulas (except MC2010 for concrete without fibers) include an identical and explicit term after considering the favorable effect of prestressing reinforcement on the concrete contribution, a line showing the level of this effect has been drawn in Figs. 4.11 and 4.12.

Figure 4.12 shows how the fiber effect is underestimated by the Codes, in particular by MC2010. Finally, Table 4.6 reports the shear contributions as a percentage attributable to stirrups, concrete and fibers.

Table 4.5 Shear strength (kN) calculated from the current design codes without safety factors

Specimen ID	V_{test}	V_{EHE08}	$V_{EC2+RILEM}$	V_{MC2010}
HF600TR/1	571.61	491.21	423.76	474.40
HF600TR/2	592.70	491.21	423.76	474.40
H600TR/3	491.34	384.99	331.55	404.34
HF600/4	392.40	281.62	290.97	249.58
HF600/5	347.20	281.62	290.97	249.58
HF400h/6	420.00	298.81	308.86	261.58
HF400/7	390.00	292.91	302.40	259.42
HF400/8	428.30	292.91	302.40	259.42
HF260/9	325.60	292.19	300.72	269.24

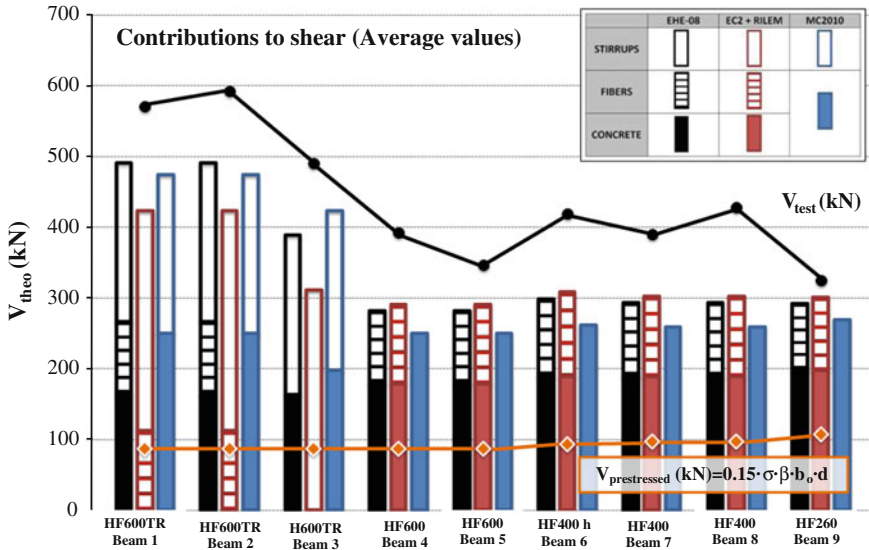


Fig. 4.11 Contributions of concrete, stirrups and fibers to the ultimate theoretical shear strength capacity (average values)

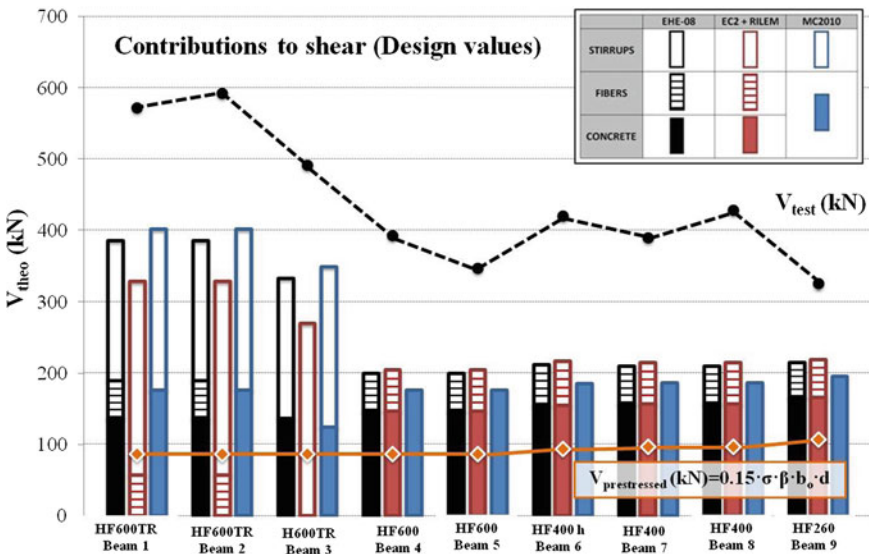


Fig. 4.12 Contributions of concrete, stirrups and fibers to the ultimate theoretical shear strength capacity (design values)

Table 4.6 Shear contributions (%) due to stirrups, concrete and fibers according to the current design codes (without safety factors)

Specimen ID	EHE08			EC2 + RILEM			MC2010		
	Stirrups	Concrete	Fibers	Stirrups	Concrete	Fibers	Stirrups	Concrete	Fibers
HF600TR/1	46	33	21	74	0	26	47	53	
HF600TR/2	46	33	21	74	0	26	47	53	
H600TR/3	58	42	0	100	0	0	56	44	0
HF600/4	0	63	37	0	61	39	0	100	
HF600/5	0	63	37	0	61	39	0	100	
HF400h/6	0	63	37	0	61	39	0	100	
HF400/7	0	64	36	0	62	38	0	100	
HF400/8	0	64	36	0	62	38	0	100	
HF260/9	0	68	32	0	66	34	0	100	

4.4.4.1 Flange Effect on Shear Strength

Some authors [14–18] have studied the effect of flange width on shear capacity with “I” and T-beams. Zsutty [17] proposed an equation to calculate the shear carried by concrete with a factor h_f (flange thickness). However he considered it reasonable to ignore the strengthening effect of the flange for design purposes. Current Design Codes do not include this effect in their formulation for plain concrete members. However, in the RILEM model factor (k_f) takes into account the flange contribution to shear due to fibers appearing.

The k_f factor in Codes EHE08 and RILEM, which takes into account flange contribution in the T-sections calculated by the formula in *Introduction to Part III*, is equal to 1 for rectangular sections and increases when there is a flange. With the cases presented here, k_f is equal to 1.5 for flange widths of up to 400 mm and we detected no flange effect among the beams in the present study with flange widths of these sizes. In contrast, k_f equaled 1.35 for the smallest flange width tested (260 mm).

In Fig. 4.13, the EC2 safety margins were plotted for the steel fiber-only beams. In this graph, the theoretical values were obtained with the EC2 formulations, and the RILEM proposal was added to evaluate the shear contribution due to steel fibers (EC2 formulations do not include the k_f factor, but it is included in RILEM). Four different options were therefore calculated:

1. $k_f = 1.5$.
2. $k_f = 1$.
3. k_f was applied exactly as proposed in the RILEM approach.
4. k_f was applied as proposed in the RILEM approach, but without its limitations (see *Introduction to Part III*).

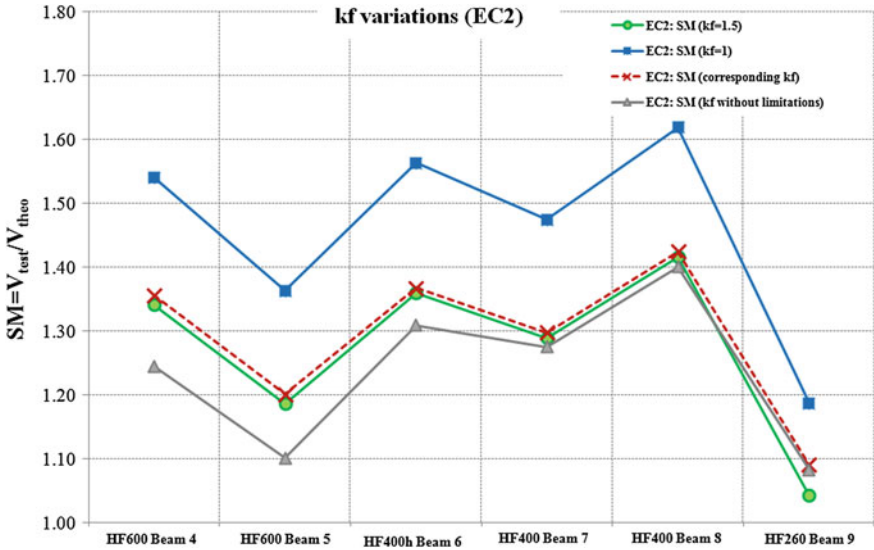


Fig. 4.13 SM variations when different flange factor values are applied

When k_f was not applied (2nd option), highly conservative SM (safety margin) values were obtained (Fig. 4.13). If the 4th option is observed (k_f without limitation) it is clear that SM is lowered for 600 mm flange widths, meaning that the application of limitations is necessary.

In Sect. 4.4.3 it was concluded that, although the beam with the smallest flange width ($b_f = 260$ mm) presented the lowest shear strength, it was not possible to confirm any clear influence of the flange width as no clear differences in shear strength were observed for beams with flange widths up to 400 mm. This is in complete agreement with the results given in Fig. 4.13, in which the most balanced option (when comparing the theoretical and experimental results) may be obtained by applying the corresponding k_f value (3rd option) for the cases in which $h_f > 400$ mm. Only the beam with a low b_f value ($b_f = 260$ mm) was not conservative enough with this criterion. In this case it cannot be considered that the flange width has an influence on shear strength and therefore $k_f = 1$ should be applied.

4.4.4.2 Assessment of Shear Formulations from Current Design Codes

The safety margins (SM) obtained as V_{test}/V_{theo} (the shear test value divided by the theoretical shear value) were used as a reference to compare the results obtained from the different beams and Codes.

In order to achieve a more complete analysis of the SMs of the current Design Codes, Fig. 4.14 shows how the SMs of the different codes were plotted for the

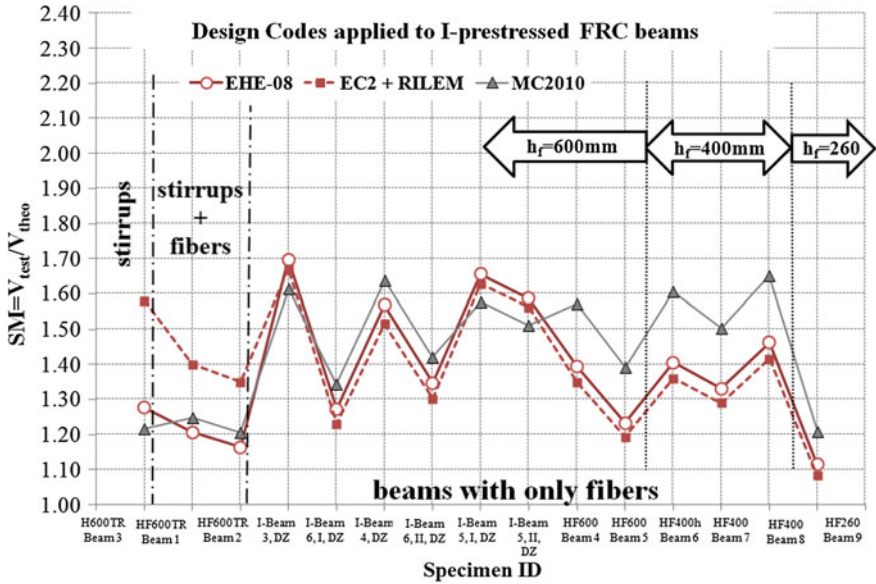


Fig. 4.14 Safety margin = V_{test}/V_{theo} without safety factors

beams tested in the experimental program presented here, along with six more beams corresponding to Minelli’s Ph.D. thesis [19]. Minelli’s beams were similar to our HF600 series (prestressed, reinforced only with fibers, a depth of 700 and 600 mm flange width).

The toughness properties of Minelli’s concretes were evaluated by means of four point-bending tests to determine equivalent strengths such as f_{eq} (0.6–3.0). These values are normally assumed to be f_{R3} in the literature. The authors observed that if the limitation for the longitudinal reinforcement according to the EC2 and EHE08 ($\rho_{l,max} = 0.02$, see *Introduction to Part III*) is applied in beams with very high amounts of longitudinal reinforcement (which is the case in Minelli’s database), the theoretical shear values are too conservative. This reasoning, coupled with Cladera’s assertion [20], by which the limitation of longitudinal reinforcement could be extended from 2 to 4 %, led the authors to apply the real value of the longitudinal reinforcement ratio for the calculations, even though it exceeded the limitations.

The graph in Fig. 4.14 is divided into three parts: beams reinforced only with stirrups, stirrups with fibers and, fiber-only. The beams were arranged in descending flange-width order.

All the Codes presented safety margins greater than “1”, which means a safe shear strength evaluation for beams reinforced with fibers only (Fig. 4.14). MC2010 shows well balanced SM for a range of flange widths (b_f). This formula (see *Introduction to Part III*) considered the whole effect of fibers as it multiplied the longitudinal reinforcement ratio by a parameter which included the compressive strength and toughness properties of the FRC. In this way, one of the fiber effects,

that of improving the dowel action by increasing the bond between the rebar and concrete matrix [21], was implicit. The improved dowel action by the fibers was too significant for beams with very high longitudinal reinforcement ratios ($\rho_l > 2\%$) to be left out of consideration, as with EC2. The application of EC2, with RILEM or EHE08 formulas, to Minelli's beams with large amounts of longitudinal reinforcement (ρ_l), led to a higher SM.

The current MC2010 formula for FRC offers a major advantage as compared to EC2 + RILEM, since in MC2010 the longitudinal reinforcement ratio is modified by the toughness properties of the FRC, which are not considered in EC2 + RILEM.

MC2010 is highly conservative for all FRC beams. It should be noted that the limit of the longitudinal reinforcement ratios was equal to 2% and was not applied in the values reported in Fig. 4.14 (otherwise, the SM obtained for the Minelli's beams would have been higher).

When stirrups were present, MC2010 with Level III of Approximation (see *Introduction to Part III*), or EHE08, were clearly better adjusted. In these cases the SM was close to 1.2 and was noticeably narrower than the values obtained for FRC (about 1.5). This may be justified by less confidence in the continuity of the FRC toughness properties. Additional studies will obviously have to be carried out to validate a more precise proposal.

4.5 Conclusions

An experimental program was carried out including shear tests on nine prestressed FRC I-beams with unequal flange dimensions. Self-compacting FRC was cast with good production continuity, according to the slump flow test, with compressive strength and flexural behavior up to industrial standards and small variations in quality. The results indicate that including steel fibers in beams with stirrups provides a more ductile behavior [22]. According to the analysis of failure modes, deflections and cracking patterns the following conclusions can be drawn:

- Steel fibers control not only the appearance of cracks but also their propagation.
- With steel fibers more cracks are created but these are narrower than without fibers and crack spacing is smaller.
- Steel fibers positively interact with traditional transverse reinforcement (additive effect).
- Fibers give concrete an enhanced tension-stiffening mechanism.
- The results obtained from the tested beams indicate that the presence of a flange does not make a clear difference to the ultimate load capacity. These results are in agreement with the fact that the flange factor in shear (k_f) does not vary for $b_f > 400$ mm, according to RILEM.
- The application of RILEM design equations leads to results which vary widely as a function of the longitudinal reinforcement ratio.

- In MC2010 the fiber contribution increases when beams have high longitudinal reinforcement ratios. MC2010 shows well-balanced safety margins for a range of flange widths (b_f) and reinforcement ratios. However, these SMs are conservative.
- Even though all the Codes underestimate the fiber effect on shear, a less conservative approach is needed in the MC2010 proposal.

4.6 Publication of These Results

The results of this paper have been published in the journal *Construction and Building Materials*:

Estefanía Cuenca; Pedro Serna. SHEAR BEHAVIOR OF PRESTRESSED PRECAST BEAMS MADE OF SELF-COMPACTING FIBER REINFORCED CONCRETE. *Construction and Building Materials*. 45, pp. 145–156. Elsevier, 2013. DOI: <http://dx.doi.org/10.1016/j.conbuildmat.2013.03.096>.

References

1. EFNARC. 2005. The European guidelines for self-compacting concrete. specification, production and use. <http://www.efnarc.org/pdf/SCCGuidelinesMay2005.pdf>.
2. Serna, P., Cuenca, E. and M.S. Alves de Oliveira, 2011. Self-compacting fiber reinforced in precast elements production for shear resistance. In *Dedicated to Innovation: 50 years MC-Bauchemie*, MC-Bauchemie Müller GmbH Co. KG.
3. Bolomey, J. 1947. The grading of aggregate and its influence on the characteristics of concrete. *Revue des Matériaux de Construction et des Travaux Publics* 147–149.
4. Bernard, E.S. 2002. Correlations in the behaviour of fibre reinforced shotcrete beam and panel specimens. *Materials and Structures* 35: 156–164.
5. di Prisco, M., Plizzari, G.A. and L. Vandewalle, 2009. Fibre reinforced concrete: New design perspectives. *Materials and Structures* 42: 1261–1281.
6. EHE-08. 2008. Instrucción de Hormigón Estructural EHE-08, Comisión Permanente del Hormigón, Ministerio de Fomento, 2008; URL (Spanish Instruction EHE-08 (english versión)). www.fomento.gob.es/MFOM/LANG_CASTELLANO/ORGANOS_COLEGIADOS/CPH/Publicaciones/EHE_ingles/.
7. Eurocode 2: Design of Concrete Structures—EN 1992-1-1, European Committee for Standardization; 2005.
8. MC2010. 2012. Fib Bulletin 65–66. Model Code—Final draft.
9. Rilem, T.C. 2003. 162-TDF: Test and design methods for steel fibre reinforced concrete, Stress-strain design method. *Final Recommendation*. *Materials and Structures* 36: 560–567.
10. Vecchio, F.J., and M.P. Collins, 1986. The modified compression field theory for reinforced concrete elements subjected to shear. *ACI Journal* 83(2): 219–231.
11. Cladera, A., and A.R. Mari, 2007. Shear strength in the new Eurocode 2. A step forward? *Structural Concrete* 8(2): 57–66.
12. Cladera, A., and A.R. Mari, 2004. Shear design procedure for reinforced normal and high-strength concrete beams using artificial neural networks. Part II: beams with stirrups. *Engineering Structures* 26: 927–936.

13. European Concrete Platform ASBL. 2008. *Commentary to Eurocode 2*. Belgium: Brussels.
14. Leonhardt, F. 1970. Shear and torsion in prestressed concrete. In FIP Congress, Prague.
15. Leonhardt, F., and R. Walther, 1964. The Stuttgart shear tests, 1961. Cement and Concrete Association.
16. Placas, A., and P.E. Regan, 1971. Shear failures of reinforced concrete beams. *Proceedings of American Concrete Institute* 68: 763–773.
17. Zsutty, T.C. 1972. Unpublished memorandum to reinforced concrete research council.
18. ACI-ASCE Committee.426. 1973. The shear strength of reinforced concrete members. *Journal of the Structural Division ASCE* 1973; 99 (6): 1091–1187.
19. Minelli, F. 2005. Plain and fiber reinforced concrete beams under shear loading: Structural behavior and design aspects. PhD thesis, Brescia, Italy: Department of Civil Engineering, University of Brescia.
20. Cladera, A., and A.R. Mari, 2004. Shear design procedure for reinforced normal and high-strength concrete beams using artificial neural networks. Part I: beams without stirrups. *Engineering Structures* 26(7): 917–926.
21. Swamy, R.N., and H.M. Bahia, 1985. The effectiveness of steel fibers as shear reinforcement. *Concrete International* 7(3): 35–40.
22. Cuenca, E., and P. Serna, 2013. Shear behavior of prestressed precast beams made of self-compacting fiber reinforced concrete. *Construction and Building Materials* 45: 145–156.

Chapter 5

Experimental Tests on Fibers Influence on the Size Effect on Shear

5.1 Introduction

In this chapter it will be discussed the possibility of steel fibers to mitigate the size effect in large beams. For that, an experimental program consisting in 9 beams with $h = 500, 1,000$ and $1,500$ mm, made with three types of concretes with 0, 50 and 75 kg/m^3 of fibers was done. The beams were tested with $a/d = 3$ for all cases. The concrete was manufactured in a concrete plant of *Italcementi Group*, while the tests were carried entirely at the laboratory “*Pietro Pisa*” of the University of Brescia.

5.2 Materials

The beams have been casted in different times using three different mix design. Specific concrete proportions have been used for mixing plain concrete (samples PC) and fiber reinforced concrete with an amount of fibers of 50 kg/m^3 (samples FRC50) and 75 kg/m^3 (samples FRC75). All mixtures have been mixed in a precast manufacturing plant of *Italcementi Group* (Fig. 5.1) situated in Mompiano (Brescia) and concrete was provided to the university by mixing trucks.

The materials used were a CEM I 42.5R cement type, sand 0/4 mm and coarse aggregates with a maximum size of 16 mm. The concretes had a water/cement ratio equal to 0.41. As it can be seen in Table 5.1, mix designs only differ on the amounts of fibers and superplasticizer. The fibers used were low carbon steel with hooked-ends: 50 mm length, 0.8 mm diameter, and a nominal aspect ratio (length/diameter) equal to 62.5. Fibers were provided by *La Matassina Group* and its product “*La Gramigna*” fibers was used (Fig. 5.2).

Table 5.1 shows the three concrete compositions.

Table 5.2 show the fibers geometry and their characteristics.



Fig. 5.1 Concrete manufacturing plant

Table 5.1 Mix design of plain and fiber reinforced concretes

Beams	PC	FRC50	FRC75
Cement type	CEM I-42.5R	CEM I-42.5R	CEM I-42.5R
Cement content (kg/m ³)	410	410	410
Sand 0/4 (kg/m ³)	1,073	1,073	1,073
Coarse aggregate 4/16 (kg/m ³)	645	645	645
Maximum aggregate size (mm)	16	16	16
Fibers (kg/m ³)	0	50	75
Water-cement ratio	0.41	0.41	0.41
Super-plasticizer (l/m ³)	4.1	4.8	5.7

Fig. 5.2 Fibers used



Table 5.2 Characteristics of the fibers adopted

Designation	50/0.80
Type of steel	Carbon
Shape	Hooked
Minimum tensile strength (MPa)	1,100
Length (mm)	50
Diameter (mm)	0.8
Aspect ratio l/ϕ	62.5

5.3 Concrete Properties and Production Control

For evaluating the mechanical properties of concrete, an exhaustive production quality control took place in the experimental program. Cylinders, cubes, round panels and prismatic specimens were produced, as shown Fig. 5.3.

The following tests were done: the slump-flow (EN 12350-8), compressive strength (EN 12390-3) and three point bending (EN 14651). The following was obtained from the flexural test: the limit of proportionality (f_{ct}) and the residual flexural tensile strength ($f_{R,j}$) which corresponds to the crack mouth opening displacements (CMOD) linked to the crack openings (in mm) of 0.5, 1.5, 2.5 and 3.5 ($j = 1, 2, 3, 4$ respectively). Figure 5.4 exhibits the dimensions of the prismatic specimens according to the EN 14651, while Fig. 5.5 shows a prismatic specimen during the three point bending test (EN 14651).

Figure 5.6 exhibits the curves obtained by the three point bending tests. Beyond the peak load, it can be observed the clear differences between plain and fiber reinforced concrete. Plain concrete has a behavior totally brittle after the peak; namely, once the specimen cracks, immediately the specimen breaks in two blocks,

Fig. 5.3 Round panel and cylinder, cubic and prismatic specimens just produced



Fig. 5.4 Flexural tensile strength test setup according to EN 14651

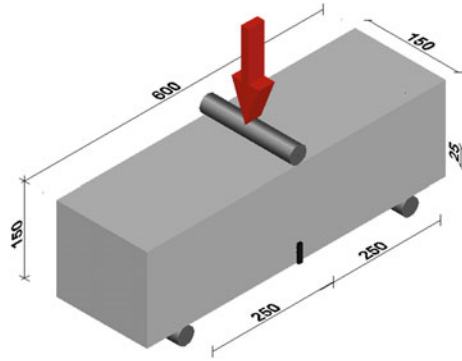
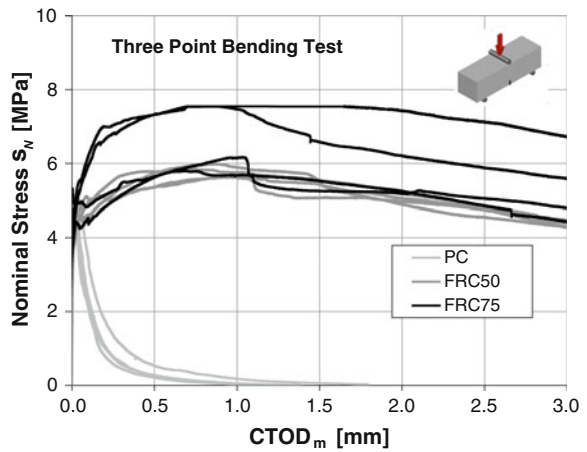


Fig. 5.5 Prismatic specimen during the flexural tensile strength test according to EN 14651



Fig. 5.6 Nominal stress-CTOD curves according to EN 14651



dissipating a small energy. On the other hand, depending on the content, fibers enhance concrete toughness. Consequently, more energy is dissipated by cracks in fiber reinforced concrete.

Table 5.3 shows the mechanical properties of the different types of concrete used: the average compressive strength (f_{cm}); the average tensile strength (f_{ctm}); the Young's modulus (E_{cm}) and the average post-cracking residual strength (f_{R1} , f_{R2} , f_{R3} , f_{R4}).

Also, round panel tests [1] were made using centrally loaded small round panels of 600 mm of diameter [2], see Fig. 5.7. In these tests, energies of fracture after cracking were determined (Fig. 5.8 and Table 5.4).

The yielding and tensile ultimate strength of the longitudinal deformed reinforcing bars were, respectively: 506 and 599 MPa for $\phi 14$ bars; 555 and 651 MPa for $\phi 20$ bars and, 518 and 612 MPa for $\phi 24$ bars. These are typical values for S500 steel, according to the current EC2 (2005).

Table 5.3 Mechanical properties of concrete and post-cracking residual strengths according to EN 14651

Beams	PC	FRC50	FRC75
Fibres V_f (%)	0.00	0.64	1.00
f_{cm} (MPa)	38.7	32.1	33.1
f_{ctm} (MPa)	3.0	2.4	2.5
E_{cm} (MPa)	33,500	30,800	32,100
$f_{R,1}$ (MPa)	–	5.4	6.0
$f_{R,2}$ (MPa)	–	5.6	6.1
$f_{R,3}$ (MPa)	–	5.0	6.0
$f_{R,4}$ (MPa)	–	4.5	5.5

Fig. 5.7 Round panel during the test



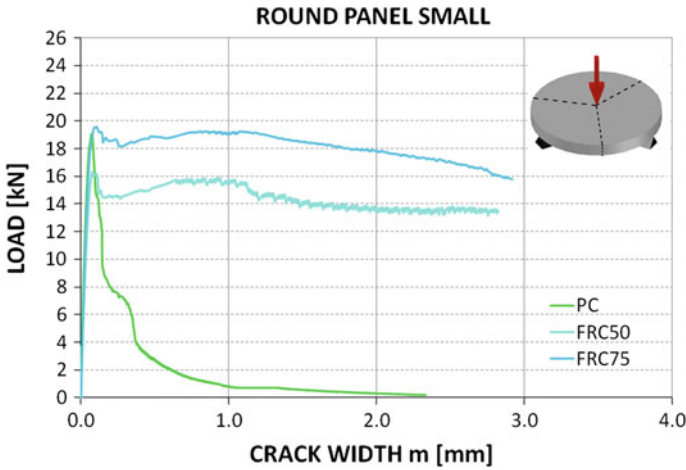


Fig. 5.8 Load-crack width curve corresponding to the specimens made of PC, FRC50 and FRC75

Table 5.4 Energy absorbed corresponding to displacements 3.75 and 30 mm (Average values)

Round panel	$G_{3.75}$ (N/mm)	G_{30} (N/mm)
PC	11.21	11.41
FRC50	53.92	93.11
FRC75	67.99	105.06

5.4 Experimental Program

5.4.1 Main Variables and Beam Production

Nine large reinforced beams without stirrups with several depths (500, 1,000 and 1,500 mm) with shear span 3 times their effective depth were casted. Figures 5.9, 5.10 and Table 5.5 show the beam cross-section and reinforcement.

The amount of longitudinal reinforcement has been designed to represent real cases. This longitudinal reinforcement implies a ρ_l between 1.01 and 1.12 % as shows Table 5.5. All the rebars used were made out of steel B 500 S type.

The experimental program variables were:

- Height (500; 1,000; 1,500 mm)
- Amount of fibers (0, 50 and 75 kg/m³)

All beams had the same width of 250 mm and gross cover of 60 mm.

In Fig. 5.11 it can be seen the formworks and their appearance just after pouring the concrete.

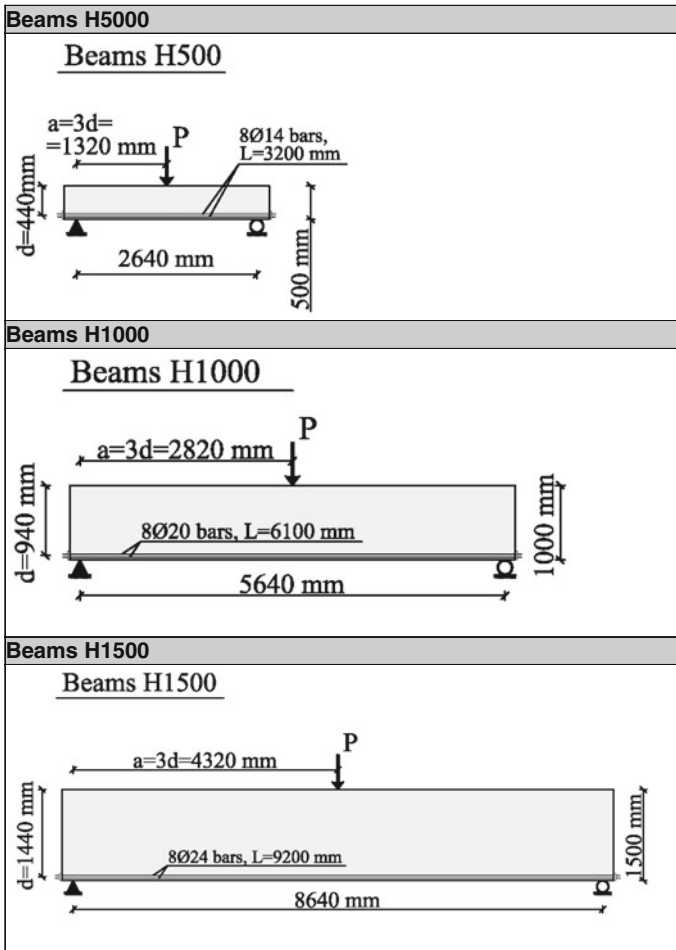


Fig. 5.9 Geometry and reinforcement details of beams (Frontal view)

5.4.2 Testing Procedure

Beams were tested under a three point loading system and a shear span-to-depth ratio (a/d) of 3. The load was applied to the beams by an electro-mechanical jack with displacement control. All tests began by imposing an initial displacement rate of 0.20 mm/min, decreased to 0.10 mm/min after the appearance of some shear crack. For beams H500 was used a jack with a load capacity of 500 kN, whereas for beams H1000 and H1500, one of 1,500 kN was used. Load was measured with a load cell at load point. Before starting the test, preliminary elastic cycles were applied to verify the correct operation of the devices. Obviously, these cycles

Fig. 5.10 Geometry and reinforcement details of beams (*Cross-sections*)

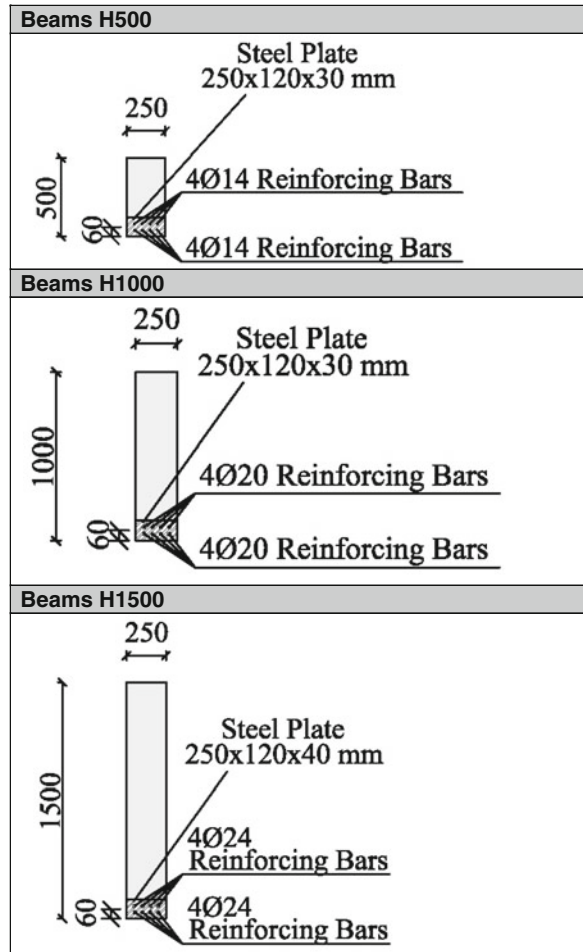


Table 5.5 Geometry characteristics of specimens

Beams	H500	H1000	H1500
Height (mm)	500	1,000	1,500
Effective depth d (mm)	440	940	1,440
Total length (mm)	3,000	5,900	9,000
Span (mm)	2,640	5,640	8,640
Shear span a (mm)	1,320	2,820	4,320
Width (mm)	250	250	250
Gross cover (mm)	60	60	60
Reinforcement longitudinal bars	8φ14	8φ20	8φ24
Reinforcement area (mm ²)	1,232	2,513	3,619
Reinforcement ratio (%)	1.12	1.07	1.01



Fig. 5.11 Formworks and beams just casted

reached peak loads well below those of the first shear cracking, reaching 30, 40 and 50 kN for beams H500, H1000 and H1500, respectively.

Figure 5.12 shows the test arrangement of the beams. To prevent movement out of plane of the beams, H1000 and H1500 steel profiles were arranged around the beam ends.

Instrumentation was available to measure: deflections, shear cracks widths, settlement of supports, shortening of top chord and elongation of bottom chord. Linear Variable Differential Transformers (LVDTs) were utilized for measuring deflections at midspan (front and back side) and support displacements. Potentiometric transducers were employed for measuring crack widths and strut shortenings. The latter were placed with an inclination of 40° (struts) and 140° (crack

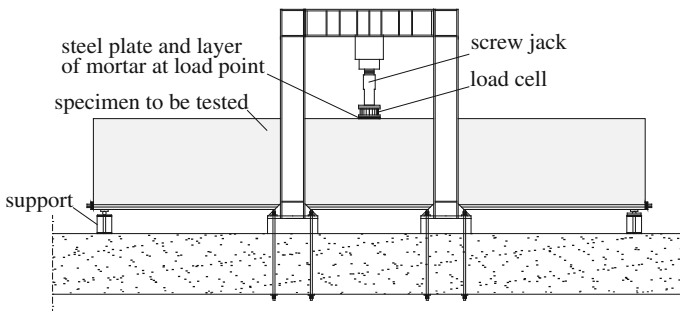


Fig. 5.12 Three point test setup for the full-scaled beams

widths) to the horizontal. This inclination was based on experimental observation of similar tests [3], in which the critical shear crack occurred at a distance of about the *effective depth* (d) from the support, directed towards the point of load application.

The instrumentation applied in the shear span for beams H1000 and H1500 (see Fig. 5.13), was slightly different from the beams H500, due to their increased shear span area. Thus, in all beams were disposed 2 potentiometric transducers for measuring strut displacements on the front side of the beam and, also, transducers for measuring crack widths on the shear span. The latter on the following: 4 transducers (2 on the front and 2 on the back side) in H500 beams and 6 (4 on the front and 2 on the back side) in H1000 and H1500 beams.

Figure 5.14 shows a front view of a H1000 beam before testing.

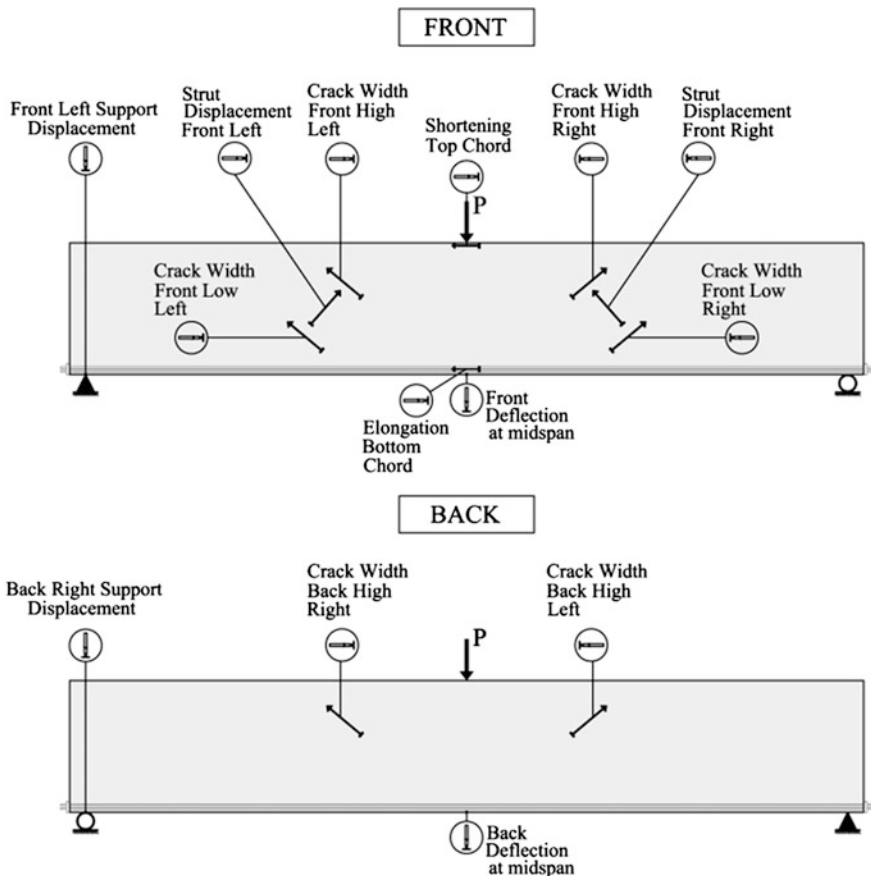


Fig. 5.13 Instrumentation details for beams H1000 and H1500



Fig. 5.14 Front view of a beam H1000 under preparation for the test

5.4.3 Results

5.4.3.1 Experimental Results

Figure 5.15 exhibits beam H1500-FRC75 ($h = 1500$ mm; 75 kg/m³ of fibers) after failure testing.

Table 5.6 reports the main experimental results: the failure mode, shear ultimate load (V_u), shear stress (v_u), ratio $v_u/f_{cm}^{1/2}$, ultimate flexure moment ($M_{u,fl}$), experimental ultimate moment (M_u), ($M_u/M_{u,fl}$) ratio and the maximum deflection at midspan (δ_u).

The experimental ultimate moment (M_u) was determined as $M_u = V_u \cdot a$ and the ultimate flexure moment ($M_{u,fl}$) was calculated according to the EC2 for the RC beams while for the FRC beams it was calculated according to the MC2010, assuming a stress-block both in compression (according also to EC2) and in tension. The latter was characterized by a constant stress, in the whole tensile area, equal to f_{FTu} (where $f_{FTu} = f_{R3}/3$). This formulation comes from the assumptions that the maximum compressive strain in the FRC, the maximum tensile strain in the steel and the maximum post-cracking tensile strain in the FRC are attained (Fig. 5.16).

As can be seen in the Table 5.6, all beams failed in shear although beams H500 FRC75 and H500 FRC50 reached their flexure capacity with yielding of the longitudinal reinforcement. Beam H500-FRC50 behaved quite ductile. This is quite clear from the Table 5.6, where the ($M_u/M_{u,fl}$) ratio exceeds unity in H500 beams made of FRC.



Fig. 5.15 Beam H1500-FRC75 after its failure

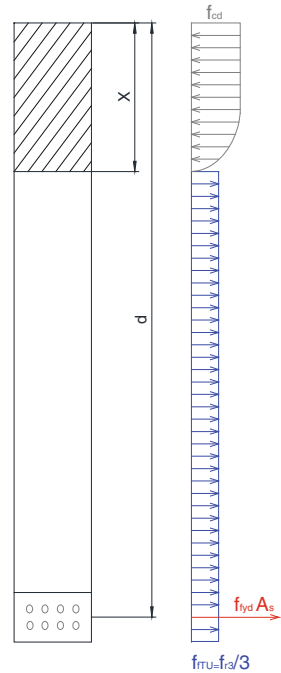
Table 5.6 Main experimental results

Specimen	Failure mode	V_u (kN)	v_u (MPa)	$v_u/(f_{cm})^{1/2}$ [-]	M_u (kN m)	$M_{u,fl}$ (kN m)	$M_u/M_{u,fl}$ [-]	Midspan displ. δ_u (mm)
H500 PC	Shear	116	1.05	0.17	153	254	0.60	3.7
H500 FRC50	Shear ^a	240	2.18	0.38	316	285	1.11	35.0
H500 FRC75	Shear ^a	235	2.13	0.37	310	293	1.06	9.1
H1000 PC	Shear	188	0.80	0.13	529	1,210	0.44	6.3
H1000 FRC50	Shear	272	1.16	0.20	767	1,325	0.58	13.6
H1000 FRC75	Shear	351	1.49	0.26	989	1,356	0.73	16.8
H1500 PC	Shear	211	0.59	0.09	911	2,511	0.36	7.0
H1500 FRC50	Shear	484	1.34	0.24	2,089	2,791	0.75	21.6
H1500 FRC75	Shear	554	1.54	0.27	2,394	2,864	0.84	23.5

^a Shear failure took place with yielding of longitudinal rebars

Furthermore, the addition of fibers increases the shear ultimate capacity. In the case of H500 beams, the addition of fibers doubled the shear ultimate capacity of PC beams. For beams H1000, the addition of 50 kg/m³ of fibers increases the shear capacity by almost 50 % from the reference beam H1000 PC; when added 75 kg/m³, the increase was equal to 86 %. Also in beams H1500, fibers double shear ultimate capacity while, from 50 to 75 kg/m³ of fibers ultimate capacity increased by 33 %.

Fig. 5.16 Stress distribution over the cross section of the beam



5.4.3.2 Load-Deflection Response

Load-deflection curves (Figs. 5.17, 5.18 and 5.19) show that, in all the beams, greater amount of fibers, the greater the shear ultimate capacity reached and that, for the same load level, greater deflections are reached for cases of 50 kg/m^3 compared with those of 75 kg/m^3 ; although this effect is less evident in H500 beams, on higher beams (H1000 and H1500) it is more evident, especially in beams H1000 which reached a higher load of 75 kg/m^3 than in the 50 kg/m^3 , as discussed above.

5.4.3.3 Cracking Pattern and the Load-Crack Width Response

Crack width-load curves (Figs. 5.20, 5.22 and 5.24) and crack patterns (Figs. 5.21, 5.23 and 5.25) show that the addition of fibers causes more smaller cracks giving to the beam a more ductile behavior.

Fibers determine an increase of the ultimate shear load and the load at which the shear crack becomes unstable. For instance, in H1500 series, an evident shear cracking began at 320 kN for the reference sample, whereas it occurred at 570 and 890 kN for the FRC50 and FRC75 beams, respectively. The same trend can be seen for sample H1000: in the reference specimen, the shear crack first developed at a load of 240 kN, whereas 456 and 482 kN were the external loads necessary to initiate the shear cracking in the two elements cast with 50 and 75 kg/m^3 of steel

Fig. 5.17 Experimental curve load versus deflection of H500 beams

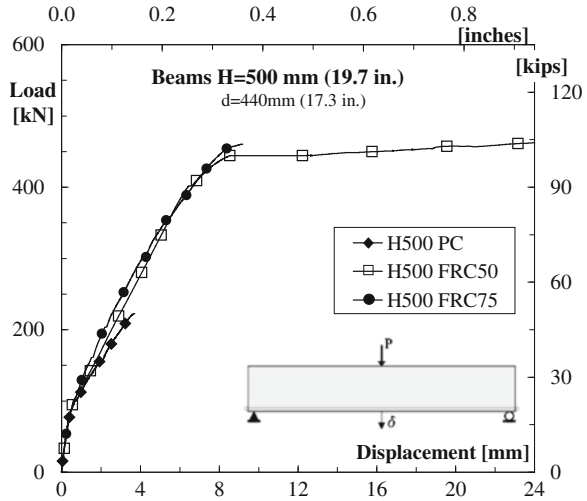
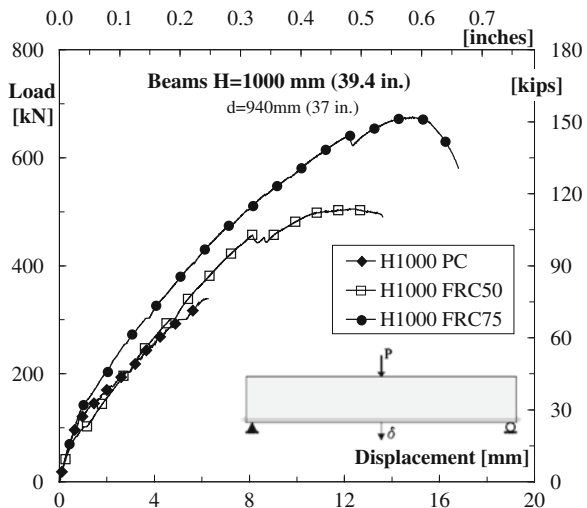


Fig. 5.18 Experimental curve load versus deflection of H1000 beams



fibers, respectively. While the plain concrete member fails early after the appearance of the first shear crack, with a maximum shear crack width of 0.25–0.50 mm, multi-cracking in shear was observed for the FRC samples, with single shear cracks wider than 1–3 mm and, even more important, steadily propagating. All flexure-shear cracks in the FRC specimens were 35–45° inclined to the horizontal.

In all beams without fibers, as the test progresses, flexure cracks are formed at midspan, then an inclined crack develops causing the collapse of the beam. By contrast, in beams reinforced with fibers, after flexure cracks, inclined shear cracks appear, developing an unstable mechanism, which cannot be predicted which of all

Fig. 5.19 Experimental curve load versus deflection of H1500 beams

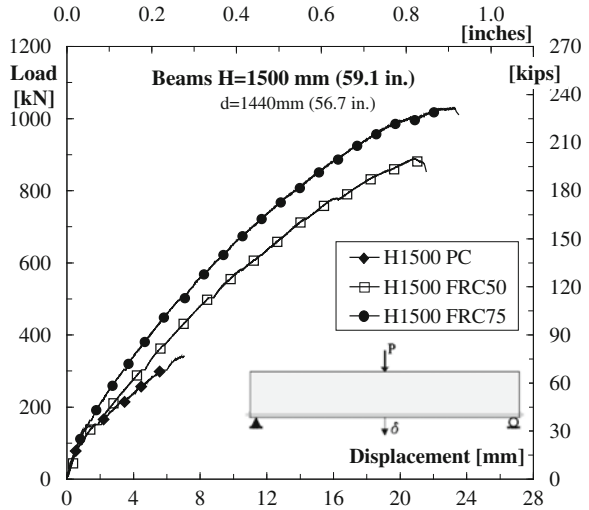
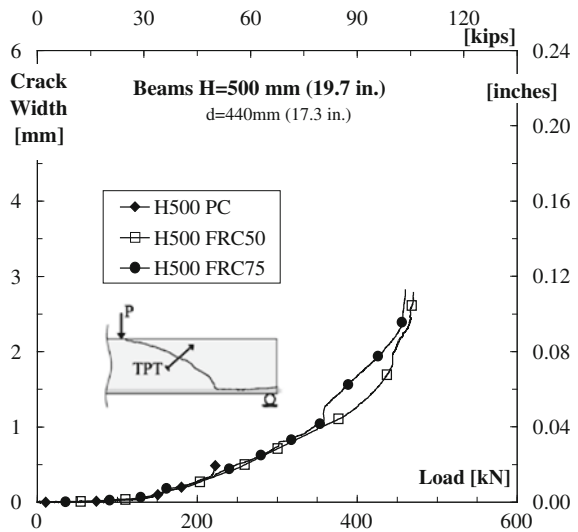
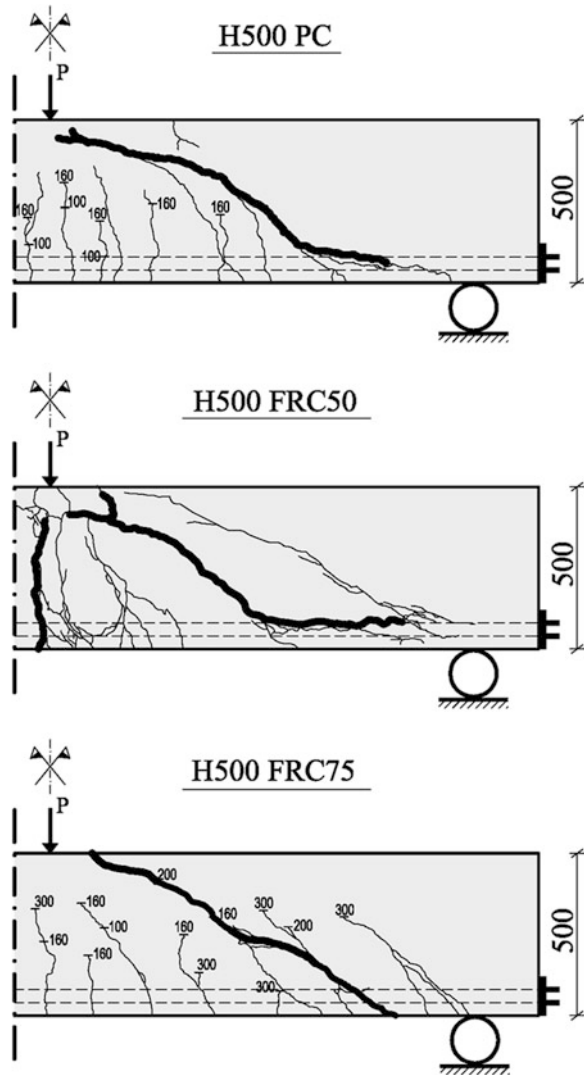


Fig. 5.20 Main shear crack width versus load (kN) of H500 beams



the inclined cracks end up causing final failure. In turn, it is observed that the addition of fibers causes shear cracks less inclined to the horizontal; the higher the amount of fibers, the smaller is the inclination of the cracks. An estimation of the inclination of the shear critical crack was also done by considering its inclination to the horizontal in a portion around the barycentric axis. As mentioned above, the experimentally determined angle θ diminished as the material toughness increased. In fact, the angle θ turned out to be equal to 44° , 41° and 38° to the horizontal, respectively for samples H1500 PC, H1500 FRC50 and H1500 FRC75. This trend

Fig. 5.21 Crack evolution for beams H500 (loads in kN)

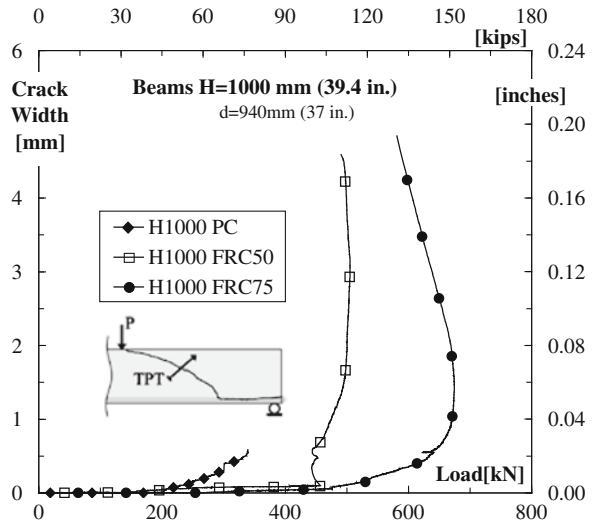


was also found in the smaller series: for samples H1000, θ ranged from 42° in the reference element, while it was equal to 37° and 34° respectively for beams FRC50 and FRC75; for beams H500, θ was 41° , 39° and 32° , respectively for elements PC, FRC50 and FRC75.

In the case of sample H1500 FRC50, the main shear crack was not recorded as it developed much closer to the support than expected (i.e., it turned out to be external to the gauge length).

To analyze the formation and subsequent propagation of shear cracks in a beam of FRC, let's consider the beam FRC50 H1500. Figure 5.26 indicates the order of

Fig. 5.22 Main shear crack width versus load (kN) of H1000 beams



appearance of each of the cracks; as we see, fibers allow stress redistribution in the beam. Therefore, after the first crack forms, there is no collapse in FRC beam as occurs in PC beams; afterwards, different shear cracks appear from the center of the span to the beam ends (Fig. 5.26), resulting in a non-cracked concrete arch (at the top of the beam) increasingly slim. Once a crack is formed, the following occurs when the latter offers a weaker path for the formation. This process is repeated until one of the cracks is not able of withstanding more stress and, eventually, causes the final failure of the beam.

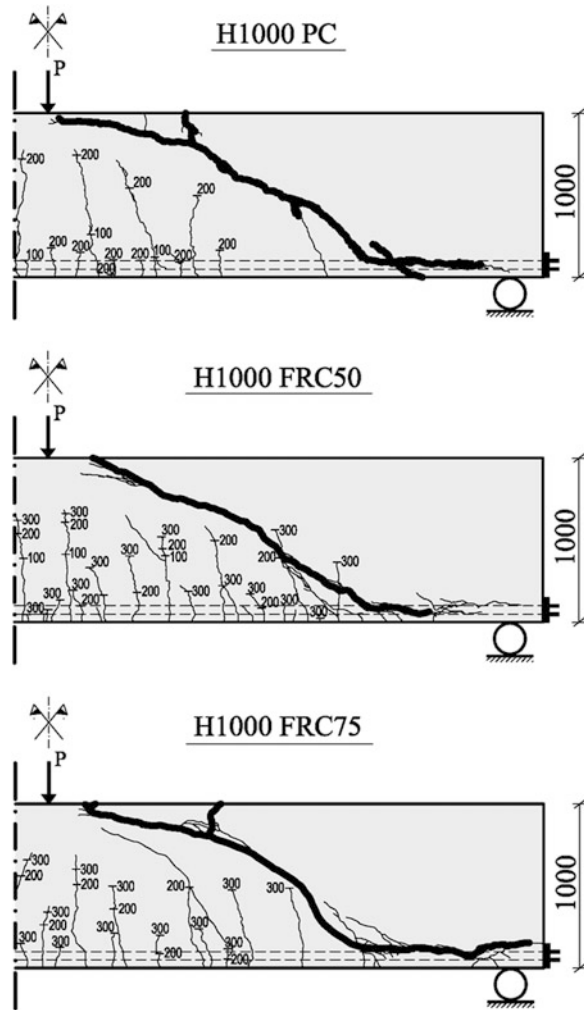
5.4.4 Study of the Size Effect

5.4.4.1 Experimental Study of the Size Effect

Figure 5.27 reports the classical size effect graph representing the experimental ultimate shear strength over the square root of the compressive strength ($v_u/f_{cm}^{1/2}$) as a function of the effective depth (d), whereas Fig. 5.28 reports the ratio $v_u/v_{u,fl}$ (experimental shear strength over the maximum shear strength in the case of flexure collapse) versus the effective depth (d), corresponding to the percentage of the maximum flexure capacity attained by the beams. In addition, the graph indicates the value of the residual tensile strength, f_{R3} for the beams tested, as it is a relevant parameter for the FRC in Design Codes.

Figure 5.27 evidences the rather good fitting between the experiments on plain concrete elements, presented herein. Figure 5.27 also shows how fibers can mitigate the size effect in high beams without stirrups. However, it seems that the results

Fig. 5.23 Crack evolution for beams H1000 (loads in kN)



from H1000 beams are lower than expected. This suggests that, as ensured Bentz [4], after 1,500 mm the decrease was very little by observing the results obtained herein, the FRC elements could also come to an asymptote. In other words, given the results shown in the Fig. 5.27, fibers could definitely mitigate the size effect for beams with effective depths higher than 1,000 mm, when the FRC is 75 kg/m³; however, to confirm these findings, further tests would be needed.

Figure 5.28 emphasizes that, with increasing f_{R3} it is possible to reach the full flexure capacity avoiding shear failure and, therefore, size effect.

Fig. 5.24 Main shear crack width versus load (kN) of H1500 beams

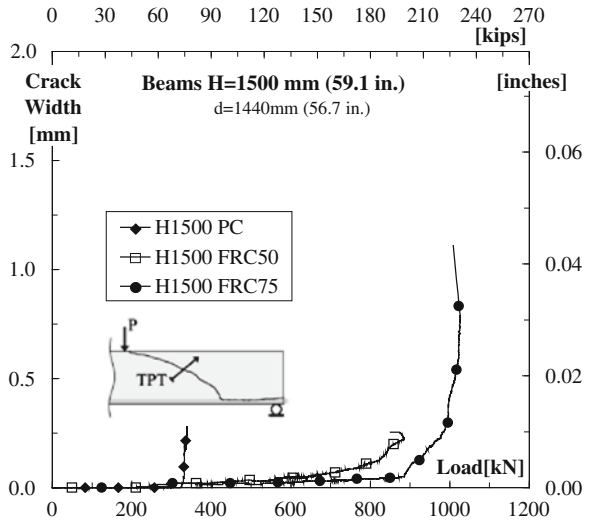
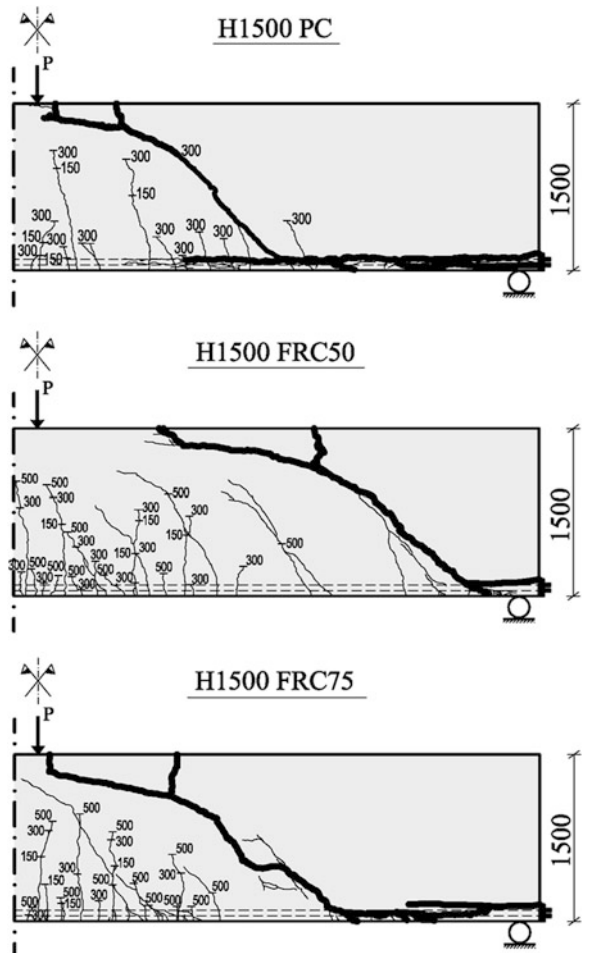


Fig. 5.25 Crack evolution for beams H1500 (loads in kN)



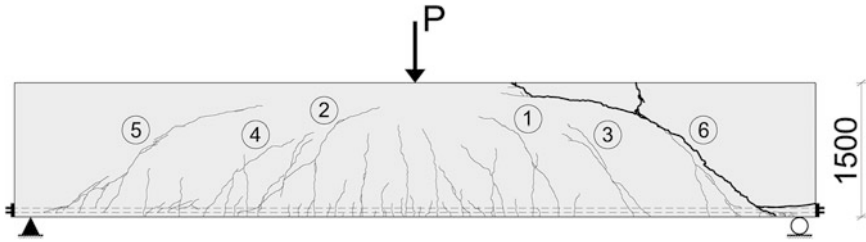


Fig. 5.26 Crack evolution for beam H1500 FRC 50

5.4.4.2 Numerical Analysis of the Size Effect

The load-deflection behavior of beams was simulated numerically with the software VecTor 2 [5]. For modeling fiber reinforced concrete in VecTor 2, it should be introduced the constitutive law of the material in tension. To get that, specifies back analyses have been done on the prismatic specimens used for the three point bending tests. Then, the stress- strain curves in tension for all concrete have been determinate by dividing the crack opening by the crack spacing [6]. Crack spacing was assumed as the distance between the bending cracks of the beam, since they are the closest to represent the behavior in tension of the material. However, from another conceptual point of view (expecting that *final failure is by shear*), it has been considered that it could be better to take as a crack spacing the separation between shear cracks. Therefore, numerical simulations were reprocessed with

Fig. 5.27 Ultimate shear strength versus effective depth

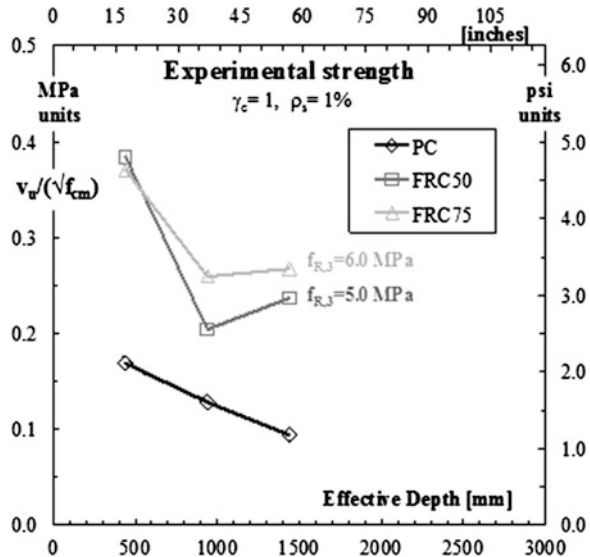
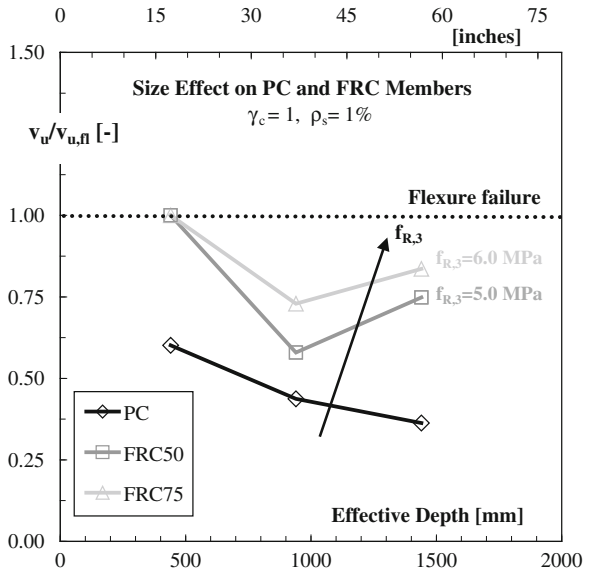


Fig. 5.28 Trend of size effect for all beams (PC and FRC)



VecTor, with the shear crack spacing, obtaining a load-deflection numerical curve closer to the experimental one.

Since the fibers allow redistribution of stresses, in the numerical models a great number of shear cracks could be observed, generating new paths of cracking, contrarily elements without fibers. Some of the shear cracks are stabilized, because new cracks appear at weaker paths. This process of crack spacing development in FRC beams is not entirely clear (see [7]); in fact, a more significant crack spacing could correspond to the distance between two active shear cracks (that are growing during crack development) and not to two consecutive shear cracks. To clarify this concept, additional tests are necessary and, in the present work, a numerical parametric study was performed to better understand the influence of different values of crack spacing; in doing so, the crack spacing was assumed as twice and four times the distance between two consecutive shear cracks. The results for beams H1000 and H1500 with 50 and 75 kg/m³ of fibers are shown from Figs. 5.29, 5.30, 5.31 and 5.32.

It can be observed a better comparison between experiments and numerical curves with a crack spacing larger than the measured one (twice or four times). This is confirmed by the plot in Figs. 5.33 and 5.34, referring to size effect. It can be therefore concluded that the proper crack spacing for the constitutive law should be referred to active shear cracks. Also, the smaller resistance of beams H1000 beams is not reproduced by the numerical analyses.

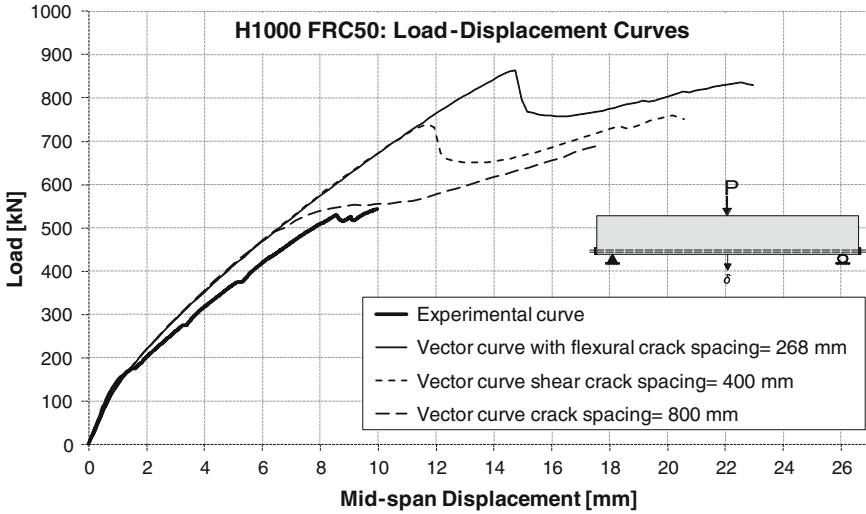


Fig. 5.29 Numerical response against experimental results for load-deflection of H1000-FRC50

Once again, the size effect plots (Figs. 5.33 and 5.34) show that fibers can mitigate the size effect and that the resistance of larger beams approaches a horizontal asymptote.

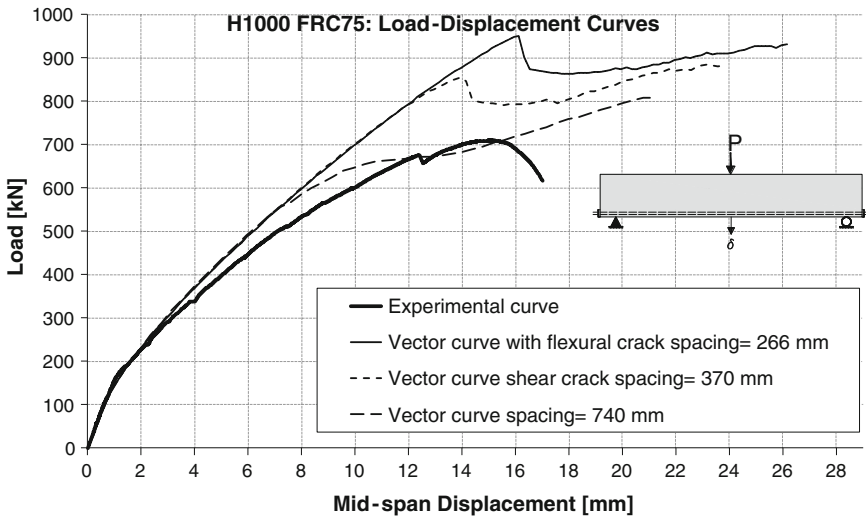


Fig. 5.30 Numerical response against experimental results for load-deflection of H1000-FRC75

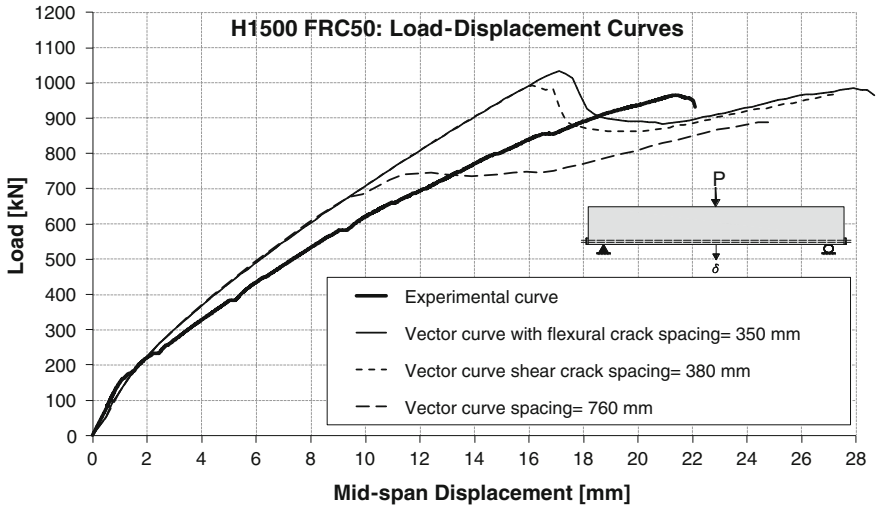


Fig. 5.31 Numerical response against experimental results for load-deflection of H1500-FRC50

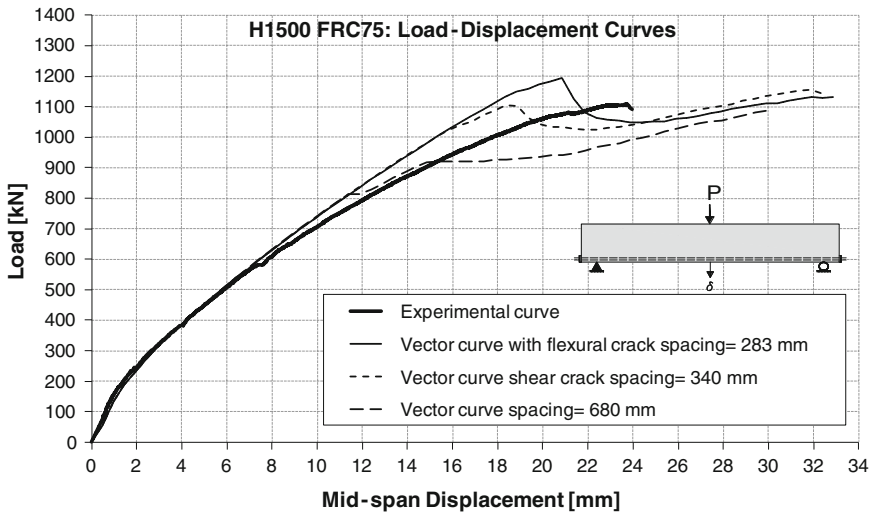


Fig. 5.32 Numerical response against experimental results for load-deflection of H1500-FRC75

Fig. 5.33 Size effect trend comparing experimental and numerical analysis with two different crack spacing: distance between bending cracks and distance between shear cracks

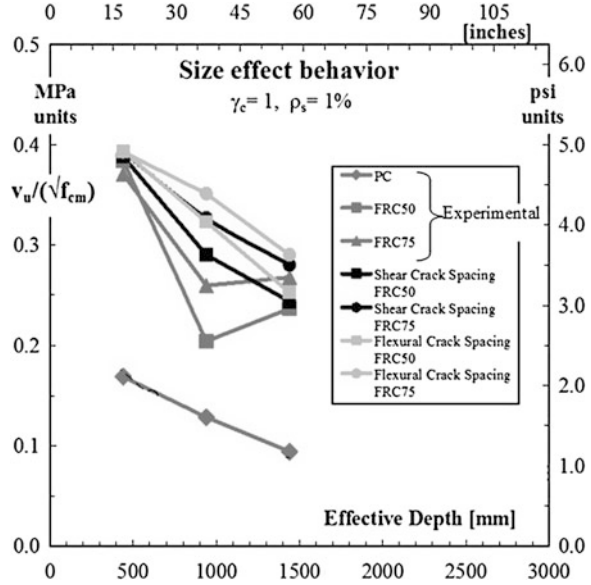
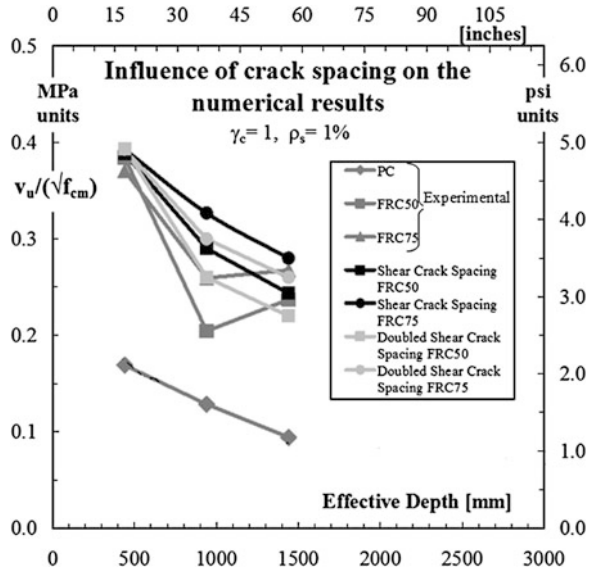


Fig. 5.34 Size effect trend comparing experimental and numerical analysis with two different crack spacing: distance between shear cracks and the double of its distance



5.4.5 Shear Values Calculated with the Current Design Codes

The nine beams herein discussed were compared against the prediction of the models included in the following Codes: RILEM [8], Spanish EHE-08 [9] and MC2010 [6].

To better compare the resistance, partial safety factors for material properties were considered in the calculation as $\gamma_c = 1$ and $\gamma_s = 1$. Moreover, average values of the material properties were utilized instead of the characteristic value present in the equations.

Table 5.7 reports the experimental and the shear theoretical values corresponding to the analyzed Design Codes.

The safety margins (SM) obtained as V_{test}/V_{theo} (the shear experimental value divided by the predicted shear value) were used as a reference parameter to compare the results obtained from the different beams and Codes. SM values are reported in Table 5.8.

The values presented in Table 5.8 are also plotted in Fig. 5.35 for both PC and FRC beams. This permits to evaluate separately PC than FRC beams since these concretes have models and behaviors totally different. As showed Chaps. 3 and 4, MC2010 for PC is based on the MCFT, and for FRC is based on variable truss

Table 5.7 Shear strength (kN) calculated from the current design codes without safety factors

Specimen ID	V_{test}	V_{EHE08}	V_{RILEM}	V_{MC2010}
H500 PC	115.68	116.38	116.38	109.15
H500 FRC50	239.53	215.93	225.61	188.68
H500 FRC75	234.53	238.76	250.42	199.39
H1000 PC	187.73	213.72	213.72	189.48
H1000 FRC50	272.14	399.54	417.60	346.50
H1000 FRC75	350.75	442.08	463.82	366.17
H1500 PC	210.98	301.27	301.27	244.34
H1500 FRC50	483.57	569.05	595.05	488.45
H1500 FRC75	554.13	630.21	661.50	516.18

Table 5.8 Safety margins calculated from the current design codes without safety factors

Specimen ID	SM_{EHE08}	SM_{RILEM}	SM_{MC2010}
H500 PC	0.99	0.99	1.06
H500 FRC50	1.11	1.06	1.27
H500 FRC75	0.89	0.94	1.18
H1000 PC	0.88	0.88	0.99
H1000 FRC50	0.68	0.65	0.79
H1000 FRC75	0.79	0.76	0.96
H1500 PC	0.70	0.70	0.86
H1500 FRC50	0.85	0.81	0.99
H1500 FRC75	0.88	0.84	1.07



Fig. 5.35 Safety margin (SM) = $V_{\text{test}}/V_{\text{theo}}$ without safety factors

analogy. Figure 5.35 shows that for H500 beams, Codes are safe, except for H500 FRC75 beam evaluated with RILEM and EHE08. Also, MC2010 evaluates properly the size effect on beams, giving safe values (SM > 1) for all beams, except for H1000 FRC50. From beams made with PC (without fibers), a decreasing line is observed and the SM decreases when effective depth increases; this line almost has safe values for all depths but, on the other hand, RILEM and EHE08 give unsafe values for H1000 PC and H1500 PC.

Finally, it can be observed that all the H1000 beams have a SM smaller than 1, indicating that something strange occurred during the tests.

5.5 Conclusions

Based on the experimental results [10], the following main conclusions can be drawn:

- Fibers substantially mitigate the size effect in shear that is increasingly reduced for increasing FRC toughness.
- FRC allows a multiple and stable shear crack development in the shear critical area, delaying (or even avoiding) the formation of the single critical shear crack.
- Fibers, even in relatively low amount, greatly influence the shear behavior of beams, basically by delaying the occurrence of the shear failure mechanism and, eventually, by altering the collapse from shear to flexure, with enhanced bearing capacity and ductility.

- It is essential to choose a proper value of the crack spacing for a good numerical simulation represented by the distance between active shear cracks; otherwise, simulations obtained will not represent well the actual behavior.
- A horizontal asymptote in the size effect law seems to be present (no further decrease of shear resistance with larger beam sizes); however, further studies are necessary to better understand the size effect in FRC and confirm this trend.
- MC2010 evaluates properly the shear behavior and the size effect on beams, having size significant for practice; RILEM and EHE08 give unsafe values for H1000 PC and H1500 PC.
- For PC beams a decreasing line on the graph SM versus increasing effective depth was observed.

5.6 Publication of These Results

The results of this paper have been published in the journal *Materials & Structures*:

Fausto Minelli; Antonio Conforti; Estefanía Cuenca; Giovanni Plizzari. ARE STEEL FIBRES ABLE TO MITIGATE OR ELIMINATE SIZE EFFECT IN SHEAR?. *Materials & Structures*. March 2014, Volume 47, Issue 3, pp 459–473. Springer. DOI: [10.1617/s11527-013-0072-y](https://doi.org/10.1617/s11527-013-0072-y).

References

1. ASTM.C1550-10a. 2002. Standard Test Method for Flexural Toughness of Fiber Reinforced Concrete (Using Centrally Loaded Round Panel). West Conshohocken: ASTM International.
2. Conti and Flelli. 2008–2009. Caratterizzazione del calcestruzzo fibrorinforzato attraverso prove su piastre sottili (in italian). Tesi di laurea, Università degli Studi di Brescia, Brescia, Italy.
3. Conforti, A. 2014. Shear behavior of deep and wide-shallow beams in fiber reinforced concrete, 232. Ph.D. Thesis, Department of Civil, Architectural, Environmental, Land Planning Engineering and of Mathematics, University of Brescia, May 2014, Aracne Editrice, Roma, ISBN 978-88-548-7009-3.
4. Bentz, E. 2005. Empirical modelling of reinforced concrete shear strength size effect for members without stirrups. *ACI Structural Journal* 102(2): 232–241.
5. Vecchio. VecTor analysis group. <http://www.civ.utoronto.ca/vector/software.html>.
6. MC2010. 2012. Fib Bulletin 65–66. Model Code—final draft.
7. Moutanac, Massicotte and Charron. 2012. Design of SFRC structural elements: flexural behavior prediction. *Materials and Structures* 45(4): 623–636.
8. RILEM, TC 162-TDF. 2003. Test and design methods for steel fibre reinforced concrete, stress-strain design method. Final recommendation. *Materials and Structures* 36: 560–567.
9. EHE-08. 2008. Instrucción de Hormigón Estructural EHE-08 (in Spanish), 702. Madrid: Ministerio de Fomento.
10. Minelli, F., Conforti, A., Cuenca, E., and G.A. Plizzari. 2014. Are steel fibres able to mitigate or eliminate size effect in shear? *Materials and Structures* 47(3): 459–473.

Chapter 6

Experimental Tests to Study the Influence on the Shear Behavior of Fibers of Different Characteristics

6.1 Introduction

Steel fiber reinforced concrete (SFRC) is a composite material that is characterized by an enhanced post-cracking behavior due to the capacity of fibers to bridge the crack faces. The enhanced toughness is mainly provided by bond and high-modulus fibers in a suitable concrete matrix. Hooked fibers are more effective than straight and crimped ones in enhancing the post-peak energy absorption capacity. The effect of fibers on compressive strength is relatively small, and different fiber types seem to act similarly in this regard [1]. Bencardino et al. [2] realized that the addition of steel fibers with high aspect ratio into a high strength concrete matrix significantly improves the post-peak behavior. In 2014, Banthia et al. [3] has ensured that, in mixes reinforced with a single fiber, the Hooked-End fiber was significantly better in shear than the Double Deformed fiber.

On the other hand, the inclusion of fibers decreases the concrete workability. This effect is more pronounced for fibers with higher aspect ratios.

Steel fibers in concrete can considerably influence shear behavior and shear capacity guarantying the minimum shear reinforcement required by the current Codes. SFRC makes possible a more distributed cracking pattern, where shear cracks are characterized by smaller crack spacing and widths [4].

Many studies have advanced the knowledge in shear behavior of FRC beams. Fiber content has a significant effect on shear behavior, but the fiber type was also found to be influential since both of them influence the FRC toughness. Fibers with a higher aspect ratio resulted in an increased shear strength due to the enhanced post-cracking behavior compared to fibers with a low aspect ratio [2, 5–7]. Hooked steel fibers with a length of 60 mm allowed a larger shear crack opening when compared to that observed in beams with 30 mm long fibers, but they were prone to problems associated with fiber lumping along the longitudinal reinforcement. In fact, horizontal clear spacing between reinforcing bars, no less than the fiber length, is recommended [8].

Most research on elements of FRC focus only on the type of fiber (shape), aspect ratio and amount of fibers [9, 10]. However, the strength of the fiber is also a very important factor to consider and there is little research about this [11].

To analyze the fiber contribution to shear capacity, Codes usually consider only the residual concrete strength at 2.5 mm crack opening in the flexural test (f_{R3}). However, it is possible to produce concretes with a similar f_{R3} but with very different post cracking behaviors. This is possible using fibers with different geometries and yielding capacity [12].

The aim of this chapter is to obtain self-compacting fiber reinforced concrete (SCFRC) with a large variability of mechanical behaviors by using different fiber types, and to analyze its effect on the shear behavior, by considering the serviceability limit state (SLS), the ultimate limit state (ULS), and also analyzing the ductility on the load/deflection and load/shear crack opening behavior of these beams. To achieve the objectives, an experimental program consisting of SCFRC double-T beams was designed. Beams were 2,400 mm long, with a double-T cross-section, a height of 350 mm and web width equal to 90 mm.

The main parameters of study were: concrete compressive strength level (30, 50, 80 MPa) and steel fibers quality [using fibers with different strength levels, lengths, and aspect ratios (length/diameter)]. The amount of steel fibers (50 kg/m³) was kept constant. Beams without fibers were produced as a reference.

6.2 Experimental Program

Three concrete matrices, characterized by their compressive strength (30, 50 and 80 MPa), named as Low (L), Medium (M) or High (H) strength, were produced. With those concrete matrixes, 16 different self-compacting concretes were derived by only adding fibers. When used, the fiber content was always 50 kg/m³. Each concrete is then defined by the compressive strength level and the fiber geometries (lengths and aspect ratio) as well as fiber strength levels. Table 6.1 shows the nominal mix designs.

Table 6.1 Mix designs (kg/m³)

	Low strength concrete (L)	Medium strength concrete (M)	High strength concrete (H)
Cement 52.5R	290	340	450
7/12 aggregate	658	731	610
Sand	954	954	1075
Filler	180	125	0
Silica fume	0	0	50
Steel fibers	50	50	50
Water	210	210	175
Superplasticizer	5.20	7.45	26.7

Five different types of hooked-end steel fibers from Bekaert© were used, both normal strength low carbon fibers (BN), with a tensile strength equal to 1,225 MPa, or high strength high carbon (BP), with a tensile strength equal 3,070 MPa.

To analyze the mix design, a characterization quality control took place in the experimental program. The following control tests were done: compressive strength test on 150×300 mm cylinder specimens (EN 12390-3) and on cubic specimens 100×100 mm. Flexural tensile strength tests (EN 14651) was performed on notched beams to determine: the limit of proportionality (f_{ct}) and the residual flexural tensile strength ($f_{R,j}$) which corresponds to the crack mouth opening displacements (CMOD) linked to the crack openings (in mm) of 0.5, 1.5, 2.5 and 3.5 ($j = 1, 2, 3, 4$ respectively).

Each type of the fiber was referenced by its aspect ratio (length/diameter), its length (in mm) and the steel strength level, according with the following structure:

$$\{Aspect\ ratio\}/\{Length\ (mm)\} BN\ or\ BP$$

Figure 6.1 shows the steel fibers used in the experimental program presented herein, consisting of twenty-two double-T beams. Beams were 2,400 mm long, with a double-T cross section, 350 mm height and web width equal to 90 mm (Fig. 6.2). All beams had a basic reinforcement, as shown in Figs. 6.2 and 6.3, without stirrups in one of the shear span (tested shear span), in order to localize the failure zone.

Beams without fibers, including or not traditional shear reinforcement in the tested shear span, were produced to be utilized as a reference.

In order to facilitate their identification, the beam ID took the following structure:

$$\{Concrete\ Compressive\ strength\ level:\ (L)\ (M)\ or\ (H)\} - \{Type\ of\ fibers\} - \{a,\ b\}$$

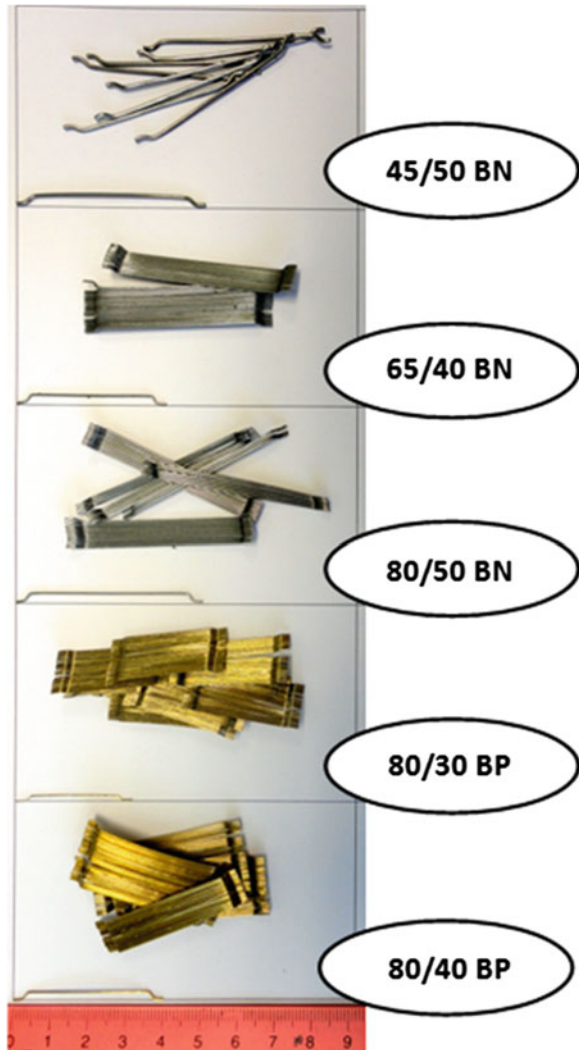
When traditional shear reinforcement in the tested shear span is provided, the type of fibers is substituted by the diameter of the employed rebar. When there were two identical beams, their beam IDs were differentiated by placing: “a” and “b” at the end of the beam ID. The experimental program is shown in Table 6.2.

Beams were subjected to a three-point test (Fig. 6.2) with an a/d ratio equal to 2.92 for all beams, except for the beams V19 (H- $\phi 6$) and V20 (L- $\phi 6$), characterized by a ratio $a/d = 3.02$, since the longitudinal reinforcement was placed 10 mm higher than the other beams (therefore, a lower effective depth (d) was present).

6.3 Result of the Concretes Characterization

Very different flexural strength and post-peak behavior were obtained even when comparing concretes made with the same matrix (Figs. 6.4 and 6.5). Concretes with a clear ductile behavior, like those made with medium strength matrix and high

Fig. 6.1 Typology of steel fibers used in this experimental program (*scale lines indicate millimeters*)



strength fibers, and others with a brittle response as those made with high strength concretes and normal strength fibers, have been obtained. Figures 6.4 and 6.5 shows that the most ductile behaviors corresponds to BP fibers, as expected, maintaining high loads at great CMOD values. On the other hand, concretes type H or M with 80/50BN or 65/40BN show a big difference between the residual f_{R3} and f_{R1} strength values and, as consequence, a brittle behavior.

Table 6.3 shows the mechanical properties of the different mixes of each beam. All the mechanical values were obtained as the average of at least three specimens,

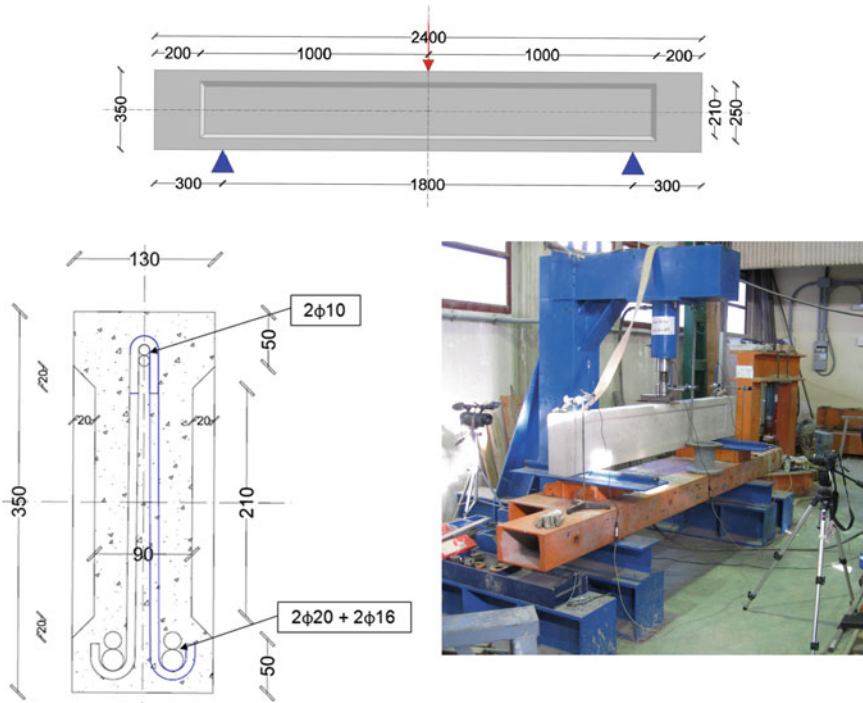


Fig. 6.2 Beams' geometry and test set-up. Dimensions in mm

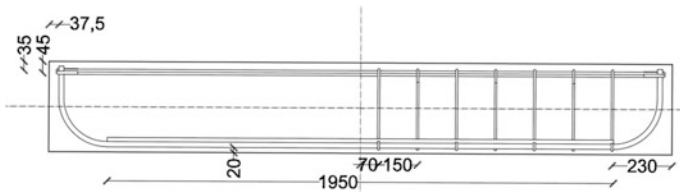


Fig. 6.3 Transverse reinforcement arrangement. Dimensions in mm

28 days after casting the beams. The $(f_{R3,m}/f_{R1,m})$ ratio is included to compare with the fiber classification proposed by the Model Code [12]. The obtained values, ranging from 0.21 to 1.16, cover all the possibilities considered by this classification, except the highest hardening behavior ($f_{R3,m}/f_{R1,m}$ ratio > 1.3). A column with the average residual strength $f_{Rm} = (f_{R1} + f_{R3})/2$ is also included.

Table 6.2 Experimental program

Reference	Beam ID	Fibers amount (kg/m ³)	Transverse reinforcement
V1	M-65/40BN-a	50	–
V2	M-80/40BP	50	–
V3	L-80/50BN-a	50	–
V4	L-65/40BN	50	–
V5	M-80/50BN	50	–
V6	H-65/40BN	50	–
V7	H-80/40BP	50	–
V8	M-0	0	–
V9	M-45/50BN	50	–
V10	L-80/40BP	50	–
V11	M-φ8	0	φ8@150 mm–1 leg
V12	M-80/30BP	50	–
V13	H-0	0	–
V14	H-80/50BN	50	–
V15	H-45/50BN	50	–
V16	H-80/30BP	50	–
V17	H-φ8	0	φ8@150 mm–1 leg
V18	M-φ6	0	φ6@200 mm–1 leg
V19	H-φ6	0	φ6@200 mm–1 leg
V20	L-φ6	0	φ6@200 mm–1 leg
V21	M-65/40BN-b	50	–
V22	L-80/50BN-b	50	–

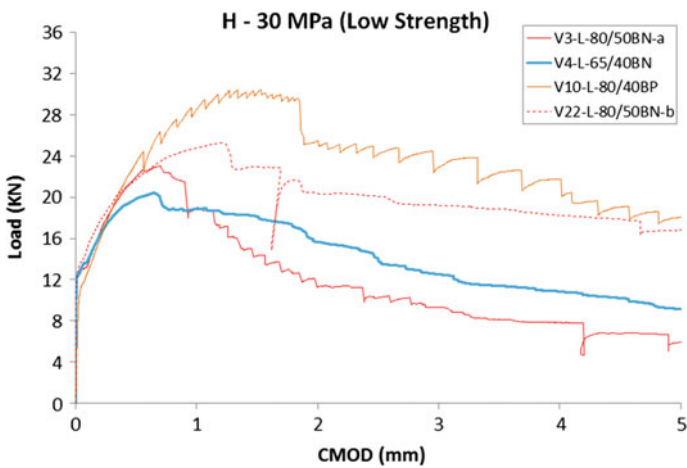


Fig. 6.4 Flexural strength curve for low strength concrete (H-30)

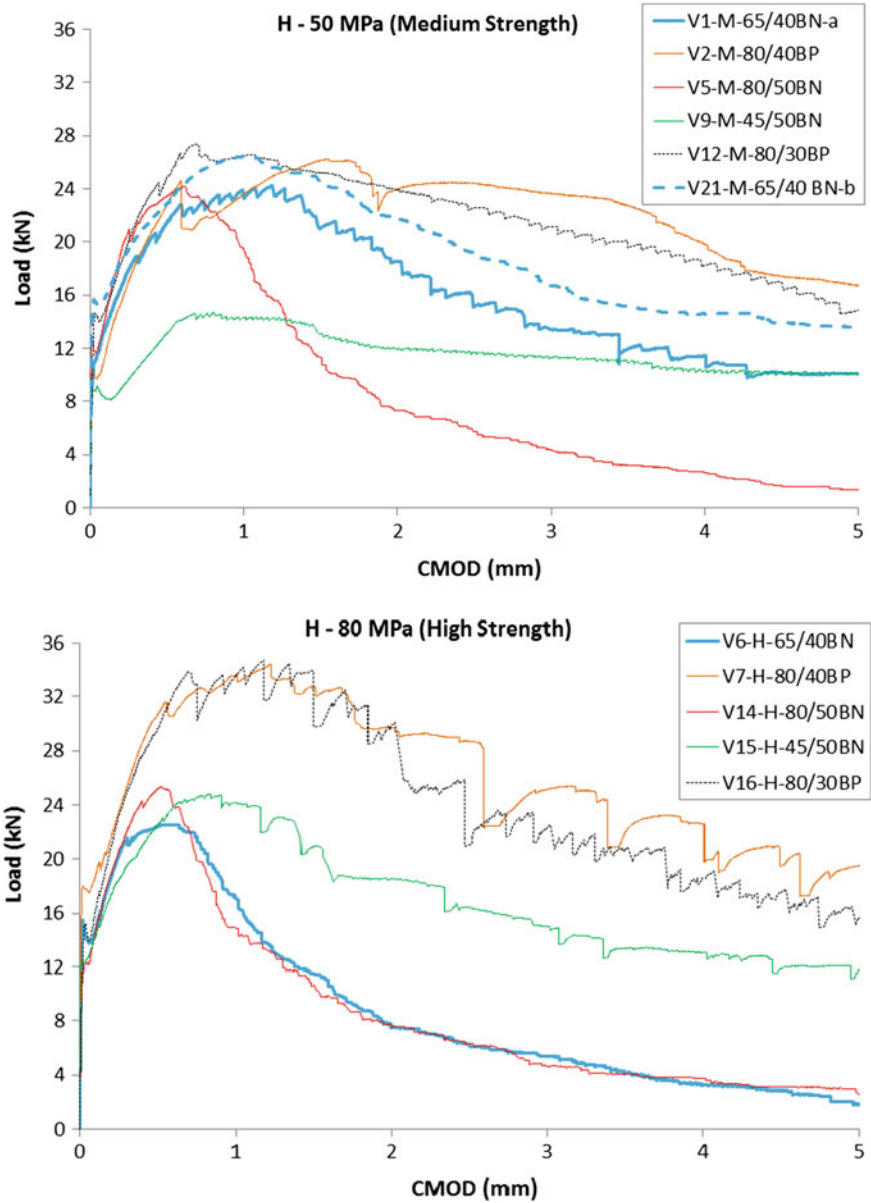


Fig. 6.5 Flexural strength curves for medium and high strength concretes (H-50 and H-80)

Table 6.3 Concrete mechanical properties (average values)

Ref.	Beam ID	f_{cm} (MPa)	$f_{R1,m}$ (MPa)	$f_{R3,m}$ (MPa)	f_{Rm} (MPa)	$f_{R3,m}/$ $f_{R1,m}$	V_{test} (kN)
V1	M-65/40BN-a	66.58	6.48	4.50	5.49	0.69	74.8
V2	M-80/40BP	71.09	8.16	9.44	8.80	1.16	100.7
V3	L-80/50BN-a	34.29	5.29	3.55	4.42	0.67	59.5
V4	L-65/40BN	33.82	5.45	3.69	4.57	0.68	56.6
V5	M-80/50BN	61.87	7.50	1.83	4.67	0.24	72.2
V6	H-65/40BN	95.95	6.34	1.30	3.82	0.21	65.7
V7	H-80/40BP	88.10	12.20	10.60	11.40	0.87	111.6
V8	M-0	50.48	–	–	–		37.5
V9	M-45/50BN	51.03	4.18	4.43	4.31	1.06	66.8
V10	L-80/40BP	40.74	7.71	8.18	7.95	1.06	81.2
V11	M- ϕ 8	50.48	–	–	–		80.9
V12	M-80/30BP	49.67	6.93	7.13	7.03	1.03	92.7
V13	H-0	85.57	–	–	–		40.4
V14	H-80/50BN	96.34	6.70	1.91	4.31	0.29	62.9
V15	H-45/50BN	84.88	7.28	5.94	6.61	0.82	68.9
V16	H-80/30BP	83.60	8.84	7.38	8.11	0.83	94.7
V17	H- ϕ 8	85.57	–	–	–		94.3
V18	M- ϕ 6	48.25	–	–	–		74.1
V19	H- ϕ 6	74.50	–	–	–		79.1
V20	L- ϕ 6	41.90	–	–	–		85.7
V21	M-65/40BN-b	45.30	6.20	5.55	5.88	0.90	55.7
V22	L-80/50BN-b	39.58	7.35	6.67	7.01	0.91	50.6

Bold values indicate beams with BP fibers

6.4 Results of the Shear Tests on Beams

All failures were produced by shear with three different failure modes:

- *Failure Mode (I)*: First crack appeared in the middle of the web with an inclination of 45° and a second crack forms close to the initial. The first crack is expanding, spreading all over the web and has a bigger width compared to the cracks created after it. An instantaneous increase is observed in all crack widths, as the bottom flange cracks, followed by a continuously increasing crack opening. In the end, new cracks are created connecting the other cracks to achieve the final failure (e.g. unreinforced beams: M-0 and H-0). Shear cracks development is shown in Fig. 6.6.
- *Failure Mode (II)*: The first crack appeared next to the point of loading and shortly after that, a second one is created, which propagates rapidly through the whole flange. The cracks spread to the support to the whole web and their width increased until the top flange was cracked. Afterwards, crack openings

Fig. 6.6 Shear crack evolution (failure mode I)

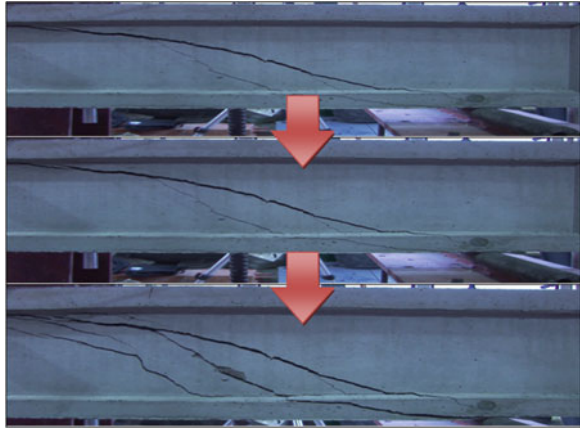
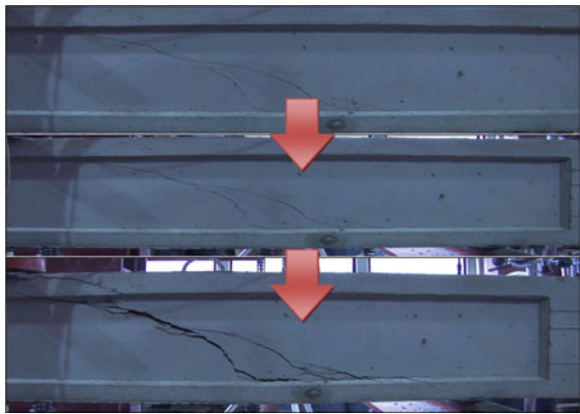


Fig. 6.7 Shear crack evolution (failure mode II)



grow very fast and produce the failure (e.g. beams L-80/50BN-a, L-65/40BN, M-80/50BN, H-65/40BN, M-45/50BN, L-80/40BP, H-80/50BN, H-80/30BP and L-80/50BN-b). Shear cracks development is shown in Fig. 6.7.

- *Failure Mode (III)*: First crack appeared in the web close to the loading point, with an inclination of about 45° . A second crack develops, with a larger inclination, closer to the support. Cracks develop slowly during the test, but cracked zones are created, where the concrete is significantly damaged, especially where cracks were clustering together. Finally, the failure occurs after the development of a crack in the top flange (e.g. beams with stirrups $\phi 8$ or BP fibers: M-80/40BP, M- $\phi 8$, M-80/30BP and H- $\phi 8$). Shear cracks evolution is shown in Fig. 6.8.

Shear strength behavior is significantly influenced by the fiber type, ranging from a low shear strength improvement (compared with unreinforced concrete) to a behavior even more ductile than that of a beam with stirrups. Low strength

Fig. 6.8 Shear crack evolution (failure mode III)



concretes with $\phi 6$ stirrups showed a very brittle post-crack behavior, while beams with BN fibers were the most ductile. For all strength levels, beams with BP fibers and reinforced beams reached the highest loads. Beams with traditional shear reinforcement show an important deflection increase just after the first crack and a greater load reduction after peak.

From those shear tests: load, deflection and crack widths were measured. Also, cracking pattern was observed by means of pictures and video recording.

Figure 6.9 shows the load-deflection response of all tested beams. The maximum loads are reported in Table 6.3.

Shear cracks widths development during the test was analyzed by analysis of pictures coordinated with loading process through the time (Fig. 6.10). In the load-deflection curves, the point markers indicate the maximum shear crack width for its corresponding load-deflection value. It can be noticed that at shear peak load, the shear crack opening was about 0.2 mm.

Observing Fig. 6.10, the beam with stirrups ($H\phi 6$) achieved the greatest deflection (at midspan) at the peak load and reached higher deflection, if compared with SFRC. The beam with BN fibers obtained crack widths slightly smaller for the same deflection, as compared to the beam with BP fibers. Obviously, the beam without any reinforcement had a completely brittle behavior.

In the Sect. 6.3 of this chapter, it was obtained that toughness properties of the FRC depended not only of the type of fibers, but also with the compressive strength of the concrete. For that, it was determined a new parameter $f_{Rm} = (f_{R1} + f_{R3})/2$. After having the test results of the beams, it is intended to know if there is a relationship between the toughness properties (using shear stress τ , determined with f_{R3} and f_{Rm}) and the experimental shear value (V_{test} in kN) and, which toughness value (f_{R3} or f_{Rm}) represents better the shear behavior to be included in the design Codes. Therefore, Fig. 6.11 shows the experimental shear strength versus the “ τ ” factor proposed by RILEM [13] ($\tau = k_f \cdot 0.7 \cdot \xi \cdot 0.18 \cdot f_{R3}$) and, in Fig. 6.12, the same tendency was analyzed but using an average residual flexure tensile strength $f_{Rm} = (f_{R1} + f_{R3})/2$

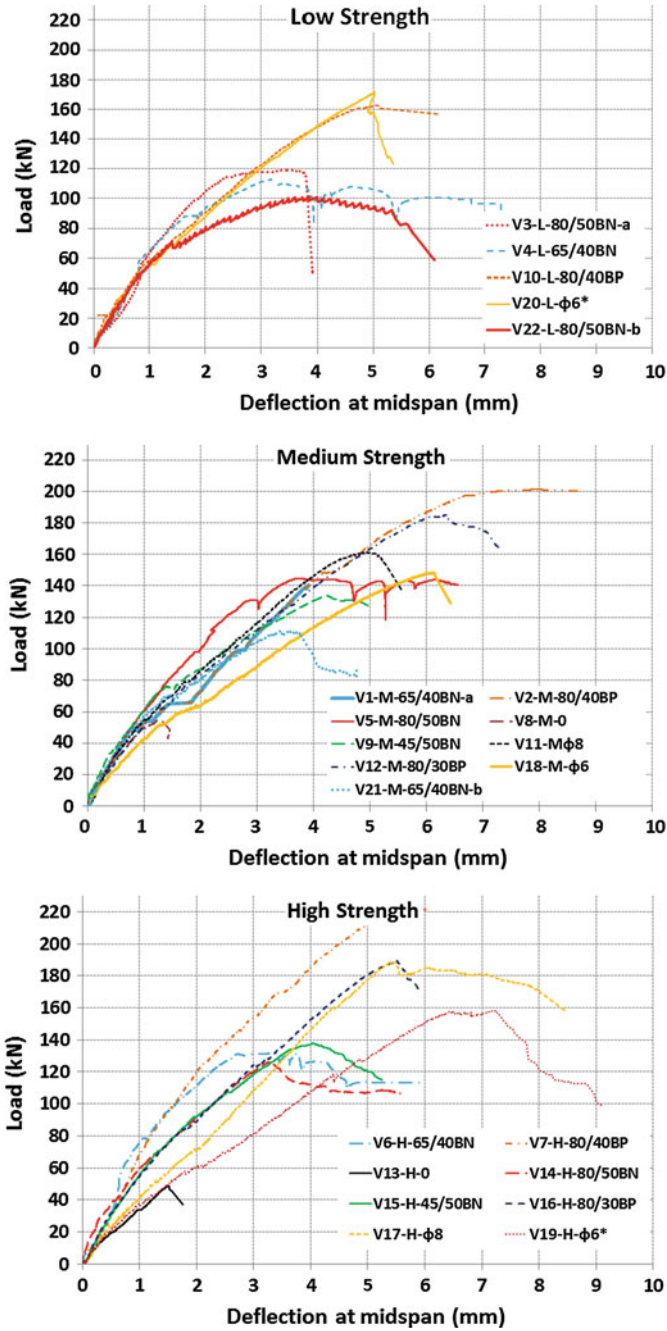


Fig. 6.9 Load-deflection at mid-span curves

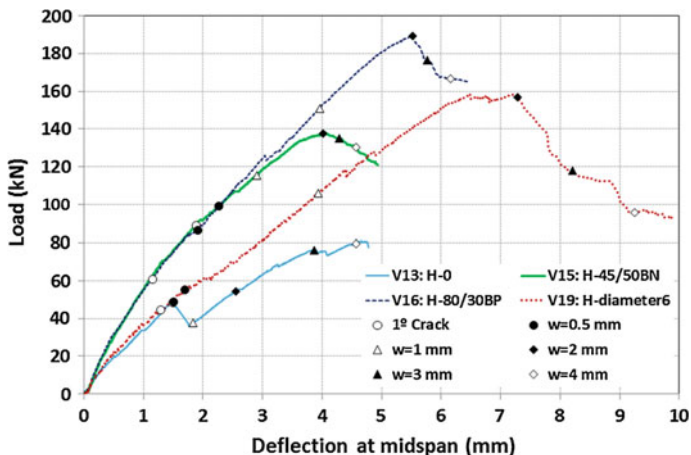


Fig. 6.10 Crack width evolution indicated over the load-deflection curve

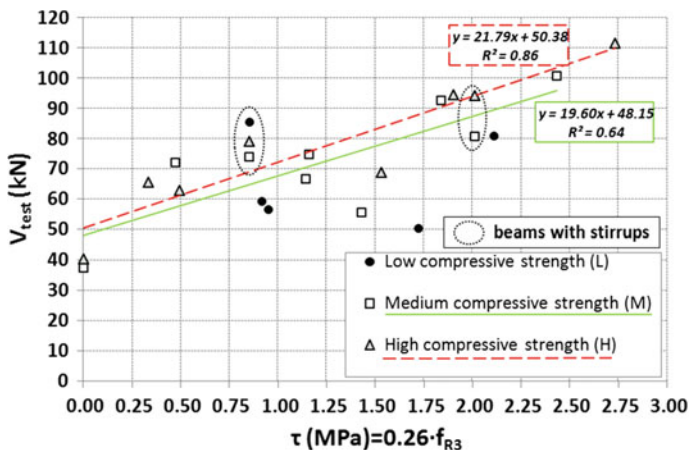


Fig. 6.11 $V_{test}-f_{R3}$ response

instead of f_{R3} . In order to analyze these same graphs (Figs. 6.11 and 6.12), the “ τ ” value for the beams with stirrups was determined through an analogy which consist on assume the V_{su} (corresponding to the stirrups contribution to shear) equal to V_{fu} (corresponding to the fibers contribution to shear) obtaining, in this way, an equivalent τ value for the shear reinforcement ($\tau = V_{su}/b \cdot d$) which obviously have the same value for both graphs (Figs. 6.11 and 6.12) corresponding to f_{R3} and the f_{Rm} , respectively. This is:

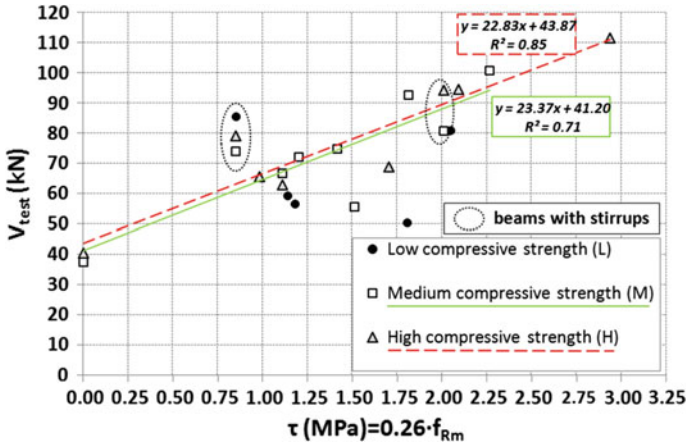


Fig. 6.12 V_{res} - f_{Rm} response; $f_{Rm} = (f_{R1} + f_{R3})/2$

$$V_{ju} = k_f \cdot 0.7 \cdot \xi \cdot 0.18 \cdot f_{R3} \cdot b \cdot d \equiv V_{su}$$

with: $k_f = 1.13$; $\xi = 1.81$; $b = 90 \text{ mm}$ for all beams

$$k_f \cdot 0.7 \cdot \xi \cdot 0.18 \cdot f_{R3} = \tau = 0.26 \cdot f_{R3}$$

For the particular case of beam V18 (M- $\phi 6$), with $\phi 6@200 \text{ mm}^{-1}$ leg:

$$0.26 \cdot f_{R3} \cdot b \cdot d \equiv V_{su} = 23511 \text{ (N)}$$

$$0.26 \cdot f_{R3} = \frac{23511}{b \cdot d} = \frac{23511 \text{ N}}{90 \text{ mm} \cdot 307.98 \text{ mm}} = 0.85$$

Equivalent τ values for all the beams with stirrups are reported in Table 6.4.

In Fig. 6.11 a linear tendency was observed. In Fig. 6.12, the same tendency was analyzed but using an average residual flexure tensile strength $f_{Rm} = (f_{R1} + f_{R3})/2$ instead of f_{R3} , and a better correlation was obtained for medium strength concretes (see continuous green line). This linear dependency was found with no influence of

Table 6.4 Equivalent τ -values for all the beams with stirrups

Reference	Beam ID	d (mm)	Transverse reinforcement	V_{su} (N)	$\tau = V_{su}/b \cdot d$
V11	M- $\phi 8$	307.98	$\phi 8@150 \text{ mm}^{-1}$ leg	55,730	2.010592
V17	H- $\phi 8$	307.98	$\phi 8@150 \text{ mm}^{-1}$ leg	55,730	2.010592
V18	M- $\phi 6$	307.98	$\phi 6@200 \text{ mm}^{-1}$ leg	23,511	0.848215
V19	H- $\phi 6$	297.98	$\phi 6@200 \text{ mm}^{-1}$ leg	22,748	0.848230
V20	L- $\phi 6$	297.98	$\phi 6@200 \text{ mm}^{-1}$ leg	22,748	0.848230

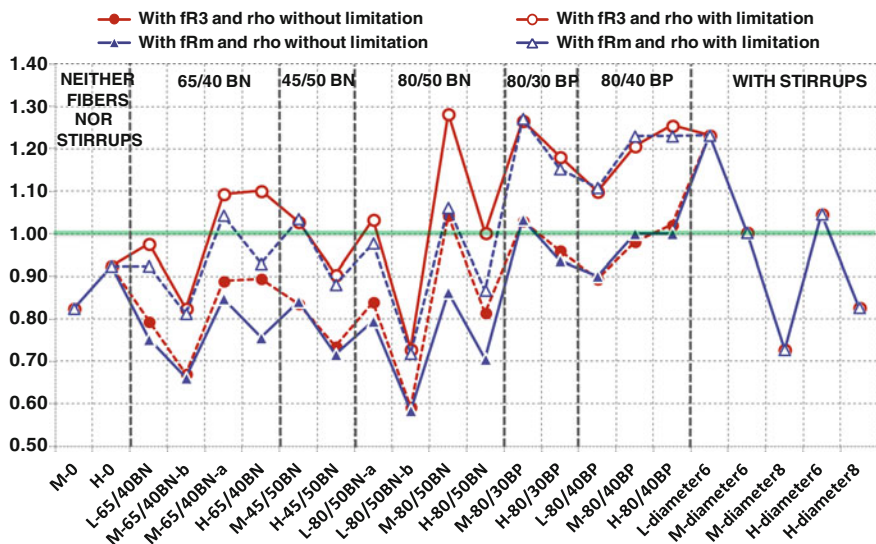


Fig. 6.13 Shear safety margins according to MC2010. *Note* rho (ρ) = longitudinal reinforcement ratio; where $\rho_{\max} = 2\%$

concrete strength when varying from 55 to 90 MPa. The linear dependency for high strength concretes is very high (see *dashed red line*), with a value $r^2 \approx 0.85$ for both cases, using f_{R3} and using f_{Rm} . For medium strength concretes the approximation to a straight line is worse than for high strength concretes, but the correlation is slightly better when f_{Rm} ($r^2 = 0.71$) is used instead of f_{R3} ($r^2 = 0.64$). In a few words, after seeing Figs. 6.11 and 6.12, it seems that parameter represent much better the tendency of the experimental shear value (with a coefficient of correlation, r^2 , close to the unit, thus, points follow approximately a straight line) for different levels of compressive strength, when f_{Rm} is used instead of f_{R3} . Therefore, f_{R3} residual strength may not be the most adequate parameter to define the shear capacity, as the average crack width along the failure crack will be smaller.

For low strength concretes shear capacity is reduced, so is reasonable the compression strength limitation ($f_{ck} \leq 60$ MPa) according to the EHE-08 [14]. Only some points are out of this tendency.

The shear safety margin (SM) obtained as V_{test} / V_{theo} (the shear test value divided by the shear theoretical value) was used as a reference parameter to compare the results obtained from the analyzed beams (see plot in Fig. 6.13). Theoretical shear values were calculated by means of the formulation of the first complete draft of Model Code 2010 [12]. Beams without fibers were calculated by applying the most accurate form (*Level III of Approximation*), which permits the calculation of ϵ_x and directly calculates the corresponding inclination of the compression stresses (θ). Level III of approximation was based directly in the equations of the Modified Compression Field Theory (MCFT) [15]. The beams with fibers were calculated by

Table 6.5 Model code 2010 (first complete draft) shear formulas

Code	Theoretical shear (V)
V_{cu} : Concrete contribution to shear; V_{fu} : Fibers contribution to shear	
MC2010 without fibers	$V_{cu} = k_v \cdot (\sqrt{f_{ck}/\gamma_c}) \cdot z \cdot b_o$ (<i>level III approximation</i>)
MC2010 with fibers	$V_{cu} + V_{fu} = [(0.18/\gamma_c) \cdot \xi \cdot (100 \cdot \rho_l \cdot C_2)^{1/3} + 0.15 \sigma_{ck}] \cdot b_o \cdot d$ $C_2 = (1 + 7.5 \cdot (f_{Ftk}/f_{ctk})) \cdot f_{ck}$

applying the formula proposed in MC2010, which includes the effect of fibers inside the concrete matrix contribution (see Table 6.5).

The reinforcement ratio for longitudinal reinforcement ($\rho_l = A_s/(b_o \cdot d)$) was equal to 3.72 % for all beams, except for beams V19 (H ϕ 6) and V20 (L ϕ 6) because of their lower effective depth (d) ($\rho_l = 3.84$ %). It should be observed that MC2010 formula limits to a maximum 2 % the ρ_l value. Figure 6.13 shows SMs obtained in four cases: using the formula with and without the ρ_l limitation ($\rho_{l,max} \leq 2$ %), and also these combinations using f_{R3} or f_{Rm} . As can be observed, in the formulations (see Table 6.5), the limitation of ρ_l in MC2010 only affects beams reinforced with fibers. The results were arranged attending to their shear reinforcement type. Firstly, results for beams without fibers and stirrups are shown followed by the beams reinforced only with fibers (firstly low carbon fibers -BN- and then, high carbon fibers -BP- being both groups ordered by increasing length of fibers). Finally, results for beams with stirrups are represented.

It can be observed that SMs were more balanced for the same type of fiber (BN or BP), when SM values were calculated using f_{Rm} instead f_{R3} ; this underlines the important role of f_{Rl} on shear strength.

Contrarily to the results on previous papers [16–19], in this program SM were lower than 1, so unsafe, when real ρ_l (without 2 % limitation) is used. In other paper [19], it was observed that, when the longitudinal reinforcement was much higher to 2 %, shear strength estimations according to MC2010 were too conservative. In the experimental program developed in this chapter, this tendency was not observed, and a low SM (lower than 1 and then unsafe) is obtained when the actual ρ value is applied. This fact may be explained as a consequence of a too small concrete cover over of the longitudinal reinforcement.

In Fig. 6.13 it can be also observed that the beams with the best fibers (fibers BP) achieved safe SM ($SM \approx 1$), this is because fibers BP make the cover more effective than with normal fibers (BN fibers). Figure 6.14 shows the beam M-0; it can be observed that failure was influenced by the small cover of the longitudinal reinforcement (see crack at the level of this reinforcement); triggering an earlier failure. Therefore, a lower SM (lower than the unit) was obtained (as can be seen in Fig. 6.14).



Fig. 6.14 Small cover of beam M-0

6.5 Conclusions

An experimental program including shear tests on twenty-two reinforced FRC beams has been developed to investigate how the quality of the fibers can influence in shear behavior and the differences on behavior between reinforced beams with fibers a with stirrups. From the obtained, the following conclusions can be drawn:

- Shear strength and load deflection response shown an important dependence on the fiber type. Low strength concretes with $\phi 6$ stirrups shows a very brittle postcracking behavior while beams with BN fibers were the most ductile. For all strength levels, beams with BP fibers and stirrups reached the highest loads. Beams with stirrups show an important deflection increase just after the first crack and a greater load reduction after the peak. Beam with stirrups reached higher deflection and crack openings, if compared with SFRC.
- The parameter f_{R3} , as a reference value for calculating shear strength, could be unsafe or overconservative. In these small beams (in this chapter), the parameter f_{Rm} (average value between f_{R1} and f_{R3}) may be more appropriate than f_{R3} .
- Beside f_{R3} , also f_{R1} , plays a major role in shear behavior and shear strength of beams. This fact suggests using equivalent energy (f_{eq}) to determine the shear strength of FRC beams in structural codes.
- In this program, safety margins obtained as V_{test}/V_{theo} (the shear test value divided by the shear theoretical value) were lower than the unit, so unsafe, when real values of the longitudinal reinforcement ratio ρ_l were used. The small cover of the main reinforcement may be the reason. Safety margins were low also for traditional reinforcements, even if stirrups yielded at failure.

References

1. Soroushian, S., and Z. Bayasi. 1991. Fiber-type effects on the performance of steel fiber reinforced concrete. *ACI Materials Journal* 88(2):129–134.
2. Bencardino, Rizzuti, Spadea and Swamy. 2013. Implications of test methodology on post-cracking and fracture behavior of steel fibre reinforced concrete. *Composites:Part B* 46:31–38.
3. Banthia, N., F. Majdazadeh, J. Wu, and V. Bindiganavile. 2014. Fiber synergy in hybrid fiber reinforced concrete in flexure and direct shear. *Cement and Concrete Composites*. 48:91–97.
4. fib, fib Bulletin 57.2010. Shear and punching shear in RC and FRC elements, Salò, Italy: Workshop proceedings 2010
5. Adhikary, B., and H. Mutsuyoshi. 2006. Prediction of shear strength of steel fiber RC beams using neural networks. *Construction and Building Materials* 20:801–811.
6. El-Niema, E. 1991. Reinforced concrete beams with steel fibers under shear. *ACI Structural Journal* 88(2):178–183.
7. Susetyo, J., P. Gauvreau, and F. Vecchio. 2011. Effectiveness of steel fiber as minimum shear reinforcement. *ACI Structural Journal* 108(4):488–496.
8. Dinh, H., G. Parra-Montesinos, and J. Wight. 2010. Shear behavior of steel fiber-reinforced concrete beams without stirrup reinforcement. *ACI Structural Journal* 107(5):597–606.
9. Parra-Montesinos, G. 2006. Shear strength of beams with deformed steel fibers. *Concrete International* 28(11):57–66.
10. Chalioris, C.E. 2013. Analytical approach for the evaluation of minimum fibre factor required for steel fibrous concrete beams under combined shear and flexure. *Construction and Building Materials*. 43:317–336.
11. Tiberti, G., F. Minelli, G. Plizzari, and F.J. Vecchio. 2014. Influence of concrete strength on crack development in SFRC members. *Cement and Concrete Composites*. 45:176–185.
12. MC2010. 2012. Fib Bulletin 65–66. Model Code—final draft, 1 and 2.
13. RILEM. 2003. RILEM TC 162-TDF: Test and design methods for steel fiber reinforced concrete. *Materials and Structures*. 36:560–567.
14. EHE08.2008. Instrucción de hormigón estructural EHE-08 (in spanish)., Ministerio de Fomento.
15. Vecchio, F., and M. Collins. 1986. The modified compression field theory for reinforced concrete elements subjected to shear. *ACI Journal* 83(2):219–231.
16. Cuenca, E., and Serna, P. 2010. Shear behavior of self-compacting concrete and fiber-reinforced concrete push-off specimens. In: *Design, Production and Placement of Self-Consolidating Concrete*, ed. Khayat, K.H., Feys, D., 429–438. RILEM Book series Volume 1. Netherlands: Springer.
17. Minelli, F., A. Conforti, E. Cuenca, G.A. Plizzari. 2014. Are steel fibres able to mitigate or eliminate size effect in shear? *Materials and Structures*. 47(3):459–473.
18. Serna, P., Cuenca E., and M. Alves-de Oliveira. 2011. Self-compacting fiber reinforced in precast elements production for shear resistance. In *Dedicated to Innovation: 50 years of MC Bauchemie*.
19. Cuenca, E., and P. Serna. 2013. Shear behavior of prestressed precast beams made of self-compacting fiber reinforced concrete. *Construction and Building Materials* 45:145–156.

Chapter 7

Experimental Tests on Hollow Core Slabs Made with FRC

7.1 Introduction

Hollow Core Slabs (HCS) are usually precast by extrusion and it is not easy to place stirrups; thus, it is difficult to guarantee shear resistance in some cases. This chapter describes an experience using Fiber Reinforced Concrete (FRC) to produce HCS by extrusion to enhance shear resistance.

In this chapter, introduction of FRC as shear reinforcement in a continuous way has been conducted in a precast plant where 26 real-scale HCS were produced. Elements were produced and tested in shear according to the following variables: amount of steel fibers (0, 50 and 70 kg/m³), two prestressing levels and a shear span/depth (a/d) ratio variable between 2.3 and 8.6.

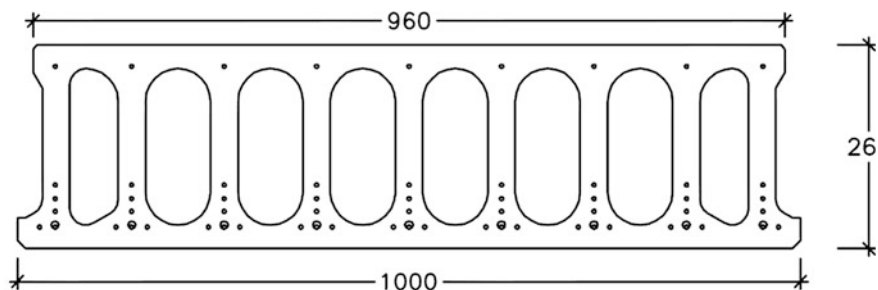
7.2 Experimental Investigation

Twenty-six HCS were tested and classified into two different series, mainly differentiated by the tension in the prestressing strands and the different design failure modes expected in them.

In Series I, HCS and their test disposition were designed in order to have a shear-flexure failure. For Series II, a program with greater variability of predictable failure modes was developed and was based on a design for more heavily prestressed HCS which includes a wider range of fiber reinforcement contents.

7.2.1 Hollow Core Slabs' Geometry

All the HCS presented the same geometry (Fig. 7.1) and a depth of 260 mm. This geometry is within the scope of application of the European Standard EN 1168+A2



Peso : 3.36 kN/m

$\xi = 0.54$

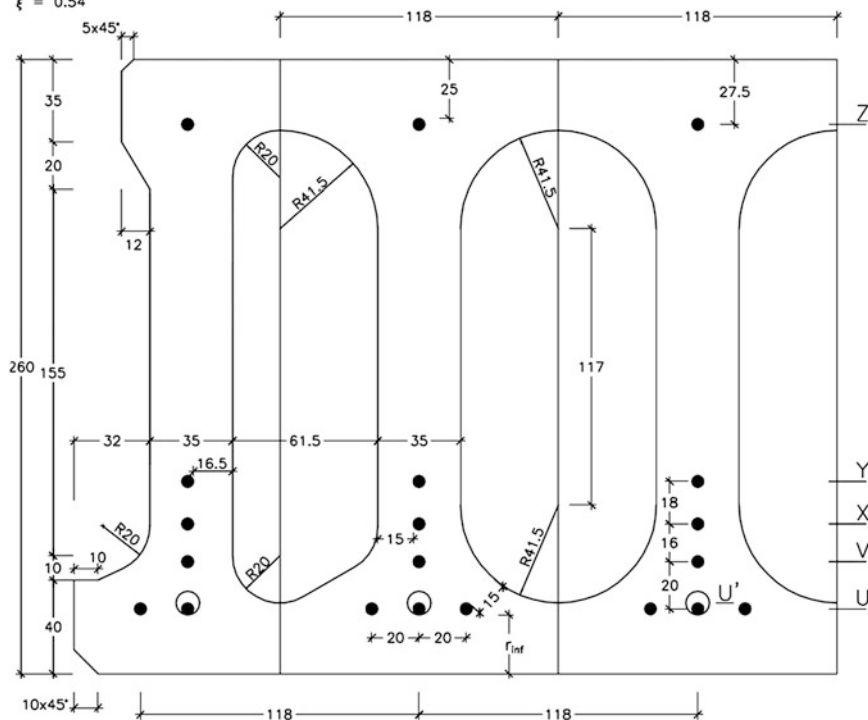


Fig. 7.1 Cross-section of HCS. Dimensions in millimeters

[1]. A different reinforcement, characterized by the number and diameter of wire or strand, its position and pretension (Fig. 7.1 and Table 7.1), was tested in each Series. In Table 7.1, “Initial tensile” is the prestressing tension applied prior to discounting prestressing losses; r_{inf} is the cover on the bottom reinforcement; ρ_l is the longitudinal reinforcement ratio (wires or 7-wire strands in this case) and σ_c is the average stress acting on the concrete cross-section due to the prestressing axial force, including prestressing losses.

Table 7.1 Reinforcement characteristics

Series	Initial tensile (MPa)	Prestressed losses (%)	r_{inf} (mm)	Reinforcement Position					ρ_l (%)	σ_c MPa
				U	U'	V	X	Z		
I	1,255	19.7	30	2 ϕ 5	5 ϕ 9.3	–	–	4 ϕ 5	0.5	2.87
II	1,255	27.2	25	25 ϕ 5	–	9 ϕ 5	4 ϕ 5	4 ϕ 5	1	5.69

As Table 7.1 shows, Series I included wires (Y 1860 C 5.0) with a diameter of 5 mm and 7-wire strands (Y 1860 S7 9.3), thus conforming a strand with a nominal diameter equal to 9.3 mm (the notation is defined in UNE 36094-97 and EN 10027-1) with a yielding stress f_{pk} equal to 1,637 MPa and a tensile strength of 1,860 MPa for the wires, a yielding stress f_{pk} equal to 1,581 MPa and a tensile strength of 1,860 MPa for strands. In Series II, on the other hand, only those wires with the same characteristics as those in Series I were used. All these values were nominal.

7.2.2 Concrete Mix Design

One important goal was to produce HCS by extrusion with very dry concretes by adding different amounts of steel fibers (0, 50 and 70 kg/m³). In order to optimize the material performance, several concrete compositions were tested.

The materials used in this study were a CEM I 52.5R cement type and calcareous crushed aggregates: 0/4 mm-sized sand, 0/6 mm-sized sand and 6/10 mm-sized gravel. The steel fibers utilized were low carbon steel with hooked-end (RC 65/40 BN), 40 mm in length, 0.62 mm in diameter, with an aspect ratio (length/diameter) equal to 65.

Two concrete admixtures were used: an accelerating high range water reducer/superplasticizer and a specific admixture for extruded concretes.

Table 7.2 presents the mix designs.

Table 7.2 Mix design of the HCS tested

(kg/m ³)	TC	FRC-50	FRC-70
Coarse aggregate (6/10 mm)		843	
Sand (0/4 mm)		690	
Sand (0/6 mm)		311	
Cement		411	
Water (liters)		198	
W/C ratio		0.48	
Fibers	0	50	70
Superplasticizer (liters)	1.5	1.5	1.6
Admixture for extruded concretes (l)	0.8	0.8	0.7
Mixing time (min)	1.5	4.3	5.4

Table 7.3 Concrete mechanical properties

Series	Concrete	f_c (MPa)	f_{R1} (MPa)	f_{R2} (MPa)	f_{R3} (MPa)	f_{R4} (MPa)
I	TC	54.2	–	–	–	–
	FRC-50	50.4	2.75	2.85	2.83	2.66
II	TC	43.8	–	–	–	–
	FRC-50	38.2	4.25	4.66	4.70	4.37
	FRC-70	35.9	5.74	6.03	5.80	5.47

Average values

Concrete without fibers was used in the daily HCS production in the precast industry that provided the FRC elements. Mechanical properties were controlled in one concrete sample by means of the compressive strength test on 150×300 mm cylinders (EN 12390-3) and the flexural tensile strength test (EN 14651). The latter were obtained with the flexural test: the residual flexural tensile strength ($f_{R,j}$), which corresponds to the crack mouth opening displacements (CMOD) linked to the crack openings of 0.5, 1.5, 2.5 and 3.5 mm ($j = 1, 2, 3, 4$ respectively).

Table 7.3 provides the mechanical properties of the different concrete mixes. All the values were obtained as an average of three specimens made with two different samples for each concrete type, 28 days after casting. As it can be observed in Table 7.3 there is a big difference between the results of same types of concrete, probably because of different casting conditions and very different external temperatures as Series I and Series II were produced in different seasons. Also, it is very important to know that the concrete was made in a precast plant during its normal cycle of production and some little details could be changed to adapt the concretes of our Series to the needs of the company.

7.2.3 HCS Production

A continuous slab was casted. It occupied a complete lane in which prestressed strands were positioned; the machine received the concrete and HCS were formed by extrusion (Fig. 7.2).

As expected [2], some problems initially occurred when a new concrete type was produced. The initial problems were related with the introduction of fibers into a very dry concrete mix to obtain an optimum concrete ready to use in the extrusion process. Yet after the preliminary adjustments in the process, these problems no longer appeared and a good surface aspect was achieved (Fig. 7.3). This fact demonstrates that it is possible to produce FRC Hollow Core Slabs in a normal daily production cycle of a precast plant.

Only some slabs had an undulated surface, webs of different widths and defects on the slab surface, which were created in some zones where fibers blocked the extrusion machine. These stretches were thrown away.



Fig. 7.2 Extrusion process

Fig. 7.3 How the surface of HCS looked



7.2.4 Test Set-Up

HCS were subjected to a four-point test bending by adapting the loading scheme shown in Fig. 7.4.

Figure 7.5 depicts the test set-up. Tests were done in the precast industry.

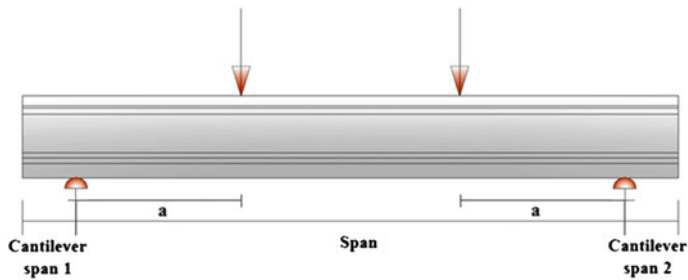


Fig. 7.4 Loading scheme adapted for the HCS test

Fig. 7.5 Test set-up. Shear diagonal tension failure



Loads and supports were disposed into two cross lines. The shear span/depth (a/d) ratio varied between 3 and 4.4 in Series I. In Series II there were three different a/d ratios: 2.3, 3.4 and 8.6. Table 7.4 indicates all these parameters. In order to facilitate their identification, the HCS *Specimen ID* took the following structure:

$$\{\text{Series: I or II}\} - \{\text{Amount of fibers (kg/m}_3\}) - \{a/d \text{ ratio}\} \{a, b, c, \dots\}$$

If there were identical HCS, they were differentiated by placing: a, b, c, etc. So, an HCS from Series II with 50 kg/m^3 of fibers, and with $a/d = 3.4$, which had other identical HCS, would be: II-50-3.4b.

In order to analyze the previous precrack effect, three HCS [II-0-3.4(P), II-50-3.4(P) and II-70-3.4(P)] were precracked before the shear test by loading the HCS with a longer span length ($a/d = 4.9$) until the maximum flexure crack width in the span reached 0.2 mm. In these precrack steps, a shear of 161kN was accomplished. After the flexure precracking tests, supports were moved to adapt them to shear tests conditions in order to have shear failure on the flexure precracked zone.

Table 7.4 Shear tests description and specimen ID to each HCS

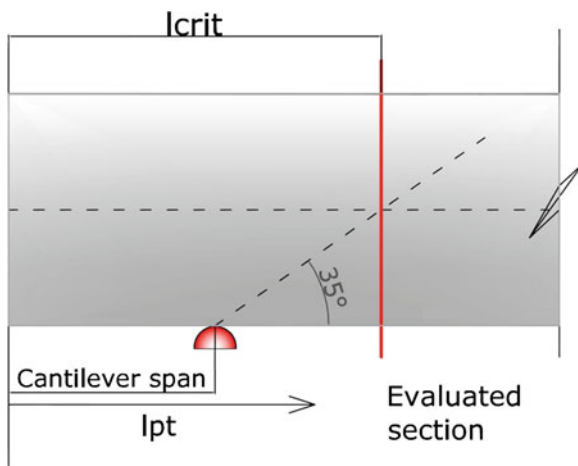
	Specimen ID	F*	a/d ratio	Cantilever span (mm)**	l_{pt} (mm)	l_{crit} (m)	V_{test} (kN)	F.M.	HCS length (mm)			
Series I	I-0-4.1	0	4.1	600	400.2	785.66	131.15	SF	3,990			
	I-0-4.3a		4.3	630		815.66	131.11	SF	3,980			
	I-0-4.3b		4.3	630		815.66	134.90	SF	4,000			
	I-50-3.1	50	3.1	120	420.1	305.66	160.19	A	2,975			
	I-50-3.9a		3.9	700		885.66	162.10	SF	4,000			
	I-50-3.9b		3.9	700		885.66	162.10	SF	4,000			
	I-50-4.3		4.3	860		1,045.66	152.61	SF	4,500			
	I-50-4.4		4.4	870		1055.66	158.62	SF	4,500			
	I-50-3.0a		3.0	120		305.66	172.95	SF	2,975			
	I-50-3.0b		3.0	2,120		2305.66	200.63	SF	4,500			
	I-50-3.1c		3.1	2,035		2220.66	189.43	SF	4,500			
	Series II		II-0-2.3	0		2.3	210	350.6	395.66	310.80	A	1,990
			II-0-3.4			3.4	270		455.66	213.10	S	2,600
II-0-3.4 (P)		3.4	2,105		2290.66	266.20	S		4,500			
II-0-8.6		8.6	250		435.66	131.60	SF		4,990			
II-50-2.3		50	2.3	500	384.1	685.66	410.00	S	2,600			
II-50-3.4a			3.4	225		410.66	236.70	S	2,580			
II-50-3.4 (P)			3.4	260		445.66	288.70	S	4,500			
II-50-3.4b			3.4	2,500		2685.66	202.00	S	5,000			
II-50-8.6		8.6	270	455.66	146.10	F	4,980					
II-70-2.3a		70	2.3	225	400.3	410.66	310.70	S	1,990			
II-70-2.3b			2.3	215		400.66	310.70	A	2,000			
II-70-3.4a			3.4	250		435.66	266.70	S	2,570			
II-70-3.4 (P)			3.4	290		475.66	315.00	S	4,500			
II-70-3.4b			3.4	290		475.66	251.40	S	4,500			
II-70-8.6			8.6	230		415.66	135.20	F	4,980			

SF Shear-flexure failure, S Web shear tension failure, F flexure failure, A Anchorage failure of strands, P Hollow core slab precracked in flexure, *F Amount of steel fibers (kg/m^3), ** Values correspond to the cantilever span nearest the failure side, l_{pt} basic value of the transmission length, l_{crit} distance between the end of the slab and the critical section, F.M. Failure mode

Table 7.4 shows the variables analyzed for each test, as well as the maximum load reached and the main failure mode. Figure 7.6 shows the section for web shear tension failures that was adopted; it is given by the intersection between the centroidal axis of the HCS and the failure line that emerges from the edge of the support with an angle of 35° to the horizontal axis, as indicated EN 1168+A2 [1], which delimitates the zone affected by the support reaction.

Several HCS were tested with a critical length (l_{crit}) below the transfer length (l_{pt}), which was evaluated according to the European standard EN 1168+A2 [1] that, refers to Eurocode 2 [3] (see Table 7.4). In some HCSs, this caused anchorage failure

Fig. 7.6 Section taken in consideration in web shear tension failure calculations



[I-50-3.1, II-0-2.3 and II-70-2.3b]. Nevertheless in HCS I-50-3.0a, which was also performed with a critical length below the required transfer length, there was no anchorage failure; the reason was that the crack which caused the failure was at a long distance from the cantilever. If there is not enough anchorage, prestressing contribution should not be considered but if, in this case, it is not considered in the calculations very high SM will be obtained. It is, therefore, evident that when the cantilever span is short, there is a partial transfer of prestressing. In Table 7.5, the parameters used in the *basic value of the transmission length* (l_{pt}) calculation, according to the Eq. (8.16) of the EC2 (here (Eq. 7.1)), are presented.

$$l_{pt} = \alpha_1 \cdot \alpha_2 \cdot \phi \cdot \sigma_{pm0} / f_{bpt} \quad (7.1)$$

where: $\alpha_1 = 1.25$ for sudden release; α_2 (Series I) = 0.19 for 3 and 7-wire strands; α_2 (Series II) = 0.25 for tendons with circular cross section; ϕ is the nominal diameter of the tendon; σ_{pm0} is the tendon stress just after release and f_{bpt} is the constant bond stress at which the prestress is transferred to the concrete at release of tendons. f_{bpt} is determinate with the Eq. (8.15) of EC2 (here (Eq. 7.2)):

$$f_{bpt} = \eta_{p1} \cdot \eta_1 \cdot f_{ctd}(t) \quad (7.2)$$

where: η_{p1} is a coefficient that takes into account the type of tendon and the bond situation at release ($\eta_{p1} = 2.7$ for indented wires and $\eta_{p1} = 3.2$ for 3 and 7-wire strands); $\eta_1 = 1.0$ in this case (good bond conditions) and $f_{ctd}(t)$ is the design tensile value of strength at time of release. All these values are presented in Table 7.5.

Recently, Elliott et al. [4] has proposed an equation for prestressed hollow core units without steel fibers manufactured using long-line techniques. The effect of this on a typical slab design is to increase $V_{Rd,c}$ by about 10 % and reduce the zone of transmission around holes by about 350 mm, which in some circumstances may benefit the failure criteria at holes.

Table 7.5 Parameters used in l_{pr} calculation

Series	Specimen ID	η_{p1}	$f_{ctd}(t)$ (MPa)	f_{bpt} (MPa)	ϕ (mm)	σ_{pm0} (MPa)	l_{pt} (mm)
I	I-0-4.1	3.20	1.74	5.56	9.3	1007.77	400.20
	I-0-4.3a	3.20	1.74	5.56	9.3	1007.77	400.20
	I-0-4.3b	3.20	1.74	5.56	9.3	1007.77	400.20
	I-50-3.1	3.20	1.66	5.30	9.3	1007.77	420.07
	I-50-3.9a	3.20	1.66	5.30	9.3	1007.77	420.07
	I-50-3.9b	3.20	1.66	5.30	9.3	1007.77	420.07
	I-50-4.3	3.20	1.66	5.30	9.3	1007.77	420.07
	I-50-4.4	3.20	1.66	5.30	9.3	1007.77	420.07
	I-50-3.0a	3.20	1.66	5.30	9.3	1007.77	420.07
	I-50-3.0b	3.20	1.66	5.30	9.3	1007.77	420.07
	I-50-3.1c	3.20	1.66	5.30	9.3	1007.77	420.07
	II	II-0-2.3	2.70	1.51	4.07	5	913.64
II-0-3.4		2.70	1.51	4.07	5	913.64	350.62
II-0-3.4 (P)		2.70	1.51	4.07	5	913.64	350.62
II-0-8.6		2.70	1.51	4.07	5	913.64	350.62
II-50-2.3		2.70	1.38	3.72	5	913.64	384.10
II-50-3.4a		2.70	1.38	3.72	5	913.64	384.10
II-50-3.4 (P)		2.70	1.38	3.72	5	913.64	384.10
II-50-3.4b		2.70	1.38	3.72	5	913.64	384.10
II-50-8.6		2.70	1.38	3.72	5	913.64	384.10
II-70-2.3a		2.70	1.32	3.57	5	913.64	400.33
II-70-2.3b		2.70	1.32	3.57	5	913.64	400.33
II-70-3.4a		2.70	1.32	3.57	5	913.64	400.33
II-70-3.4 (P)		2.70	1.32	3.57	5	913.64	400.33
II-70-3.4b		2.70	1.32	3.57	5	913.64	400.33
II-70-8.6		2.70	1.32	3.57	5	913.64	400.33

7.3 Tests Results and Analysis

7.3.1 Failure Modes

Different failure modes were observed.

7.3.1.1 Shear Failure Modes

Shear-Flexure Failure (SF)

On the shear-flexure failures (Fig. 7.7), flexure cracks initially developed but, eventually, one of them caused the failure. The failure crack was always situated in

Table 7.6 Shear resistance (kN) of the regions uncracked in bending according to EN 1168+A2 (V_{Rdc}) and RILEM (V_f)

Specimen ID	V_{test}	F.M.	V_{Rdc}	V_f RILEM	$V_{Rdc} + V_f$	$SM = \frac{V_{test}}{V_{Rdc} + V_f}$	$SM = \frac{V_{test}}{V_{Rdc}}$
II-0-2.3	310.8	A	191.58	0.00	191.58	1.62	1.62
II-0-3.4	213.1	S	207.30	0.00	207.30	1.03	1.03
II-50-2.3	410.0	S	230.04	78.77	308.81	1.33	1.78
II-50-3.4a	236.7	S	170.22	78.77	248.99	0.95	1.39
II-50-3.4b	202.0	S	258.44	78.77	337.21	0.60	0.78
II-70-2.3a	310.7	S	159.29	98.83	258.12	1.20	1.95
II-70-2.3b	310.7	A	156.75	98.83	255.58	1.22	1.98
II-70-3.4a	266.7	S	165.45	98.83	264.28	1.01	1.61
II-70-3.4b	251.4	S	174.87	98.83	273.70	0.92	1.44

F.M. Failure Mode

the shear span close to one of the load points. Firstly, the crack grew vertically to finally turn in direction by taking a shear slope near the top.

Web Shear Tension Failure of Concrete (S)

In most cases, failure was caused by diagonal shear tension (Fig. 7.5). Shear failure was produced by inclined cracks due to principal tensile stresses. On these slabs, a transverse reinforcement was not placed to resist shear, so fibers, prestressing strands and the concrete zone in compression had to resist shear stresses; if shear grew, the crack progressed upwardly to the HCS top.

Fig. 7.7 Shear-flexure failure (SF)



7.3.1.2 Flexure Failure Mode (F)

For the higher a/d ratio in Series II ($a/d = 8.6$), several flexure cracks developed vertically toward the top of the HCS, and one of these cracks continued to grow until a flexure failure (Fig. 7.8) took place.

7.3.1.3 Failure on Anchorage of Prestressing Strands (A)

During the tests, slippage on strands (Figs. 7.9 and 7.10) was also detected and, in most cases, this led to a diagonal crack.

7.3.2 Load-Deflection Response

Figure 7.11 plots the deflection on the mid-span for the most representative HCS of series I.

As expected, HCS I-50-3.1 failed through anchorage and the failure was brittle. All the other HCS failed through shear-flexure and showed a ductile failure. The maximum load increased when shear span diminished. HCS with fibers exhibited greater shear capacities.

In Figs. 7.12, 7.13 and 7.14, the load-deflections curves of Series II are plotted and classified by fibers amount according to the shear span (a/d) ratio. Three behaviors are distinguished. HCS with $a/d = 2.3$ accomplished the greatest loads with brittle failure through a diagonal shear (S).

Fig. 7.8 Flexure failure



Fig. 7.9 Sliding of the strands in concrete



Fig. 7.10 Crack caused by tension shear and anchorage failure simultaneously



In these cases, and especially when the critical length l_{crit} was close to the transfer length l_t (II-0-2.3 and II-70-2.3b), final failure was caused by anchorage. For HCS II-70-2.3a had a web shear tension failure occurred accompanied by anchorage failure, therefore, in situations like this, it is not entirely clear whether it is a shear tension failure or an anchorage failure (see Fig. 7.10). The lowest ultimate loads corresponds to the HCS with $a/d = 8.6$. In this supports-loads distribution, the highest deflections were achieved, showing clear ductile flexural failure (F) or shear-flexure (SF). In these cases, behavior was similar for the three types of concrete as the influence of fibers was only marginal, compared with the influence of the prestressing.

The HCS with an a/d ratio = 3.4 showed intermediate behavior by always cracking through web shear tension failure (S). The tendency of increasing shear capacity with an increasing amount of fibers is reported.

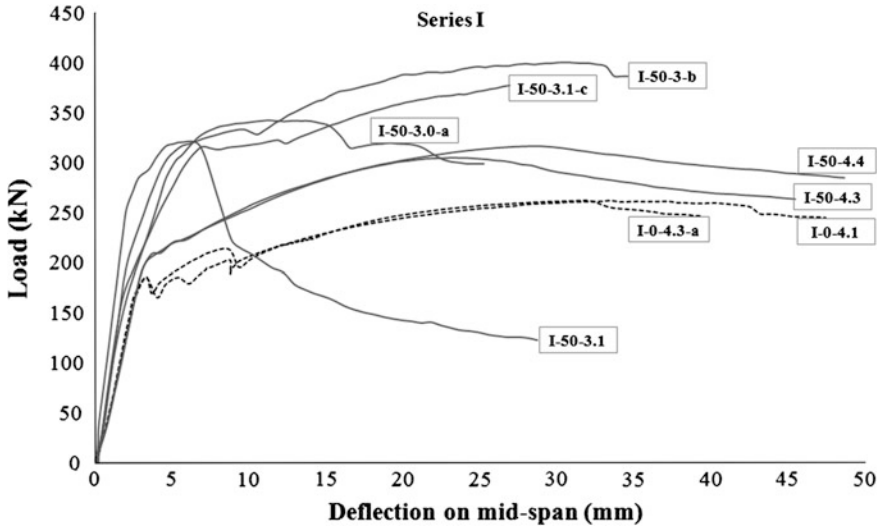


Fig. 7.11 Load-deflection response (Series I)

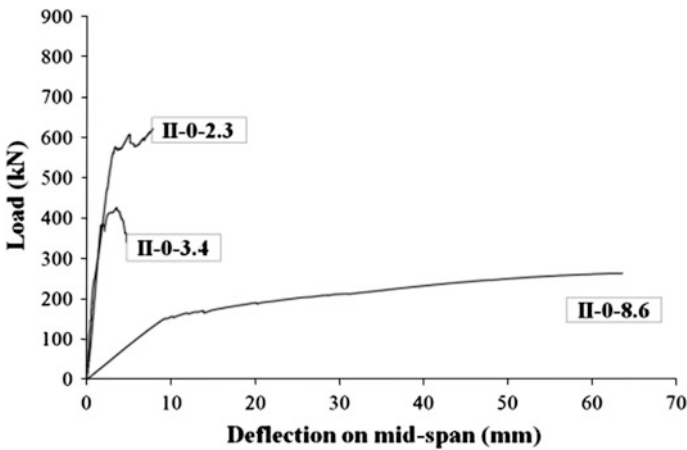


Fig. 7.12 Series II: HCS with 0 kg/m³ of fibers

For the a/d ratio equal to 3.4, we can see (Fig. 7.15) that the HCS [II-0-3.4(P), II-50-3.4(P) and II-70-3.4(P)], accomplished a more ductile behavior with greater loads than their equivalent specimens non precracked. Moreover, dependence on fiber amount was clearly evident.

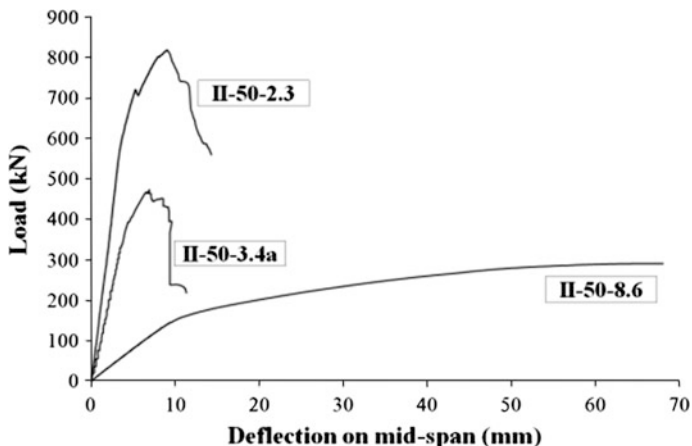


Fig. 7.13 Series II: HCS with 50 kg/m³ of fibers

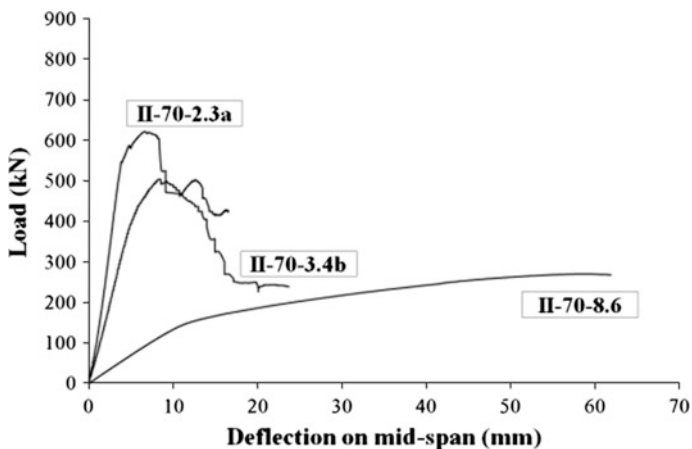


Fig. 7.14 Series II: HCS with 70 kg/m³ of fibers

7.3.3 Shear Values According to Current Design Codes and Failure Modes Discussion

7.3.3.1 Current Design Codes

Some authors like Pisanty [5], among others, claimed that the model proposed in EC2 [3] to evaluate the uncracked shear capacity of prestressed elements overestimated the real ultimate strength. For this reason, the standard EN 1168+A2 [1] proposes a reduction of shear resistance proposed by the EC2 [3] for regions uncracked in bending by means of the reduction factor $\varphi = 0.8$ (see Table III.3).

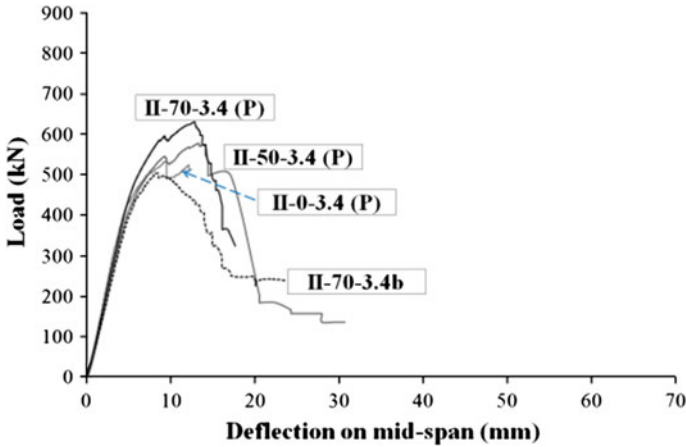


Fig. 7.15 Series II: HCS with $a/d = 3.4$

MC2010 [6] consider that shear tension failure can occur in regions uncracked in flexure (bending) when the principal tensile stress in the web reaches the tensile strength of concrete. MC2010 [6] ensures that this type of failure is relevant especially for precast elements like prestressed hollow core slabs. In other words, EC2 [3] considers a region as uncracked in bending when flexure stress is lower than tensile concrete strength.

Therefore, the shear capacity by diagonal shear tension was calculated for the critical section (Fig. 7.6) assuming the region as uncracked in bending using the formula of EN 1168+A2 [1] (Eq. 7.3). As this standard has no formulation to take into account fiber contribution, it was calculated by following the RILEM proposal [7]; the values are indicated in Table 7.7 (see Notation in Table III.3). The safety margins (SM) were obtained as V_{test}/V_{theo} (the shear test value divided by the shear theoretical value).

Table 7.7 Current codes shear formulas for elements without stirrups

	Code	Theoretical shear (V)
		V_{cu} = Concrete contribution; V_{fu} = Fibers contribution
Regions cracked in bending	EN 1168+A2 [1] + RILEM [7]	$V_{cu} = [(0.18/\gamma_c) \cdot \xi \cdot (100 \cdot \rho_1 \cdot C_2)^{1/3} + 0.15 \cdot \sigma_{ck}] \cdot b_o \cdot d$; $C_2 = f_{cv}$ $V_{fu} = k_f \cdot 0.7 \cdot \xi \cdot 0.18 \cdot (f_{R4k}/\gamma_c) \cdot b_o \cdot d$
	MC2010 [6] Without fibers:	$V_{cu} = k_v \cdot (\sqrt{f_{ck}}/\gamma_c) \cdot z \cdot b_o$ (Level III Approximation)
	MC2010 [6] With fibers:	$V_{cu} + V_{fu} = [(0.18/\gamma_c) \cdot \xi \cdot (100 \cdot \rho_1 \cdot C_2)^{1/3} + 0.15 \cdot \sigma_{ck}] \cdot b_o \cdot d$ $C_2 = (1 + 7.5 \cdot (f_{Ftuk}/f_{ctk})) \cdot f_{ck}$
Regions uncracked in bending	EN 1168+A2 [1] + RILEM [7]	$V_{cu} = \phi \cdot (I \cdot b/S) \cdot \sqrt{f_{ct}^2 + \beta \cdot \alpha_1 \cdot \sigma_{cd} \cdot f_{ct}}$ $V_{fu} = k_f \cdot 0.7 \cdot \xi \cdot 0.18 \cdot (f_{R4k}/\gamma_c) \cdot b_o \cdot d$

$$V_{Rdc} = \varphi \cdot (I \cdot b/S) \cdot \sqrt{(f_{ct}^2 + \beta \cdot \alpha_1 \cdot \sigma_{cd} \cdot f_{ct})} \quad (7.3)$$

To obtain real predictable resistance, the partial safety factors for material properties were considered in the calculation as $\gamma_c = 1$ and $\gamma_s = 1$ (Tables 7.6 and 7.8). Moreover, average values were utilized instead of characteristic values present in the formulas.

On the other hand, when failure took place in a region cracked in bending, shear strength capacity was calculated by the formulation of standard EN 1168+A2 [1] under cracked conditions (based on EC2 [3]) and by adding fibers contribution

Table 7.8 Shear values (kN) calculated without safety factors using codes and assuming regions cracked in bending (average values compression and residual flexural strength)

Specimen ID	V _{test}	F.M.	V _{FLEXURE}	SM (F)	V _{EN1168 +RILEM}	SM (V) EN1168+RILEM	V _{MC2010}	SM (V) MC2010
I-0-4.1	131.15	SF	133.86	0.98	100.55	1.30	104.16	1.26
I-0-4.3a	131.11	SF	126.63	1.04	102.25	1.28	101.80	1.29
I-0-4.3b	134.90	SF	125.21	1.08	102.25	1.32	101.31	1.33
I-50-3.1	160.19	A	196.42	0.82	149.18	1.07	128.10	1.25
I-50-3.9a	162.10	SF	153.86	1.05	149.18	1.09	128.10	1.27
I-50-3.9b	162.10	SF	153.86	1.05	149.18	1.09	128.10	1.27
I-50-4.3	152.61	SF	139.87	1.09	149.18	1.02	128.10	1.19
I-50-4.4	158.62	SF	137.79	1.15	149.18	1.06	128.10	1.24
I-50-3.0a	172.95	SF	199.25	0.87	149.18	1.16	128.10	1.35
I-50-3.0b	200.63	SF	197.82	1.01	149.18	1.34	128.10	1.57
I-50-3.1c	189.43	SF	197.12	0.96	149.18	1.27	128.10	1.48
II-0-2.3	310.80	A	560.58	0.55	150.10	2.07	182.42	1.70
II-0-3.4	213.10	S	373.72	0.57	150.10	1.42	182.42	1.17
II-0-3.4 (P)	266.20	S	373.72	0.71	150.10	1.77	182.42	1.46
II-0-8.6	131.60	SF	149.49	0.88	150.10	0.88	115.25	1.14
II-50-2.3	410.00	S	546.11	0.75	224.62	1.83	200.81	2.04
II-50-3.4a	236.70	S	364.07	0.65	224.62	1.05	200.81	1.18
II-50-3.4 (P)	288.70	S	364.07	0.79	224.62	1.29	200.81	1.44
II-50-3.4b	202.00	S	364.07	0.55	224.62	0.90	200.81	1.01
II-50-8.6	146.10	F	144.13	1.01	224.62	0.65	200.81	0.73
II-70-2.3a	310.70	S	540.50	0.57	243.15	1.28	207.60	1.50
II-70-2.3b	310.70	A	540.50	0.57	243.15	1.28	207.60	1.50
II-70-3.4a	266.70	S	360.34	0.74	243.15	1.10	207.60	1.28
II-70-3.4 (P)	315.00	S	360.34	0.87	243.15	1.30	207.60	1.52
II-70-3.4b	251.40	S	360.34	0.70	243.15	1.03	207.60	1.21
II-70-8.6	135.20	F	144.13	0.94	243.15	0.56	207.60	0.65

P Hollow core slab precracked in flexure, * Bond failure; Failures: SF Shear-flexure failure, S Web shear tension failure, S Web shear tension failure, F Flexure failure, A Anchorage failure of strands, F.M. Failure Mode

according to RILEM [7] and MC2010 [6]. To obtain the elements' shear theoretical values, each HCS can be approximated to a single double T beam; when the web width b_o was the sum of all the webs widths which composed the HCS. For the calculations, the fact that all the webs contributed in the same manner to resist shear was taken into account. However, some authors, like Elliott et al. [8], suggested that the shear capacity of HCS is not the same as the shear capacity of each component section, unless web widths are exactly equal; since shear failure finally occurs in the critical web. Therefore, it seems reasonable to calculate shear by not taking into account all the webs of the HCS. As HCS were treated as a sum of the double T beams, the contribution of the flange to the shear was considered in the calculations for the HCS made from fibers, by means of factor k_f (Table III.2), proposed in the RILEM guidelines. This value (k_f) was equal to 1.036 for all the cases. Neither EN 1168+A2 nor MC2010 considered flanges contribution to shear. For the HCS without fibers, MC2010 shear strength was calculated by applying the most accurate form (Level III of Approximation), which permitted the calculation of ε_x (see Table III.1 in the introduction to Part III) and directly calculated the corresponding inclination of the compression stresses (θ). Level III of Approximation was based directly on the equations of the Modified Compression Field Theory (MCFT) [9]. The resistance of HCS with fibers were calculated by applying the formula proposed in MC2010 (see Table 7.7), which included the effect of fibers inside the concrete matrix contribution. All the formulas used to calculate shear strength are clearly summarized in Table 7.7.

Code formulae included limitations on several parameters, such as the ρ_l reinforcement ratio for longitudinal reinforcement, the ζ factor which considers size effect, the σ_{ck} average stress acting on the concrete cross-section for an axial force due to prestressing actions, and the minimum concrete contribution due to shear V_{cu} , as presented in Table III.2 (see introduction to Part III). None of these limitations affected the values calculated in the beams tested in these Series. The safety margins ($SM = V_{test}/V_{theo}$) were used as a reference parameter to compare the results obtained from the different beams and Codes. Table 7.8 shows the shear values (experimental and theoretical) and their SM; it also indicates the shear values corresponding to the flexure failure mode and their corresponding SM. The ultimate flexural moment was calculated by taking into account the fibers contribution, according to MC2010 [6]. In the SM columns (Table 7.8), the values exceeding the unit are shown in boldface.

7.3.3.2 Series I: Shear Values According to Current Design Codes

By way of general conclusion, and as expected, all the slabs of Series I presented a failure mode through shear-flexure, therefore theoretical shear values were calculated in regions cracked in bending.

Figure 7.16 plots the SM of all the HCS in Series I, except HCS (I-50-3.1), which had a failure through bonding. We can observe that the shear SM and the flexure SM are higher than the unit. These results demonstrate that exceeding both

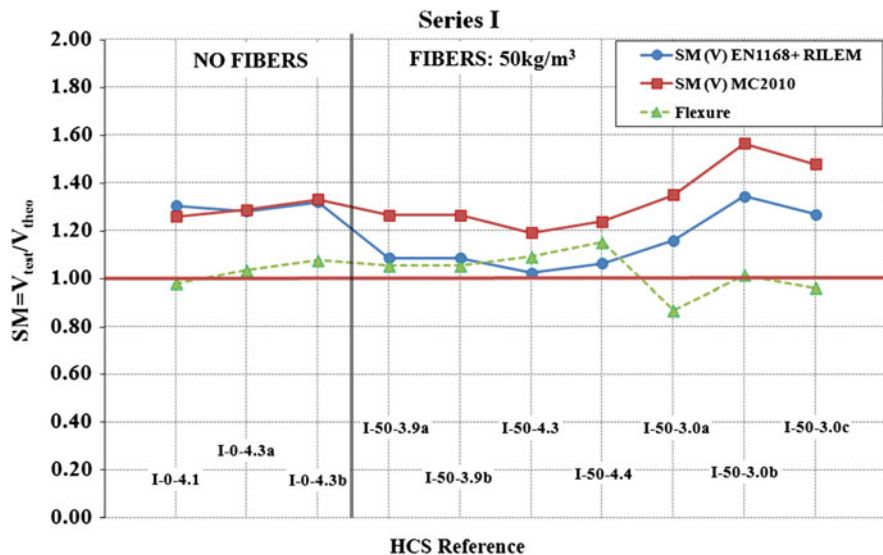


Fig. 7.16 Shear safety margins in regions cracked in bending (Series I)

shear and flexural theoretical strengths at the same time it is possible. However, three HCS (I-50-3.0a, I-50-3.0b and I-50-3.1c) achieved higher SM values in shear due to the lower a/d value. We can also notice how the MC2010 provisions are better balanced than those from EN1168 + RILEM, and that EN1168 + RILEM are less conservative than MC2010 when fibers are present.

7.3.3.3 Series II: Shear Values According to Current Design Codes

Series II had, in the majority, diagonal tensile failures, as it is shown in Table 7.8. Theoretically, pure diagonal tensile failures should be calculated using the formula for regions uncracked in bending; however, it is possible that a small flexure crack was produced prior to the diagonal tension failure. For this reason, it was decided to calculate the theoretical shear value also under the hypothesis of region cracked in bending (Fig. 7.17) to compare which of these two hypotheses is closer to the experimental value. Figure 7.18 shows HCS from Series II which had web shear tension failures calculated according to both hypotheses: cracked or uncracked in bending.

Figure 7.17 plots the shear and flexure SM for the tested Series II HCS, assuming regions cracked in bending according to EN1168. As with Series I, MC2010 was better balanced than EN1168 when comparing the elements with or without fibers for the same a/d . In any case, the results are very similar for both Code provisions. Nevertheless, a clear sensitivity to the a/d ratio was detected. Shear SM were greater for the HCS with a low a/d , and obtained values close to 2.

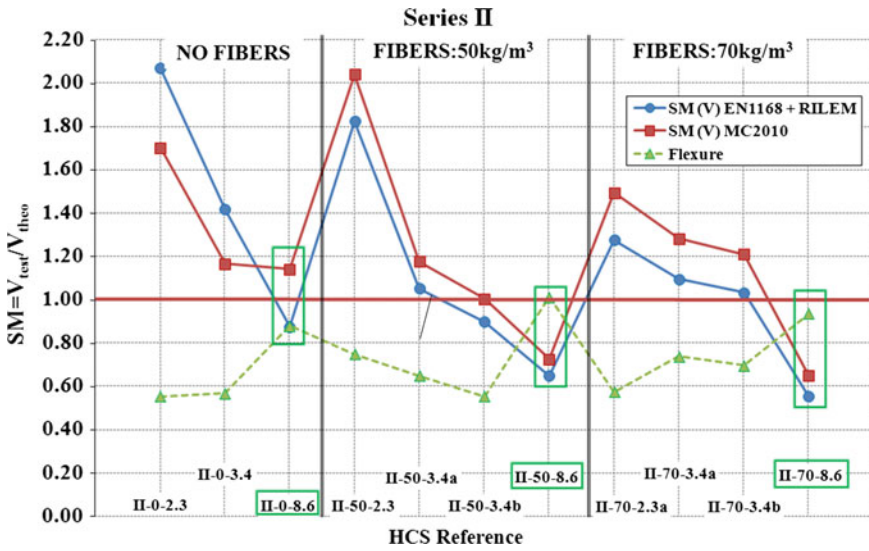


Fig. 7.17 Shear safety margins assuming regions cracked in bending (Series II)

On the other hand, shear strength values were more balanced when a/d ratio was higher (3.4). Only HCS II-50-3.4b shows a shear SM lower than 1; it may be justified by a bad surface finishing. Evidently when flexural failure was observed (II-0-8.6, II-50-8.6, II-70-8.6), failure loads did not reach the theoretical shear strength (see rectangular boxes in Fig. 7.17).

In Fig. 7.18, only HCS with web shear tension failures have been represented, plotting together the SM values calculated with both hypotheses: regions cracked in bending (as were plotted in Fig. 7.17) and regions uncracked in bending (Table 7.6), which means pure shear tension failures. As it can be seen in Fig. 7.18, for all HCS, except the II-50-3.4b (because of bad surface finishing), less SM were obtained assuming uncracked region.

Precracking HCS before shear testing implied an increase in bearing load that was equal to 24.92, 31.62 and 21.60 % for HCS made with 0, 50 and 70 kg/m³ of fibers, respectively (Fig. 7.19). It is evident that flexural precracking makes diagonal tension crack propagation difficult and improves HCS behavior, observing that precracked HCS reached higher ultimate loads than their analogous non precracked (Table 7.8). This behavior occurs since, in regions previously precracked, the previous cracks intercept the stress fields and generate new cracks that do not correspond with the most unfavorable. From this Series, it can be observed that Codes are more conservative for the HCS without fibers, this is when brittle failures are expected; on the other hand, for ductile members, Codes give less SM [10], [11]. This fact, which the present work detects, agrees with the observations made by Peaston et al. [2]. In Fig. 7.20 is represented the capacity achieved in flexure at the time of failure (in Fig. 7.20 called SM in flexure) versus a/d ratio. It can be

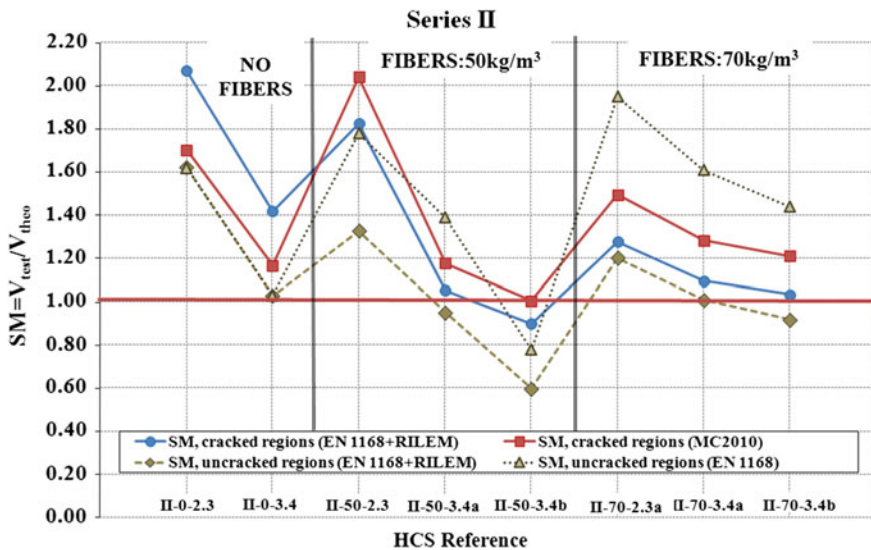


Fig. 7.18 Shear safety margins of HCS with web shear tension failure (Series II)

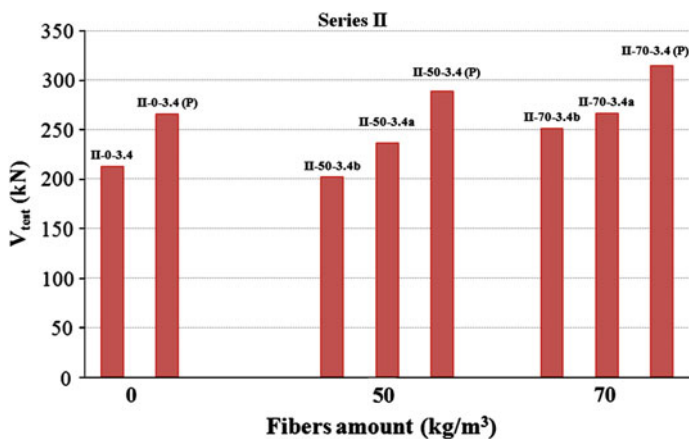


Fig. 7.19 Pre-crack influence on shear strength for HCS with $a/d = 3.4$

observed that the FRC slabs which had a shear-tension failure were over Kani's valley. Also, [12] those with shear-flexure failures had flexural capacities greater than expected, according to Kani's valley [12]. These results agree with Imam et al. [13], who suggested that the region of diagonal failure disappears completely in Kani's valley when increasing fiber amount and efficiency.

In this way, use of fibers is a possible solution to overcome shear failure since fibers are capable of increasing element strength to its full flexural capacity.

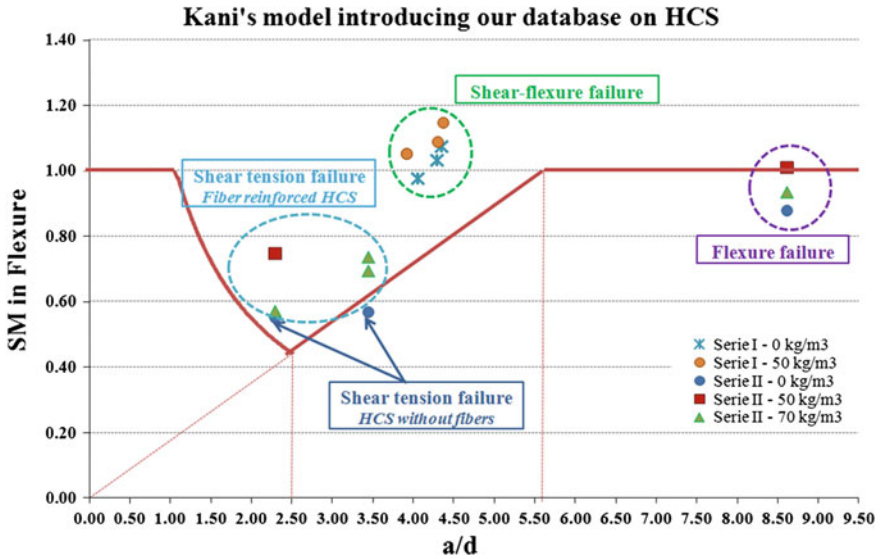


Fig. 7.20 Own database inside Kani's valley

7.4 Conclusions

According to the tests, the following conclusions can be drawn:

- It is possible to produce fiber-reinforced concrete hollow core slabs (HCS) without encountering technical problems.
- An extensive experimental program has been developed to analyze the shear strength and failure behavior of HCS with different failure modes. The effect of fiber amount and shear span on behavior has been analyzed.
- HCS with fibers reached higher shear capacities than those without fiber reinforcement, and when characterized a more ductile behavior. This is a key advantage given the impossibility of placing transverse reinforcements in extruded HCS.
- A clear influence of the a/d ratio on shear strength and on shear behavior has also been detected.
- Model Code 2010 and European standard EN1168+A2 approaches were used to evaluate the HCS shear capacity for both traditional and FRC elements, assuming regions cracked in bending. In the EN1168 approach, the fibers effect was introduced as proposed by RILEM. Codes provisions are very similar and are very conservative when the HCS made with FRC shear strength are calculated for loads applied with low a/d and brittle failures caused by web shear tension failure (S). However, they are well adjusted for high values of the a/d ratio and ductile failures caused by flexure (F) or shear-flexure (SF).

- The model proposed in EN1168 to evaluate the shear capacity in regions uncracked in bending provides a better approximation for HCS with web shear tension failures (S).
- The HCS previously precracked in flexure showed an enhanced shear behavior, and obtain higher safety margins (20–30 %) than those of uncracked HCS.
- Use of fibers is a possible solution to overcome shear failure since fibers are capable of increasing element strength to its full flexural capacity, thus attenuating Kani's valley.

7.5 Publication of These Results

The results of this paper were accepted in *Composites Part B: Engineering Journal* the 2nd June 2012 and therefore will be published in this journal with the following reference [14].

References

1. UNE-EN 1168+A2. 2006. Precast concrete products. Hollow core slabs.
2. Peaston, Elliott and Paine. 1999. Steel fiber reinforcement for extruded prestressed Hollow Core Slabs. *ACI Special Publication* 182: 87–107.
3. EC2. 2004. Eurocode 2: Design of concrete structures—EN 1992-1-1.
4. Elliott. 2013. Transmission length and shear capacity in prestressed concrete hollow core slabs. *Magazine of Concrete Research* 1–18.
5. Pisanty. 1992. The shear strength of extruded hollow-core slabs. *Materials and Structures* 25: 224–230.
6. MC2010. 2012. fib Bulletin 65–66. Model code—final draft.
7. RILEM. 2003. RILEM TC 162-TDF: Test and design methods for steel fibre reinforced concrete. *Final Recommendation* 36: 560–567.
8. Elliott, Peaston and Paine. 2002. Experimental and theoretical investigation of the shear resistance of steel fibre reinforced prestressed concrete X-beams. Part I: Experimental work. *Materials and Structures* 35: 519–527.
9. Vecchio and Collins. 1986. The modified compression field theory for reinforced concrete elements subjected to shear. *ACI Journal* 83(2): 219–231.
10. Cladera and Mari. 2006. Shear design of reinforced and prestressed concrete beams: a proposal for code procedure. *Hormigón y Acero* 242(4): 51–63.
11. Cladera and Mari. 2004. Shear design procedure for reinforced normal and high-strength concrete beams using artificial neural networks. Part II: beams with stirrups. *Engineering Structures* 26: 927–936.
12. Kani. 1964. The Riddle of Shear Failure and its solution. *ACI Journal* 61(4): 441–467.
13. Imam, Vandewalle, Mortelmans and V. Gemert 1997. Shear domain of fibre-reinforced high-strength concrete beams. *Engineering Structures* 19(9): 738–747.
14. Cuenca and Serna. 2013. Failure modes and shear design of prestressed hollow core slabs made of fiber-reinforced concrete. *Composites: Part B* 45(1): 952–964.

Part IV
Shear Database

Chapter 8

Shear Database and Study of the Parameters Influencing Shear Behavior

8.1 Introduction

After thorough review of the literature on structural elements with shear failure, and after conducting several experimental programs whose values were compared later with the theoretical values obtained with the three selected Design Codes to calculate shear in elements reinforced with fibers, it was found that it would be useful and also necessary to build a large database of elements failing in shear in order to have a large number of cases that allow to better evaluate resisting phenomena and the validity of building Codes. For this reason, this chapter shows the analysis of that database.

The structure of this chapter is the following: Sect. 8.2 explains how the data have been selected. Data are analyzed separately in four cases: *Case 1* encompasses the concrete beams with any shear reinforcement (*neither fibers nor stirrups*); *Case 2* concerns beams with only stirrups (*no fibers*); *Case 3* refers to beams with only fibers (*no stirrups*) and *Case 4* concerns beams with fibers and stirrups. In each of these four cases the influence of the following parameters is analyzed: d , a/d , f_{cm} , f_{R3} , ρ , σ_c , and amount of fibers and stirrups.

In Sect. 8.7 particular cases, that are subsets of the entire database, have been analyzed. The subsets have been organized to study the influence of single factors but also double interactions (interaction between 2 parameters). For each subset, an analysis of variance (ANOVA) has been performed and, to analyze the influence of each level of parameter in the SM, LSD have been determined. On the other hand, interaction graphs have been done to analyze the interaction between two different parameters into the SM.

Section 8.8 describes the conclusions of the influence of each parameter (d , a/d , etc.) in the safety margin (SM).

Finally, in Sect. 8.9 are listed some suggestions or modifications to the selected Codes according to the results and trends observed in this chapter.

8.2 Data Selection

In total, 215 structural elements were used to prepare a complete database to analyze the shear behavior and the influence of each parameter on shear out of 363 elements of the experimental database. As can be seen, 148 elements were eliminated for various reasons. In particular, the following data were removed:

1. those with different failure modes to shear;
2. those beams which are not known in some detail;
3. the beams containing a mixture of more than one fiber type;
4. those which are not available any value of strength; and,
5. all those elements with ratios a/d smaller than 2.5, in which arching action is dominant [1–4].

The present database was made by using elements from other databases (as performed by the University of Brescia (Italy) and RILEM databases), plus all the elements tested in shear in the Brite/Euram project [5], beams tested by Dupont and Vandewalle [6], other beams [7] as well as the elements tested within the present PhD thesis.

The input parameters used were: the shear span-to-depth ratio (a/d); the effective depth (d); the concrete cylinder compressive strength (f_c); the residual flexural tensile strength (f_{R3}) corresponding to a crack mouth opening displacement $\text{CMOD} = 2.5$ mm, according to the Standard EN 14651 [8]; the reinforcement ratio for longitudinal reinforcement (ρ_l); the average stress acting on the concrete cross-section for an axial force due to prestressing actions (σ_c); the amount of steel fibers (kg/m^3) and transverse reinforcement area per unit length ($A_{s\sigma}/s$). The output value is the safety margin (SM) obtained as V_{test}/V_{theo} (the shear test value divided by the shear theoretical value).

A large shear database has been obtained, that covers a great interval of the main parameters influencing shear. Table 8.1 summarizes the ranges of the different values used in this shear database.

The theoretical shear (V_{theo}) was calculated for each of the beams according to three structural Codes: the Spanish Standard EHE08 [9], the RILEM approach [10] and the Final Draft of Model Code 2010 [11]. In this chapter, the limitations to the parameters according to the Codes (*see* Table 5.2 in the introduction to Part III) were applied.

Table 8.1 Range of parameters in the complete database (N = 215 elements)

Parameter	Minimum	Maximum
d (mm)	102	1,440
a/d	2.50	4.69
f_{cm} (MPa)	17	96.34
f_{R3} (MPa)	0	10.60
Amount of fibers (kg/m^3)	0	240
ρ (%)	0.41	5.82
σ_c (MPa)	0	12
$A_{s\sigma}/s$ (cm^2/m)	0	4.90

EHE-08 formulation considers fibers contribution separately from concrete, which is based in EC2 [12] while the contribution of the fibers is based on RILEM [10]. The MC2010 [11] considers fiber reinforced concrete (FRC) as a composite material when fibers represent a distributed reinforcement; contribution of fibers is modeled as a modifier of the longitudinal reinforcement ratio throughout a factor that includes the toughness properties of FRC [4]. The shear formulations of these Codes are summarized in Table 5.2 (see *Introduction to Part III*).

8.3 Case 1: Beams Made Without Shear Reinforcement (Concrete Neither Fibers Nor Stirrups)

Tables 8.2 and 8.3 summarize the ranges of the different parameters used in this case, differencing between reinforced and prestressed beams respectively.

8.3.1 Influence of the a/d Ratio

If safety margins ($SM = V_{test}/V_{theo}$) are represented versus a/d for each Code: EHE08 [9], MC2010 [11] and RILEM [10] distinguishing elements without (filled squares) or with prestressing (empty squares), several tendencies are detected. It can be observed that EHE08 is more conservative for prestressed elements (Fig. 8.1).

According to MC2010 (Fig. 8.2) and RILEM (Fig. 8.3), for the same a/d , when $a/d \geq 4$, reinforced and prestressed elements have similar SM. In Fig. 8.2, it can be observed that in one case a great safety margin take place (SM close to 2.4). When $a/d \geq 4$, RILEM safety margins are very close to the unit (Fig. 8.3).

In Fig. 8.4, SMs are represented for each beam of this subset (Case 1: *Beams without shear reinforcement*). Each column represents one beam of this subset and on each column there are three points corresponding to its SM according to the

Table 8.2 Range of parameters in the shear database of reinforced beams made without shear reinforcement (N = 37 elements)

Parameter	Minimum	Maximum	Average	CoV (%)
d (mm)	197	1,440	395.38	65.59
a/d	2.50	4.69	3.19	21.61
f_{cm} (MPa)	20	85.57	36.90	34.50
f_{R3} (MPa)	–	–	–	–
Amount of fibers (kg/m^3)	–	–	–	–
ρ (%)	0.99	3.72	1.76	47.47
σ_c (MPa)	–	–	–	–
$A_{s\alpha}/s$ (cm^2/m)	–	–	–	–

Table 8.3 Range of parameters in the shear database of prestressed beams made without shear reinforcement (N = 6 elements)

Parameter	Minimum	Maximum	Average	CoV (%)
d (mm)	226.47	550	282.16	42.46
a/d	3.27	4.30	380	11.72
f_{cm} (MPa)	43.80	54.20	50.25	9.30
f_{R3} (MPa)	–	–	–	–
Amount of fibers (kg/m ³)	–	–	–	–
ρ (%)	0.41	3.03	1.06	87.28
σ_c (MPa)	2.87	10.18	4.77	54.24
A_{sd}/s (cm ² /m)	–	–	–	–

Fig. 8.1 Beams without shear reinforcement (neither fibers nor stirrups). SM (EHE08) versus a/d

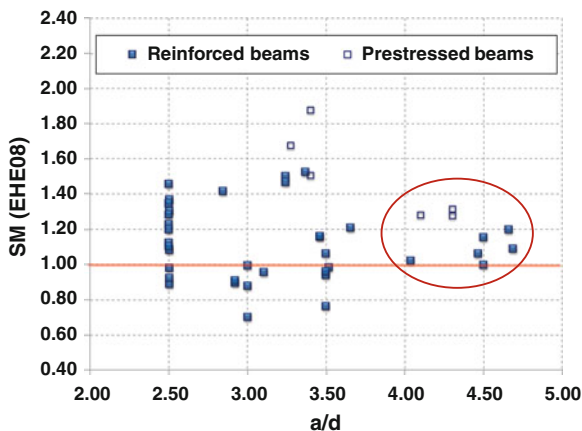
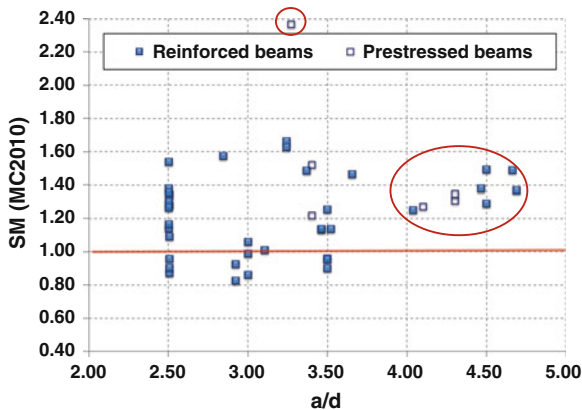


Fig. 8.2 Beams without shear reinforcement (neither fibers nor stirrups). SM (MC2010) versus a/d



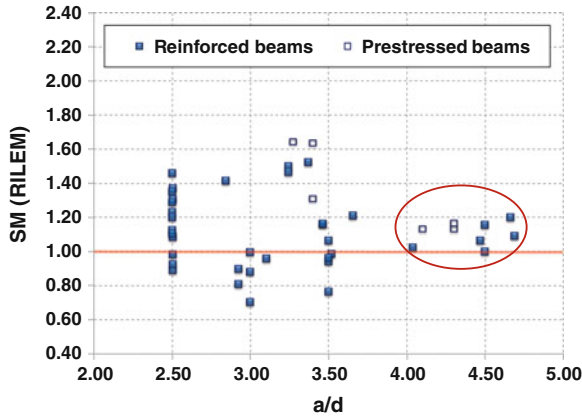


Fig. 8.3 Beams without shear reinforcement (neither fibers nor stirrups). SM (RILEM) versus a/d

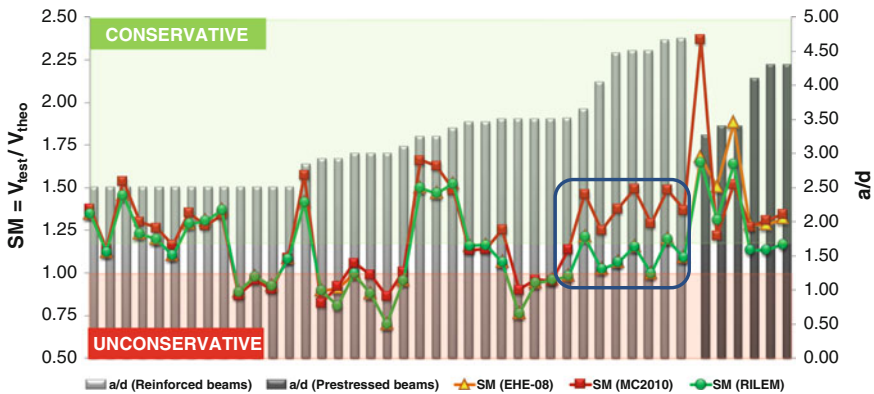


Fig. 8.4 SM represented versus a/d for beams without any reinforcement (neither stirrups nor fibers)

Codes: EHE08, MC2010 and RILEM. Beams are sorted in ascending order according to their value of a/d (right vertical axis), so that the height of each column indicates the value of a/d of each beam (*as can be read on the right vertical axis*). On the other hand, SM values of each beam can be obtained through the left vertical axis. Also, reinforced beams are represented by light grey columns (left side of the graph), while dark grey columns are prestressed beams (right side of the graph). Moreover, the upper side of the graph (*green shaded*), is the area in which Codes are conservative ($SM > 1$), whereas the lower side area (*red shaded*), when $SM < 1$. For example, the first beam, starting from the left, it is a reinforced beam, because the column is in light grey; the height of the column indicates that, if one reads on the right vertical axis, the beam has an $a/d = 2.5$. In turn, if one focus on the 3 points on the column, then SM values are obtained moving to the left vertical axis.

With this graph it has been possible to observe that for $a/d > 3.5$ the MC2010 was the most conservative (Fig. 8.4).

8.3.2 Influence of the Effective Depth, d . Size Effect

If experimental shear stress ($v_u = V_{\text{test}}/b \cdot d$) is represented versus effective depth (d), a clear tendency (size effect) is observed, as expected; in fact, shear stress decreased when effective depth increase (Fig. 8.5).

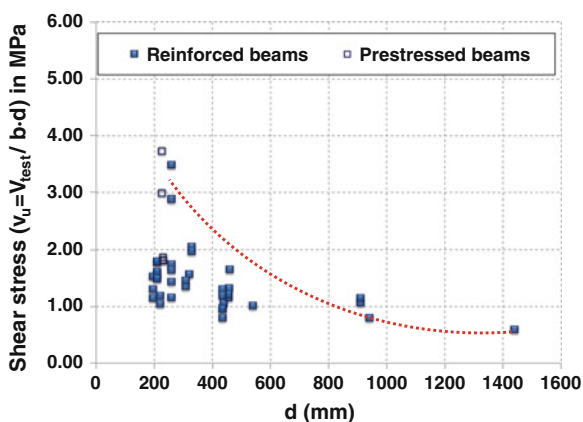
It can be observed that, when $d > 900$ mm (specifically $d = 1,440$ mm in this case), all Codes are unsafe (Fig. 8.6). On the other hand, for $d < 900$ mm, all Codes give similar values.

Figure 8.6 also shows that all Codes are conservative for $d < 200$ mm, although MC2010 underestimates the effect of the effective depth (d) in this range (see square a, in Fig. 8.6). Codes are unconservative for reinforced beams with $d > 900$ mm (see square b, in Fig. 8.6). Prestressed beams are always conservative for all Codes (see square c, in Fig. 8.6). Finally it is noted that, for one of the prestressed beams, the MC2010 gives higher SM, it appears that the MC2010 underestimates the effect of prestressing, as discussed below (see square d, in Fig. 8.6).

8.3.3 Influence of the Concrete Compressive Strength, f_c

Trends on SM due to concrete compressive strength are not observed in beams without shear reinforcement.

Fig. 8.5 Beams without shear reinforcement (neither fibers nor stirrups). Size effect



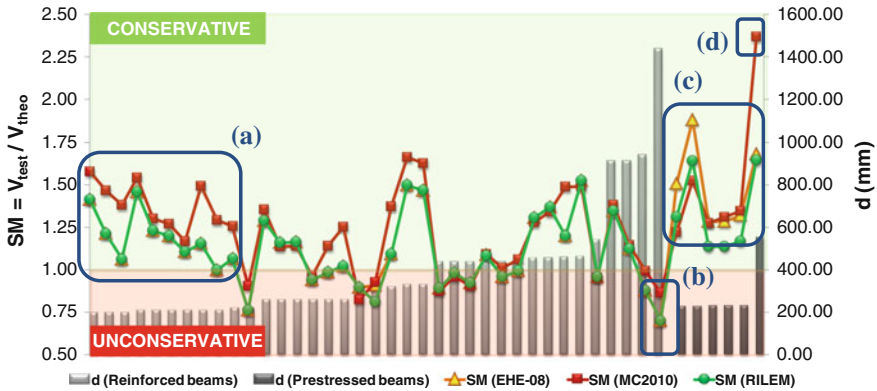


Fig. 8.6 Beams without shear reinforcement (neither fibers nor stirrups). SM versus d (mm)

8.3.4 Influence of the Amount of Longitudinal Reinforcement, ρ_l

In prestressed beams without any shear reinforcement, SM increase when increase ρ_l in the range $\rho_l \leq 2\%$. When $\rho_l \gg 2\%$, SM according to MC2010 in prestressed beams increases quickly (Fig. 8.7).

8.3.5 Influence of the Prestressing Stress, σ_c

Prestressed beams are always safe according to all Codes (Fig. 8.8). It can be observed that shear experimental stress and SM of all Codes increase linearly with σ_c (Fig. 8.9).

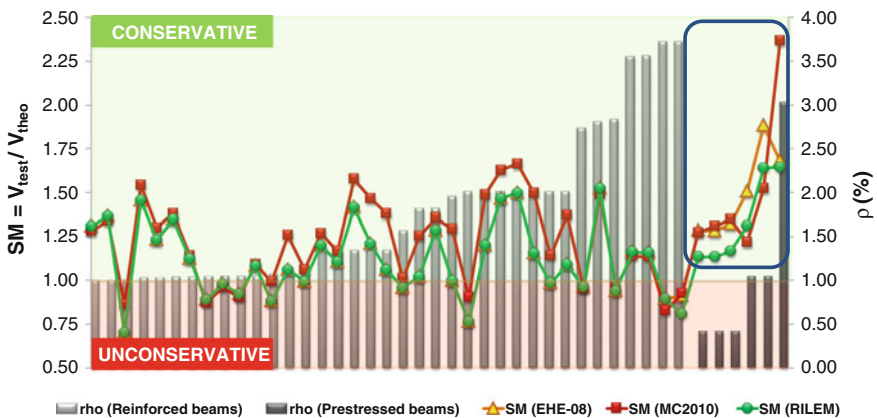


Fig. 8.7 Beams without shear reinforcement. SM represented versus ρ (%)

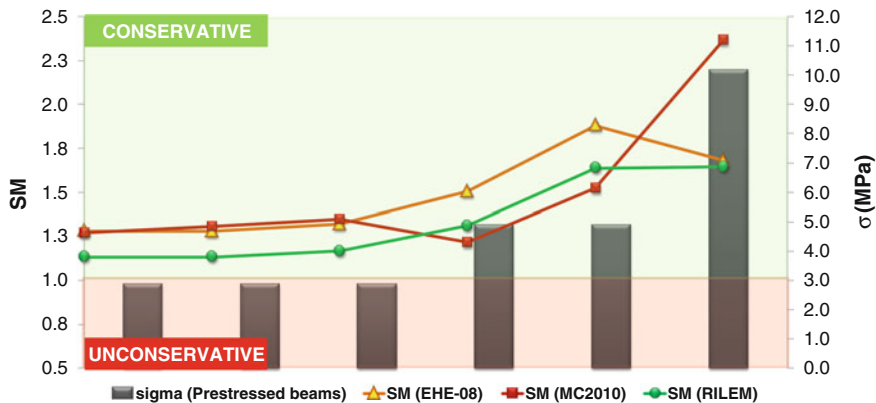


Fig. 8.8 SMs represented versus σ_c (MPa) for beams without shear reinforcement

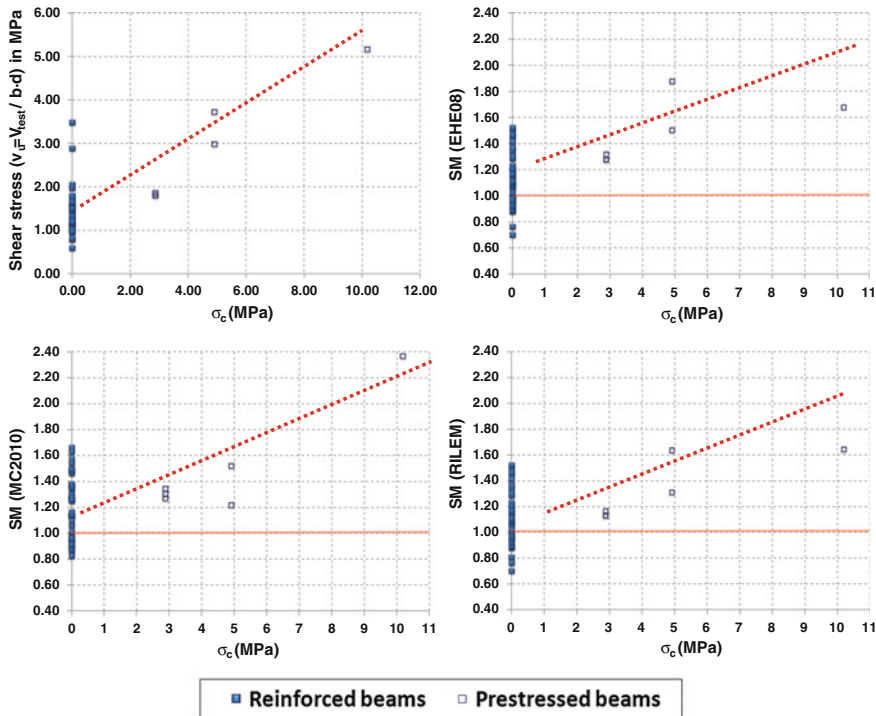


Fig. 8.9 Beams without shear reinforcement (neither fibers nor stirrups). Influence of σ_c

Table 8.4 Summary of statistics of reinforced beams without shear reinforcement

Reinforced beams (plain concrete)			
	EHE-08	MC2010	RILEM
Minimum	0.70	0.82	0.70
Maximum	1.52	1.66	1.52
Average	1.12	1.21	1.11
Standard deviation	0.21	0.24	0.21
CoV (%)	18.38	19.45	18.74
5th percentile (%)	0.86	0.87	0.80
95th percentile (%)	1.47	1.59	1.47

8.3.6 General Behavior of Codes for Beams Without Shear Reinforcement

By determining the main statistics corresponding to the reinforced beams (Table 8.4), it is observed that all Codes (EHE08, MC2010 and RILEM) have coefficients of variation (CoV) in the same order. The 5th percentile values for all Codes are not very close to the unit, this fact makes not possible to ensure the designation of safe predictions. Analyzing

Table 8.5, it is clear that all Codes are conservative for prestressed beams, EHE08 and RILEM present similar CoV, being the RILEM more adjusted for this subset. MC2010 have a great CoV, but it is due to only one point with a very high SM which corresponds to a stress σ_c with a value around 10 MPa since, as stated, it appears that the MC2010 underestimates the effect of prestressed giving high values of SM when $\sigma_c \geq 10$ MPa.

Table 8.5 Summary of statistics of prestressed beams without shear reinforcement

Prestressed beams (plain concrete)			
	EHE-08	MC2010	RILEM
Minimum	1.28	1.22	1.13
Maximum	1.88	2.37	1.65
Average	1.49	1.51	1.34
Standard deviation	0.22	0.40	0.22
CoV (%)	15.07	26.38	16.63
5th percentile (%)	1.28	1.23	1.13
95th percentile (%)	1.83	2.16	1.64

8.4 Case 2: Beams with Stirrups (No Fibers)

8.4.1 Parameters Influence on Shear for Beams with Only Stirrups

Table 8.6 summarizes the ranges of the different parameters used in this case: beams only reinforced transversally with stirrups, without fibers. In this Sect. 8.4, only reinforced beams are analyzed since, in case 2 (beams with stirrups), there is only one prestressed beam and one element is not representative for the analysis.

With respect to the a/d ratio, safety margins (SM) do not show any trend over the range studied ($2.5 \leq a/d \leq 3.5$). In the range ($400 < d < 900$ mm) it is observed that SM increases with increasing values of the effective depth (d). For beams with $f_c > 70$ MPa, SM are unconservative; however, since there are two reinforced beams with $f_c > 70$ MPa, these values are not sufficient to ensure this tendency. Referring to the amount of longitudinal reinforcement (ρ_l) and its influence on SM, no trends are detected; it is only observed an increasing trend in shear stresses with the increase of ρ_l .

Also in this case, the only prestressed beam reinforced with stirrups is safe according all the Codes. No clear trends are obtained on the influence of the transverse reinforcement area ($A_{s\sigma}/s$) on the shear stress or SM.

8.4.2 General Behavior of Codes for Beams with Only Stirrups

As shows Table 8.7, EHE-08 presents the largest dispersion and also the lower 5th percentile. MC2010 is the Code with less CoV. Anyway, all Codes present low values of 5th percentile, and this could be indicate that Codes does not give very safe values for this particular subset, consisting in a sample of beams reinforced only with stirrups.

Table 8.6 Range of parameters in the shear database of reinforced beams with only stirrups (N = 22 elements)

Parameter	Minimum	Maximum	Average	CoV (%)
d (mm)	220	910	392.72	51.89
a/d	2.50	3.52	2.99	12.85
f_{cm} (MPa)	25.90	85.57	44.57	33.12
f_{R3} (MPa)	–	–	–	–
Amount of fibers (kg/m^3)	–	–	–	–
ρ (%)	0.99	3.84	2.46	44.97
σ_c (MPa)	–	–	–	–
$A_{s\sigma}/s$ (cm^2/m)	1.40	4.90	2.51	42.98

Table 8.7 Summary of statistics of beams reinforced only with stirrups

Reinforced beams (beams with stirrups)			
	EHE-08	MC2010	RILEM
Minimum	0.69	0.73	0.72
Maximum	1.71	1.52	1.70
Average	1.05	1.06	1.12
Standard deviation	0.25	0.20	0.25
CoV (%)	24.16	18.40	22.41
5th percentile (%)	0.71	0.76	0.79
95th percentile (%)	1.41	1.38	1.47

8.5 Case 3: Beams with Fibers (No Stirrups)

Tables 8.8 and 8.9 summarize the ranges of the different parameters used in this case (beams only reinforced with fibers), differentiating between reinforced and prestressed beams, respectively.

8.5.1 Influence of the a/d Ratio and the Effective Depth, d

No trends are observed in the range studied for beams reinforced only with fibers.

8.5.2 Influence of the Concrete Compressive Strength, f_c

Reinforced beams presented low SM for high compressive strength levels ($f_c > 70$ MPa), of course, there are other beams with low SM, but the general trend is that with high strength, Codes tend to be less safe.

Table 8.8 Range of parameters in the shear database of beams reinforced only with fibers (N = 102)

Parameter	Minimum	Maximum	Average	CoV (%)
d (mm)	102	1,440	360.80	59.59
a/d	2.50	4.69	3.24	18.60
f_{cm} (MPa)	17.00	96.34	38.86	41.32
f_{R3} (MPa)	1.22	10.60	3.65	49.24
Amount of fibers (kg/m^3)	15	240	63.31	66.33
ρ (%)	0.99	3.72	2.23	39.80
σ_c (MPa)	–	–	–	–
$A_{s\alpha}/s$ (cm^2/m)	–	–	–	–

Table 8.9 Range of parameters in shear database of prestressed beams with only fibers (N = 26)

Parameter	Minimum	Maximum	Average	CoV (%)
d (mm)	226.47	738.89	440.93	48.79
a/d	2.84	4.40	3.40	11.15
f_{cm} (MPa)	35.90	77.00	55.38	22.78
f_{R3} (MPa)	2.83	8.61	4.95	39.19
Amount of fibers (kg/m ³)	50	70	55	12.61
ρ (%)	0.41	5.82	2.23	92.52
σ_c (MPa)	2.87	12.00	7.16	50.05
A_{so}/s (cm ² /m)	–	–	–	–

8.5.3 Influence of the Residual Tensile Strength (CMOD = 2.5 mm), f_{R3}

Reinforced beams with $f_{R3} > 5$ MPa present low SM. Shear stresses increases when f_{R3} also increases for both, reinforced and prestressed beams. It can be observed that the slopes are different between reinforced and prestressed beams, due to the effect of prestressing which also produce higher shear stresses (Fig. 8.10).

8.5.4 Influence of the Amount of Longitudinal Reinforcement, ρ_l

In Fig. 8.11, experimental shear stresses are represented versus the longitudinal reinforcement percentage. As it can be observed, no trend is detected in reinforced beams while, in prestressed beams, when ρ_l increases also the shear stress increases.

Fig. 8.10 Experimental shear stress versus f_{R3} for beams reinforced only with fibers

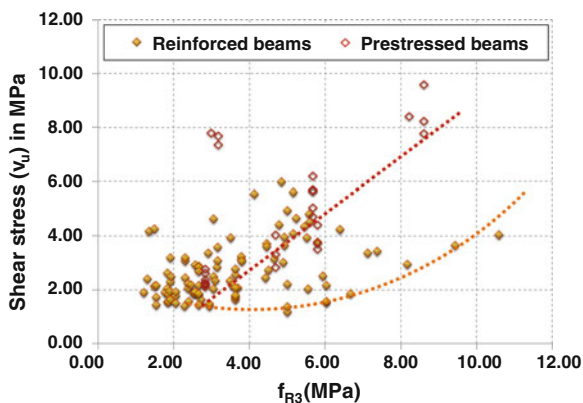
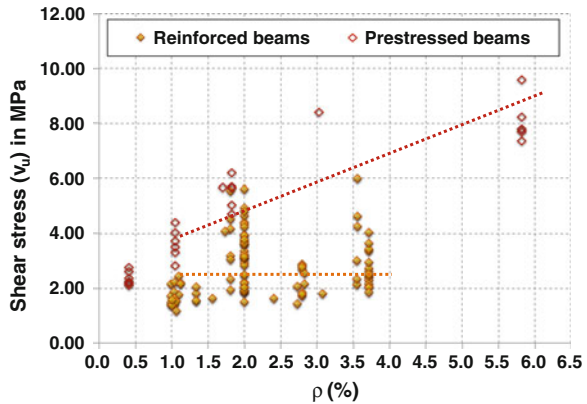


Fig. 8.11 Experimental shear stress versus ρ (%) for beams reinforced only with fibers



In Fig. 8.12, safety margins (SM) are represented versus ρ_l according to Codes EHE08 and RILEM; in both Codes, the same trend is observed.

Figure 8.13 shows the SM determined according to the MC2010, versus ρ_l . For high ρ_l (values that exceed the maximum limitation of ρ_l ($\rho_l \leq 2\%$)) excessively high values of SM are obtained. In Fig. 8.13, it can be also observed that the trends of prestressed beams are different between MC2010 and EHE and RILEM. In the case of EHE and RILEM, SM increases approximately linearly with ρ_l but, on the other hand, SM of MC2010 initially increases more quickly than EHE & RILEM, but for values higher than the limit value ($\rho_l = 2\%$), SM are very high and, therefore, very conservative.

In Fig. 8.14, SM of all studied Codes (EHE, MC2010 and RILEM) are represented versus ρ_l for all beams of this particular subset (only with fiber reinforcement).

Some reinforced beams (*see square a in Fig. 8.14*) show high SMs; the reason is that these beams have a real value of ρ_l greater than 2% (*the exact value is unknown*), but the data come from elements of the database of other authors. Therefore, the calculations are using a value lower than the actual ρ_l , resulting in a lower predicted value. In reinforced beams, when $\rho_l \geq 3\%$, SMs of all Codes reduce (*see square b in Fig. 8.14*), when ρ_l increases. In prestressed beams, when ρ_l increases, SM also increases; however, when $\rho_l \geq 5\%$, it seems that MC2010 underestimates the effect of prestressed (*see square c in Fig. 8.14*).

8.5.5 Influence of the Stress Due to Prestressing Actions, σ_c

In Fig. 8.16 beams with fibers are ordered by increasing σ_c , SMs are represented with respect to σ_c (Fig. 8.15) and, to f_c (Fig. 8.16). In general, observing both graphs, it is observed that MC2010 is always the most conservative. RILEM & EHE are most balanced for all levels of f_c and σ_c whereas MC2010 is more

Fig. 8.12 Safety margin (V_{test}/V_{theo}) versus ρ (%) according to EHE08 and RILEM

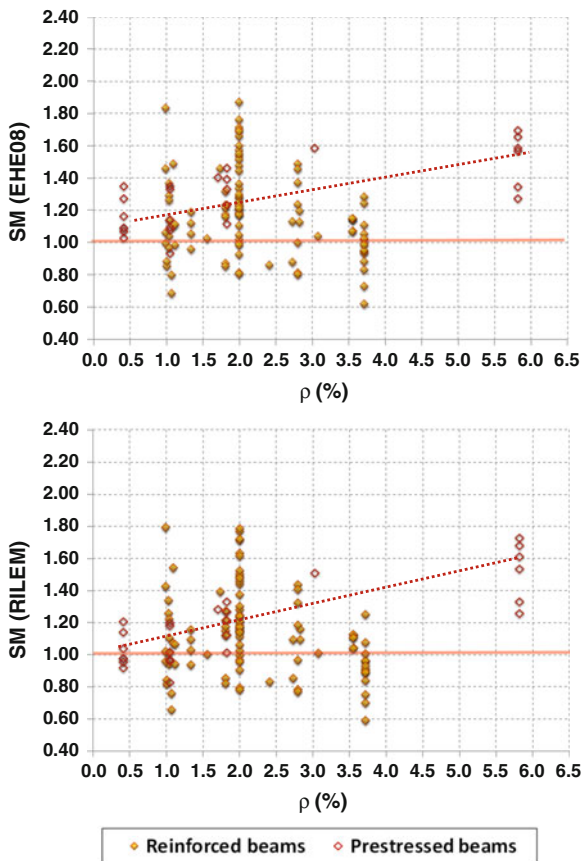
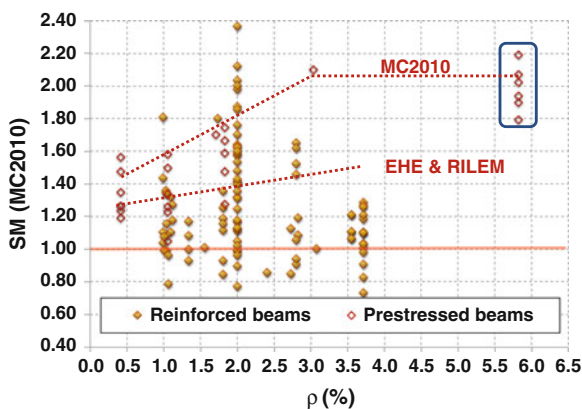


Fig. 8.13 Safety margin (V_{test}/V_{MC2010}) versus ρ (%)



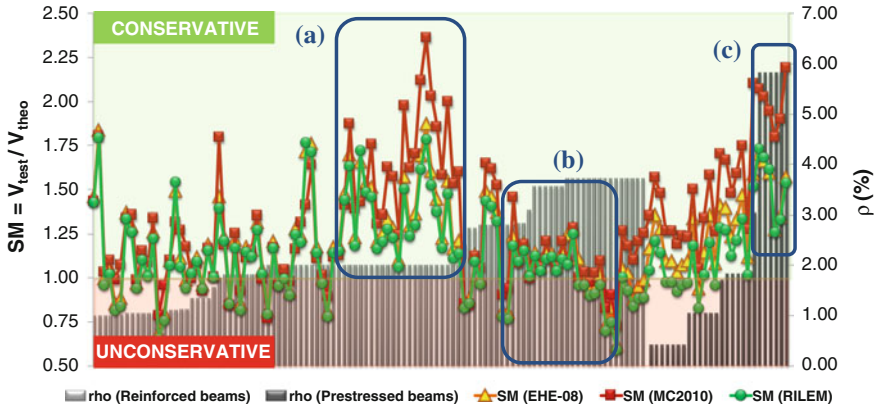


Fig. 8.14 Beams transversally reinforced with fibers. SM represented versus ρ (%)

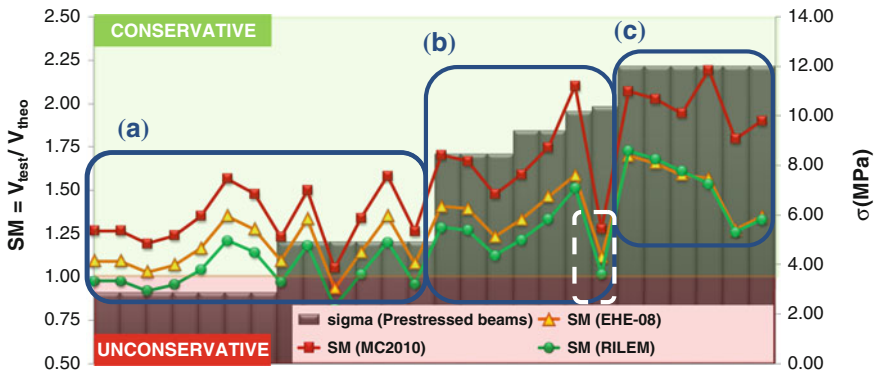


Fig. 8.15 Beams transversally reinforced with fibers. SM represented versus σ_c (MPa)

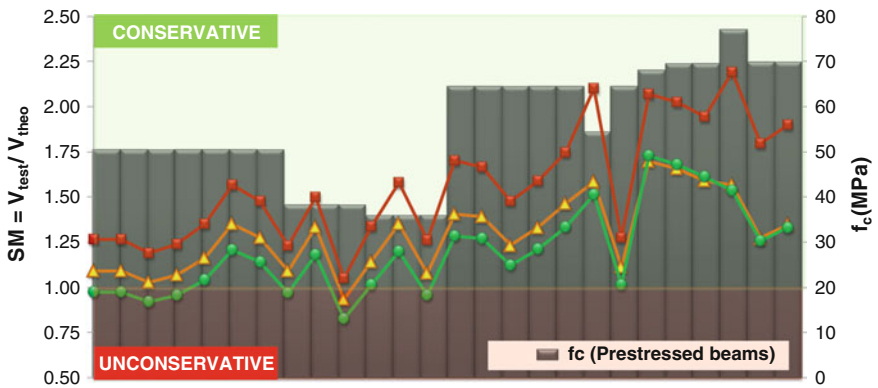


Fig. 8.16 Beams transversally reinforced with fibers. SM represented versus f_c (MPa)

conservative for high levels of f_c and σ_c . The first prestressed elements correspond to hollow core slabs (see square A in Fig. 8.15). One beam (see dashed line square B in Fig. 8.15) has a clearly lower value of SM than its analogous beam (see square B in Fig. 8.15), this is because the beam has a flange width ($b_f = 260$ mm) much lower than its analogous ($b_f = 400\text{--}600$ mm). Therefore, RILEM & EHE Codes, which take into account the contribution of the flange width in beams reinforced with fibers are overestimating the contribution of a flange which is very small. In beams with flanges of considerable size ($b_f > 400$ mm), MC2010 gives higher SM than the other two codes (RILEM and EHE), which means that determines a lower shear theoretical value since it neglects the contribution of flanges to shear (see Chap. 4).

8.5.6 Influence of the Amount of Fibers, Kg/m^3

Reinforced and prestressed beams with fibers are always safe ($\text{SM} > 1$) for all Codes, according to this database, when the amount of fibers is greater than 125 kg/m^3 (Fig. 8.17).

8.5.7 General Behavior of Codes for Beams with Only Fibers

Tables 8.10 and 8.11 show that, for the beams reinforced with fibers, MC2010 presents the greater CoV (%) but, it is the safest Code, with the highest value of 5th percentile (in reinforced and prestressed beams). Codes are safer for prestressed beams.

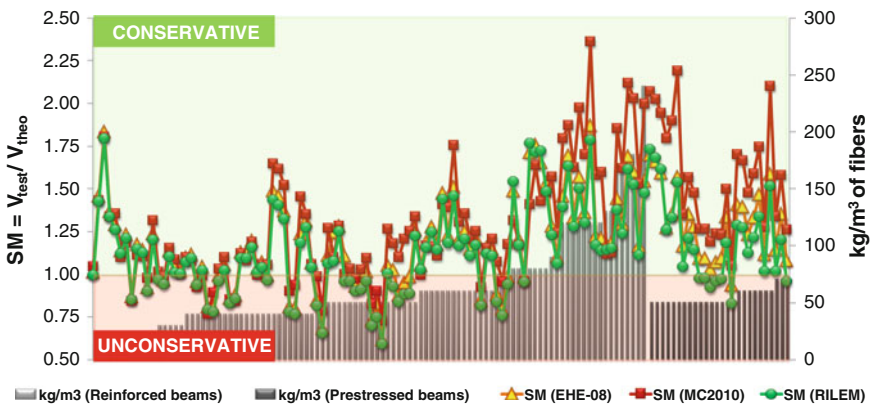


Fig. 8.17 Beams transversally reinforced with fibers. SM represented versus kg/m^3 of fibers

Table 8.10 Summary of statistics of reinforced beams only with fibers

Reinforced beams (beams with fibers)			
	EHE-08	MC2010	RILEM
Minimum	0.62	0.73	0.59
Maximum	1.87	2.36	1.79
Average	1.17	1.25	1.13
Standard deviation	0.26	0.32	0.26
CoV (%)	22.32	25.81	23.07
5th percentile (%)	0.80	0.84	0.77
95th percentile (%)	1.69	1.87	1.63

Table 8.11 Summary of statistics of prestressed beams only with fibers

Prestressed beams (beams with fibers)			
	EHE-08	MC2010	RILEM
Minimum	0.93	1.05	0.83
Maximum	1.70	2.19	1.73
Average	1.29	1.57	1.20
Standard deviation	0.21	0.32	0.24
CoV (%)	15.92	20.23	20.20
5th percentile (%)	1.04	1.20	0.93
95th percentile (%)	1.64	2.10	1.66

8.6 Case 4: Beams with Fibers and Stirrups

Table 8.12 summarizes the ranges of the different parameters used in beams transversally reinforced with stirrups and fibers. A table for prestressed beams has no sense in this case, because only two prestressed beams are available in the database.

Influences in SM due to the parameters: a/d , d , f_{cm} and $A_{s\sigma}/s$ were not detected.

Table 8.12 Range of parameters in the shear database of reinforced beams with only fibers (N = 19)

Parameter	Minimum	Maximum	Average	CoV (%)
d (mm)	210	650	293.68	34.65
a/d	3.10	4.50	3.53	10.06
f_{cm} (MPa)	38.00	50.67	45.33	9.91
f_{R3} (MPa)	1.22	8.54	3.19	56.33
Amount of fibers (kg/m ³)	15	60	39.95	42.52
ρ (%)	1.56	3.56	2.99	26.41
σ_c (MPa)	–	–	–	–
$A_{s\sigma}/s$ (cm ² /m)	1.40	3.53	2.18	34.50

8.6.1 Influence of the Residual Tensile Strength, f_{R3}

Figure 8.18 shows the SM of all Codes versus the residual tensile strength f_{R3} , it can be observed that for reinforced beams the most conservative is the EHE while, for prestressed beams the RILEM is the safest, the MC2010 is the most balanced Code, as it maintains the same SM levels for reinforced and prestressed beams.

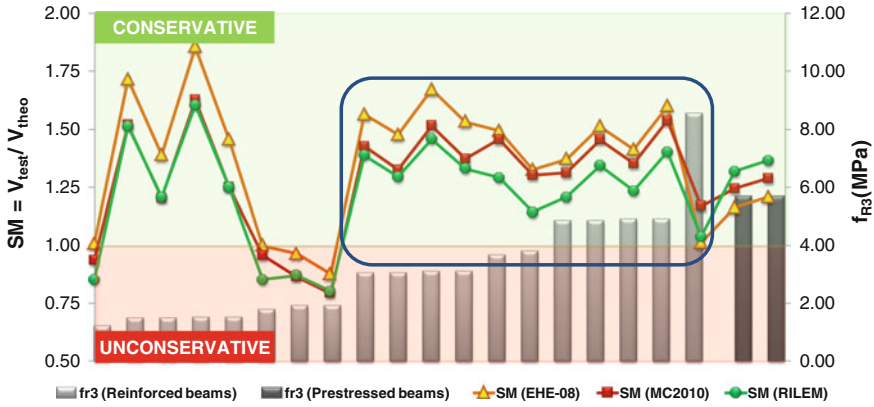


Fig. 8.18 Beams transversally reinforced with fibers + stirrups. SM represented versus f_{R3} (MPa)

8.6.2 Influence of the Longitudinal Reinforcement Percentage, ρ_l

In Fig. 8.19 it can be observed that reinforced beams with $\rho_l \leq 2\%$ and $f_{R3} < 1.5$ MPa are all in the side of unsafety (SM < 1). Reinforced beams with

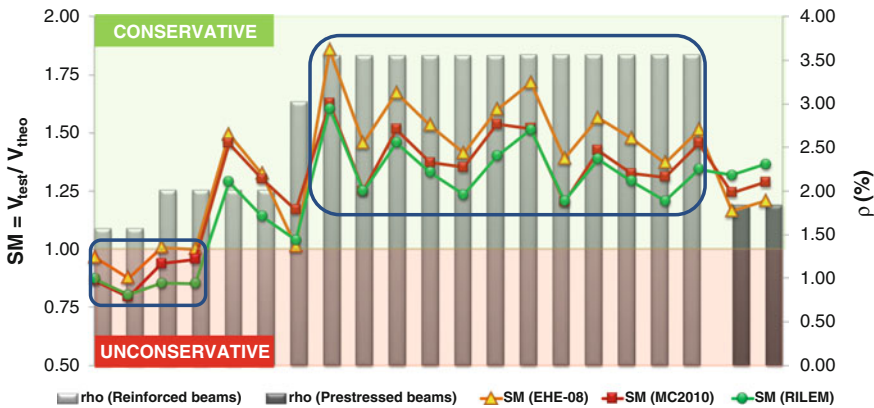


Fig. 8.19 Beams transversally reinforced with fibers + stirrups. SM represented versus ρ (%)

$\rho_l = 3.5 \%$ have similar levels of SM for all Codes. The MC2010 is the most balanced in both: reinforced and prestressed.

8.6.3 Influence of the Stress Due to Prestressing Actions, σ_c

In this subset (beams reinforced with fibers and stirrups) there are only two pre-stressed beams, so they are not enough to formulate strong conclusions, but it seems that when both reinforcements are present (fibers + stirrups) SM for prestressed beams is higher.

Table 8.13 Summary of statistics of reinforced beams only with fibers

Reinforced beams (fibers and stirrups)			
	EHE-08	MC2010	RILEM
Minimum	0.88	0.79	0.80
Maximum	1.85	1.63	1.60
Average	1.38	1.28	1.21
Standard deviation	0.27	0.23	0.23
CoV (%)	19.82	18.29	18.82
5th percentile (%)	0.96	0.86	0.85
95th percentile (%)	1.73	1.55	1.52

8.6.4 General Behavior of Codes for Beams with Stirrups and Fibers

EHE08 has a CoV slightly greater than MC2010 and RILEM, but EHE08 also is the safer Code for this subset, presenting the greatest value of the 5th percentile (Table 8.13). Table 8.14 summarizes the main conclusions obtained in Sects. 8.3–8.6.

Table 8.14 Main conclusions of Sects. 8.3–8.6

Parameter	Neither fibers nor stirrups	Beams only with stirrups	Beams only with fibers	Beams with fibers and stirrups
d (mm)	EHE08, MC2010 and RILEM: For $d = 1,440$ mm, SM are unsafe and, for	In the range $400 < d < 900$ mm, SM increases when increases for reinforced beams	–	–

(continued)

Table 8.14 (continued)

Parameter	Neither fibers nor stirrups	Beams only with stirrups	Beams only with fibers	Beams with fibers and stirrups
	$d < 900$ mm similar SM are obtained			
a/d	EHE08: For the same a/d prestressed beams are more conservative MC2010 and RILEM: For the same a/d (when $a/d \geq 4$), reinforced and prestressed elements have \approx SM	(No trends for the analyzed range $2.5 \leq a/d \leq 3.5$)	–	–
f_{cm} (MPa)	–	For $f_c > 70$ MPa, SM are unconservative	Reinforced beams with $f_c > 70$ MPa, present low SM	–
f_{R3} (MPa)	–	–	Reinforced beams with $f_{R3} > 5$ MPa, present low SM	EHE08 is the most conservative for reinforced beams. For prestressed RILEM is the safest. MC2010 is the most balanced Code (similar SM for reinforced and prestressed)
Amount of fibers (kg/m^3)	–	–	For amount of fibers $> 125 \text{ kg/m}^3$, Codes are safe (SM > 1)	–
ρ (%)	In prestressed beams, SM increase with ρ for $\rho \leq 2$ %. For $\rho \gg 2$ % SM in prestressed beams increases quickly	–	EHE08 and RILEM: No trends are observed for reinforced beams. For prestressed, shear stress increases with ρ . MC2010: when $\rho > 5$ %, prestressed is underestimated	Reinforced beams with $\rho > 2$ % and $f_{R3} < 1.5$ have SM < 1 . MC2010 is the most balanced for reinforced and prestressed beams

(continued)

Table 8.14 (continued)

Parameter	Neither fibers nor stirrups	Beams only with stirrups	Beams only with fibers	Beams with fibers and stirrups
σ_c (MPa)	MC2010: Underestimates the effect of prestressing. EHE08, MC2010 and RILEM: SM increase linearly with σ_c and, prestressed beams are always safe	EHE08, MC2010 and RILEM: All prestressed beams are safe (SM > 1)	EHE08 and RILEM are most balanced for all levels of f_c and σ_c whereas MC2010 is always the most conservative	For reinforced beams EHE08 is the most conservative while, for prestressed is the RILEM MC2010 is the most balanced (similar SM for reinforced and prestressed)
A_{sa}/s (cm ² /m)	–	–	–	–

–: No influence have been detected

8.7 Particular Cases

8.7.1 Introduction

Throughout this chapter, the role of the factors influencing shear strength in the safety margin (SM) in three design Codes (EHE, MC2010 and RILEM) have been analyzed in different cases: beams without any shear reinforcement, beams with only stirrups, beams with only steel fibers and finally, beams with stirrups and fibers.

At this point, in which the influence of the different factors on the SM is reported, it is presented the possible influence of the interactions of different factors on the SM. For this purpose, the analysis of variance “ANOVA” will be used.

ANOVA makes the following assumptions:

- *Independence of cases.* This is an assumption of the model that simplifies the statistical analysis.
- *Normality.* The distributions of the residuals are normal.
- *Equality (or “homogeneity”) of variances, called homoscedasticity.* The variance of data in groups should be the same.

The one-way ANOVA examines the influence of an independent variable (factor) in the dependent variable, in this case, SM. The two-way analysis of variance is an extension to the one-way analysis since there are two independent variables (hence the name two-way).

Whenever possible, in two-way ANOVAs, interactions of simple factors and their possible influence on the dependent variable (SM in this case) will be studied.

The independent variables in a two-way ANOVA are called factors. The idea is that there are some variables, factors, which affect the dependent variable. Each factor will have two or more levels within it, and the degrees of freedom for each factor is one less than the number of levels.

ANOVA procedure will be described very briefly; herein further details of the fundamentals of ANOVA can be found in [13].

Below, the results obtained from several ANOVAs are summarized. The analyses were done for some experimental programs from the shear database analyzed in the previous sections. In this way, the ANOVA was done each time for series with the same geometry and cross-section and other constant variables, to have an ANOVA as robust as possible.

8.7.2 Brite Series 1

In this section, the beams from Series 1 of the *Subtask 4.2—Trial Beams in Shear of Brite-Euram project* [5] are going to be analyzed. This Serie 1 was carried out in the *Technical University of Braunschweig (UBS) by Rosenbusch J. and Teutsch M.* In Table 8.15 the constant variables within the same Series are indicated. In Table 8.16, the input data for the ANOVA analysis are presented, differencing the factors (independent variables) of the dependent variable (safety margin, SM) for all these subsections. In this case the three factors are: f_{R3} , A_{sw}/s and Code, having the factor f_{R3} four levels and, the other two factors, three levels. So, the number of complete cases is:

$$\text{No complete cases} = (\text{No of levels})^{\text{No of factors}} = 3^2 \times 4^1 = 36 \text{ complete cases}$$

The ANOVA Table 8.17 decomposes the variability of safety margin on shear (SM) in contributions due to several factors. Since the sum of squares Type III has been chosen, the contribution of each factor is measured by removing the effects of other factors. P-values, test the statistical significance of each factor. Since six p-values are less than 0.05, these factors have a statistically significant shear on SM on a 95.0 % confidence level.

Table 8.15 Constant variables between the beams within the same series (Brite Series 1)

Constant variables
Cross-section 200 × 300 mm: Rectangular reinforced (no prestressed) beams
$\rho_l = 3.56 \%$
$a/d = 3.5$
3 point test

Table 8.16 Factors and dependent variable analyzed in the ANOVA analysis of Brite Series 1

<i>Factors (independent variables)</i>
f_{r3} (MPa): 0, 1.49, 3.05, 4.85
Transverse reinforcement, A_{sv}/s (cm ² /m): 0, 1.4, 2.8
Codes: EHE08, MC2010, RILEM
<i>Dependent variable</i>
Shear safety margin (SM)

Table 8.17 Analysis of variance (ANOVA) for SM on shear—type III sums of squares (Series 1)

Source of variation	Sum of Squares	d.f	Mean square	F-ratio	p-value
<i>Main effects</i>					
A: f_{R3} (MPa)	0.0750528	3	0.0250176	22.99	0.0000
B: A_{sv}/s (cm ² /m)	0.631839	2	0.315919	290.25	0.0000
C: Code	0.0546722	2	0.0273361	25.12	0.0001
<i>Interactions</i>					
AB	0.132739	6	0.0221231	20.33	0.0000
AC	0.0419722	6	0.00699537	6.43	0.0032
BC	0.0184944	4	0.00462361	4.25	0.0227
<i>Residual</i>	0.0130611	12	0.00108843		
<i>Total (corrected)</i>	0.967831	35			

All F-ratios are based on the residual mean square error

In this case, Series 1, have been possible to study double interactions, because there are enough *residual degrees of freedom (d.f.)*, this is:

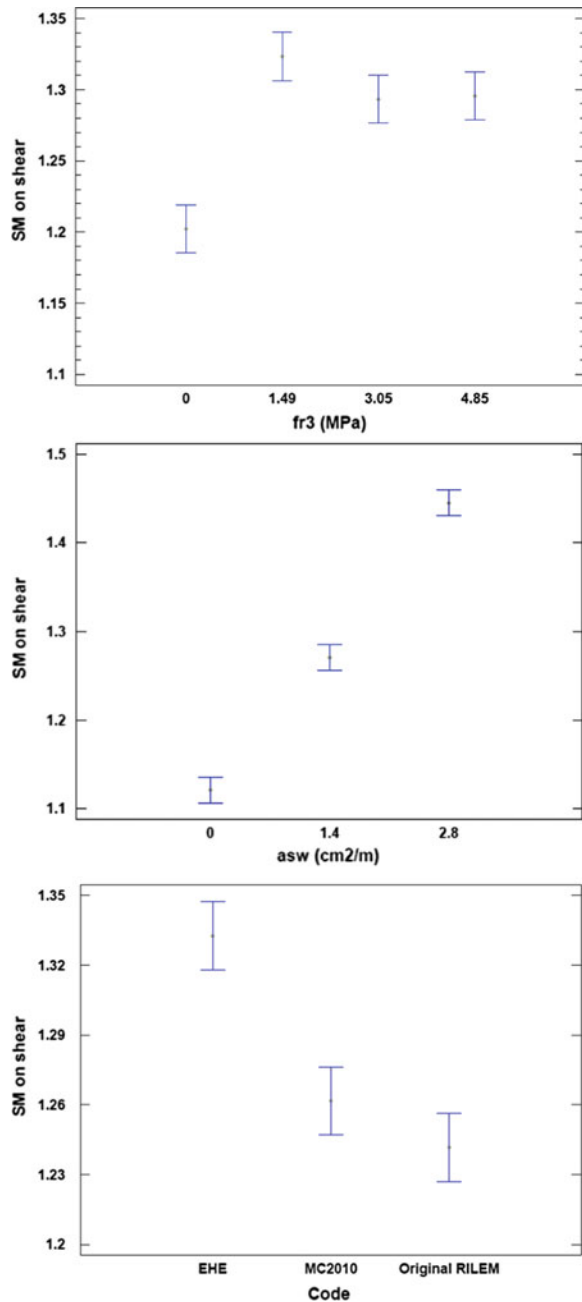
$$\begin{aligned}
 &\text{d.f. (effect A) = 3; d.f. (effect B) = 2; d.f. (effect C) = 2} \\
 &\text{d.f. (interaction AB) = 6; d.f. (interaction AC) = 6; d.f. (interaction BC) = 4} \\
 &\text{d.f. (residual) = d.f. (total) - d.f. (simple effects) - d.f. (interactions) = 35 - 3 - 2 - 2 - 6 - 6 - 4 = 12}
 \end{aligned}$$

As *d.f. (residual) = 12* then double interactions can be studied.

So in this case there are enough degrees of freedom to study interactions. Higher order interactions could be considered but, in general, not occur almost in practice, and is also difficult to interpret [14]. Henceforth, only double interactions will be studied. There is a double interaction between two factors, whether the effect of one of them is different according to the variant of the other factor considered. By means of ANOVA table, one knows what simple effects and what interactions are statistically significant, being those with p-value < 0.005. But a significant value of p-value only would indicate that at least one of the levels of this factor differs from the others, but does not specify which ones differ. A simple way to clarify this issue

is through the establishment of LSD (*abbreviation of “Least Significant Difference”*) intervals for the mean for each level of each effect. The average difference between the two levels will be significant if the respective LSD intervals (Fig. 8.20)

Fig. 8.20 Means and 95.0 % LSD intervals (Brite Series 1)



do not overlap. As it can be observed, there are not significant differences between the several f_{R3} values. There are not differences in SM between MC2010 and RILEM but only significant differences between the EHE08 and the other two Codes. In this test Series, Codes are safer; in fact, as one increases the amount of transverse reinforcement, SM increases linearly.

LSD intervals are used when the effects are qualitative values, in this case, two of the three effects are quantitative; therefore, for a comprehensive statistical analysis, it would be suitable to decompose the quantitative effect in their linear and quadratic components but, the analysis just done is considered sufficient to study these particular cases.

As it can be observed in the ANOVA table, in this Series all interactions were statistically significant.

In Figs. 8.21, 8.22 and 8.23 are shown the surface charts for this case; these graphs show how is affected the dependent variable (SM) for each combination among the various levels of two simple effects.

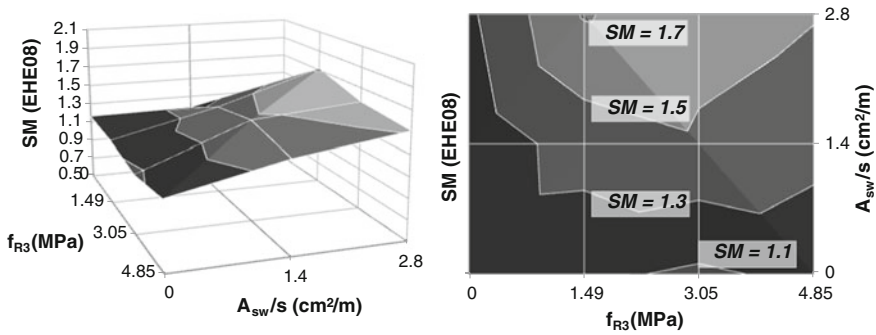


Fig. 8.21 Influence of the interaction between f_{R3} and A_{sw}/s in the SM according to EHE08

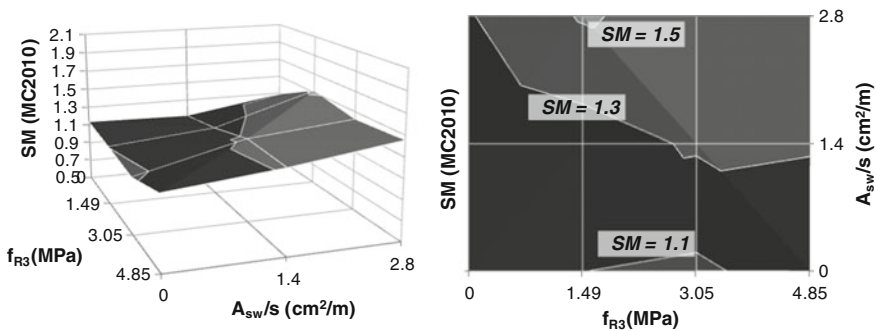


Fig. 8.22 Influence of the interaction between f_{R3} and A_{sw}/s in the SM according to MC2010

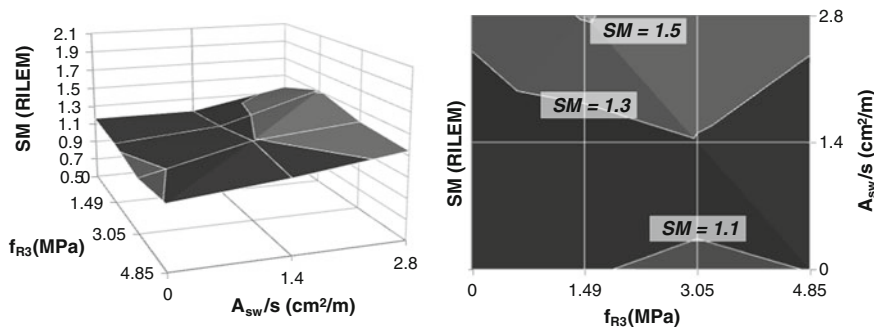


Fig. 8.23 Influence of the interaction between f_{R3} and A_{sw}/s in the SM according to RILEM

The influence of the interaction of f_{R3} and A_{sw}/s on the safety margins (SM), according to the EHE08, MC2010 and RILEM, are plotted respectively in Figs. 8.21, 8.22 and 8.23. In each of these figures, two perspectives are represented. In the left picture a surface chart and, on the right, the same graph is represented as a topographic map indicating in each isoline (also called contour line) its corresponding SM value. In this Series, in particular, Codes are safer for greater amounts of transverse reinforcement; this trend is detected for all f_{R3} values. It is illogical that the Codes are more conservative with increasing the amount of transverse reinforcement. However, since results from this series do not provide a firm conclusion, more research is required on this topic.

8.7.3 Brite Series 2

In this subsection, the Series 2 of the *Subtask 4.2—Trial Beams in Shear of Brite-Euram project* [5] are going to be analyzed. This Serie 2 was carried out in the *Katholieke Universiteit Leuven (KUL)* by Dupont D. and Vandewalle L. In Table 8.18 the constant variables within the same Series are indicated.

In Table 8.19, the input data for the ANOVA analysis are presented, differencing the factors (independent variables) of the dependent variable (safety margin, SM) for all these subsections. In this case the three factors are: f_{R3} , ρ_l and Code, having the factor Codes three levels and, the other two factors, two levels. So, the number of complete cases is:

$$N_{\text{complete cases}} = (N_{\text{of levels}})^{N_{\text{of factors}}} = 2^2 \times 3^1 = 12 \text{ complete cases}$$

Table 8.18 Constant variables between the beams within the same series (Brite Series 2)

Constant variables
Cross-section 200×300 mm: Rectangular reinforced (no prestressed) beams
No stirrups
$a/d = 2.5$
4 point test

Table 8.19 Factors and dependent variable analyzed in the ANOVA analysis of Brite Series 2

<i>Factors (independent variables)</i>	
f_{R3} (MPa):	1.35, 4.13
ρ_l (%):	1.16, 1.81
Codes:	EHE08, MC2010, RILEM
<i>Dependent variable</i> Shear safety margin (SM)	

The ANOVA table (Table 8.20) decomposes the variability of safety margin on shear (SM) in contributions due to several factors. Since six p-values are less than 0.05, these factors have a statistically significant shear on SM on a 95.0 % confidence level.

By means of LSD intervals (Fig. 8.24), in this Series 2, it can be observed that there are significant differences in SM between both levels of f_{R3} and ρ_l . In this case, Codes are more conservative for small f_{R3} and when ρ_l increases. There are also differences with different design Codes. In this case, the MC2010 is the safest while RILEM is the closest to the experimental results.

As it was seen in the ANOVA (Table 8.20), in this Series all interactions were statistically significant. By means of surface charts (Figs. 8.25, 8.26 and 8.27), it is possible to evaluate the influence of the interactions on the shear SM.

8.7.4 Brite Series 3

In this subsection, the Series 3 of the *Subtask 4.2—Trial Beams in Shear of Brite-Euram project* [5] are analyzed. This Serie 3 was carried out in the *Universitat Politècnica de Catalunya (UPC)* by *Gettu R., Barragán B. E., Martín M.A., Ramos G. and Burnett I.*

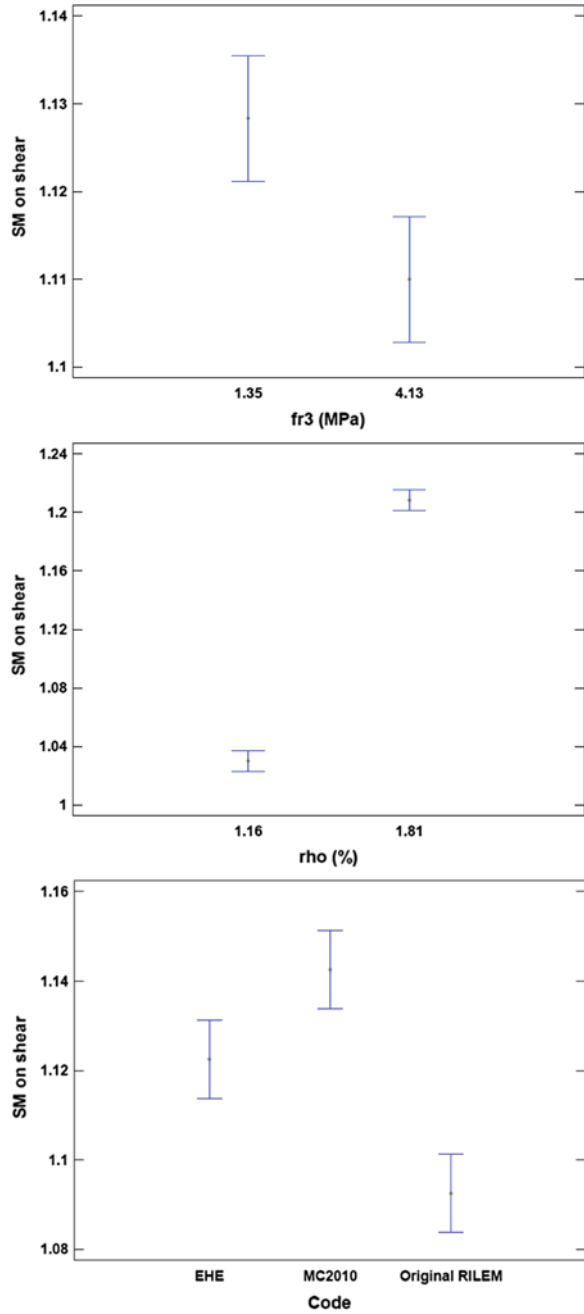
Two different analyses have been done related to this Series 3.

Table 8.20 Analysis of variance (ANOVA) for SM on shear—type III sums of squares (Series 2)

Source of variation	Sum of Squares	d.f	Mean square	F-ratio	p-value
<i>Main effects</i>					
A: f_{R3} (MPa)	0.00100833	1	0.00100833	30.25	0.0315
B: ρ (%)	0.0954083	1	0.0954083	2862.25	0.0003
C: Code	0.00506667	2	0.00253333	76.00	0.0130
<i>Interactions</i>					
AB	0.00140833	1	0.00140833	42.25	0.0229
AC	0.00826667	2	0.00413333	124.00	0.0080
BC	0.00166667	2	0.000833333	25.00	0.0385
<i>Residual</i>	0.0000666667	2	0.0000333333		
<i>Total (corrected)</i>	0.112892	11			

All F-ratios are based on the residual mean square error

Fig. 8.24 Means and 95.0 % LSD intervals (Brite Series 2)



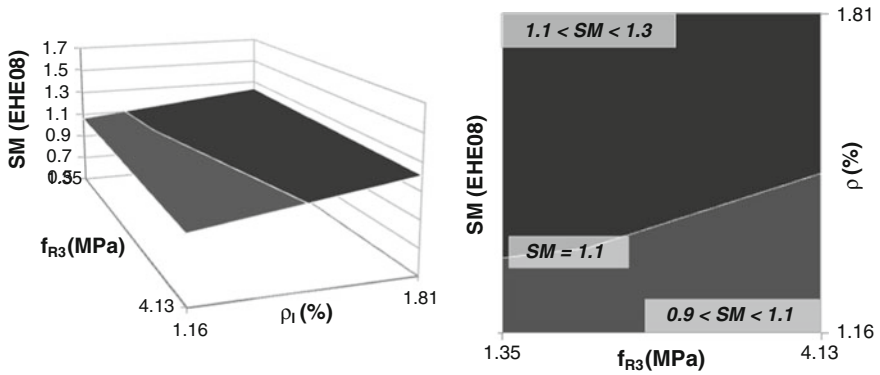


Fig. 8.25 Influence of the interaction between f_{R3} and ρ in the SM according to EHE08

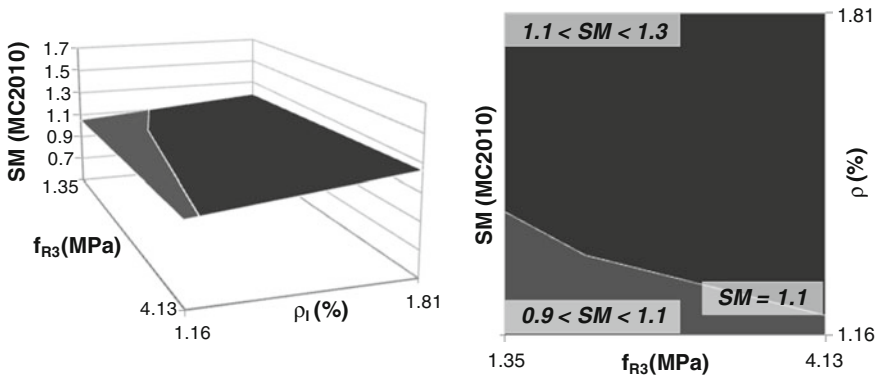


Fig. 8.26 Influence of the interaction between f_{R3} and ρ in the SM according to MC2010

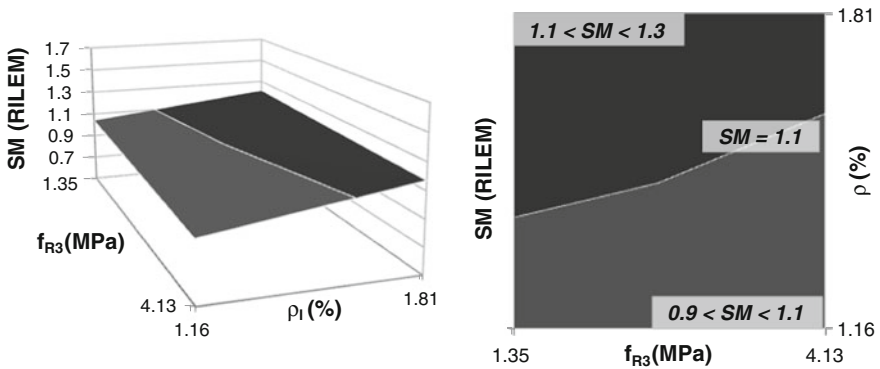


Fig. 8.27 Influence of the interaction between f_{R3} and ρ in the SM according to RILEM

8.7.4.1 Brite Series 3: Analysis I

In Table 8.21 the constant variables within the same Series are indicated. In Table 8.22, the input data for the ANOVA analysis are presented, differencing the factors (independent variables) of the dependent variable (safety margin, SM). In this case the two factors are: b_f and Code, having both factors three levels. So, the number of complete cases is: $N_{\text{complete cases}} = (N_{\text{of levels}})^{N_{\text{of factors}}} = 3^2 = 9$ complete cases.

The ANOVA table (Table 8.23) shows that both factors are significant. Since both p-values are less than 0.05, these factors have a statistically significant shear on SM on a 95.0 % confidence level.

By means of LSD intervals (Fig. 8.28), in this Series 3-I, it can be observed that there are significant differences in SM between both levels of b_f and Code. In this case, Codes are more conservative for smaller flange widths (b_f), SM decreases when b_f increases. Also there are differences according to the design Codes used. In this case the MC2010, is the safest.

In this case, there are not enough degrees of freedom to study interactions so, only simple effects have been studied.

8.7.4.2 Brite Series 3: Analysis II

In Table 8.24 the constant variables within the same Series are indicated. In Table 8.25, the input data for the ANOVA analysis are presented, differencing the

Table 8.21 Constant variables between the beams within the same series (Brite Series 3-I)

<i>Constant variables</i>
Cross-section shape: Doble-T reinforced (no prestressed) beams
No stirrups
3 point test
$a/d = 3.5$
40 kg/m ³ of fibers RC 65/60BN
$b_w = 200$ mm
ρ_l (%) = 2.8
$h = 500$ mm
$hf = 150$ mm

Table 8.22 Factors and dependent variable analyzed in the ANOVA analysis of Brite Series 3-I

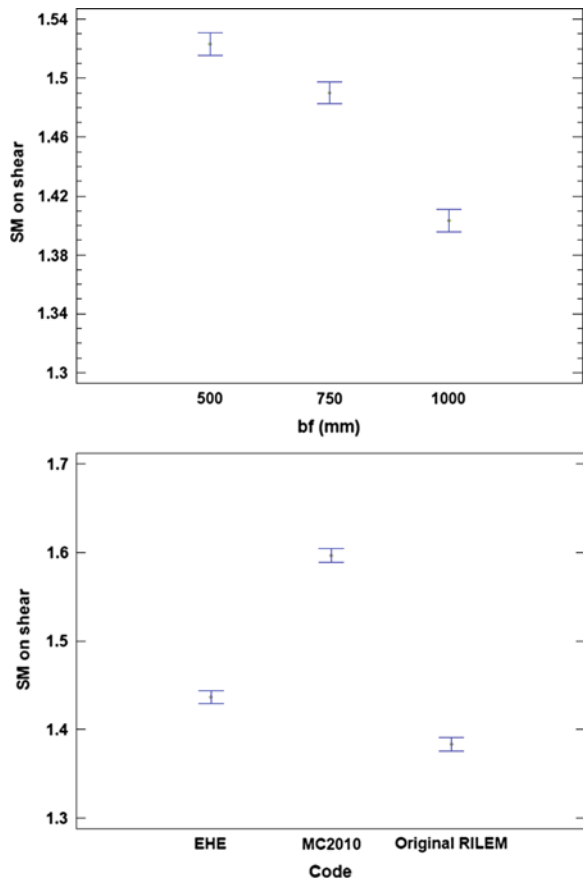
<i>Factors (independent variables)</i>
b_f (mm): 500, 750, 1000
Codes: EHE08, MC2010, RILEM
<i>Dependent variable</i>
Shear safety margin (SM)

Table 8.23 Analysis of variance (ANOVA) for SM on shear—type III sums of squares (Series 3-I)

Source of variation	Sum of Squares	d.f	Mean square	F-ratio	p-value
<i>Main effects</i>					
A: b_f (mm)	0.0230222	2	0.0115111	259.00	0.0001
B: Code	0.0739556	2	0.0369778	832.00	0.0000
<i>Residual</i>	0.000177778	4	0.0000444444		
<i>Total (corrected)</i>	0.0971556	8			

All F-ratios are based on the residual mean square error

Fig. 8.28 Means and 95.0 % LSD intervals (Brite Series 3-I)



factors (independent variables) of the dependent variable (safety margin, SM). In this case the two factors are: h_f and Code, having both factors three levels. So, the number of complete cases is:

$$\text{No complete cases} = (\text{No of levels})^{\text{No of factors}} = 3^2 = 9 \text{ complete cases}$$

Table 8.24 Constant variables between the beams within the same series (Brite Series 3-II)

<i>Constant variables</i>
Cross-section shape: Doble-T reinforced (no prestressed) beams
No stirrups
3 point test
$a/d = 3.5$
40 kg/m ³ of fibers RC 65/60BN
$b_w = 200$ mm
ρ_f (%) = 2.8
$h = 500$ mm
$b_f = 500$ mm

Table 8.25 Factors and dependent variable analyzed in the ANOVA analysis of Brite Series 3-II

<i>Factors (independent variables)</i>
h_f (mm): 100, 150, 230
Codes: EHE08, MC2010, RILEM
<i>Dependent variable</i>
Shear safety margin (SM)

The ANOVA table (Table 8.26) shows that both factors are significant. Since both p-values are less than 0.05, these factors have a statistically significant shear on SM on a 95.0 % confidence level.

By means of LSD intervals (Fig. 8.29), in this Series 3-II, it can be observed that there are not significant differences in SM between the different levels inside the same factor. In this particular case, Series 3-II, there are not significant differences between flange depth of 100 and 150 mm, being the Codes unconservative but, the SM corresponding to $h_f = 230$ mm is clearly different than the other two. There are not significant differences between EHE and RILEM; only MC2010 is different than the other two reaching the greatest SM in shear.

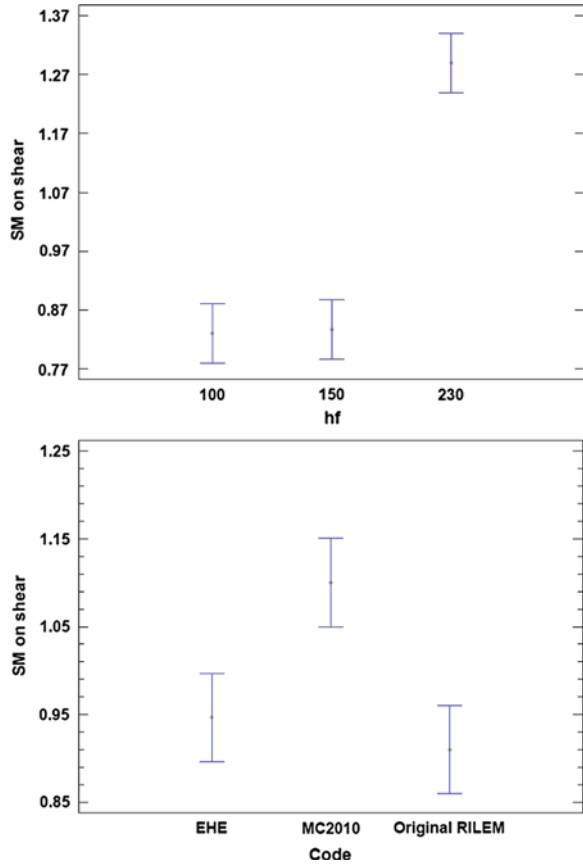
In this case, there are not enough degrees of freedom to study interactions so, only simple effects have been studied.

Table 8.26 Analysis of variance (ANOVA) for SM on shear—type III sums of squares (Series 3-II)

Source of variation	Sum of Squares	d.f	Mean square	F-ratio	p-value
<i>Main effects</i>					
A: h_f (mm)	0.417156	2	0.208578	105.46	0.0003
B: Code	0.0609556	2	0.0304778	15.41	0.0132
<i>Residual</i>	0.00791111	4	0.00197778		
<i>Total (corrected)</i>	0.486022	8			

All F-ratios are based on the residual mean square error

Fig. 8.29 Means and 95.0 % LSD intervals (Brite Series 3-II)



8.7.5 Study of Size Effect on Shear

In this subsection, the beams of Chap. 5, tested at the University of Brescia (Italy), are statistically analyzed. In Table 8.27, the constant variables within the same Series are indicated. In Table 8.28, the input data for the ANOVA analysis are presented, differencing the factors (independent variables) of the dependent variable (safety margin, SM) for all these subsections. In this case, the three factors are: d , f_{R3} , and Code, having all factors three levels. So, the number of complete cases is:

$$N_{\text{complete cases}} = (N_{\text{of levels}})^{N_{\text{of factors}}} = 3^3 = 27 \text{ complete cases}$$

The ANOVA table (Table 8.29) shows that all main effects and two interactions have significant differences since their p-values are less than 0.05.

By means of LSD intervals (Fig. 8.30), in this Series, it can be observed that, for the effect “effective depth (d)”, there are significant differences between the three levels, being the SM corresponding to $d = 440$ mm clearly different from the other two. SM increases when increases the fiber content, but there are not significant differences

Table 8.27 Constant variables between the beams within the same series (size effect beams)

<i>Constant variables</i>
Cross-section shape: Rectangular reinforced (no prestressed) beams
No stirrups
3 point test
$a/d = 3.0$
Type of fibers: La Gramigna © $l_f/d_f = 62.5$; $l_f = 50$ mm
$b_w = 250$ mm
$\rho_l (\%) = 1.12$
Compressive strength level assumed constant: 38.65 MPa for PC; 32.07 MPa for FRC50; 33.08 MPa for FRC75

Table 8.28 Factors and dependent variable analyzed in the ANOVA analysis of size effect beams

<i>Factors (independent variables)</i>
d (mm): 440, 940, 1,440
f_{R3} (MPa): 0, 5.00, 6.00
Codes: EHE08, MC2010, RILEM
<i>Dependent variable</i>
Shear safety margin (SM)

Table 8.29 Analysis of variance (ANOVA) for SM on shear—type III sum of squares (size effect)

Source of variation	Sum of Squares	d.f	Mean square	F-ratio	p-value
<i>Main effects</i>					
A: d (mm)	0.313956	2	0.156978	409.51	0.0000
B: f_{R3} (MPa)	0.00682222	2	0.00341111	8.90	0.0092
C: Code	0.153356	2	0.0766778	200.03	0.0000
<i>Interactions</i>					
AB	0.141889	4	0.0354722	92.54	0.0000
AC	0.00142222	4	0.000355556	0.93	0.4939
BC	0.00988889	4	0.00247222	6.45	0.0127
<i>Residual</i>	0.00306667	8	0.000383333		
<i>Total (corrected)</i>	0.6304	26			

All F-ratios are based on the residual mean square error

between concrete without fibers and with $f_{R3} = 5$ MPa. There are significant differences between the different, but MC2010 is, in this case, the safest Code.

As was seen in the ANOVA table (Table 8.29), in this Series two interactions were statistically significant: d with f_{R3} (AB), and f_{R3} with Code (BC). By means of surface charts (Figs. 8.31, 8.32 and 8.33), it is possible to evaluate the influence of the interactions on the shear SM.

Fig. 8.30 Means and 95.0 % LSD intervals (size effect beams)

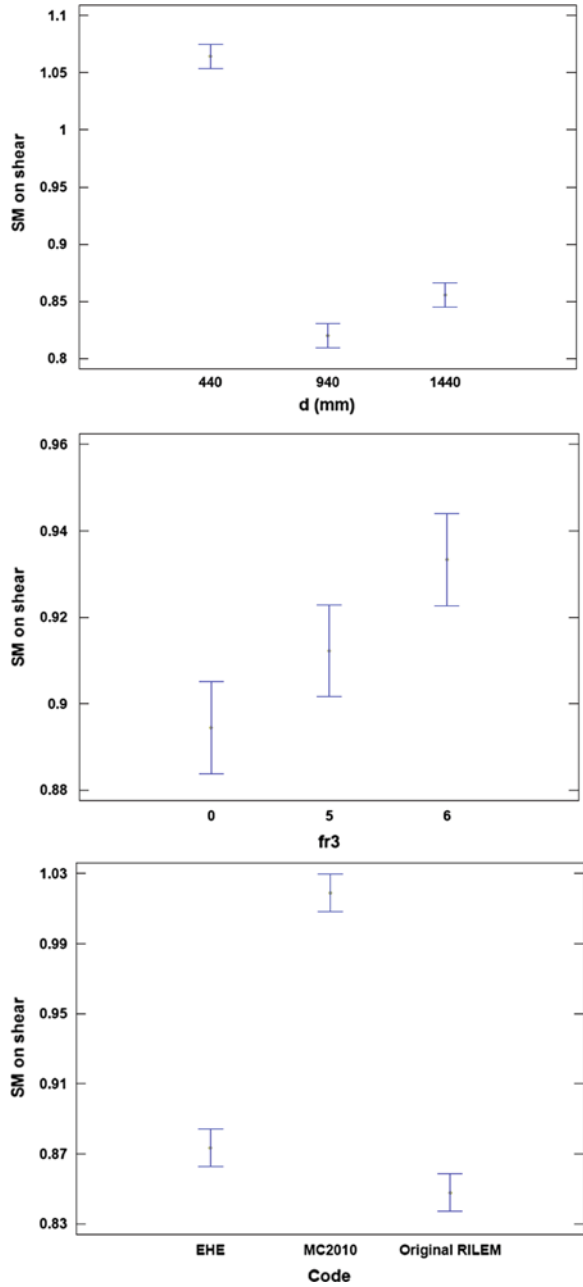


Fig. 8.31 Influence of the interaction between f_{R3} and d in the SM according to EHE08

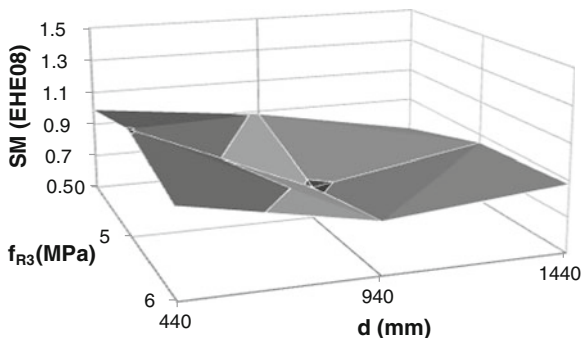


Fig. 8.32 Influence of the interaction between f_{R3} and d in the SM according to MC2010

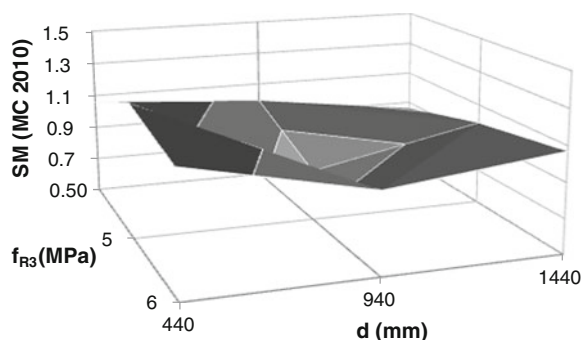
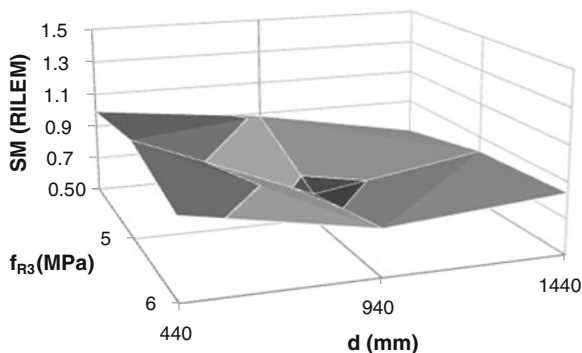


Fig. 8.33 Influence of the interaction between f_{R3} and d in the SM according to RILEM



The surface charts show clearly that the combination $f_{R3} = 5$ MPa with $d = 940$ mm has a lower SM, according to the three Codes considered, and that fibers can mitigate size effect.

However, only one beam was tested for each combination so to obtain decisive conclusions further research in this topic will be needed.

8.7.6 Beams with Different Types of Fibers

In this section, the beams of Chap. 6, tested at the *Universitat Politècnica de València (Spain)*, are statistically analyzed by means of two different analysis, combining the compressive strength levels with several types of steel fibers with different lengths, aspect ratio and steel strength.

8.7.6.1 Beams with Different Fibers Types: Analysis I

In Table 8.30, the constant variables within the same Series are indicated. In Table 8.31, the input data for the ANOVA analysis is presented, differencing the factors (independent variables) of the dependent variable (safety margin, SM). In this case, the three factors are: compressive strength level (*Low, L; Medium, M; High, H*), fibers type (*65/40BN, 80/50BN, 80/40BP*) and Codes (*EHE, MC2010, RILEM*), having all factors three levels. So, the number of complete cases is:

$$\text{No complete cases} = (\text{No of levels})^{\text{No of factors}} = 3^3 = 27 \text{ complete cases}$$

The ANOVA table (Table 8.32) shows that all main effects and two interactions have significant differences, since their p-values are less than 0.05.

By means of LSD intervals (Fig. 8.34), in this Series, it can be observed that, according to the compressive strength level only, there are significant differences between the low compressive level and the other two. In this particular case, only beams made with fibers 80/50BN have SM significantly different than the other two types. Codes give SM values significantly different, being MC2010 the safest and the RILEM unconservative.

As it can be seen in Table 8.32, all main effects have a clear influence on the SM; furthermore, interactions between compressive strength and fiber type (AB), and between fiber type and Code (BC) present significant differences on SM. By means

Table 8.30 Constant variables between the beams within the same series (f_c and f_{R3} beams-I)

<i>Constant variables</i>
Cross-section shape
ρ (%) = 3.72
3 point test
50 kg/m ³ of steel fibers

Table 8.31 Factors and dependent variable analyzed in the ANOVA analysis of f_c and f_{R3} beams-I

<i>Factors (independent variables)</i>
Compressive strength level: Low (L), Medium (M), High (H)
Fibers type: 65/40BN, 80/50BN, 80/40BP
Codes: EHE08, MC2010, RILEM
<i>Dependent variable</i>
Shear safety margin (SM)

Table 8.32 ANOVA for SM on shear—type III sums of squares (f_c and f_{R3} beams-I)

Source of variation	Sum of squares	d.f	Mean square	F-ratio	p-value
<i>Main effects</i>					
A: Compressive strength	0.104674	2	0.052337	33.81	0.0001
B: Fiber type	0.0444741	2	0.022237	14.36	0.0023
C: Code	0.101252	2	0.0506259	32.70	0.0001
<i>Interactions</i>					
AB	0.112326	4	0.0280815	18.14	0.0004
AC	0.0126815	4	0.00317037	2.05	0.1802
BC	0.0933481	4	0.023337	15.07	0.0009
<i>Residual</i>	0.0123852	8	0.00154815		
<i>Total (corrected)</i>	0.481141	26			

All F-ratios are based on the residual mean square error

of surface charts (Figs. 8.35, 8.36 and 8.37), it is possible to evaluate the influence of the interactions on the shear SM.

Analyzing the surface charts of this Series, it seems that all Codes give SM very close to the unit, so they are very safe for all the combinations. RILEM and EHE are unsafe when high strength fibers (80/40BP) are used. Of the three codes, in general, the MC2010 seems to be the safest. In general, Codes have low SM for concretes with low compressive strength and high strength fibers (80/40BP). On the other hand, Codes have greater SM for concretes with medium compressive strength and fibers 80/50BN.

8.7.6.2 Beams with Different Fibers Types: Analysis II

In Table 8.33, the constant variables within the same Series are indicated. In Table 8.34, the input data for the ANOVA analysis is presented, differencing the factors (independent variables) of the dependent variable (safety margin, SM). In this case, the three factors are: compressive strength level (*Medium, M; High, H*), fibers type (*45/50BN, 65/40BN, 80/50BN, 80/30BP, 80/40BP*) and Codes (*EHE, MC2010, RILEM*), having all factors three levels. So, the number of complete cases is:

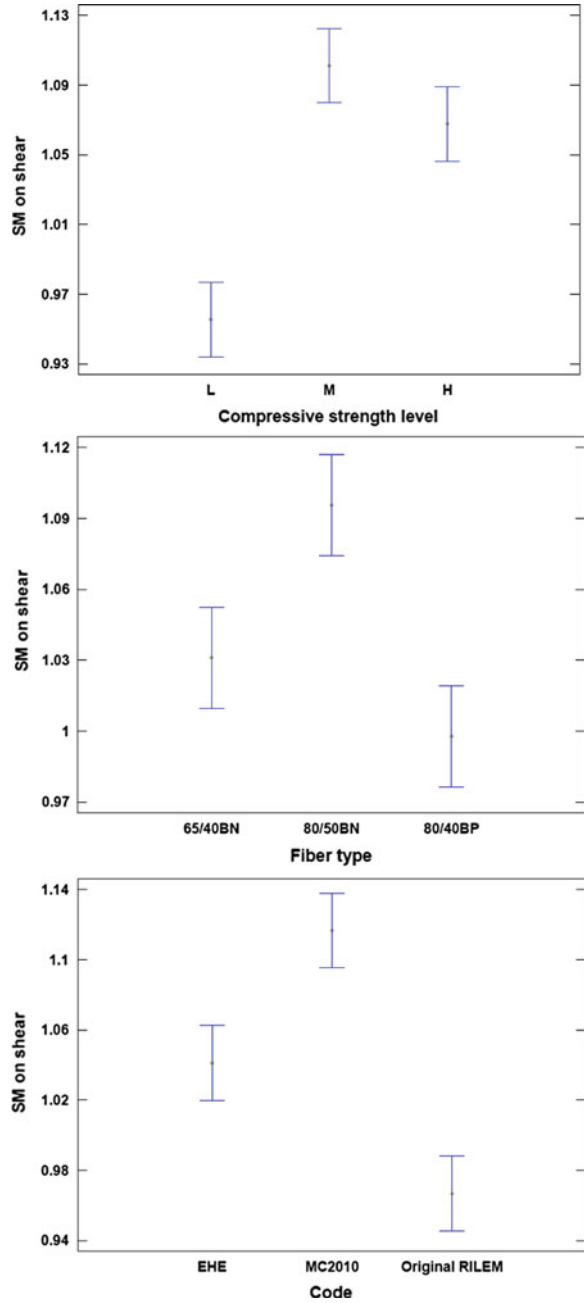
$$N_{\text{complete cases}} = (N_{\text{of levels}})^{N_{\text{of factors}}} = 2^1 \times 5^1 \times 3^1 = 30 \text{ complete cases}$$

The ANOVA table (Table 8.35) shows that all main effects and two interactions have significant differences since their p-values are less than 0.05.

By means of LSD intervals (Fig. 8.38), in this Series, it can be observed that:

- *Compressive strength level.* there are significant differences. For high compressive strengths, Codes are more adjusted (less conservative).
- *Fiber type.* With fibers made with normal strength fibers (BN), Codes are more conservative when fibers are slenderer and longer. For high strength fibers (BP), the shorter are the more conservative for EHE and RILEM, as discussed in the interaction plots and surface charts.

Fig. 8.34 Means and 95.0 % LSD intervals (f_c and f_{R3} beams-I)



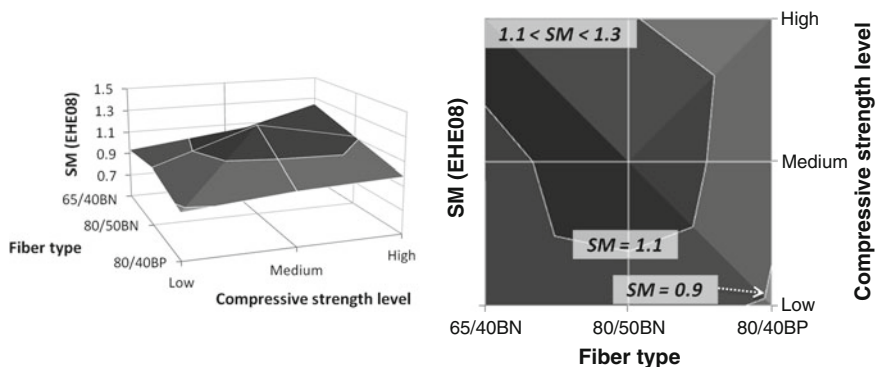


Fig. 8.35 Influence of the interaction between *fiber type* and f_c level in SM according to EHE08

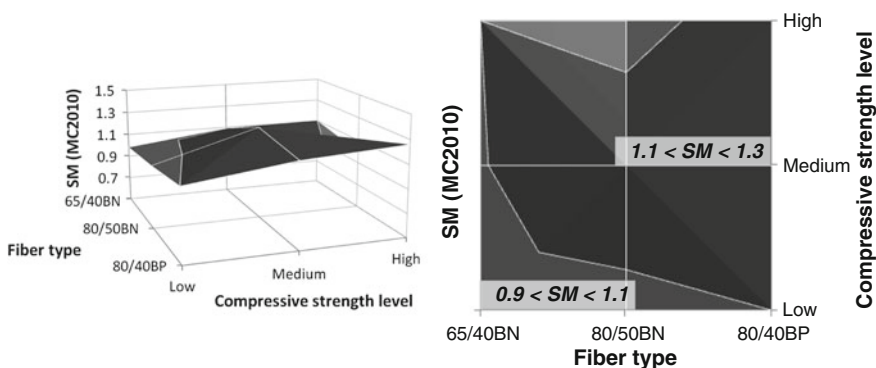


Fig. 8.36 Influence of the interaction between *fiber type* and f_c level in SM according to MC2010

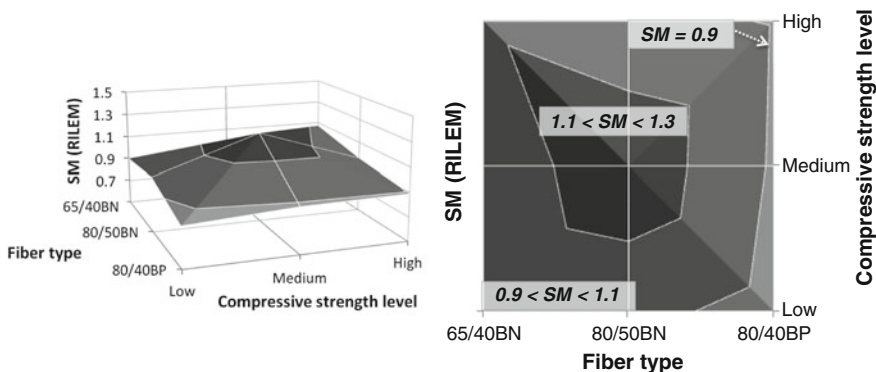


Fig. 8.37 Influence of the interaction between *fiber type* and f_c level in SM according to RILEM

Table 8.33 Constant variables between the beams within the same series (f_c and f_{R3} beams-II)

<i>Constant variables</i>
Cross-section shape
ρ (%) = 3.72
3 point test
50 kg/m ³ of steel fibers

Table 8.34 Factors and dependent variable analyzed in the ANOVA analysis of f_c and f_{R3} beams-II

<i>Factors (independent variables)</i>
Compressive strength level: Medium (M), High (H)
Fibers type: 45/50BN, 65/40BN, 80/50BN, 80/30BP, 80/40BP
Codes: EHE08, MC2010, RILEM
<i>Dependent variable</i>
Shear safety margin (SM)

Table 8.35 ANOVA for SM on shear—type III sums of squares (f_c and f_{R3} beams-II)

Source of variation	Sum of squares	d.f	Mean square	F-ratio	p-value
<i>Main effects</i>					
A: Compressive strength	0.0264033	1	0.0264033	22.65	0.0014
B: Fiber type	0.213753	4	0.0534383	45.84	0.0000
C: Code	0.148087	2	0.0740433	63.51	0.0000
<i>Interactions</i>					
AB	0.119313	4	0.0298283	25.59	0.0001
AC	0.00920667	2	0.00460333	3.95	0.0641
BC	0.0984467	8	0.0123058	10.56	0.0016
<i>Residual</i>	0.00932667	8	0.00116583		
<i>Total (corrected)</i>	0.624537	29			

All F-ratios are based on the residual mean square error

- *Code*. There are significant differences between all Codes. MC2010 is the safest, and the mean value of SM for RILEM is below the unit. EHE gives SM very close to the unit.

As it can be seen in Table 8.35, all main effects have a clear influence on the SM; furthermore, interactions between compressive strength and fiber type (AB), and between fiber type and Code (BC) present significant differences on SM. By means of surface charts (Figs. 8.39, 8.40 and 8.41), it is possible to evaluate the influence of the interactions on the shear SM.

Fig. 8.38 Means and 95.0 % LSD intervals (f_c and f_{R3} beams-II)

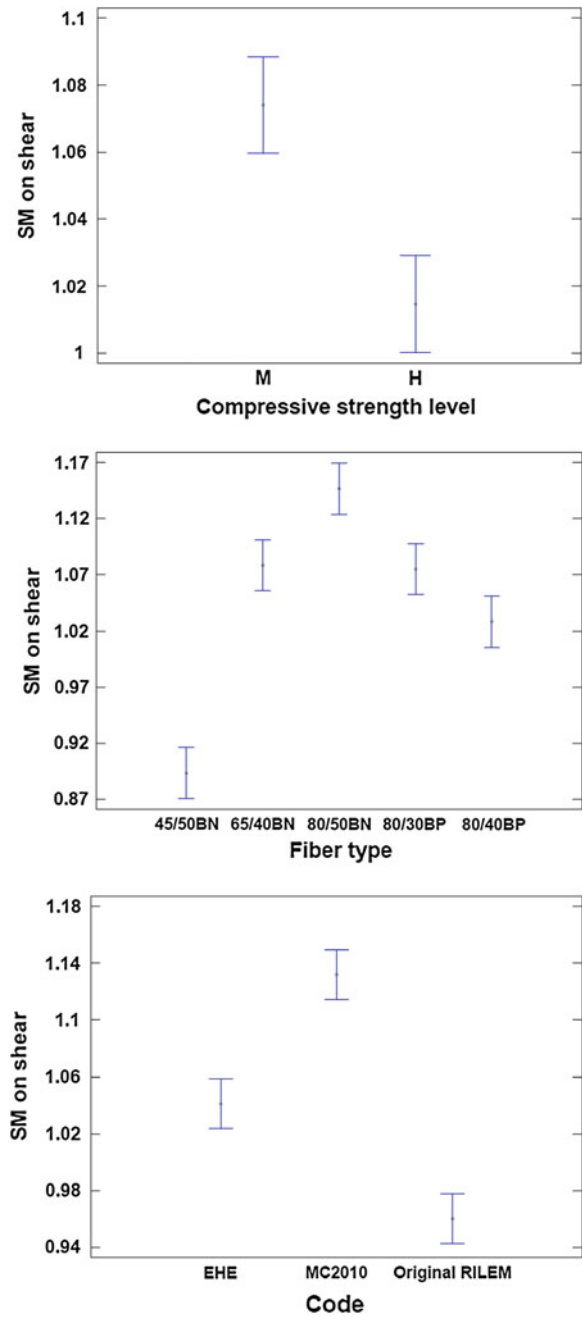


Fig. 8.39 Influence of the interaction between *fiber type* and f_c level in SM according to EHE08

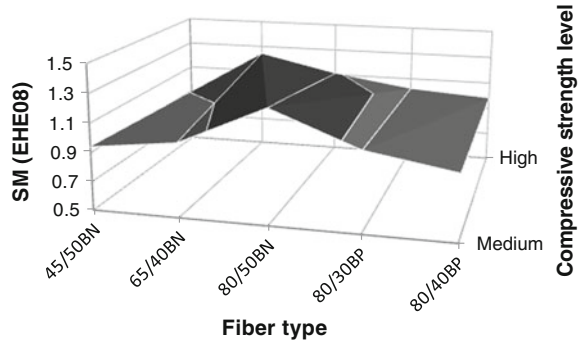


Fig. 8.40 Influence of the interaction between *fiber type* and f_c level in SM according to MC2010

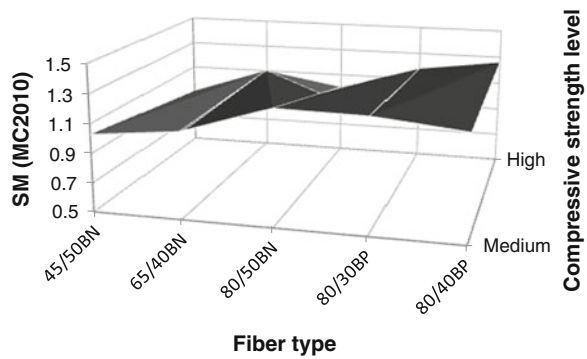
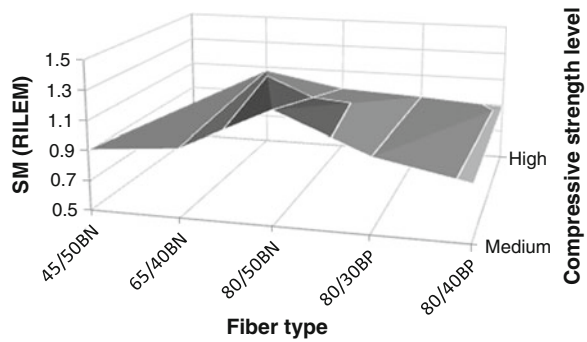


Fig. 8.41 Influence of the interaction between *fiber type* and f_c level in SM according to RILEM



By means of the surface charts, it can be observed that MC2010 is the safest; it only gives the lower results (SM around the unit) when using long fibers (50 mm). When fibers are long and shortly slender (45/50BN), MC2010 gives results slightly unsafe for both levels of compressive strength. When fibers are long and very slender (80/50BN), SM is low in high strength concrete.

RILEM is the most unconservative Code, followed by the EHE08. For this Series SM are always greater than the unit for beams of medium compressive strength and fibers 80/50BN.

When Codes gives $SM < 1$, it means that they estimate theoretical shear values too high; in this case, it seems that Codes are overestimating the effect of fibers. 45/50BN are fibers longer and less slender than the other types of fibers used; therefore, for the same amount of steel, less fibers are into the concrete. This fact, coupled with high compressive strength, results in a brittle matrix and, in this case, Codes should be more conservative.

8.8 Conclusions According to the Analyzed Shear Database

After analyzing a shear database consisting of 215 structural elements, it was detected the influence of each parameter influencing shear.

In the following, Codes will be compared with the experimental results available in the considered database, under the assumption that the partial safety factors are equal to the unit; therefore, the comparisons will not refer to the safety because, in this case, this safety factor have to be considered.

8.8.1 Influence of Effective Depth, d

For effective depth (d) of about 200 mm, Codes were always conservative for all cases except for beams with only stirrups (*see square in solid line*, Fig. 8.42).

When $d \geq 900$ mm, in beams without any shear reinforcement (neither stirrups nor fibers), the analyzed Codes underestimate the shear strength; on the contrary, in beams with stirrups, Codes were too conservative. In beams with only fibers as shear reinforcement, Codes give intermediate results (*see square in dashed line*, Fig. 8.42). So when stirrups are not present, Codes underestimate the shear strength for $d \geq 900$ mm.

It should be underlined that both, stirrups and fibers, can mitigate size effect in shear (Fig. 8.43).

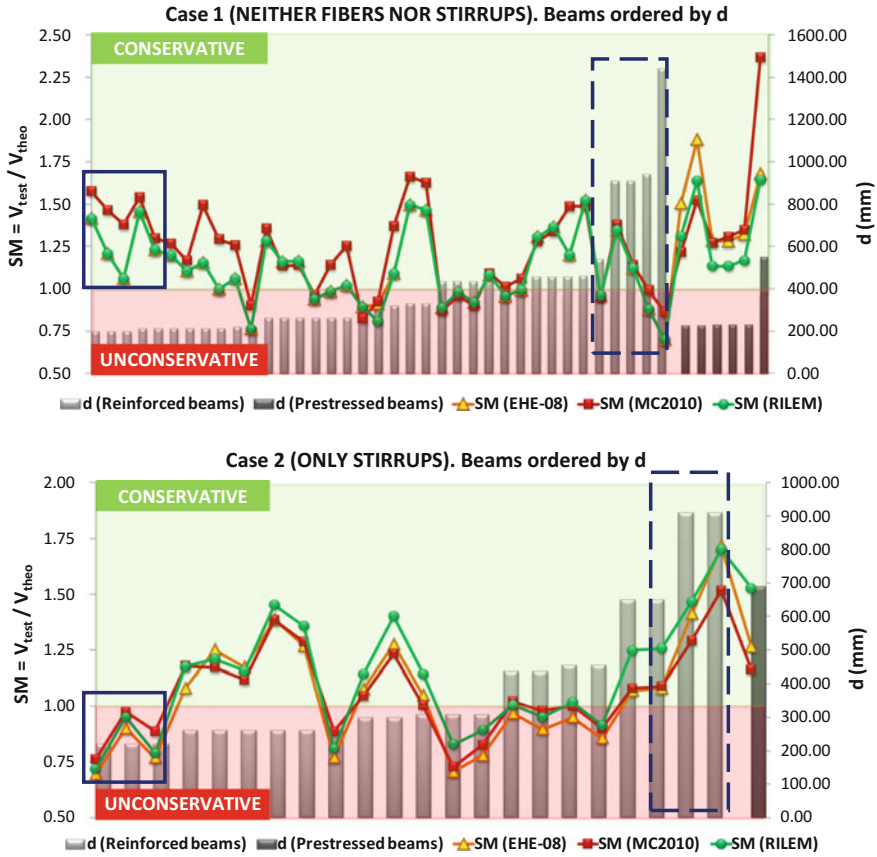


Fig. 8.42 Influence of effective depth (d) on shear safety margins

8.8.2 Influence of the a/d Ratio

For the range $2.5 \leq a/d \leq 3.5$, particular trends are not observed, independently of the reinforcement type (fibers and/or stirrups).

8.8.3 Influence of the Concrete Compressive Strength, f_c

For all concrete beams, with different types of shear reinforcement, when concrete compressive strength (f_c) was higher than 70 MPa, Codes underestimate the shear strength (Fig. 8.44).

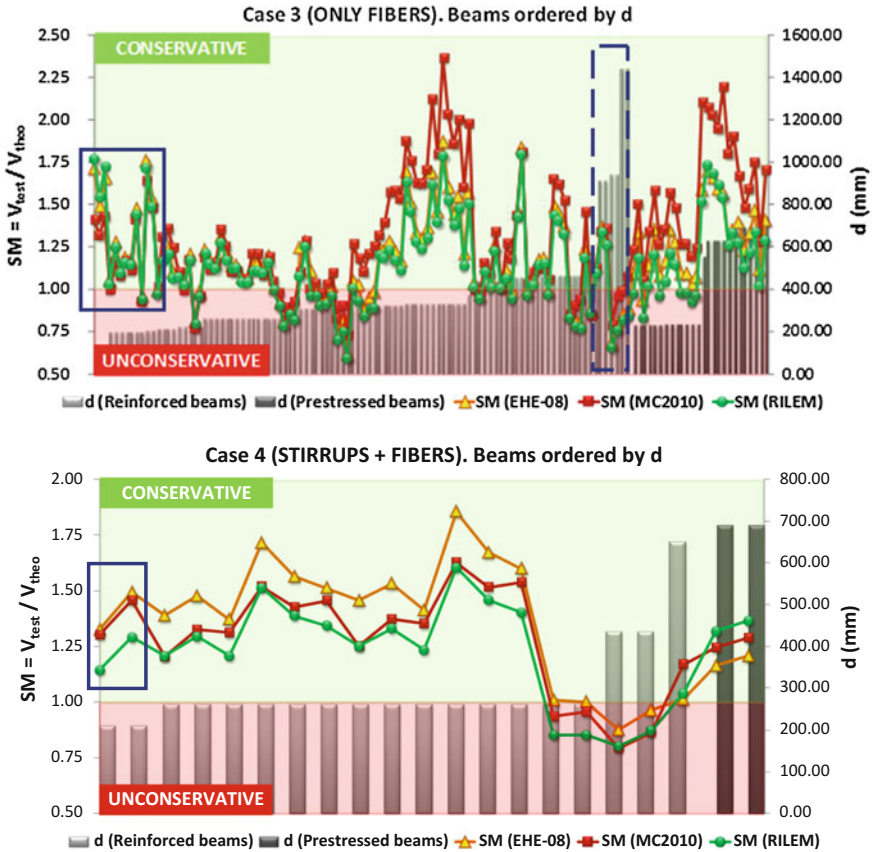


Fig. 8.42 (continued)

8.8.4 Influence of the Residual Tensile Strength, f_{R3}

For beams with only fibers as shear reinforcement, the SMs are generally higher than the unit, with a high scatter (Fig. 8.45). The scatter is smaller in beams with both fibers and stirrups, but a lower number of results are available in the database (Fig. 8.45).

But fundamentally, it was evidenced that the shear should not rely solely on the value of f_{R3} for all types of FRC (with any type of fiber and any concrete compressive strength), since residual strength for smaller crack opening (f_{R1}) also influences the shear strength.

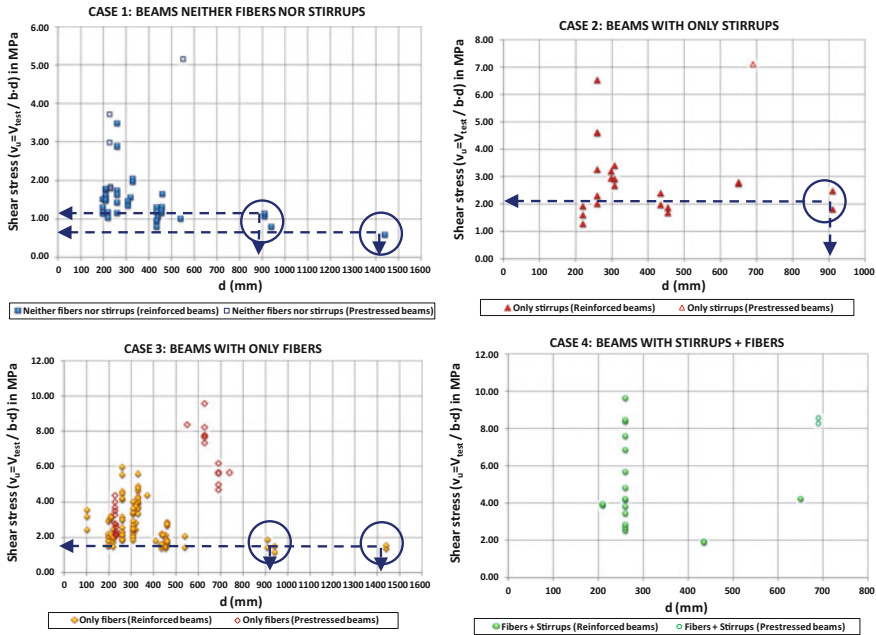


Fig. 8.43 Influence of effective depth (d) on experimental shear stress

Hence parameters f_{R1} and f_{R3} should be linked to correctly estimate the theoretical shear value, as evidenced in Chap. 6 when an alternative parameter $f_{Rm} = (f_{R1} + f_{R3})/2$ was proposed.

Furthermore, in large beams, a crack opening corresponding to f_{R3} , is not reached and a residual strength value related to f_{R1} should be considered. Reinforced beams with more than 125 kg/m^3 of fibers, evidenced $SM > 1$. In beams with combined reinforcement, for amounts of fibers greater than 40 kg/m^3 , SM was always higher than 1 (Fig. 8.46).

8.8.5 Influence of the Amount of Longitudinal Reinforcement, ρ_l

Since $\rho > 3.5 \%$ in reinforced beams, SM began a descent, to more ρ , less SM. This was observed in all cases, except when there were a combination of stirrups and fibers (Fig. 8.47). For reinforced beams with stirrups and fibers, where $\rho < 2 \%$ and $f_{R3} < 1.5 \text{ MPa}$, Codes were unsafe (Fig. 8.48). In prestressed beams, for all cases and all Codes, more ρ , more SM (Fig. 8.47).

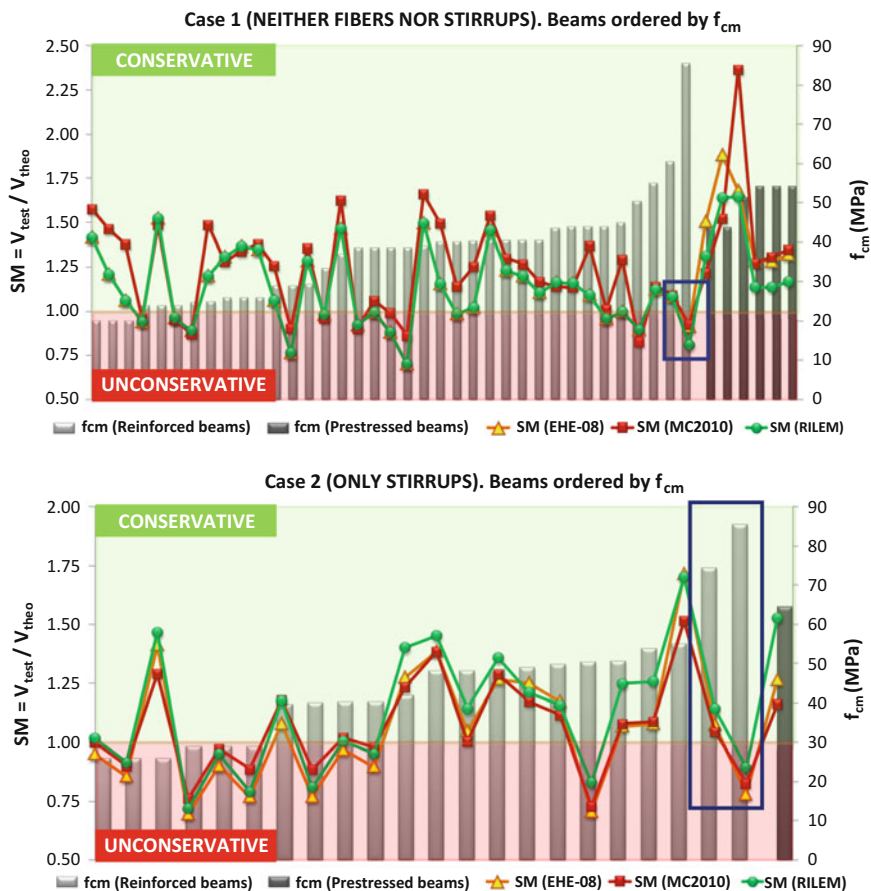


Fig. 8.44 Influence of the concrete compressive strength (f_c) on shear safety margins

8.8.6 Influence of the Stress Due to the Prestressing Actions, σ_c

Codes were always conservative for prestressed beams since they underestimate the effective shear strength experimentally determined. However, in beams with combined shear reinforcement (fibers and stirrups), prestressed beams had SM levels similar of those of beams without prestressing (Fig. 8.49).

For beams without any shear reinforcement, SM of the prestressed beams had a clear dependence of prestressing, since the SM increased with the prestressing stress. In beams with shear reinforcement only, a larger scatter was observed

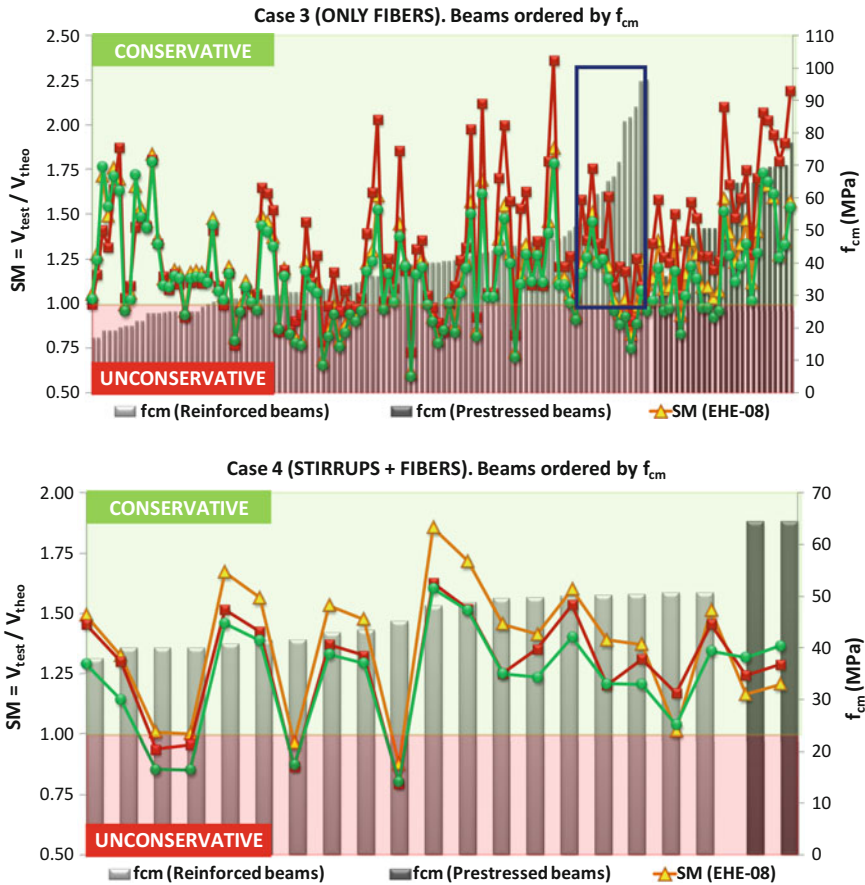


Fig. 8.44 (continued)

(Fig. 8.49). In these beams, MC2010 underestimated the effect of prestressing. In all Codes the SM decreased for prestressing stresses higher than 10 MPa (Fig. 8.49).

8.9 Suggestions for Design Codes According to Shear

After analyze a large database consisting of 215 structural elements failing in shear, and determined the expected shear strength according to three different Design Codes, it was possible to evidence the role of the simple parameters and among these, the ones that could be better evaluated.

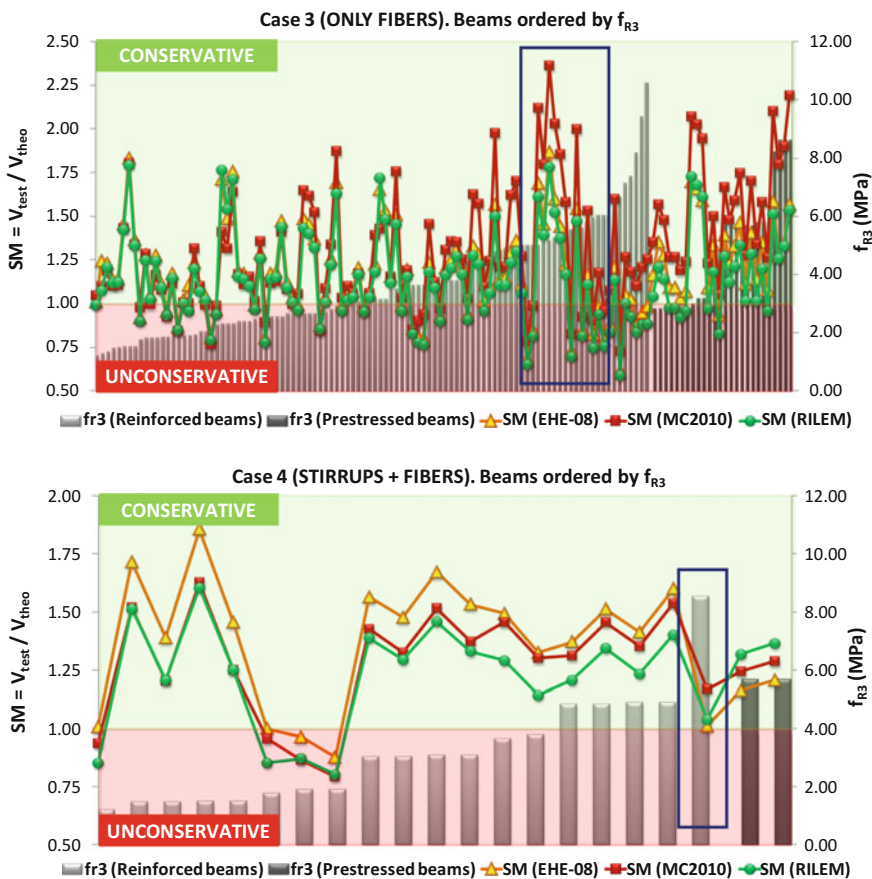


Fig. 8.45 Influence of the residual tensile strength (f_{R3}) on shear safety margins

Unfortunately, although a lot of beams were included in the database, it was not possible to study the influence that each parameter has on the shear safety margin of each Code, but also the influence of some interactions between these parameters that seem to be particularly important.

The analyses performed on the database allowed observing that existing building Codes can be significantly improved and that every time new concrete matrices are developed with enhanced mechanical properties, the existing Codes may be no longer suitable.

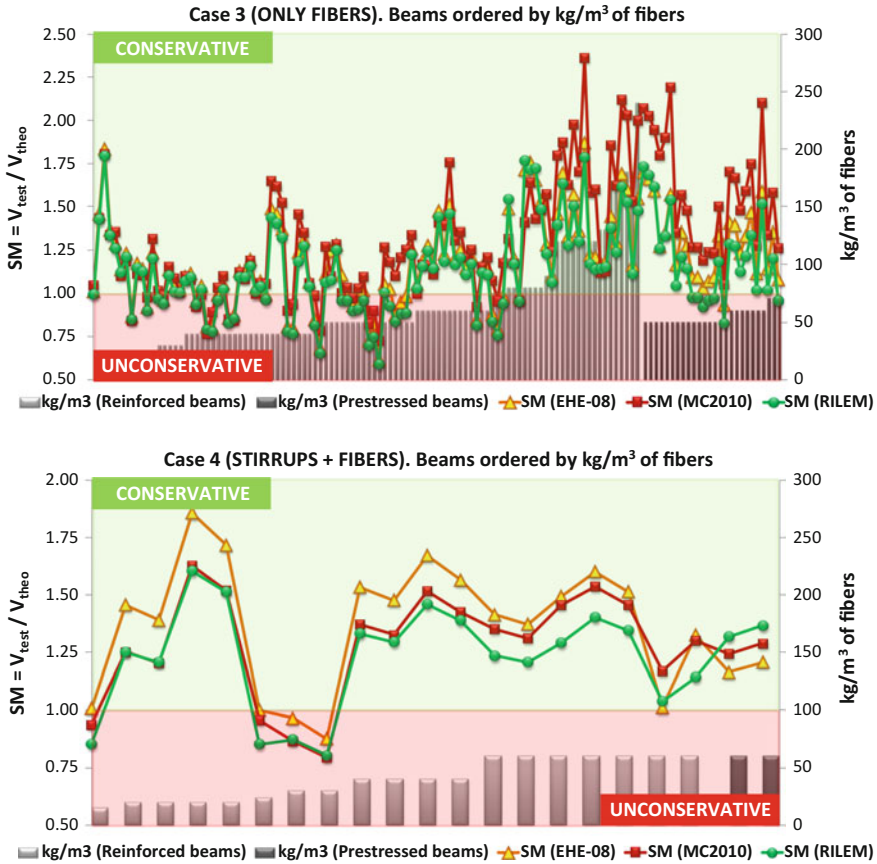


Fig. 8.46 Influence of the amount of steel fibers (kg/m³) on shear safety margins

In the present work, some suggestions for improvements to existing Codes were made. In particular, the following suggestions are proposed:

- Codes are not reliable for calculating shear strength when $a/d < 2.5$, since the arch action is very pronounced and shear strength provided by Codes is markedly conservative. For proper calculation of these cases, other methods should be used as the method of struts and ties.
- The larger the crack width at Ultimate Limit State becomes, the stronger the size-effect will be. Furthermore, it should be considered that the size factor is influenced by the fiber length and, therefore, by the FRC toughness. The latter is a mechanical property that better characterizes the material behavior. Therefore, in fiber reinforced elements, the parameter governing the size effect should depend on the FRC toughness in addition to the element size.

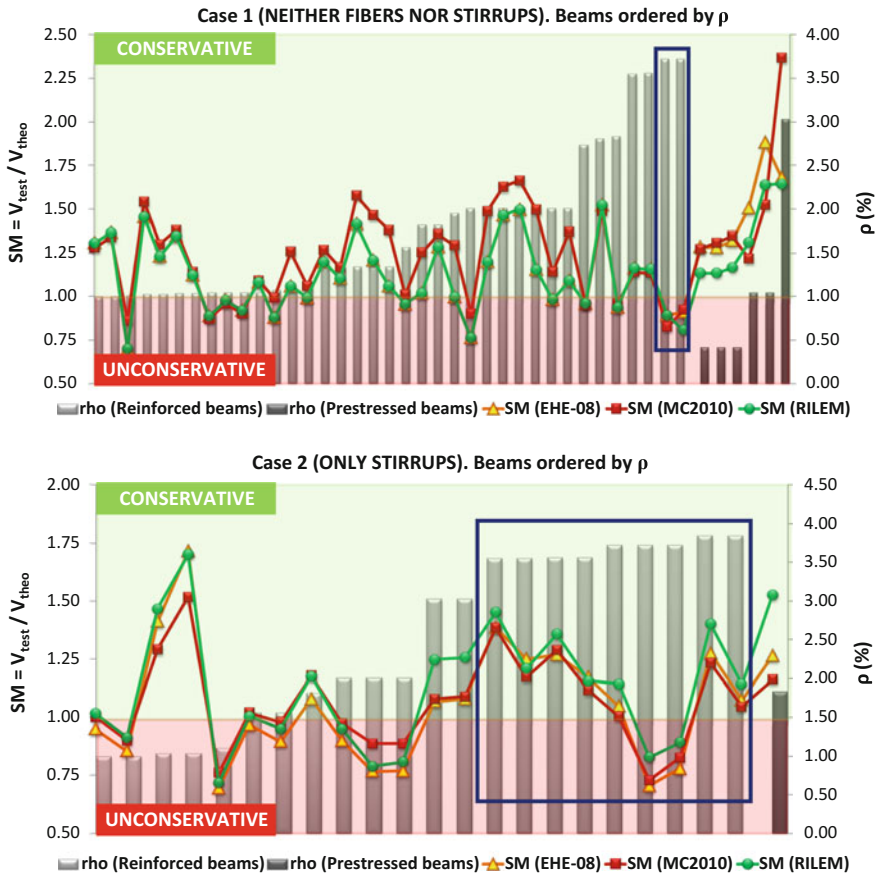


Fig. 8.47 Influence of the amount of longitudinal reinforcement (ρ_l) on shear safety margins

- After analyzing the database, it was found that, for small elements without stirrups (e.g. $d = 200$ mm), Codes gave conservative SM, and that, for larger elements, without stirrups, Codes overestimates the shear strength.
- For small depths will interest to decrease the SM by increasing the theoretical shear, for that, size effect factor (ζ) must be increased. In contrast, for great depths, SM will be increased by reducing the theoretical shear by diminishing the size effect factor (ζ). Therefore, the size effect rules proposed by Codes should be connected accordingly.

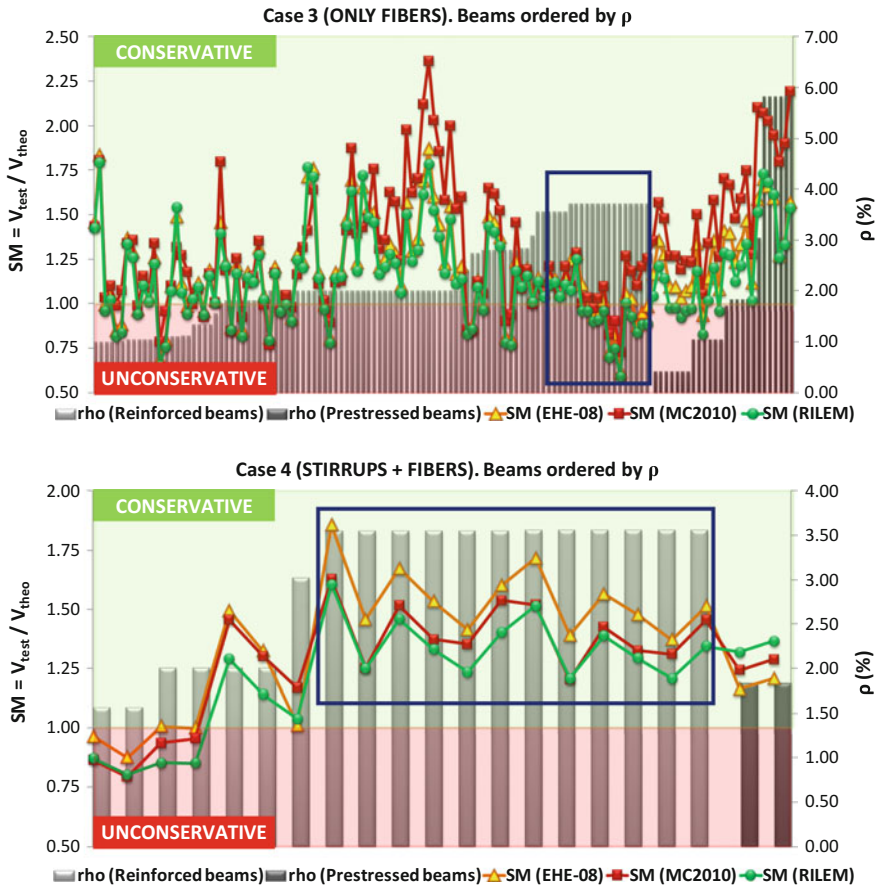


Fig. 8.47 (continued)

- It has been observed that Codes overestimate the shear strength of beams made of high strength concrete ($f_c > 70$ MPa). Therefore, structural codes should provide rules that take into account the shear strength, when $f_c > 70$ MPa, as does the EHE when limits the compressive strength ($f_c \leq 60$ MPa) and the MC2010 for elements without fibers ($(f_{ck})^{1/2} \leq 8$ MPa). In fact, the Model Code ensures that its limitation in f_{ck} is provided due to the larger observed variability in shear strength of higher strength concrete, particularly for members without stirrups. However, concrete compressive strength also influences the FRC toughness.

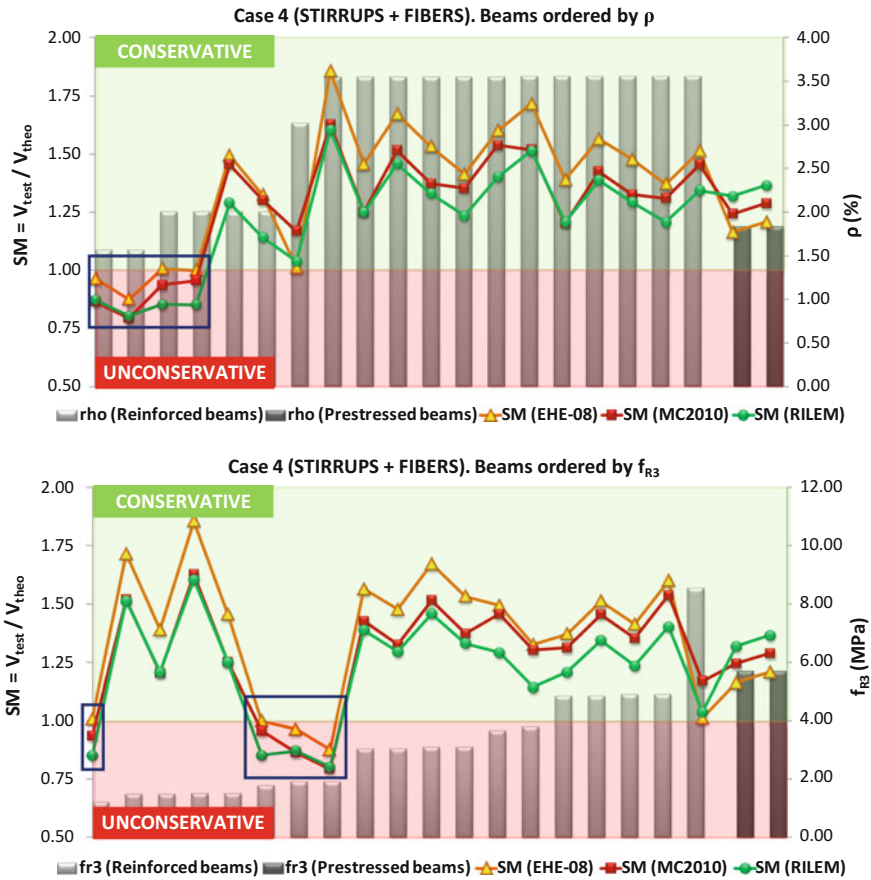


Fig. 8.48 Influence of ρ_l and f_{R3} on shear safety margins

- Beside fracture parameter f_{R3} , parameter f_{R1} should be considered for shear strength, since it depends also on the smaller cracks. A parameter that better represents the shear strength in FRC could be represented by the average value $f_{Rm} = (f_{R1} + f_{R3})/2$.
- Codes are highly conservative for prestressed beams, better and more appropriate rules for considering the compressive stress in the beams should be proposed.

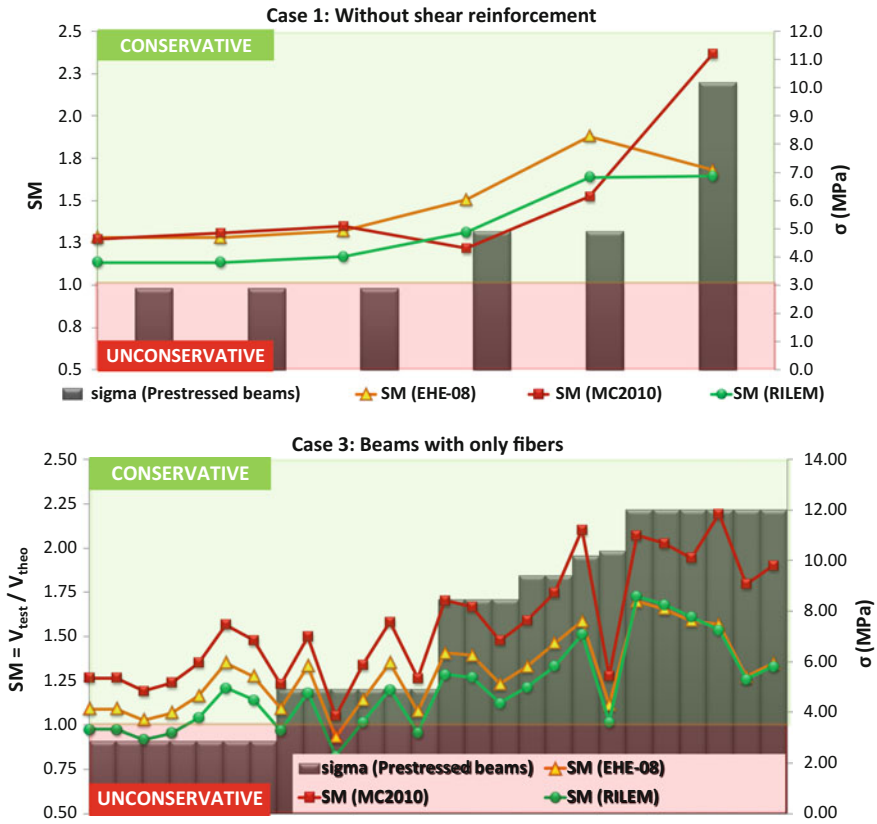


Fig. 8.49 Influence of the stress due to prestressing actions (σ_c) on shear safety margins

References

- Muttoni, A., and M.F. Fernández-Ruiz. 2010. Shear in slabs and beams: should they be treated in the same way? In *fib Bulletin 57. Shear and punching shear in RC and FRC elements. Workshop Proceedings*, p. 268.
- Cladera, A., and A.R. Mari. 2006. Shear design of reinforced and prestressed concrete beams: A proposal for code procedure. *Hormigón y Acero* 242(4): 51–63.
- Di-Prisco, M., G. Plizzari, and L. Vandewalle. 2010. MC2010: Overview on the shear provisions for FRC. In *fib Bulletin 57. Shear and punching shear in RC and FRC elements. Workshop proceedings*, 268 pp.
- Bentz, E. 2010. MC2010: Shear strength of beams and implications of the new approaches. In *fib Bulletin 57. Shear and punching shear in RC and FRC elements. Workshop proceedings*, ed. F. Minelli and G. Plizzari, 268 pp. Italy: University of Brescia.
- Rosenbusch, J., M. Teutsch, D. Dupont, L. Vandewalle, R. Gettu, B. Barragán, M.A. Martín, G. Ramos, and I. Burnett. 2002. Subtask 4.2: Trial beams in shear. In *Brite-Euram Project: Test and design methods for steel fibre reinforced concrete*.
- Dupont, D., and L. Vandewalle. 2003. Shear capacity of concrete beams containing longitudinal reinforcement and steel fibers. *ACI Special Publication* 216: 79–94.

7. Conforti, A., E. Cuenca, F. Minelli, and G. Plizzari. 2011. Can we mitigate or eliminate size effect in shear by utilizing steel fibers? In *Proceedings of fib symposium PRAGUE 2011*.
8. EN14651:2005+A1. 2005. Test method for metallic fibre concrete—measuring the flexural tensile strength (limit of proportionality (LOP), residual).
9. EHE-08. 2008. Instrucción de Hormigón Estructural EHE-08 (in Spanish), Ministerio de Fomento, 702 pp.
10. RILEM. 2003. TC 162-TDF. Test and design methods for steel fibre reinforced concrete, stress-strain design method. Final recommendation. *Materials and Structures* 36: 560–567.
11. MC2010. 2012. Fib Bulletin 65–66. Model Code—final draft.
12. EC2. 2005. Eurocode 2: Design of concrete structures—EN 1992-1-1.
13. Montgomery, D.C., and G.C. Runger. 1996. *Probabilidad y Estadística aplicadas a la Ingeniería*. New York: McGraw Hill.
14. Romero, R., and L. Zúnica. 2010. *Métodos estadísticos en Ingeniería*, UPV.

Part V
Conclusions and Future Research

Chapter 9

Conclusions

This thesis presents a comprehensive experimental program for analyzing the behavior of FRC beams with different dimensions, production processes and transverse reinforcement.

The analysis of the results confirms that steel fibers improve the shear behavior of beams and that their contribution may be highly beneficial in many cases and practically indispensable in others.

The main conclusions can be summarized as follows (subscript indicates the chapter referred to):

- A self-compacting fiber-reinforced concrete (SCFRC) of consistent quality can be cast in a continuous process, as shown by the slump flow test, compressive strength and flexural behavior under normal site conditions (Chap. 4).
- Adding steel fibers to beams with stirrups improves ductility as steel fibers control cracking and help to prevent cracks from spreading (Chap. 4).
- With steel fibers more cracks are created but they are smaller than in plain concrete and the crack spacing is also smaller (Chap. 4).
- Beam flanges clearly improve shear behavior, as they prevent failure by compression in the top beam layer. This effect should be included in the Codes in the form of a *flange coefficient* (k_f) for all types of concrete. An improvement in shear behavior with flange width was also observed, although there were two exceptional cases with no improvements: small flange widths (in relation to web width) and large flange widths (depending on the other dimensions of the cross section) in which shear improvement remains constant over a certain flange width (Chap. 4).
- The RILEM approach does not model the positive effect of fibers on the dowel action, as fibers do not affect the longitudinal reinforcement term, so that RILEM considers fibers and longitudinal reinforcement to be completely independent. On the other hand, MC2010 considers the positive effect of fibers on the dowel action, so that the fibers' contribution increases with high longitudinal reinforcement ratios (Chap. 4).

- Fibers substantially mitigate the size effect in shear: the effect of the descending trend in this factor becomes less steep with increasing FRC toughness and shear failure (and size effect) appears at higher effective depths in members (Chap. 5).
- The constitutive law of FRC in tension is obtained from the prismatic specimen results (EN 14651). It is therefore necessary to consider an appropriate critical length (L_r) for each specific case (Chap. 5).
- Even small amounts of fibers greatly influence the shear behavior of beams, basically by delaying the occurrence of the shear failure mechanism and by altering the collapse from shear to flexure, with enhanced bearing capacity and ductility (Chap. 5).
- Fibers mitigate the size effect in shear, which declines with increased FRC toughness (Chap. 5).
- Even though fibers have positive effects when added to stirrups, their contribution does not represent an optimized practical solution for at least two reasons. The first is mechanically-based, since fibers and stirrups do not come into action at the same time and their contributions cannot simply be added together. The second is practically-based, since the main advantage of using fibers consists of avoiding the use of stirrups and larger stirrup spacing. The only exception is that fibers control the formation and propagation of new cracks, but when they do show up the fiber mitigates their effects.
- A large amount of longitudinal reinforcement can be efficient for shear resistance, provided that it is well anchored and has sufficient cover. In these conditions the limitation on the amount of longitudinal reinforcement (ρ_l) of 2 %, generally imposed by Design Codes should not be applied (Chap. 6).
- Shear strength and load deflection response markedly depend on the fiber type (quality of steel and geometry of steel fiber) and its combination with the compressive strength of the concrete matrix. It is possible to have a brittle post-cracking (high compressive concrete strength + low steel strength fibers) or a very ductile behavior (low or medium compressive concrete strength + high steel strength fibers) (Chap. 6).
- The combined effects of the structural system that comes into play in the structural member (position and amount of longitudinal reinforcement, section shape and dimensions), including the joint effects of stirrups and fibers, depend on the evolution of shear-crack width. Thus, for certain structural arrangements, the use of the fracture parameter f_{R3} as a reference value for calculating shear strength may be unsafe or over-conservative. In some circumstances, as in small beams, the average value between f_{R1} and f_{R3} may be more appropriate (Chaps. 6 and 8).
- Given the impossibility of placing stirrups in extruded Hollow Core Slabs (HCS), adding steel fibers to concrete certainly improves shear resistance, as it was demonstrated that it is possible to produce HCS without any technical problems (Chap. 7).
- According to the database analyzed, it seems that Design Codes are always conservative for prestressed beams and they also seem to overestimate the shear strength of beams made with high strength concretes ($f_c > 70$ MPa) (Chap. 8).

Chapter 10

Recommendations for Future Research

The following recommendations are based on the experimental and numerical results of the present study:

- A new push-off test should be performed subject to direct shear loads, with good control of crack width, in order to improve the response of the test in determining aggregate interlock in different concrete matrixes, at different levels of compressive strength and with different kinds of steel fibers.
- Improvements should be proposed for the current formulations in the Design Codes.
- FRC should be included in building codes for its toughness, but not only based on the f_{R3} parameter, as it is not representative for all types of FRC.